Application of Parameter Estimation for Diffusions and Mixture Models

Nolsøe, Kim

Publication date:
2007

Document Version
Publisher's PDF, also known as Version of record

Application of Parameter Estimation for Diffusions and Mixture Models

Kim Nolsøe

Kongens Lyngby 2006
IMM-PHD-2006-168

Technical University of Denmark
Informatics and Mathematical Modelling
Building 321, DK-2800 Kongens Lyngby, Denmark
Phone +45 45253351, Fax +45 45882673
reception@imm.dtu.dk
www.imm.dtu.dk

IMM-PHD: ISSN 0909-3192

Preface

This thesis was prepared at Informatics and Mathematical Modelling (IMM), the Technical University of Denmark and Universidad Politécnica de Cartagena in partial fulfillment of the requirements for acquiring the Ph.D. degree in engineering. The project was partially supported by the European Commission through the Research Training Network DYNSTOCH under the Human Potential Programme.

The topic of the Ph.D. thesis is parameter estimation for diffusion processes and Bayesian conformational analysis of ring molecules. The thesis consists of an introduction and six papers written during the Ph.D, study, published/submitted to international journals.

The work was supervised by Henrik Madsen (Informatics and Mathematical Modelling (IMM)) and Mathieu Kessler (Universidad Politécnica de Cartagena (UPCT)).

Lyngby, June 2006

Kim Nolsøe

Summary

The first part of this thesis proposes a method to determine the preferred number of structures, their proportions and the corresponding geometrical shapes of an m-membered ring molecule. This is obtained by formulating a statistical model for the data and constructing an algorithm which samples from a posterior distribution. The sampling algorithm is constructed from a Markov chain which allows the dimension of each sample to vary, this is obtained by utilizing the Reversible jumps methology proposed by Peter Green. Each sample is constructed such that the corresponding structures are physically realizable; this is obtained by utilizing the geometry of the structures. Determining the shapes, number of structures and proportions for an m-membered ring molecule is of interest, since these quantities determine the chemical properties.

The second part of this thesis deals with parameter estimation for diffusions. The first idea is in an optimal way to incorporate prior information in the estimation equation $G^*(\theta; X_{t_1}, \ldots, X_{t_n}) = 0$, used to find an estimator of the unknown parameter θ. The general idea is to introduce an new optimality criterion which optimizes the correlation with the posterior score function. From an application point of view this methology is easy to apply, since the optimal estimating function $G^*(\theta; X_{t_1}, \ldots, X_{t_n})$ is equal to the classical optimal estimating function, plus a correction term which takes into account the prior information. The methology is particularly useful in situations where prior information is available and only few observations are present. The resulting estimators in some sense have better properties than the classical estimators. The second idea is to formulate Michael Sørensens method "prediction based estimating function" for measurement error models. This is obtained by constructing an estimating function through projections of some chosen function of $Y_{t_{i+1}}$ onto functions of previous observations $Y_{t_i}, \ldots, Y_{t_0}$. The process of interest $X_{t_{i+1}}$ is partially observed through a measure-

ment equation $Y_{t_{i+1}} = h(X_{t_{i+1}}) + \text{noice}$, where $h(.)$ is restricted to be a polynomial. Through a simulation study we compare for the CIR process the obtained estimator with an estimator derived from utilizing the extended Kalman filter. The simulation study shows that the two estimation methods perform equally well.

Resumé

Den første del af afhandlingen foreslår en metode til at bestemme det forestukkende antal af strukturer, deres procentvise forekomster samt de tilsvarende strukturelle former for et ringmolekyle bestående af m-atomer. Dette opnås ved at formulere en statistisk model for data og konstruere en algoritme som sampler fra en posteriori fordeling. Selve samplingsalgoritmen er konstrueret udfra en Markovkæde, hvor dimensionen af hver sample kan variere, hvilket opnås ved at benytte metoden "reversible hop" introduseret af Peter Green. Hver sample er dannet således at de tilsvarende strukturelle former er fysisk realiserbare; dette opnås ved at udnytte den geometri som strukturene har. Grunden til at de geometriske former samt den procentuelle sammensætning er interessante, er at disse størrelser afgør de kemiske egenskaber for ringmolekylet.

Den anden del af afhandlingen omhandler parameterestimation for diffusionsprocesser. Den første ide er på en optimal måde at introducere priorinformation i estimationsligningen $G^*(\theta; X_{t_1}, \ldots, X_{t_n}) = 0$, der bruges til at finde en estimator for parameteren θ. Dette opnås ved at introducere et nyt optimalitetskriterium, der maksimerer korrelationen med posterior-scorefunktionen. Fra et anvendelses mæssigt synspunkt er denne metode let at benytte, da den optimale estimations funktion $G^*(\theta; X_{t_1}, \ldots, X_{t_n})$ er identisk med den optimale klassiske estimations funktion, plus et korrektionsled der tager hensyn til den specificerede prior. Metoden er særlig brugbar, når der er priorinformation om parametrene tilrådighed samt kun få observationer. De opnåede parameterestimater har i en hvis forstand bedre egenskaber end de klassiske. Den anden ide er at formulere Michael Sørensens metode "Prediktions baserede estimationsfunktioner" for modeller med målefejl. Dette opnås ved at danne en estimations funktion konstrueret af en funktion af $Y_{t_{i+1}}$, som projekteres på funktioner af $Y_{t_i}, \ldots, Y_{t_0}$. Den interessante Proces $X_{t_{i+1}}$ er indirekte observeret igennem en måleligning $Y_{t_{i+1}} = h(X_{t_{i+1}}) +$ støj, hvor funktio-

nen h skal være polynomiel. Vi sammenligner gennem et simulationsstudie for CIR processen de opnåede estimater med estimater fundet ved at benytte det udvidede Kalman filter. Simulationsstudiet viste at de to metoder opnår sammenlignelige resultater.

Papers included in the thesis

I K. Nolsøe, M. Kessler, J. Pérez, H. Madsen Bayesian Conformational Analysis of m-membered rings through Reversible Jump MCMC. *Journal of Chemometrics* 2005.

II J. Pérez, L. García, M. Kessler, K. Nolsøe, E. Pérez, J.L Serrano, J.F. Martínez, R. Carrascosa. A statistical method for the conformational classification of eight-membered rings. Application to copper complexes double bridged by phosphate, phosphonate or phosphinate ligands. *Inorganica Chimica Acta*. 2005.

III J. Pérez, K. Nolsøe, M. Kessler, L. García, E. Pérez, J.L Serrano. Bayesian Methods for the conformational classification of eight-.membered rings. *Acta Crystallographica, Serie B* 2005.

IV M. Kessler, K. Nolsøe, María C. Bueso, and José Pérez Model Based Conformational Analysis of Ring Molecules. *Elsevier status submitted*

V K. Nolsøe, M. Kessler, H. Madsen Estimating Functions with Prior Knowledge, (EFPK) for Diffusions. *Technical report* 2006.

VI K. Nolsøe, J. Nygaard Nielsen and H. Madsen PREDICTION-BASED ESTIMATING FUNCTIONS FOR DIFFUSION PROCESSES WITH MEASUREMENT NOISE. *RevStat status submitted* 2006.

Notation

$1_A(x)$	Indicator function $1_A(x) = \begin{pmatrix} 1, & x \in A \\ 0, & \text{else} \end{pmatrix}$.
$Be(\alpha, \beta)$	Beta distribution.
$D_k(\alpha_1, \ldots, \alpha_k)$	Dirichlet distribution.
$G(X_{t_0}, \ldots, X_{t_n}; \theta)$	Estimating function.
$E_f[h(X)]$	Expectation of $h(X)$ under the distribution $f(x)$.
$IG(\alpha, \beta)$	Inverse gamma distribution.
$l(x; \theta)$	Likelihood.
$N(\mu, \sigma^2)$	Normal distribution.
$x_{1:n}$	Observations $x_1, \ldots, x_n$.
$\pi(\theta \mid x_{1:n})$	Posterior density.
$\pi_u(\theta \mid x_{1:n})$	(possibly **u**n-normalized) posterior density.
$p(\theta)$	Prior density.
$U(x_{t_0}, \ldots, x_{t_n}; \theta)$	Score function.
$X \sim f, X \sim N(\mu, \sigma^2)$	Stochastic variables generated from the density function f or the stochastic variable $N(\mu, \sigma^2)$.
Ω_x	State space of X.
$K(X_i, X_{i+1})$	Transition kernel.
$U_{\{1,\ldots,M\}}$	Uniform distribution discrete.
$U_{[a,b]}$	Uniform distribution.
W_t	Wiener process.

Contents

Chapter 1

An (MCMC) application to 3-dimensional ring structures

This chapter motivates the works presented in Paper I, II, III and IV. We define and illustrate basic concepts used in these articles by applying the methology on simple examples. Further an introduction to basic terms assumed known in these papers will be presented.

Paper I describes a method to classify the geometrical structures called the *conformations*, of m-membered ring molecules and the corresponding proportions, see Figure 1.1 For a certain ring molecule it is interesting to determine the pos-

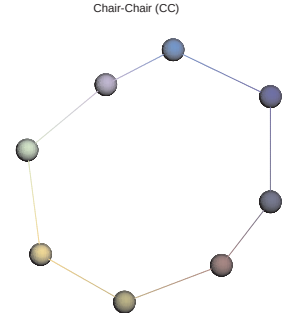

Figure 1.1: One conformation of an 8-membered ring molecule.

sible conformations and its proportions, since these terms specify the chemical properties of the molecule, see [16]. The conformations can be determined from quantum mechanical energy considerations, resulting in a set of *canonical* conformations, see Figure 1.2. However, it is well known from experimental data

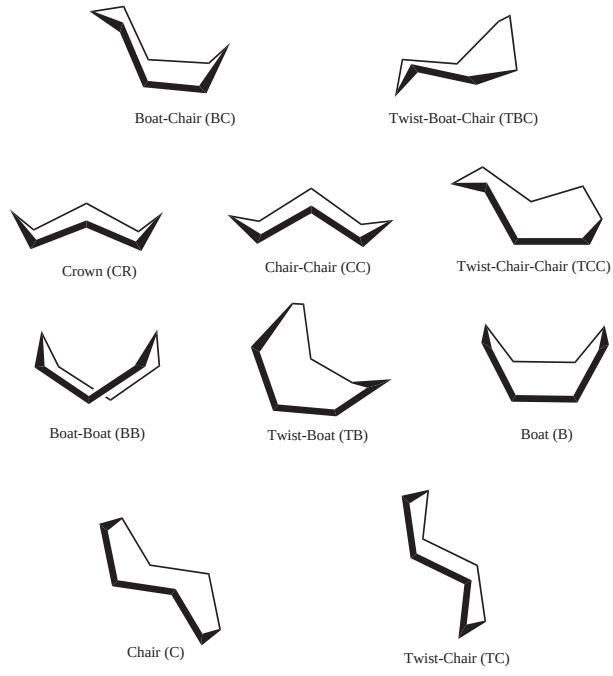

Figure 1.2: The 10 canonical conformations for cyclooctane (8-membered ring molecule).

that some of these canonical conformations are almost never observed. Statistical descriptive methods have been applied to detect preferred conformations by clustering the observed structures into a number of conformations. A review of different statistical methods can be found in [23]. The main objection to these methods is that no probabilistic model is specified for the data.

Our proposed method is build on a probabilistic model for the data together with the specification of prior distributions. The model and the priors determine the posterior distribution. From the posterior distribution sampling algorithms were constructed applying an extended version of the Metropolis-Hastings algorithm called the Reversible jump algorithm [9] (introduced in Section 1.3). Basically the Reversible jump algorithm enables one to sample from models where the dimension (the number of conformations) is unknown. The sampling was further refined by imposing some restrictions on each sample (introduced in Section 1.4), such that

each proposed sample represents a reasonable chemical structure.

We start out by motivating the use of simulation to estimate the distribution of a parameter θ.

Throughout the whole chapter the mathematical details will be omitted when they do not help to illustrate the general ideas.

1.0.1 Bayesian statistics

For known θ let the probability density of $(X_1, \ldots, X_n) = X_{1:n}$ be $f(x_{1:n}|\theta)$, $f(x_{1:n}|\theta)$ represents the model for the data. Given $x_{1:n}$, $f(x_{1:n}|\theta)$ describes a function $l : \theta \mapsto l(x_{1:n}|\theta)$ called the *likelihood function*. Let $p(\theta)$ represent the *prior* of the parameter θ describing our knowledge of θ before $x_{1:n}$ was available, $h(x_{1:n})$ is the marginal probability density of $X_{1:n}$.

The *posterior* distribution of θ, $\pi(\theta|x_{1:n})$, describing the distribution of θ when $x_{1:n}$ is available, is related to the likelihood function and the prior distribution through Bayes rule

$$\pi(\theta|x_{1:n}) = \frac{l(x_{1:n}|\theta)p(\theta)}{h(x_{1:n})} \propto l(x_{1:n}|\theta)p(\theta). \tag{1.1}$$

Observe from (1.1) that the posterior probability density, is proportional to the likelihood $l(x_{1:n}|\theta)$ multiplied by the prior probability density $p(\theta)$

$$\pi(\theta|x_{1:n}) \propto l(x_{1:n}|\theta)p(\theta) \equiv \pi_u(\theta|x_{1:n}). \tag{1.2}$$

$\pi_u(\theta|x_{1:n})$ is the un-normalized posterior distribution, meaning that $\pi(\theta|x_{1:n}) = \frac{\pi_u(\theta|x_{1:n})}{c}$, with c being the unknown normalization constant. Denote by Ω_θ the state space of θ.

The probability density of interest in this thesis is the posterior probability $\pi(\theta|x_{1:n})$. $\pi(\theta|x_{1:n})$ is specified through the product of the two known expressions of $l(x_{1:n}|\theta)$ and $p(\theta)$, hence the posterior density is only described up to a normalization constant c.

It might seem logical to determine c by calculating the integral

$$c = \int_{\Omega_{x_1} \otimes \cdots \otimes \Omega_{x_n}} \pi_u(\theta) dx_1 \cdots dx_n. \tag{1.3}$$

However in general calculations of these integrals are complicated to carry out. Without further comments we mention that numerical approximations to the in-

tegral in (1.3) such as the Laplace approximation exist but are outside the scope of this presentation.

Example 1 (A mixture model of two components) *Consider the mixture model of two normal distributions $N(\mu_1, \sigma_1^2)$ and $N(\mu_2, \sigma_2^2)$, which e.g. could describe the height of a random person not specifying whether person i is a boy or a girl. Let X_i represent the height of an individual, then $X_{1:n}$ is i.i.d. with*

$$X_i \sim w_1 N(\mu_1, \sigma_1^2) + (1 - w_1) N(\mu_2, \sigma_2^2). \tag{1.4}$$

(1.4) represents the model for the data given the parameters $(w_1, \mu_1, \mu_2, \sigma_1^2, \sigma_2^2)$. The density of $f(x|w_1, \mu_1, \mu_2, \sigma_1^2, \sigma_2^2)$ for a certain choice of $(w_1, \mu_1, \mu_2, \sigma_1^2, \sigma_2^2)$ is illustrated in Figure 1.3 Next the priors are specified, to simplify assume that

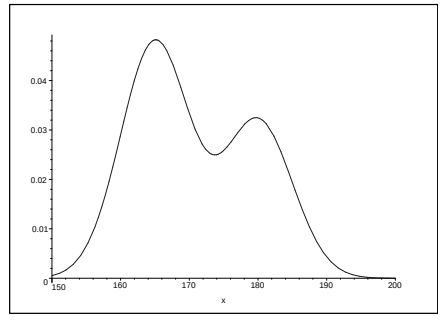

Figure 1.3: Density of the mixture model specified by $f(x|w_1, \mu_1, \mu_2, \sigma_1^2, \sigma_2^2)$ from (1.4).

σ_1^2, σ_2^2 and w_1 are known, hence $\theta = (\mu_1, \mu_2)$. Let the priors for μ_1 and μ_2 be normal distributed $\mu_1 \sim N(\alpha, \sigma^2)$ (μ_1 is a stochastic variable with the distribution $N(\alpha, \sigma^2)$, (a small μ can represent either a stochastic variable or parameter understood from the context, standard notation in most scientific papers)) and $\mu_2 \sim N(\alpha, \sigma^2)$. Resulting in the expression of the prior for θ,

$$p(\theta) = \varphi(\mu_1; \alpha, \sigma^2)\varphi(\mu_2; \alpha, \sigma^2) \tag{1.5}$$

with $\varphi(\mu; \alpha, \sigma^2) = \frac{1}{\sqrt{2\pi\sigma^2}} \exp(-\frac{(\mu-\alpha)^2}{2\sigma^2})$.

Having carried out an experiment $x_{1:n}$ the likelihood $l(x_{1:n}|\theta)$ is specified through the model (1.4)

$$l(x_{1:n}|\theta) = \prod_{i=1}^{n} \{w_1 \varphi(x_i; \mu_1, \sigma_1^2) + (1 - w_1)\varphi(x_i; \mu_2, \sigma_2^2)\} \tag{1.6}$$

together with the expression of the prior $p(\theta)$ in (1.5) the posterior distribution is

determined through (1.1) up to a normalization constant

$$\pi(\mu_1, \mu_2|x_{1:n}) \propto \Big[\prod_{i=1}^{n}\{w_1\varphi(x_i;\mu_1,\sigma_1^2)+(1-w_1)\varphi(x_i;\mu_2,\sigma_2^2)\}\Big]\varphi(\mu_1;\alpha,\sigma^2)\varphi(\mu_2;\alpha,\sigma^2). \tag{1.7}$$

1.1 Monte Carlo Simulation

Vaguely formulated Monte Carlo simulation is a stochastic technique constructed from some random variables. Applying this technique, simulation from these random variables is conducted a large number of times, such that you afterwards are able to describe some properties with a certain precision not easily or possibly solved analytically, eg. the mean or the variance. Monte Carlo simulation has been applied in a large amount of areas ranging from e.g. high energy physics experiments to simulation of bingo games. To introduce the idea we will illustrate how the value $\pi = 3.1415...$, (which obviously has nothing to do with $\pi(\theta|x_{1:n})$ the posterior distribution) can be determined by Monte Carlo simulation.

Example 2 (Simulating $\pi = 3.1415...$) *Simulate n points* $(\theta_1^{(1)}, \theta_2^{(1)}), \ldots, (\theta_1^{(n)}, \theta_2^{(n)})$ *from* $U_{[0;1]} \otimes U_{[0;1]}$, *determine the number of points* $m = \sum_{i=1}^{n} 1_A(\theta_1^{(i)}, \theta_2^{(i)})$, *where* $1_A(\theta_1^{(i)}, \theta_2^{(i)})$ *is the indicator function* $1_A(\theta) = \begin{cases} 1 & \text{if } \theta \in A \\ 0 & \text{if } \theta \notin A \end{cases}$ *and A is specified by* $A : \{(\theta_1^{(i)}, \theta_2^{(i)})|\theta_1^{(i)} \in [0;1], \theta_2^{(i)} \in [0;1], \theta_1^{2(i)} + \theta_2^{2(i)} < 1\}$. *From simple geometry it follows that* $\hat{\pi} = \frac{4m}{n}$.

In this thesis the type of Monte Carlo simulation called Monte Carlo Integration has been applied. Monte Carlo Integration shortly put allows for estimation of $E_f[h(\Theta)]$ with h being any function and $f(\theta)$ the distribution function generating the samples. Let $\theta_{1:n}$ represents samples from $f(\theta)$ then the empirical average of $h(\theta)$ is given by

$$\bar{h}_m = \frac{1}{m}\sum_{i=1}^{m} h(\theta_i) \tag{1.8}$$

by the strong law of large numbers see e.g. [11]

$$\bar{h}_m \to E_f[h(\Theta)], \quad \text{for } m \to \infty. \tag{1.9}$$

Assume that we are interested in estimating $P(\Theta \in A)$ based on the samples $\theta_{1:m}$ generated from $f(\theta)$, this can be obtained from

$$\hat{P}(\Theta \in A) = \frac{1}{m}\sum_{i=1}^{m} 1_A(\theta_i). \tag{1.10}$$

To be convinced about this first observe from (1.8) and (1.9) $\frac{1}{m}\sum_{i=1}^{m} 1_A(\theta_i) \to E_f[1_A(\Theta)], \quad \text{for } m \to \infty$. Next rewrite $E_f[1_A(\Theta)]$

$$E_f[1_A(\Theta)] = \int 1_A(\theta) f(\theta) d\theta = \int_A f(\theta) d\theta = P(\Theta \in A).$$

In other words based on $\pi_u(\theta|x_{1:n})$ Monte Carlo simulation can be applied to estimate $\pi(\theta|x_{1:n})$ if it is possible to construct algorithms which samples from $\pi(\theta|x_{1:n})$.

1.1.1 The Accept-Reject algorithm

Probably the simplest conceptual way of sampling from $\pi(\theta|x_{1:n})$ through an expression of $\pi_u(\theta|x_{1:n})$ is the Accept-Reject algorithm 1. More generally stated Algorithm 1 enables one to sample from any un-normalized probability density $f(\theta)$ through a *proposal* distribution $g(\theta)$, given that a constant M exists such that $M > \frac{f(\theta)}{g(\theta)}, \quad \forall \theta \in \Omega_\theta$.

Algorithm 1 Accept-Reject.

Require: $\exists M$ such that $M > \frac{f(\theta)}{g(\theta)}, \quad \forall \theta \in \Omega_\theta$

1: **for** i from 1 to k **do**
2: Generate $\Theta^* \sim g$ and $U \sim U_{[0;1]}$
3: **if** $U < \frac{f(\Theta^*)}{Mg(\Theta^*)}$ **then**
4: $\Theta_i = \Theta^*$
5: **end if**
6: **end for**

Θ is distributed as the normalized f since

$$\begin{aligned} P(\Theta \le \theta) &= P(\Theta^* < \theta | U \le \frac{f(\Theta^*)}{Mg(\Theta^*)}) = \frac{P(\Theta^* < \theta, U \le \frac{f(\Theta^*)}{Mg(\Theta^*)})}{P(U \le \frac{f(\Theta^*)}{Mg(\Theta^*)})} \\ &= \frac{\int_{-\infty}^{\theta}\int_0^{\frac{f(\theta)}{Mg(\theta)}} dug(\theta)d\theta}{\int_{-\infty}^{\infty}\int_0^{\frac{f(\theta)}{Mg(\theta)}} dug(\theta)d\theta} = \frac{\int_{-\infty}^{\theta} f(\theta)d\theta}{\int_{-\infty}^{\infty} f(\theta)d\theta}. \end{aligned}$$

Algorithm 1 may seem to be a quite reasonable approach in general to sample from the normalized probability distribution in (1.7). However in practice the dimension of Ω_θ can be large and its structure complicated, making the search for a reasonable $g(\theta)$ and a sufficiently large M an inappropriate way to proceed. In practice an unsatisfying number of proposed samples are thrown away when the fraction $\frac{f(\theta)}{Mg(\theta)}$ in large parts of Ω_θ is very small. We illustrate the challenges one encounter when applying Algorithm 1 for even a simple example in practice by considering Example 3.

Example 3 (Example 1 continued) *The target distribution $\pi(\theta|x_{1:n})$, $\theta = (\mu_1, \mu_2)$ we determined up to a normalization constant in Example 1, (1.7).*

$$\pi_u(\mu_1, \mu_2|x_{1:n}) = \Big[\prod_{i=1}^{n}\{w_1\varphi(x_i;\mu_1,\sigma_1^2)+(1-w_1)\varphi(x_i;\mu_2,\sigma_2^2)\}\Big]\varphi(\mu_1;\alpha,\sigma^2)\varphi(\mu_2;\alpha,\sigma^2).$$

As pointed out several times $\pi_u(\mu_1, \mu_2|x_{1:n})$ is not a distribution function since $\int_{\Omega_\theta}\pi_u(\mu_1, \mu_2|x_{1:n})d\theta \neq 1$. We apply Algorithm 1 to sample from $\pi(\mu_1, \mu_2|x_{1:n})$. Hence an appropriate $g(\theta)$ has to be specified and a value of M determined. The $g(\theta)$ function is almost free to choose as long as $\exists M$ such that $M > \frac{\pi_u(\theta|x_{1:n})}{g(\theta)}$, $\forall\theta \in \Omega_\theta$, choose $g(\mu_1) = \varphi(\mu_1;\alpha,\sigma^*)$ and $g(\mu_2) = \varphi(\mu_2;\alpha,\sigma^*)$ to specify the proposal distribution, with appropriate choices of α and σ^*.

In Figure 1.4 (a) the contour plot of $\pi_u(\theta|x_{1:n})$ is presented. The additional plots present $\pi_u(\mu_1, \mu_2|x_{1:n})$ for the most critical μ_2, the value of $\mu_2 = k$ where $\frac{\pi_u(\mu_1,\mu_2=k|x_{1:n})}{g(\mu_1,\mu_2=k)}$ is largest for a certain μ_1. In (b) a sufficiently large M has not been applied, (c) M is too large, (d) a constant M has been chosen appropriately.

1.1.2 Markov chain

Another approach to sample from $\pi(\theta|x_{1:n})$ avoiding the difficulties of searching for an appropriate proposal distribution $g(\theta)$, satisfying $\exists M$ such that $M > \frac{f(\theta)}{g(\theta)}$, $\forall\theta \in \Omega_\theta$ and a sufficiently large M, is to construct a *Markov chain* $\{\theta_0, \Theta_1, \ldots, \Theta_N\}$, see Figure 1.5 which has $\pi(\theta|x_{1:n})$ as the stationary or invariant distribution.

The sequence $\{\theta_0, \Theta_1, \ldots, \Theta_N\}$ is a *Markov* chain if $P(\Theta_{i+1} \in B|\theta_0, \ldots, \theta_i) = P(\Theta_{i+1} \in B|\theta_i)$, $\forall i = 0, \ldots, N-1, \forall B$, see [18] for an introduction to Markov chain. We construct the sequence from an arbitrary starting point θ_0, Θ_1 is generated from the *transition kernel* $\mathcal{K}(\theta_0, \theta_1)$ and so forth. The transition kernel is a density function for all $\theta_i \in \Omega_\theta$, such that $P(\Theta_{i+1} \in B|\Theta_i = \theta_i) = \int_B \mathcal{K}(\theta_i, d\theta_{i+1}) = \int_B \mathcal{K}(\theta_i, \theta_{i+1})d\theta_{i+1}$, standard notation in many books for con-

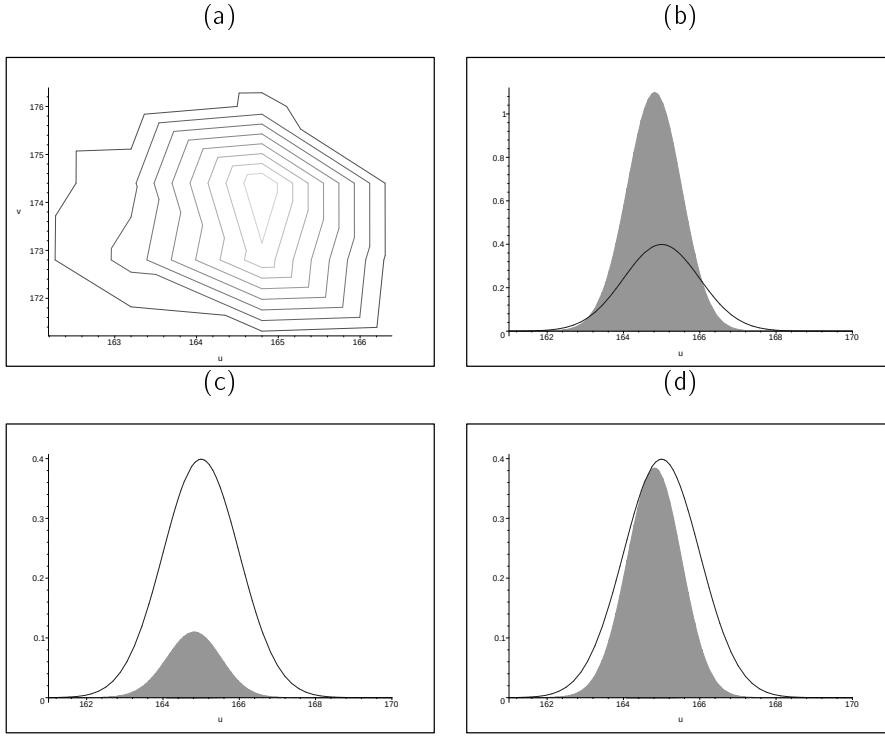

Figure 1.4: (a) contour plot of $\pi_u(\theta|x_{1:n})$. Plots of $\frac{\pi_u(\mu_1,\mu_2=k|x_{1:n})}{M}$ (filled) and $g(\mu_1)$ (black solid line) for different values of M.

tinuous state spaces, see e.g. [18] p. 235. Note that in general $P(\Theta_{i+1} \in B|\Theta_i = \theta_i)$ is not related to $\pi(\theta_i|x_{1:n})$.

If $\pi(\theta|x_{1:n})$ is the *stationary distribution* of the Markov chain and $\Theta_i \sim \pi(\theta|x_{1:n})$ then it implies that $\Theta_{i+1} \sim \pi(\theta|x_{1:n})$

$$\int_{\theta_i \in \Omega_\theta} \pi(\theta_i|x_{1:n})\mathcal{K}(\theta_i, \theta_{i+1})d\theta_i = \pi(\theta_{i+1}|x_{1:n}). \tag{1.11}$$

In other words when the chain has run for a "long" time such that $\Theta_i \sim \pi(\theta|x_{1:n})$ (loosely speaking the dependency on θ_0 is very small

$$P^j(\theta_0, \Theta_i \in A) = \int_{\Omega_\theta \otimes \cdots \otimes \Omega_\theta \otimes A} \mathcal{K}(\theta_0, \theta_1) \cdots \mathcal{K}(\theta_{i-1}, \theta_i)d\theta_1 \cdots d\theta_{i-1} \approx \int_A \pi(\theta|x_{1:n})d\theta,$$

geometric ergodicity see e.g. [18]), then $\Theta_{i+j} \sim \pi(\theta|x_{1:n})$, $j = 1, \ldots$, if $\mathcal{K}(\theta_i, \theta_{i+1})$ the transition kernel is chosen appropriately to fulfill (1.11).

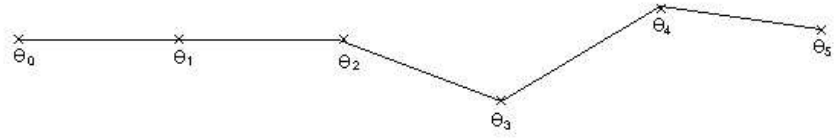

Figure 1.5: A Markov chain.

At first sight it may seem to be quite a task to construct such a transition kernel. This is however surprisingly simple with only few conditions to be satisfied.

We will assume that the transition kernel has been constructed in a reasonable way making it irreducible and aperiodic. Irreducibility loosely speaking means that all states communicates, such that in a finite number of steps there is a positive probability to go from any $\theta_i \in \Omega_\theta$ to any $\theta_{i+j} \subseteq \Omega_\theta$, $j = 1, \ldots$. Aperiodicity loosely speaking means that the chain has no deterministic repeating patterns. The fundamental condition is that of reversibility.

Definition 1.1 Reversibility (Detailed balance): A Markov chain with the transition kernel $\mathcal{K}(\theta_i, \theta_{i+1})$ is reversible w.r.t $\pi(\theta|x_{1:n})$ if

$$\pi(\theta_i|x_{1:n})\mathcal{K}(\theta_i, \theta_{i+1}) = \pi(\theta_{i+1}|x_{1:n})\mathcal{K}(\theta_{i+1}, \theta_i), \quad \forall \theta_i, \theta_{i+1} \in \Omega_\theta, \tag{1.12}$$

the definition from [18].

Lemma 1.2 *If a Markov chain is reversible w.r.t. $\pi(\theta|x_{1:n})$, then $\pi(\theta|x_{1:n})$ is the stationary distribution.*

Proof. For i "large" assume that $\pi(\theta|x_{1:n})$ is the stationary distribution of Θ_i, we will prove for a reversible chain that $\pi(\theta|x_{1:n})$ is the stationary distribution of Θ_{i+1}

$$\begin{aligned}
P(\Theta_{i+1} \in A) &= \int_A \int_{\Omega_\theta} \mathcal{K}(\theta_i, \theta_{i+1})\pi(\theta_i|x_{1:n})d\theta_i d\theta_{i+1} \\
&= \int_A \int_{\Omega_\theta} \mathcal{K}(\theta_{i+1}, \theta_i)\pi(\theta_{i+1}|x_{1:n})d\theta_i d\theta_{i+1} \\
&= \int_A \pi(\theta_{i+1}|x_{1:n}) \int_{\Omega_\theta} \mathcal{K}(\theta_{i+1}, \theta_i)d\theta_i d\theta_{i+1} \\
&= \int_A \pi(\theta_{i+1}|x_{1:n})d\theta_{i+1}.
\end{aligned}$$

The next section describes how it is possible to construct such a transition kernel in general which makes the chain reversible.

1.1.3 The Metropolis-Hastings algorithm

The Metropolis-Hastings Algorithm 2, see [18], starts in an arbitrary $\theta_0 \in \Omega_\theta$ then through a chosen *proposal distribution* $q(\theta|\theta_0)$ a new *candidate* Θ is generated. Θ is either included in the chain or thrown away depending on the acceptance ratio

$$\rho(\theta_0, \Theta) = \min\{\frac{\pi(\Theta|x_{1:n})q(\theta_0|\Theta)}{\pi(\theta_0|x_{1:n})q(\Theta|\theta_0)}, 1\} \tag{1.13}$$

if the proposal is rejected the old θ_0 is used as the next state. For a short while consider a symmetric proposal $q(\theta|\theta_0) = q(\theta_0|\theta)$ e.g. $\Theta|\theta_0 \sim N(\theta_0, \sigma^2)$ in this case the expression of acceptance ratio reduces to the ratio between the posterior of Θ and the posterior of θ_0 $\min\{\frac{\pi(\theta|x_{1:n})}{\pi(\theta_0|x_{1:n})}, 1\}$. A proposal with a higher ratio $\frac{\pi(\theta|x_{1:n})}{\pi(\theta_0|x_{1:n})}$ than 1 will for sure be accepted while a proposal with smaller ratio with the probability $\frac{\pi(\theta|x_{1:n})}{\pi(\theta_0|x_{1:n})}$ might be accepted.

Note that the acceptance rate contains the term $\frac{\pi(\theta|x_{1:n})}{\pi(\theta_0|x_{1:n})}$ which obviously equals the ratio

$$\frac{\pi(\theta|x_{1:n})}{\pi(\theta_0|x_{1:n})} = \frac{\frac{\pi(\theta|x_{1:n})}{c}}{\frac{\pi(\theta_0|x_{1:n})}{c}} = \frac{\pi_u(\theta|x_{1:n})}{\pi_u(\theta_0|x_{1:n})},$$

hence evaluation of (1.13) is done through the un-normalized densities.

Algorithm 2 Metropolis-Hastings.

Require: Given θ_0
1: **for** i from 0 to N **do**
2: Generate $\Theta^* \sim q(\theta^*|\theta_i)$ and $U \sim U_{[0;1]}$
3: **if** $U < \min\{\frac{\pi(\Theta^*)q(\theta_i|\Theta^*)}{\pi(\theta_i|x_{1:n})q(\Theta^*|\theta_i)}, 1\}$ **then**
4: $\Theta_{i+1} = \Theta^*$
5: **else**
6: $\Theta_{i+1} = \theta_i$
7: **end if**
8: **end for**

Now we convince ourselves that the Metropolis-Hastings algorithm 2 is reversible w.r.t. $\pi(\theta|x_{1:n})$! Each new proposal θ_{1+i} is accepted with the probability $\rho(\theta_i, \theta_{i+1})$ (1.13)

and it is rejected with the probability $1 - \rho(\theta_i, \theta_{i+1})$ resulting in the expression of the transition kernel

$$\mathcal{K}(\theta_i, \theta_{i+1}) = \rho(\theta_i, \theta_{i+1}) q(\theta_{i+1}|\theta_i) + r(\theta_i)\delta_{\theta_i}(\theta_{i+1}). \tag{1.14}$$

with

$$r(\theta_i) = 1 - \int_{\Omega_\theta} \rho(\theta_i, \theta_{i+1}) q(\theta_{i+1}|\theta_i) d\theta_{i+1},$$

see [18] for a more detailed explanation of the expression of $r(\theta_i)$.

Lemma 1.3 *The transition kernel (1.14) for the Metropolis-Hastings algorithm is reversible w.r.t.* $\pi(\theta|x_{1:n})$.

Proof.To prove reversibility for the Metropolis-Hastings algorithm, the expression of (1.14) is inserted into (1.12), following the proof in [18] p. 235,

$$\begin{aligned} & (\rho(\theta_i, \theta_{i+1}) q(\theta_{i+1}|\theta_i) + r(\theta_i)\delta_{\theta_i}(\theta_{i+1}))\pi(\theta_i|x_{1:n}) \qquad (1.15) \\ = \; & (\rho(\theta_{i+1}, \theta_i) q(\theta_i|\theta_{i+1}) + r(\theta_{i+1})\delta_{\theta_{i+1}}(\theta_i))\pi(\theta_{i+1}|x_{1:n}) \quad \forall \theta_i, \theta_{i+1} \in \Omega_\theta \end{aligned}$$

we will split up the proof in two parts, and to simplify just prove the first part (1.16), for a demonstration of (1.17) see [18]. (1.15) is correct if

$$\begin{aligned} & \rho(\theta_i, \theta_{i+1}) q(\theta_{i+1}|\theta_i)\pi(\theta_i|x_{1:n}) \qquad (1.16) \\ = \; & \rho(\theta_{i+1}, \theta_i) q(\theta_i|\theta_{i+1})\pi(\theta_{i+1}|x_{1:n}) \quad \forall \theta_i, \theta_{i+1} \in \Omega_\theta \end{aligned}$$

and

$$\begin{aligned} & r(\theta_i)\delta_{\theta_i}(\theta_{i+1})\pi(\theta_i|x_{1:n}) \qquad (1.17) \\ = \; & r(\theta_{i+1})\delta_{\theta_{i+1}}(\theta_i)\pi(\theta_{i+1}|x_{1:n}) \quad \forall \theta_i, \theta_{i+1} \in \Omega_\theta. \end{aligned}$$

hold. Rewriting $\rho(\theta_i, \theta_{i+1}) q(\theta_{i+1}|\theta_i)\pi(\theta_i|x_{1:n})$ by inserting the expression of $\rho(\theta_i, \theta_{i+1})$ from (1.13) yields

$$\begin{aligned} & \pi(\theta_i|x_{1:n})\rho(\theta_i, \theta_{i+1}) q(\theta_{i+1}|\theta_i) \\ = \; & \pi(\theta_i|x_{1:n}) \min\{\frac{\pi(\theta_{i+1}|x_{1:n}) q(\theta_i|\theta_{i+1})}{\pi(\theta_i|x_{1:n}) q(\theta_{i+1}|\theta_i)}, 1\} q(\theta_{i+1}|\theta_i) \\ = \; & \min\{\pi(\theta_{i+1}|x_{1:n}) q(\theta_i|\theta_{i+1}), \pi(\theta_i|x_{1:n}) q(\theta_{i+1}|\theta_i)\} \\ = \; & \pi(\theta_{i+1}|x_{1:n}) \min\{1, \frac{\pi(\theta_i|x_{1:n}) q(\theta_{i+1}|\theta_i)}{\pi(\theta_{i+1}|x_{1:n}) q(\theta_i|\theta_{i+1})}\} q(\theta_i|\theta_{i+1}) \\ = \; & \pi(\theta_{i+1}|x_{1:n})\rho(\theta_{i+1}, \theta_i) q(\theta_i|\theta_{i+1}). \end{aligned}$$

Example 4 (Continuation of Example 3) *Consider the two-dimensional mixture model from Example 3, with the extension that the previously assumed known parameters σ_1^2, σ_2^2 and w_1 are unknown. Choose standard priors for $\theta = (\mu_1, \mu_2, \sigma_1^2, \sigma_2^2, w_1)$*

$$\begin{aligned} \mu_j|\sigma_j^2 &\sim N(\alpha, \sigma^2) \\ \sigma_j^2 &\sim IG(\beta, \gamma) \\ W_1 &\sim Be(1,1). \end{aligned}$$

These priors together with the likelihood expression in (1.6) specify $\pi(\theta|x_{1:n})$. To run the Algorithm 2 some proposal distributions $q(\theta_{i+1}|\theta_i)$ have to be chosen

$$\begin{aligned} \mu_j^{(i+1)}|\mu_j^{(i)} &\sim N(\mu_j^{(i)}, \sigma_\mu^2) \\ \sigma_j^{2^{(i+1)}}|\sigma_j^{2^{(i)}} &\sim \sigma_j^{2^{(i)}} + LN(0, \sigma_\sigma^2) \\ W_1^{(i+1)}|w_1^{(i)} &\sim w_1^{(i)} + LN(0, \sigma_{w_1}^2), \end{aligned}$$

and the expression of the acceptance rate in (1.13) is found

$$\rho(\theta^{(i)}, \theta^{(i+1)}) = min\{\frac{\pi_u(\theta^{(i+1)}|x_{1:n})q(\theta^{(i)}|\theta^{(i+1)})}{\pi_u(\theta^{(i)}|x_{1:n})q(\theta^{(i+1)}|\theta^{(i)})}, 1\}.$$

by inserting the expressions the of the proposal distributions and the un-normalized posterior distributions. Running the chain for a "long" time the samples $\theta^{(N-m:N)}$ from the posterior distribution are obtained.

From practical considerations the parameters $(\sigma_\mu^2, \sigma_\sigma^2, \sigma_{w_1}^2)$ have to be adjusted to obtain an acceptable acceptance rate, a rule of thumb is $\sim [.3; .7]$.

1.2 Label switching

Example 4 deals with sampling from the posterior distribution specified up to a normalization constant for a mixture model of two normal distributions through the Metropolis-Hastings algorithm. Imagine that based on the samples $\theta^{(1:m)}$ from (4) the aim is to estimate the marginal distributions of $\mu_1, \mu_2, \sigma_1^2, \ldots, w_1$,

by calculating the empirical marginal means as described in Subsection 1.1

$$\hat{P}(\mu_1 \in A) = \frac{1}{m}\sum_{i=1}^{m} 1_{\mu_1^{(i)} \in A} \tag{1.18}$$

$$\hat{P}(\mu_2 \in A) = \frac{1}{m}\sum_{i=1}^{m} 1_{\mu_2^{(i)} \in A} \tag{1.19}$$

$$\vdots \tag{1.20}$$

$$\hat{P}(w_1 \in A) = \frac{1}{m}\sum_{i=1}^{m} 1_{w_1^{(i)} \in A}. \tag{1.21}$$

However there is no guaranty that this strategy will work, since the posterior distribution is invariant under permutations of the variable labels

$$\pi(\mu_1, \mu_2, \sigma_1^2, \sigma_2^2, w_1) = \pi(\mu_2, \mu_1, \sigma_2^2, \sigma_1^2, 1 - w_1).$$

A situation where labels have been switched is illustrated in Figure 1.6 (b). This

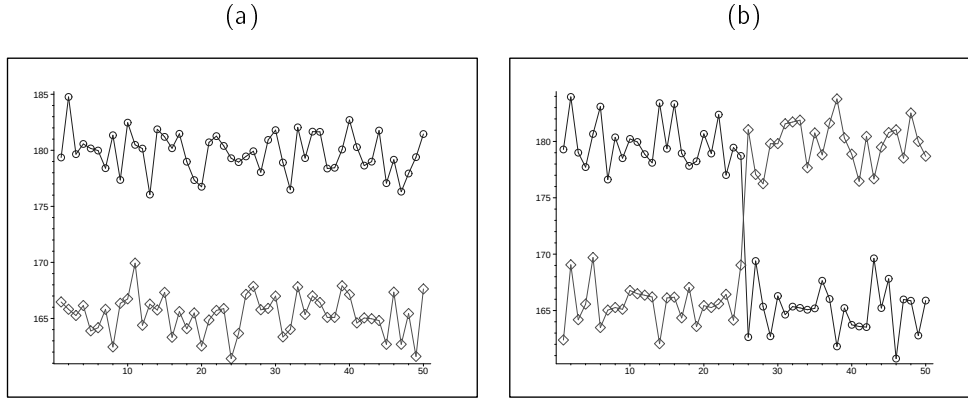

Figure 1.6: Samples $(\mu_1^{(1:m)}, \mu_2^{(1:m)})$ from a mixture model of two normal distributions described in Example 1, (1.6).

effect obviously results in unintended estimated values of the marginal distributions of $(\mu_1, \mu_2, \ldots, w_1)$ if (1.18) – (1.21) are used carelessly. In the next subsection this phenomenon is discussed in more details in a more general setup.

1.2.1 Mixture model of k components

In this subsection we will consider the k dimensional mixture model

$$X \sim p_1 f_1(x;\theta_1) + \cdots + p_k f_k(x;\theta_k),$$

and the problems related to sampling from the corresponding posterior distribution, specified through the model and some priors.

A pathological characteristic of this model class is that the likelihood is invariant under permutations of the variable labels

$$\begin{aligned} l(x_{1:n};\theta_1,\ldots,\theta_{k-1},\theta_k) &= l(x_{1:n};\theta_1,\ldots,\theta_k,\theta_{k-1}) \\ &\vdots \\ &= l(x_{1:n};\theta_k,\theta_{k-1},\ldots,\theta_1). \end{aligned}$$

For practical situations where the priors often are chosen indistinguishably $p_i(\theta_i) = p_j(\theta_j) \quad \forall i,j = 1,\ldots,k$, the posterior distribution is likewise invariant under permutations of the variable labels making the marginal distributions indistinguishable. Sampling from such distributions the labels can switch, a phenomenon referred to as *label switching*.

To avoid label switching we could introduce a truncated prior $p^{ic}(.)$ which breaks the symmetry of the posterior distribution and specifies a truncated posterior distribution

$$\pi^{ic}_{\theta_1,\ldots,\theta_k}(\theta|x_{1:n}) = \pi(\theta|x_{1:n}) 1_{\theta_1<\cdots<\theta_k}. \tag{1.22}$$

$1_{\theta_1<\cdots<\theta_k}$ indicates the indicator function which is 1 if $\theta_1 < \cdots < \theta_k$ and else 0, $\theta_1 < \cdots < \theta_k$ should be interpreted correctly (θ_j can be a vector) further described in Subsection 1.2.1.1.

Sampling from (1.22) can be carried out as previously described applying the Metropolis-Hastings algorithm, using some proposal distribution $q(.|\bar{\theta}^{(i)})$, where the bar indicates that $\bar{\theta}^{(i)}$ is a sample from the truncated posterior distribution, specified in (1.22). The proposal is accepted with the probability

$$\rho(\bar{\theta}^{(i)},\theta^{(i+1)}) = \min\{1, \frac{\pi^{ic}_{\theta_1,\ldots,\theta_k}(\theta^{(i+1)}|x_{1:n}) q(\bar{\theta}^{(i)}|\theta^{(i+1)})}{\pi^{ic}_{\theta_1,\ldots,\theta_k}(\bar{\theta}^{(i)}|x_{1:n}) q(\theta^{(i+1)}|\bar{\theta}^{(i)})}\}.$$

These steps are summed up in Algorithm 3. The problem with this approach is that $\pi^{ic}_{\theta_1,\ldots,\theta_k}(\theta^{(i+1)}|x_{1:n})$ is zero if the constraints $\theta_1 < \cdots < \theta_k$ do not hold.

Algorithm 3 Sampling from the truncated posterior distribution (the essential Metropolis-Hastings steps), (first approach).

1: Generate $\Theta^{(i+1)}|\bar{\theta}^{(i)}$ from $q(.|\bar{\theta}^{(i)})$, where e.g. $\bar{\theta}_1^{(i)} < \cdots < \bar{\theta}_k^{(i)}$.
2: Accept $\Theta^{(i+1)}$ with probability $\rho(\bar{\theta}^{(i)}, \Theta^{(i+1)}) = \min\{1, \frac{\pi^{ic}_{\theta_1,\ldots,\theta_k}(\Theta^{(i+1)}|x_{1:n})\, q(\bar{\theta}^{(i)}|\Theta^{(i+1)})}{\pi^{ic}_{\theta_1,\ldots,\theta_k}(\bar{\theta}^{(i)}|x_{1:n})\, q(\Theta^{(i+1)}|\bar{\theta}^{(i)})}\}$.
3: Note that $\Theta^{(i+1)}$ only can be accepted if it fulfills $\Theta_1^{(i+1)} < \cdots < \Theta_k^{(i+1)}$.

Hence the proposal is rejected if labels are switched, even though this proposal might have been accepted if labels had been reordered.

Second approach to sample from (1.22) is sketched by Algorithm 4. Applying

Algorithm 4 Reordering the proposal (the essential Metropolis-Hastings steps), (first improvement).

1: Generate $\Theta^{(i+1)}|\bar{\theta}^{(i)}$ from $q(.|\bar{\theta}^{(i)})$, where e.g. $\bar{\theta}_1^{(i)} < \cdots < \bar{\theta}_k^{(i)}$.
2: Reorder $\bar{\Theta}^{(i+1)} = \nu_j(\Theta^{(i+1)})$, such that $\bar{\Theta}_1^{(i+1)} < \cdots < \bar{\Theta}_k^{(i+1)}$.
3: Accept $\bar{\Theta}^{(i+1)}$ with probability $\rho(\bar{\theta}^{(i)}, \bar{\Theta}^{(i+1)}) = \min\{1, \frac{\pi^{ic}_{\bar{\Theta}^{(i+1)}}(\bar{\Theta}^{(i+1)}|x_{1:n})\, q(\bar{\theta}^{(i)}|\bar{\Theta}^{(i+1)})}{\pi^{ic}_{\bar{\Theta}^{(i+1)}}(\bar{\theta}^{(i)}|x_{1:n})\, q(\bar{\Theta}^{(i+1)}|\bar{\theta}^{(i)})}\}$.

Algorithm 4 the advantage is that the proposals are reordered through a reordering function $\nu_j(.)$, which permutes the indices of $\theta = (\theta_1, \ldots, \theta_k)$ such that the permuted $\bar{\theta} = (\theta_{\nu_j(1)}, \ldots, \theta_{\nu_j(k)})$ obeys a certain ordering $\theta_{\nu_j(1)} < \cdots < \theta_{\nu_j(k)}$.

Third approach, which is the one we used in our papers, samples from (1.22) are obtained by applying Algorithm 5. To understand why the reordered samples

Algorithm 5 Reordering the samples, after $\theta^{(N-m:N)}$ have been generated (the essential Metropolis-Hastings steps), (second improvement).

1: Generate $\Theta^{(i+1)}|\theta^{(i)}$ from $q(.|\theta^{(i)})$.
2: Accept $\Theta^{(i+1)}$ with probability $\rho(\theta^{(i)}, \Theta^{(i+1)}) = \min\{1, \frac{k!\,\pi(\Theta^{(i+1)}|x_{1:n})\, q(\theta^{(i)}|\Theta^{(i+1)})}{k!\,\pi(\theta^{(i)}|x_{1:n})\, q(\Theta^{(i+1)}|\theta^{(i)})}\}$.

from Algorithm 5 represent samples from (1.22) we first express the posterior

distribution $\pi(\theta|x_{1:n})$ in terms of $\pi^{ic}_{\theta_1,\ldots,\theta_k}(\theta|x_{1:n})$ for all the possible ordering of θ

$$\begin{aligned}
\pi(\theta|x_{1:n}) &= \frac{1}{k!}(\pi(\theta|x_{1:n},\nu_1(.)) + \cdots + \pi(\theta|x_{1:n},\nu_{k!}(.))) && (1.23)\\
&= \frac{1}{k!}(\pi(\theta|x_{1:n},\nu_1(.))1_{\nu_1(\theta_1)<\cdots<\nu_1(\theta_k)} + \cdots + \pi(\theta|x_{1:n},\nu_{k!}(.))1_{\nu_{k!}(\theta_1)<\cdots<\nu_{k!}(\theta_k)}) && (1.24)\\
&= \frac{1}{k!}(\pi^{ic}_{\theta_{\nu_1(1)},\ldots,\theta_{\nu_1(k)}}(\theta|x_{1:n}) + \cdots + \pi^{ic}_{\theta_{\nu_{k!}(1)},\ldots,\theta_{\nu_{k!}(k)}}(\theta|x_{1:n})). && (1.25)
\end{aligned}$$

(1.23) since $\pi(\theta|x_{1:n})$ is invariant under permutations of the variable labels, (1.24) since each term $\pi(\theta|x_{1:n},\nu_j(.))$ is unchanged multiplying with the corresponding identifiability constraints, (1.25) applying the definition of $\pi^{ic}_{\theta_{\nu_j(1)},\ldots,\theta_{\nu_j(k)}}(\theta|x_{1:n})$.

For a certain ordering of θ e.g. $\theta = (\theta_{\nu_j(1)},\ldots,\theta_{\nu_j(k)})$ such that $\theta_{\nu_j(1)} < \cdots < \theta_{\nu_j(k)}$, $\pi(\theta|x_{1:n},\nu_j(.))$ can be evaluated by inserting in (1.25)

$$\pi(\theta|x_{1:n},\nu_j(.)) = \frac{1}{k!}\pi^{ic}_{\theta_{\nu_j(1)},\ldots,\theta_{\nu_j(k)}}(\theta|x_{1:n})$$

since only one of the terms on the right hand side (1.25) will be different from 0, isolating $\pi^{ic}_{\theta_{\nu_j(1)},\ldots,\theta_{\nu_j(k)}}(\theta|x_{1:n})$ yields

$$\pi^{ic}_{\theta_{\nu_j(1)},\ldots,\theta_{\nu_j(k)}}(\theta|x_{1:n}) = k!\pi(\theta|x_{1:n},\nu_j(.))$$

The point is that $\pi^{ic}_{\theta_{\nu_j(1)},\ldots,\theta_{\nu_j(k)}}(\theta|x_{1:n})$ is expressed in terms $\pi(\theta|x_{1:n},\nu_j(.))$ and $\pi(\theta|x_{1:n},\nu_j(.))$ can be evaluated by $\pi(\theta|x_{1:n})$ since the posterior was invariant under any permutation permutation of the variable labels. Hence step 2 and step 3 in Algorithm 4 can be exchanged and as a consequence the reordering can be carried out after $\theta^{(N-m:N)}$ have been generated.

The reordering is in no way unique and has been considered by several authors see [17], [21] [20] [5] or [4]. In the next subsection different identifiability constraints are considered to obtain a certain ordering.

1.2.1.1 Identifiability constraints

In (1.26), (1.27) and (1.28) three possible identifiability constraints on subsets of $\theta^{(i)} = (\theta^{(i)}_1,\ldots,\theta^{(i)}_k)$, with $\theta^{(i)}_j = (w^{(i)}_j,\mu^{(i)}_j,\sigma^{2^{(i)}}_j)$ are presented

$$\mu^{(i)}_1 < \mu^{(i)}_2 < \cdots < \mu^{(i)}_k, \quad \forall i \qquad (1.26)$$

$$\sigma^{2^{(i)}}_1 < \sigma^{2^{(i)}}_2 < \cdots < \sigma^{2^{(i)}}_k, \quad \forall i \qquad (1.27)$$

$$w^{(i)}_1 < w^{(i)}_2 < \cdots < w^{(i)}_k, \quad \forall i. \qquad (1.28)$$

These identifiability constraints each in general leads to a different marginal distribution.

An alternative way of reordering the samples is by using a loss function based on e.g. Kullback-Leiber distances

$$\text{loss}(\theta, \hat{\theta}) = \int \log(\frac{\pi(\theta|x_{1:n})}{\pi(\hat{\theta})})\pi(\theta|x_{1:n})dx_{1:n}.$$

This identifiability constraint represents a global way of taking into account a weighted average of the ordering described in (1.26), (1.27) and (1.28), see I for a description of reordering using Kullback-Leiber distances.

To sum up: Before (not taking identifiability constraints into account) the acceptance rate in the Metropolis-Hastings algorithm was

$$\rho(\theta^{(i)}, \theta^{(i+1)}) = \min\{\frac{\pi_u(\theta^{(i+1)}|x_{1:n})q(\theta^{(i)}|\theta^{(i+1)})}{\pi_u(\theta^{(i)}|x_{1:n})q(\theta^{(i+1)}|\theta^{(i)})}, 1\}.$$

Introducing identifiability constraints through the truncated prior the new acceptance rate is

$$\rho(\theta^{(i)}, \theta^{(i+1)}) = \min\{\frac{l(x_{1:n}|\theta^{(i+1)})k!p(\theta^{(i+1)})q(\theta^{(i)}|\theta^{(i+1)})}{l(x_{1:n};\theta^{(i)})k!p(\theta^{(i)})q(\theta^{(i+1)}|\theta^{(i)})}, 1\}.$$

No matter which reordering one apply it is observed that for the mixture models a factor $k!$ is introduced in the expression of the posterior distribution. This factor has no influence when sampling from the models considered so fare since it is a common factor in the expression of the acceptance rate for the Metropolis-Hastings algorithm. However we have discussed the origin of this factor since it is crucial in the next section where jumps between different models will be allowed.

1.3 Reversible Jump MCMC

In Example 3 and Example 4 the dimension of θ was fixed for each sample and the target distribution contained in both cases a two-dimensional normal mixture model. Imagine for such a model that e.g. the Metropolis-Hastings algorithm has been applied to generate the samples $\theta^{(1:m)}$ based on a dataset represented by the histogram in Figure 1.7 (*a*). Then from the estimated posterior distribution the best model fit has been determined and plotted in Figure 1.7 (*a*). *But what if the number of things you do not know is one of the things you do not know? (Peter Green).* The reversible jump MCMC algorithm also referred to as the trans-dimensional MCMC or the Metropolis-Hastings-Green algorithm introduced in [9],

is a Markov chain methology which extends the Metropolis-Hastings algorithm to allow for varying dimension of θ. This is obtained by the construction of a reversible transition kernel on the state space $\bigcup_k \{k\} \times \Theta_k$, k is an indicator of the model, which has $\pi(\theta, k)$ as the stationary distribution. A brilliant idea which determines how well different models fit data, when it has been specified how to *jump* between $\pi(\theta|k)$ and $\pi(\theta'|k')$ for all $k, k' \in \bigcup_k \{k\}$. The *target* distribution $\pi(\theta, k)$ is easily expressed in terms of the conditional distribution $\pi(\theta|k)$ and the distribution of $\pi(k)$. Applying the reversible jump MCMC algorithm on e.g. a dataset represented by the histograms in Figure 1.7 (a) and (b) the reversible jump MCMC algorithm produces a $\pi(k)$ presented in Figure (c), from this Figure we observe that $k = 2$ and $k = 3$ describe data best. The best actual fits of $k = 2$ and $k = 3$ are presented in respectively Figure 1.7 (a) and (b). The list

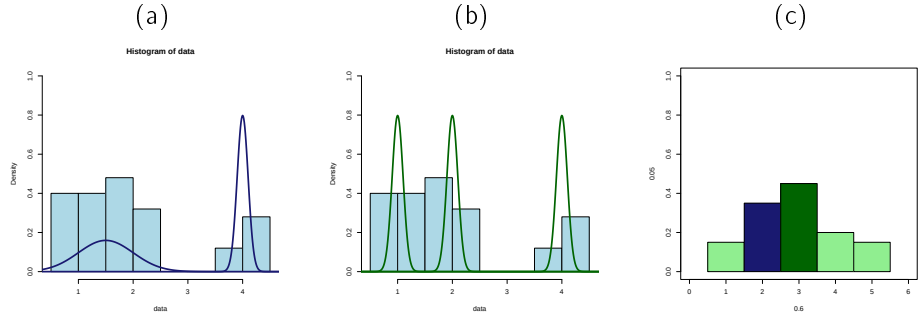

Figure 1.7: Histograms of data from a mixture model of normal distributions. In (a) a two-dimensional mixture model is fitted the data, In (b) a three-dimensional mixture model is fitted the data. Histogram (c) is a plot of $\pi(k)$, the posterior distribution of the model dimension.

of applications where the reversible jump MCMC algorithm successfully has been applied is long, among which we mention k-dimensional mixture models for Normal distributions [17], image analysis, exploring jumps for financial data, $ARMA(p, q)$ models with p and q unknown, structural conformations for ring molecules Paper I.

To be more specific the transition kernel from (1.14) in Subsection 1.1.2

$$\mathcal{K}(x, x') = \rho(x, x')q(x'|x) + r(x)\delta_x(x') \tag{1.29}$$

is constructed for $x = (k, \theta)$ and $x' = (k', \theta')$ where k and k' are allowed to be different, and $\mathcal{K}(x, x')$ is chosen appropriately to make the chain reversible w.r.t. $\pi(k, \theta)$

$$\pi(x)\mathcal{K}(x, x') = \pi(x')\mathcal{K}(x', x), \forall x, x'. \tag{1.30}$$

Readers are referred to [9] or [22] for a derivation of the reversible jump MCMC algorithm in a general setup. In the following the basic idea is sketched. As done

in Subsection 1.1.3 we will just consider

$$\rho(x, x^{'})q(x^{'}|x)\pi(x) = \rho(x^{'}, x)q(x|x^{'})\pi(x^{'}), \tag{1.31}$$

corresponding to a move to an other space which is accepted, what is missing to prove reversibility is

$$r(x)\delta_x(x^{'})\pi(x) = r(x^{'})\delta_{x^{'}}(x)\pi(x^{'}), \tag{1.32}$$

see [22]. Hence we will focus on finding the $\rho(x, x^{'})$ which satisfy

$$\pi(x)q(x^{'}|x)\rho(x, x^{'}) = \pi(x^{'})q(x|x^{'})\rho(x^{'}, x),\ \forall x, x^{'}. \tag{1.33}$$

As presented in various articles and books the reversibility criterion is alternatively presented as

$$\int_A\int_B \pi(x)q(x^{'}|x)\rho(x, x^{'})dxdx^{'} = \int_A\int_B \pi(x^{'})q(x|x^{'})\rho(x^{'}, x)dxdx^{'},\ \forall A, B, x \in B, x^{'} \in A, \tag{1.34}$$

A and B being any set. The complication is that $x^{'}$ is generated from x and u through a function $h_1 : \mathcal{R}^{d_k} \times \mathcal{R}^{d_u} \rightarrow \mathcal{R}^{d_{k'}}$ with U being a stochastic variable generated from a distribution with the probability density g. Denote P_k the probability of being in Θ_k and $P_{kk'}$ the probability of jumping from Θ_k to $\Theta_{k'}$ then

$$q(x^{'}|x) = g(.)P_{kk'}. \tag{1.35}$$

and $\pi(x)$ is expressed in terms of the conditional distribution of being in space k,

$$\pi(x) = \pi(.|k)P_k. \tag{1.36}$$

Generating x from $x^{'}$ we will do deterministically through the function $h_2 : \mathcal{R}^{d_{k'}} \rightarrow \mathcal{R}^{d_k}$, let respectively $P_{k'k}$ and $P_{k'}$ represent the probability of jumping from $\Theta_{k'}$ to Θ_k and the probability of being in $P_{k'}$, $q(x|x^{'})dx$ is then expressed as

$$q(x|x^{'}) = P_{k'k}, \tag{1.37}$$

the expression of $\pi(x^{'})$ is expressed in terms of the conditional distribution of being in space $k^{'}$

$$\pi(x^{'}) = \pi(.|k^{'})P_{k'}. \tag{1.38}$$

See Figure 1.8 for an illustration. It has been assumed that the transformation from (x, u) to $x^{'}$ is a diffeomorphism and that the dimension of u is chosen such that $d_k + d_u = d_{k'}$ (referred to as dimension matching). Inserting (1.35), (1.36), (1.37) and (1.38) in (1.34) yields

$$\int\int \pi(\theta|k)g(u)P_{kk'}P_k\rho(x, x^{'})d\theta du = \int \pi(\theta^{'}|k^{'})P_{k'k}P_{k'}\rho(x^{'}, x)d\theta^{'} \tag{1.39}$$

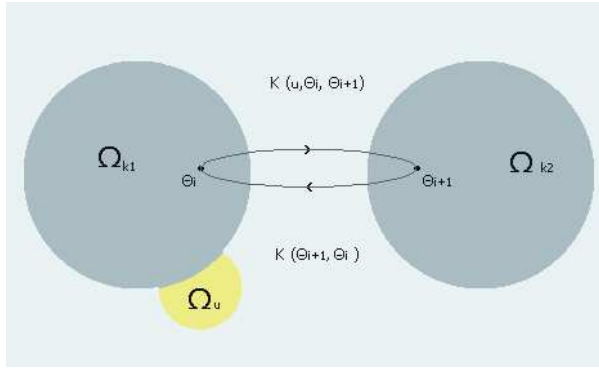

Figure 1.8: Jumps between Θ_k and $\Theta_{k'}$ by introducing a $u \in \Omega_u$.

changing the variable $d\theta'$ through the jacobian reduces (1.39) to

$$\int\int \pi(\theta|k)g(u)P_{kk'}P_k\rho(x,x')d\theta du = \int\int \pi(\theta'|k')P_{k'k}P_{k'}|\frac{\partial\theta'}{\partial(\theta,u)}|\rho(x',x)d\theta du. \tag{1.40}$$

equating the two integrands one realize, analogically to the derivation in Subsection 1.1.3 that the expression

$$\rho(x,x') = \min\{1, \frac{\pi(\theta'|k')P_{k'k}P_{k'}}{\pi(\theta|k)g(u)P_{kk'}P_k}|\frac{\partial\theta'}{\partial(\theta,u)}|\} \tag{1.41}$$

makes (1.40) true for all x and x'.

The jump types, (how to propose (k',θ') in (k,θ) through transformations h_1 and h_2) are in no way unique, among the most commonly mentioned are *birth/death* moves and *split/merge* moves. In general depending on the structure of the state space certain appropriate jumps will exist making the chain converge more or less rapidly. Let us see how the methology apply on a mixture model of normal distributions. For this model the simplest possible jumps *birth/death* are considered, see [17] for a derivation also considering the *split/merge* moves. The presentation is limited to these jump types since the *birth/death* move was the one used in our application. Note Actually the *split/merge* moves were implemented as well but it turned out that is was very difficult to get reasonable acceptance rates for these move types.

1.3.1 Continuation of Example 4

The ordinary Metropolis-Hastings algorithm cannot be applied when the dimension of θ, d_k is unknown. To illustrate the reversible jump MCMC algorithm we will apply the methology for a k-dimensional mixture model of normal distributions where k is unknown, see [3] for details describing the split/merge moves.

From the model the expression of the likelihood is found:

$$l(y_{1:n}|\theta_k) = \prod_{i=1}^{n}\sum_{j=1}^{k} \frac{w_j}{\sqrt{2\pi\nu_j}} \exp[-\frac{(y_i-\mu_j)^2}{2\nu_j}]$$

with

$$\theta_k = \{w_{1:k}, \mu_{1:k}, \nu_{1:k}\}.$$

Let the priors be

$$\begin{aligned} K &\sim U_{\{1,\ldots,M\}} \\ W_{1:k} &\sim D_{\{1,\ldots,1\}} \\ \mu_{1:k} &\sim N(0,\kappa) \\ \nu_{1:k} &\sim IG(\alpha,\beta). \end{aligned}$$

From the likelihood and the expressions of the priors $\pi(x)$ and $\pi(x')$ in (1.41) are determined.

To determine $|\frac{\partial\theta'}{\partial(\theta,u)}|$ and $g(u)$, assume that the current state is $x = (k, \theta_k)$ and the chain moves to a space $x' = (k+1, \theta_{k+1})$ with the dimension $d_{k+1} - d_k = 3$ larger constructed in the simplest possible way through a *birth* move. First $g(u)$ is chosen in an intelligent way to make h_1 and h_2 as simple as possible. Choose $g(u) = g_1(u_1)g_2(u_2)g_3(u_3)$ such that $U \sim g(u)$ with $U = (U_1, U_2, U_3)$

1. $U_1 \sim Be(1,k) \Leftrightarrow g_1(u_1) = k(1-u_1)^{k-1}1_{[0;1]}(u_1)$
2. $U_2 \sim N(0,\kappa)$
3. $U_3 \sim IG(\alpha,\beta)$.

Then define the function $h_1 : \mathcal{R}^{d_k} \times \mathcal{R}^{d_u} \to \mathcal{R}^{d_{k'}}$ by

$$\begin{aligned} w_j^{'} &= (1-u_1)w_j \text{ for } j = 1, \ldots, k \\ w_{k+1}^{'} &= u_1 \\ \mu_j^{'} &= \mu_j \text{ for } j = 1, \ldots, k \\ \mu_{k+1}^{'} &= u_2 \\ \nu_j^{'} &= \nu_j \text{ for } j = 1, \ldots, k \\ \nu_{k+1}^{'} &= u_3. \end{aligned}$$

Next $|\frac{\partial \theta_{k+1}^{'}}{\partial(\theta_k, u)}|$ is determined

$$|\frac{\partial \theta_{k+1}^{'}}{\partial(\theta_k, u)}| = \begin{vmatrix} \frac{\partial w_2^{'}}{\partial w_2} & \cdots & \frac{\partial w_2^{'}}{\partial w_k} & \frac{\partial w_2^{'}}{\partial u_1} \\ \vdots & \ddots & & \\ \frac{\partial w_k^{'}}{\partial w_2} & \cdots & \frac{\partial w_k^{'}}{\partial w_k} & \frac{\partial w_k^{'}}{\partial u_1} \\ \frac{\partial w_{k+1}^{'}}{\partial w_2} & \cdots & \frac{\partial w_{k+1}^{'}}{\partial w_k} & \frac{\partial w_{k+1}^{'}}{\partial u_1} \end{vmatrix} = \begin{vmatrix} (1-u_1) & \cdots & 0 & -w_2 \\ \vdots & \ddots & & \\ 0 & \cdots & (1-u_1) & -w_k \\ 0 & \cdots & 0 & 1 \end{vmatrix} =$$

to be $(1-u_1)^{k-1}$ since only $k-1$ free parameters exist in $w_{1:k}$. Inserting in (1.41) yields

$$\rho(x, x^{'}) = \min\{1, \frac{l(y_{1:n}|\theta_{k+1}^{'})p(\theta_{k+1}^{'})P_{k'k}P_{k'}(1-u_1)^{k-1}}{l(y_{1:n}|\theta_k)p(\theta_k)g_1(u_1)g_2(u_2)g_3(u_3)P_{kk'}P_k}\}, \tag{1.42}$$

next $\frac{p(\theta_{k+1}^{'})}{p(\theta_k)g_2(u_2)g_3(u_3)}$ is determined

$$\frac{p(\theta_{k+1}^{'})}{p(\theta_k)g_2(u_2)g_3(u_3)} = \frac{\frac{1}{k+1}}{\frac{1}{k}} = \frac{k}{k+1}, \tag{1.43}$$

(from the dirichlet priors) and (1.43) together with the expression of $g_1(u_1)$ is inserted in (1.42) resulting in

$$\rho(x, x^{'}) = \min\{1, \frac{l(y_{1:n}|\theta_{k+1}^{'})P_{k'k}}{l(y_{1:n}|\theta_k)(k+1)P_{kk'}}\}, \tag{1.44}$$

further simplifies to (taking into account the identifiability constraint which introduces a factor $(k+1)!$ in the numerator and a factor $k!$ in the denominator)

$$\rho(x, x^{'}) = \min\{1, \frac{l(y_{1:n}|\theta_{k'})P_{k'k}P_{k'}}{l(y_{1:n}|\theta_k)P_{kk'}P_k}\} = \min\{1, A\}, \tag{1.45}$$

when imposing some identifiability constraints on the sampling algorithm as considered in Section 1.2.1.1. Through almost identical calculations the expression of the death move results in an expression of the acceptance rate which is $\rho(x, x^{'}) = \min\{1, \frac{1}{A}\}$.

1.4 Sampling with restrictions

This section is meant as an appetizer to sampling with restrictions applied in the Papers I, II, III and IV, further described in Paper I. The idea is to utilize the geometry of a certain structure, combined with a set of restrictions assumed fulfilled when sampling. For the application in the papers the ring molecules have a rather complicated three-dimensional shape, making the presentation of the basic idea more involved, hence the idea is now motivated through a simple toy example.

Imagine that some measurements of the angles in a triangle are available $b_{1:3}^{(1:n)}$ and based on this data, a statistical model for the observations and specified priors for the parameters $\mu_{1:3}$ in the model, we want to sample from the posterior distribution of $\mu_{1:3}$, see Section 1.4.1 for more details. The simplest way to do this not violating the geometry of the triangle, would be to generate μ_1 and μ_2 through some proposal distributions and calculate $\mu_3 = 180° - \mu_1 - \mu_2$. We will say that μ_3 has been generated through a function F-mapping, which in this case only utilizes that the sum of the angles should equal 180°.

In Section 1.4.2 we continue with this example, however we will extend the idea inspired by the applications in the papers, such that descriptive parameters for the triangle includes distances, this obviously makes the F-mapping more involved.

1.4.1 The Toy example

Assume that we are interested in determining the angles $\theta = (\mu_b^{123}, \mu_b^{231}, \mu_b^{312})$ in a triangle as illustrated in Figure 1.9, based on n measurements obtained with a certain precision $x_{1:n} = (b_{123}^{(1:n)}, b_{231}^{(1:n)}, b_{312}^{(1:n)})$. The notation $b_{123} = \angle P_1P_2P_3$, $b_{231} = \angle P_2P_3P_1$, $b_{312} = \angle P_3P_1P_2$, $d_{12} = |P_1P_2|$, $d_{23} = |P_2P_3|$ and $d_{31} = |P_3P_1|$ is used.

To do this we formulate a statistical model for the data and apply the Metropolis-Hastings algorithm to generate samples from the posterior distribution first without restrictions. Afterwards restrictions will be imposed on the sampling algorithm to demonstrate how the restrictions improve the algorithm. The restrictions we will impose on each sample straight away leads to the final result, which then may seem silly, the example is only meant as a toy example with no practical interest.

Assume that $x^{(i)} = (b_{123}^{(i)}, b_{231}^{(i)}, b_{312}^{(i)})$ is described by 3 independent normal distributions $b_j^{(i)} = N(\mu_b^j, \sigma_b^2)$ for $j = \{123, 231, 312\}$ and that the prior for $\theta = (\mu_b^{123}, \mu_b^{231}, \mu_b^{312})$ is i.i.d. with $\mu_b^j \sim U(0, 180)$ for $j = \{123, 231, 312\}$, σ_b^2 is

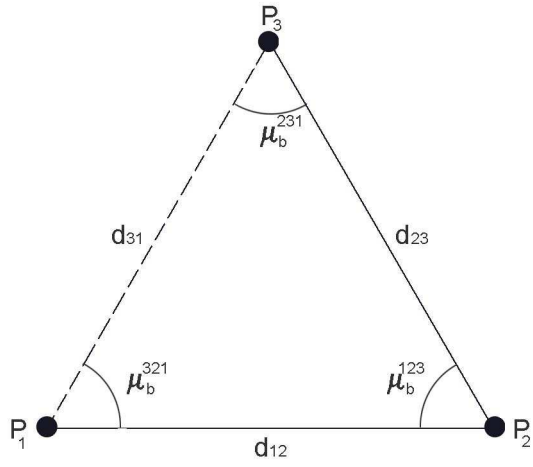

Figure 1.9: The triangular structure investigated by sampling with and without utilizing restrictions.

assumed known. To apply the Metropolis-Hastings algorithm we specify a proposal distribution, let $\mu_b^{j(i+1)}|\mu_b^{j(i)} \sim N(\mu_b^{j(i)}, \sigma_\Delta^2)$ for $j = \{123, 231, 312\}$. These simple choices of the proposal and prior distributions lead to an expression of the acceptance rate in the Metropolis-Hastings algorithm evaluated by the likelihood ratio

$$\rho(\theta^{(i)}, \Theta^{(i+1)}) = \min\{\frac{l(x_{1:n}; \Theta^{(i+1)})}{l(x_{1:n}; \theta^{(i)})}, 1\}.$$

The posterior distribution is illustrated for a dataset generated with $\mu_b^{123} = \mu_b^{231} = \mu_b^{312} = 60°$ and $\sigma_b^2 = 1$ in Figure 1.10 (b).

1.4.2 The Toy example, sampling with restrictions

Simulations with restrictions utilize the geometrical shape of the structure in combination with a subset of restrictions assumed fulfilled for each sample. From basic geometry it is well known that the sum of the angles in a triangle should equal 180°, which inspires us to do something more sophisticated than freely simulate the tree angles for each new proposal. Obviously many possible options exists to utilize the fact that the angle sum should equal 180°, we will use one inspired by the actual problem related to simulation of ring molecules. The subset of parameters best known for these structures are the distances between neighboring atoms

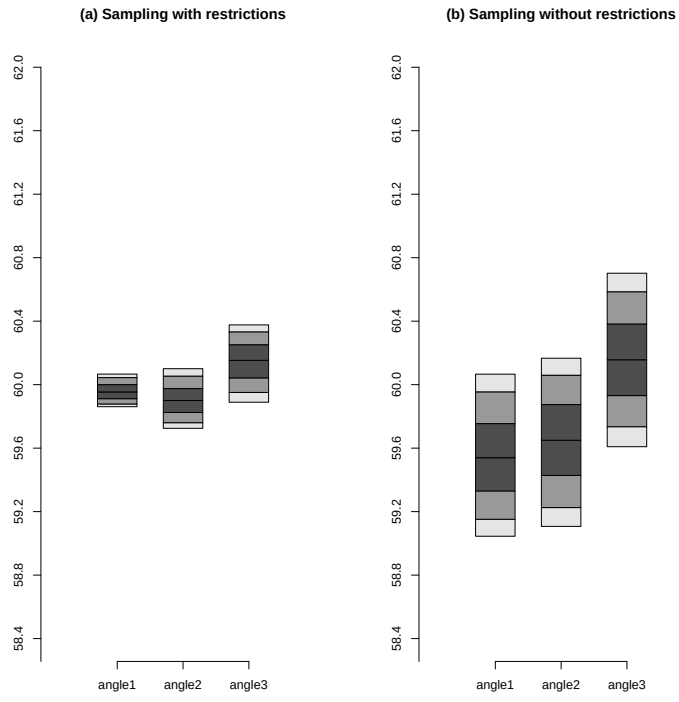

Figure 1.10: Posterior distribution of $\theta = (\mu_b^{123}, \mu_b^{231}, \mu_b^{312})$ the angles in a triangle. $x_{1:n}$ was generated from $N(60,1) \otimes N(60,1) \otimes N(60,1)$. Boxes in the figures refer to different confidence intervals in the posterior distributions. In plot (a) restrictions on $(\mu_d^{12}, \mu_d^{23}, \mu_d^{31})$ has been applied to improve the sampling of $(\mu_b^{123}, \mu_b^{231}, \mu_b^{312})$.

and bond angles for consecutive atoms in the chain, since the distances and the bond angles to some extend only depend on the actual atoms in the ring.

Introduce the parameter $\theta = (\mu_b^{123}, \mu_d^{12}, \mu_d^{23})$ which uniquely describes a triangle. Assume that μ_d^{12} and μ_d^{23} fulfill the restrictions

$$\mathfrak{R}(\theta; A_1, A_2) = \{ \ \mu_d^j \in A_j \text{ for } j = 1,2, \quad A_1 = A_2 = N(\mu_d, \sigma_d^2) 1_{[0.05;0.95]} \tag{1.46}$$

$(N(\mu_d, \sigma_d^2) 1_{[0.05;0.95]}$ refers to an interval specified by the 0.05 and 0.95 fractiles in a distribution with the mean μ_d and variance $\sigma_d^2)$. Through F-mapping $\bar{\theta} = (\bar{\mu}_b^{231}, \bar{\mu}_b^{312}, \bar{\mu}_d^{31})$ is determined by simple geometry $(\bar{\mu}_d^{31}, \bar{\mu}_b^{231}, \bar{\mu}_b^{312}) = \text{F-mapping}(\theta)$

with

$$\bar{\mu}_d^{31} = \sqrt{(\mu_d^{12})^2 + (\mu_d^{23})^2 - 2\mu_d^{12}\mu_d^{23} cos(\mu_b^{123})} \quad (1.47)$$

$$\bar{\mu}_b^{231} = sin^{-1}(\frac{\mu_d^{12} sin(\mu_b^{123})}{\mu_d^{13}}) \quad (1.48)$$

$$\bar{\mu}_b^{312} = 180 - \mu_b^{123} - \bar{\mu}_b^{231} \quad (1.49)$$

Assume further that $\bar{\theta}$ fulfills (1.50)

$$\Re(\bar{\theta}; A_3) = \{\ \bar{\mu}_d^3 \in A_3, \quad A_3 = N(\mu_d, \sigma_d^2)1_{[0.05;0.95]} \quad (1.50)$$

The proposal $\Theta^{(i+1)}$ is generated as described by the steps in Algorithm 6

Algorithm 6 Triangles example: Generating a proposal fulfilling some restrictions.

Require: A sample $\theta^{(i)}$ fulfilling $\mathcal{R}(\theta^{(i)}; A_1, A_2)$ and $\mathcal{R}(\bar{\theta}^{(i)}; A_3)$

1: **repeat**

2: Sample:

$$\mu_d^{12^{(i+1)}} | \mu_d^{12^{(i)}} \sim N(\mu_d^{12^{(i)}}, \sigma_{\epsilon_d}^2)1_{N(\mu_d^{12}, \sigma_{\epsilon_d}^2)_{[0.05;0.95]}}$$

$$\mu_d^{23^{(i+1)}} | \mu_d^{23^{(i)}} \sim N(\mu_d^{23^{(i)}}, \sigma_{\epsilon_d}^2)1_{N(\mu_d^{23}, \sigma_{\epsilon_d}^2)_{[0.05;0.95]}}$$

$$\mu_b^{123^{(i+1)}} | \mu_b^{123^{(i)}} \sim N(\mu_b^{123^{(i)}}, \sigma_{\epsilon_b}^2)$$

3: Calculate: $\mu_d^{31^{(i+1)}}, \mu_b^{231^{(i+1)}}$ and $\mu_b^{312^{(i+1)}}$ by F-mapping specified by (1.47)-(1.49).

4: **until** $\mu_d^{31^{(i+1)}} \sim N(\mu_d^{31}, \sigma_{\epsilon_d}^2)1_{[0.05;0.95]}$

The whole sampling sweep is presented in Algorithm 7

Applying the Metropolis-Hastings algorithm on a simulated data resulted in Figure 1.10 (*b*). Imposing the restrictions that each sample $(\mu_d^{12^{(i)}}, \mu_d^{23^{(i)}}, \mu_d^{31^{(i)}})$ should fulfill (1.46) and (1.50) with $\mu_d = 1$ and $\sigma_d^2 = .001$ applying Algorithm 7 resulted in Figure 1.10 (*a*). Obviously applying the restrictions resulted in a posterior distribution of θ with the most likely values of $(\mu_b^{123}, \mu_b^{231}, \mu_b^{312})$ being closer to the true values used to generate the dataset, since the restrictions on $(\mu_d^{12}, \mu_d^{23}, \mu_d^{31})$ only allow triangles with $\mu_b^{123} \approx \mu_b^{231} \approx \mu_b^{312}$.

Algorithm 7 Toy example: The Metropolis-Hastings with F-mapping.

1: Generate $\Theta^{(i+1)}|\theta^{(i)}$ from Algorithm 6 and $U \sim U_{[0;1]}$.
2: **if** $U < \rho(\theta^{(i)}, \Theta^{(i+1)})$ **then**
3: Accept the candidate

$$\rho(\theta^{(i)}, \theta^{(i+1)}) = \frac{l(x_{1:n};\theta^{(i+1)})p(\theta^{(i+1)})q(\theta^{(i+1)}|\theta^{(i)})}{l(x_{1:n};\theta^{(i)})p(\theta^{(i)})q(\theta^{(i)}|\theta^{(i+1)})} = \frac{l(x_{1:n};\theta^{(i+1)})p(\theta^{(i+1)})}{l(x_{1:n};\theta^{(i)})p(\theta^{(i)})}$$

with

$$\begin{aligned}\frac{l(x_{1:n};\theta^{(i+1)})}{l(x_{1:n};\theta^{(i+1)})} &= \exp\{-\frac{1}{2\sigma_b^2}\Big[\sum_{j=1}^{n}(b_{123}^{(j)} - \mu_b^{123^{(i+1)}})^2 + \sum_{j=1}^{n}(b_{231}^{(i)} - \mu_b^{231^{(i+1)}})^2 \\ &\quad + \sum_{j=1}^{n}(b_{312}^{(j)} - \mu_b^{312^{(i+1)}})^2\Big] + \frac{1}{2\sigma_b^2}\Big[\sum_{j=1}^{n}(b_{123}^{(j)} - \mu_b^{123^{(i)}})^2 \\ &\quad + \sum_{j=1}^{n}(b_{231}^{(j)} - \mu_b^{231^{(i)}})^2 + \sum_{j=1}^{n}(b_{312}^{(j)} - \mu_b^{312^{(i)}})^2\Big]\}\end{aligned}$$

and

$$\begin{aligned}\frac{p(\theta^{(i+1)})}{p(\theta^{(i)})} &= \exp\{-\frac{1}{2\sigma_{\epsilon_d}^2}\Big[(\mu_d^{12^{(i+1)}} - \mu_d^{12})^2 + (\mu_d^{23^{(i+1)}} - \mu_d^{23})^2 + (\mu_d^{31^{(i+1)}} - \mu_d^{31})^2 \\ &\quad -(\mu_d^{12^{(i)}} - \mu_d^{12})^2 - (\mu_d^{23^{(i+1)}} - \mu_d^{23})^2 - (\mu_d^{31^{(i+1)}} - \mu_d^{31})^2\Big]\}\end{aligned}$$

4: **else**
5: $\Theta^{(i+1)} = \theta^{(i)}$
6: **end if**

Chapter 2

Estimating Functions for Diffusions

This chapter motivates the work in Paper V and VI. We define and illustrate basic concepts used in these articles by applying the methology on simple examples. Further an introduction to basic terms assumed known will be presented.

Paper V describes a method to introduce prior knowledge in the *estimating function* $G(\theta; X_{t_0}, \ldots, X_{t_n})$, (introduced in Section 2.2, $G : \mathbb{R}^p \times E^{n+1} \to \mathbb{R}^p, \theta \in \Theta \subseteq \mathbb{R}^p$ and the state space of X_{t_i} is $E \subseteq \mathbb{R}$ for $i = 0, \ldots, n$). From $G(\theta; X_{t_0}, \ldots, X_{t_n})$ an estimator of θ is found by solving the *estimating equation* $G(\hat{\theta}; x_{t_0}, \ldots, x_{t_n}) = 0$. Estimating functions have turned out to be a convenient technique to easily derive estimators with good properties. The optimal $G(\theta; X_{t_0}, \ldots, X_{t_n})$, $G^*(\theta; X_{t_0}, \ldots, X_{t_n})$ is found by maximizing the correlation with the score function, see Section 2.2.3.

The prior knowledge is introduced in $G(\theta; X_{t_0}, \ldots, X_{t_n})$ through a function $f : \mathbb{R}^p \to \mathbb{R}^p$, which is allowed to be specified either through moment restrictions (eg. $E[\Theta] = m_1 \in \mathbb{R}^p$ and $Var[\Theta] = v_1 \in \mathbb{R}^p$) or through the prior distribution of $\Theta \sim p(\theta), p : \mathbb{R}^p \to \mathbb{R}^p$ $G(\theta; X_{t_0}, \ldots, X_{t_n}) + f(\theta)$. The optimal way of specifying $f^*(\theta)$ and $G^{**}(\theta; X_{t_0}, \ldots, X_{t_n})$ in this new class of estimating functions is obtained through a new optimality criterion imitating the posterior score function. What makes the method especially attractive from a practical point of view, is that the optimal $G^{**}(\theta; X_{t_0}, \ldots, X_{t_n})$ is identical to the optimal $G^*(\theta; X_{t_0}, \ldots, X_{t_n})$. The optimal $f^*(\theta)$ is found by maximizing the correlation with the prior distribution

of Θ. Hence the method can in practice be used in situations where the optimal estimation function has been found as an add-on utilizing the previously determined $G^*(\theta; X_{t_0}, \ldots, X_{t_n})$. The methology is especially well suited when prior information is available and only a limited number of observations are present, since in these cases it is well known that the optimal estimator derived from likelihood methods can result in poor estimators.

Paper VI formulates the estimation method proposed in [19] (Prediction based estimating functions) for measurement error models, where the process of interest X_t, described by (2.1), is indirectly observed through the measurement equation in (2.2)

$$\begin{aligned} dX_t &= a(X_t;\theta)dt + b(X_t;\theta)dW_t; \quad X_0 = x && (2.1)\\ Y_{t_i} &= h(X_{t_i}) + \varepsilon_{t_i}, && (2.2) \end{aligned}$$

with $a : E \times \Theta \mapsto \mathbb{R}$ and $b : E \times \Theta \mapsto \mathbb{R}$.

The general idea, here sketched in a simplified version, is to construct an estimating function

$$G(\theta; Y_{t_0}, \ldots, Y_{t_n}) = \sum_{i=0}^{n} g_i(Y_{t_0}, \ldots, Y_{t_i}; \theta), \tag{2.3}$$

where $g_i(Y_{t_0}, \ldots, Y_{t_i}; \theta)$ in $\mathbb{R}^p$ is constructed utilizing the fact that the projection error $f(Y_{t_i}) - (b_{i-1}(\theta)h_{i-1}(Y_{t_{i-1}}) + \cdots + b_0(\theta)h_0(Y_{t_0}) + a(\theta))$ is orthogonal to each of the elements in $\{1, h_{i-1}(Y_{t_{i-1}}), \ldots, h_0(Y_{t_0})\}$, where f, h_j, a and b_j take value in $\mathbb{R}$. The optimality criterion used to find $G^*(\theta; Y_{t_0}, \ldots, Y_{t_n})$ is further discussed in Section 2.2.3, the expression of $G^*(\theta; Y_{t_0}, \ldots, Y_{t_n})$ is presented in a more general setup in Paper VI.

Remember from classical statistics that the linear projection carried out to determine $a(\theta), b_0(\theta), \ldots, b_{i-1}(\theta)$ is expressed in terms of the conditional moments $E_\theta[f(Y_{t_i})|h_j(Y_{t_j})], j = 0, \ldots, i-1$ and $Var_\theta[f(Y_{t_i})|h_j(Y_{t_j})], j = 0, \ldots, i-1$, which through the measurement equation (2.2) are related to conditional moments of the process X_t. As a result an estimating function is build from the conditional moments of the process X_t evaluated at $(Y_{t_1}, \ldots, Y_{t_n})$.

For measurement error models a standard way within engineering to estimate the parameters is eg. through the extended Kalman filters, these filters can rather easily be applied in many setups, a drawback utilizing this methology however is that in general it is not easy to describe the statistical properties of the derived estimators. For a simple choice of the a and the b functions we compared the

estimators derived from the extended Kalman filter with the ones applying prediction based estimating functions through a small simulation study. We found for the CIR model that the extended Kalman filter performs almost as good as the estimating functions.

The diffusions represents a class of problems where likelihood theory is difficult to apply, since the transition distribution only rarely can be determined. However for many models it is possible to find expressions of the conditional moments and from these moments construct estimating equations which in a certain sense are optimal. Moreover under weak regularity conditions the obtained estimators are consistent.

Throughout the whole chapter the mathematical details will be omitted when they do not help to illustrate the general idea.

2.1 Stochastic differential equations

Introduce some randomness in the Ordinary differential equations (ODE) $\frac{dX_t(\omega)}{dt} = a(X_t(\omega);\theta)$ by

$$\frac{dX_t(\omega)}{dt} = a(X_t(\omega);\theta) + b(X_t(\omega);\theta)\xi_t(\omega). \tag{2.4}$$

Let the dependency of ω be understood implicitly, the functions a and b take values in $\mathbb{R}$. The noise term ξ_t is introduced through $\xi_t = "\frac{dW_t}{dt}"$ which inserted in (2.4) multiplying through by dt yields

$$dX_t = a(X_t;\theta)dt + b(X_t;\theta)dW_t. \tag{2.5}$$

Interpreted correctly (2.5) is a Stochastic Differential Equation (SDE). (2.5) in its integral form is

$$X_t = X_{t_0} + \int_{t_0}^{t} a(X_s;\theta)ds + \underbrace{\int_{t_0}^{t} b(X_s;\theta)dW_s}_{\text{Stochastic integral}}. \tag{2.6}$$

Now we will give some meaning to the symbols introduced by specifying the W_s process. Let W_s be a standard Wiener process with $W : [0;\infty[\to \mathbb{R}$ specified by

1. $W_{t_0} = 0$ with probability one (w.p.1)
2. $W_t - W_s \sim N(0, t-s)$

3. The increments $W_{t_1} - W_{t_0}, W_{t_2} - W_{t_1}, \ldots, W_{t_n} - W_{t_{n-1}}$ with $t_0 < t_1 < \cdots < t_n$ are independent

4. Sample path continuous.

Since the sample path of W_t is nowhere differentiable (2.5) and "$\frac{dW_t}{dt}$" do not make sense without the correct interpretation. The interpretation of (2.5) is supplied through the integral form (2.6). Note that the standard Wiener process does not have bounded variation

$$\sup \sum_{j=0}^{n-1} |W_{t_{j+1}} - W_{t_j}| = \infty, \text{ where the partitions are taking over any } [t_0; t_n].$$

Hence the stochastic integral in (2.6) is not a Riemann-Stieltjes integral.

Consider the integer $\int_{t_0}^{t_n} f(X_s, W_s) dW_s$, choosing the evaluation point $\tau_j \in]t_j; t_{j+1}]$ to be the starting point of each subinterval $\tau_j = t_j$ specifies a sum

$$\int_{t_0}^{t_n} f(X_s, W_s) dW_s = \underbrace{\lim}_{n \to \infty} \sum_{j=0}^{n-1} f(X_{t_j}, W_{t_j}) \{W(t_{j+1}) - W(t_j)\}, \tag{2.7}$$

which is the Itô integral of f w.r.t. the filtration generated by $W(t)$, where the limit is in L^2 of $p(t_{i+1} - t_i, x_{t_i}, x_{t_{i+1}}; \hat{\theta})$.

Implications of this formula is that the ordinary chain rule does not apply and evaluation of the Itô integral $\int_0^T f(X_s, W_s) dW_s$ is far more complicated than evaluation of ordinary Riemann-Stieltjes integrals. Note that e.g.

$$\int_0^T W_s dW_s = \frac{1}{2}(W_T^2 - T),$$

while

$$\int_0^T dW_s = W_T, \tag{2.8}$$

applying (2.7) evaluating the sums.

It can be shown that the chain rule for stochastic integrals, known as the Itô formula for a one-dimensional stochastic process takes the form

$$d\varphi(t, X_t) = [\frac{\partial \varphi}{\partial t} + a(X_t; \theta) \frac{\partial \varphi}{\partial x} + \frac{1}{2} b^2(X_t; \theta) \frac{\partial^2 \varphi}{\partial x^2}] dt + b(X_t; \theta) \frac{\partial \varphi}{\partial x} dW_t,$$

where X_t is described by (2.5) and φ is a function $[0; T] \times \mathbb{R} \to \mathbb{R}$ with partial derivatives $\frac{\partial \varphi}{\partial t}$, $\frac{\partial \varphi}{\partial x}$ and $\frac{\partial^2 \varphi}{\partial x^2}$.

Example 5 (The Geometric Brownian motion) *Consider the Geometric Brownian motion described by the stochastic differential equation*

$$dX_t = \mu X_t dt + \sigma X_t dW_t \tag{2.9}$$

used extensively in mathematical finance to model stock prices. To determine the process X_t (2.9) is transformed applying the Itô formula for $Y_t = \varphi(t, X_t) = \ln(X_t)$

$$dY_t = (\mu - \frac{1}{2}\sigma^2)dt + \sigma dW_t. \tag{2.10}$$

Finally Y_t is determined by writing (2.10) on integral form

$$\begin{aligned} Y_t &= Y_0 + \int_0^t (\mu - \frac{1}{2}\sigma^2)ds + \int_0^t \sigma dW_t \\ &= Y_0 + (\mu - \frac{1}{2}\sigma^2)t + \sigma W(t) \sim N(Y_0 + (\mu - \frac{1}{2}\sigma^2)t, \sigma^2 t). \end{aligned}$$

2.1.1 Likelihood inference for SDE´s

Assume that $p(t-s, x, y; \theta)$ is the transition density for the SDE specified by (2.5) with $\theta \in \Theta$ and $x, y \in E$. Ideally inference of θ is carried out through the likelihood function

$$l(x_{t_0}, \ldots, x_{t_n}; \theta) = \prod_{i=0}^{n-1} p(t_{i+1} - t_i, x_{t_i}, x_{t_{i+1}}; \theta), \tag{2.11}$$

based on a realization of the process $(x_{t_0}, \ldots, x_{t_n})$, since it holds under weak regularity conditions, that the maximum likelihood estimator is efficient.

The maximum likelihood estimator is found by introducing the score function $U(x_{t_0}, \ldots, x_{t_n}; \theta)$ as the partial derivative w.r.t. the parameter θ of the logarithm of the likelihood function and then solve

$$U(x_{t_0}, \ldots, x_{t_n}; \hat{\theta}) = \sum_{i=0}^{n-1} \partial_\theta \log(p(t_{i+1} - t_i, x_{t_i}, x_{t_{i+1}}; \hat{\theta})) = 0 \tag{2.12}$$

where $\partial_\theta f$ denotes $\partial_\theta f = (\frac{\partial f}{\partial_{\theta_1}}, \ldots, \frac{\partial f}{\partial_{\theta_p}})^T$ and T refers to transposition.

Unfortunately even for simple choices of the functions a and b in (2.5) no explicit expression exists of $p(t_{i+1} - t_i, x_{t_i}, x_{t_{i+1}}; \theta)$, which in general makes likelihood estimation a difficult approach to apply for diffusions.

Example 6 (Example 5 continued) *The solution to (2.9) was determined through the Itô formula and evaluation of the Itô integral* $\int_0^T dW(s)$ *postulated in (2.8) resulting in the expression of the transition distribution*

$$Y_{t_{i+1}}|y_{t_i} \sim N(y_{t_i} + (\mu - \frac{1}{2}\sigma^2)(t_{i+1} - t_i), \sigma^2(t_{i+1} - t_i)). \tag{2.13}$$

Assume that the measurements $(x_{t_0}, \ldots, x_{t_n})$ *are available and the model in (2.9) describes the data, further let* $\Delta_i = t_{i+1} - t_i$. *To estimate* $\theta = (\mu, \sigma^2)$ *(2.13) is inserted in the log likelihood function derived from (2.11)*

$$l(x_{t_0}, \ldots, x_{t_n}; \theta) = const - \frac{1}{2}\sum_{i=0}^{n-1} \log(\sigma^2) + \frac{(\log(x_{t_{i+1}}) - (\log(x_{t_i}) + (\mu - \frac{1}{2}\sigma^2)\Delta_i))^2}{\sigma^2\Delta_i}$$

(const represents a value not depending on parameter θ*), which inserted in (2.12) leads to a system of equations for* $(\hat{\mu}, \hat{\sigma^2})$

$$\begin{aligned} 0 &= \log(\frac{x_{t_n}}{x_{t_0}}) - (\hat{\mu} - \frac{1}{2}\hat{\sigma^2})(t_n - t_0) \\ 0 &= -n\hat{\sigma^2} - \hat{\sigma^2}\log(\frac{x_{t_n}}{x_{t_0}}) - (\hat{\mu} - \frac{1}{2}\hat{\sigma^2})(t_n - t_0) \\ &\quad + \sum_{i=0}^{n-1} \frac{\left[\log(x_{t_{i+1}}) - \log(x_{t_i}) - (\hat{\mu} - \frac{1}{2}\hat{\sigma^2})\Delta_i\right]^2}{\Delta_i}. \end{aligned}$$

2.2 Estimating Functions for SDE´s

Estimating functions represents an estimation technique constructed from some moments or some conditional moments of the process, the observations and the p-dimensional parameter $\theta \in \Theta$. The idea is that determination of these moments or conditional moments in general are far easier to compute than the transition distribution needed for the likelihood methology to work. General introduction to estimating function theory dates back to [6], see also [8, 10, 15].

Special attention has been devoted to the construction of martingale estimating functions due to the nice convergence results for martingales. martingale estimating functions from the linear family for discretely observed SDEs was considered in [1]. Requiring the estimating function to be a martingale implies that the asymptotic properties may be obtained without letting the time between measurements tend to zero. Unfortunately it also implies that the estimating functions involve conditional moments and that the optimal estimating functions involve derivatives

of these moments with respect to the parameters, which, most often, must be computed by simulation, see [14] for some approximate methods.

When the parameters of interest are only present in the diffusion term b, it can be recommendable to consider estimating functions involving higher order conditional moments. In [12] a class of simple estimating functions that provides explicit expressions for the estimators of the parameters in univariate SDEs is proposed. These estimating functions can only be used to estimate parameters appearing in the stationary density, because it is based on unconditional moments. However, the martingale property is lost and asymptotically efficient estimators are not available. In [13] another class of estimating functions that are based on eigenfunctions of the generator associated with the SDE is proposed, see also [2].

Let us start out quite generally by considering the estimating function $G : (X_{t_0}, \ldots, X_{t_n}; \theta) \mapsto G(X_{t_0}, \ldots, X_{t_n}; \theta) \subseteq \mathbb{R}^p$.

What structure to impose on G for stochastic differential equations specified by (2.5)?

Condition 1 (An unbiased estimating function) *$G(X_{t_0}, \ldots, X_{t_n}; \theta)$ should fulfill*

$$E_\theta[G(X_{t_0}, \ldots, X_{t_n}; \theta)] = 0.$$

We are able to identify the true value θ_0 of θ assuming

$$E_{\theta_0}[G(X_{t_0}, \ldots, X_{t_n}; \theta)] = 0 \text{ only when } \theta = \theta_0.$$

When the estimating function G has been fully specified the estimator of θ is found by solving the estimating equation

$$G(x_{t_0}, \ldots, x_{t_n}; \hat{\theta}) = 0. \tag{2.14}$$

Condition 1 ensures that in average (2.14) is fulfilled.

Condition 2 (Markov property of SDE´s) *$G(X_{t_0}, \ldots, X_{t_n}; \theta)$ is constructed such that $G(X_{t_0}, \ldots, X_{t_n}; \theta) = \sum_{i=0}^{n-1} g(X_{t_i}, X_{t_{i+1}}; \theta;)$ with g being an appropriate function $g : (X_{t_i}, X_{t_{i+1}}; \theta) \mapsto g(X_{t_i}, X_{t_{i+1}}; \theta) \subseteq \mathbb{R}^p$ to be specified.*

The diffusion process specified by (2.5) is a Markov process which implies that the likelihood function takes the form (2.11). When constructing estimating functions as an approximation to the score function, Condition 2 seems to be a reasonable function class to consider. Basically Condition 2 just says that since the score

function is constructed from the sum of $\partial_\theta \log(p(t_{i+1} - t_i, x_{t_i}, x_{t_{i+1}}; \hat{\theta}))$ the most obvious simplification would be to construct the estimating function as sums of $g(X_{t_i}, X_{t_{i+1}}; \theta)$ choosing g somehow to approximate $\partial_\theta \log(p(t_{i+1} - t_i, x_{t_i}, x_{t_{i+1}}; \hat{\theta}))$.

Choosing a specific functional form of the g function g_N specifies a certain class of estimating functions $\mathcal{G}_N$

$$\begin{aligned}\mathcal{G}_N \quad = \quad & \{G_N : (\theta; X_{t_0}, \ldots, X_{t_n}) \mapsto G_N(\theta; X_{t_0}, \ldots, X_{t_n}) \text{ s.t.} \\ & G_N(\theta; X_{t_0}, \ldots, X_{t_n}) = \sum_{i=0}^{n-1} g_N(X_{t_{i+1}}, X_{t_i}, \Delta_i; \theta) \text{ with} \\ & g_N(X_{t_{i+1}}, X_{t_i}, \Delta_i; \theta) = \sum_{j=1}^{N} \alpha_j(X_{t_i}, \Delta_i; \theta) h_j(X_{t_{i+1}}, X_{t_i}, \Delta_i; \theta), \ \forall\theta, \forall\Delta_i, \forall x\}.\end{aligned} \tag{2.15}$$

The h_j functions $h_j : (X_{t_i}, X_{t_{i+1}}; \theta) \mapsto h_j(X_{t_i}, X_{t_{i+1}}; \theta) \subseteq \mathbb{R}$ are chosen such that $E_\theta[h_j(X_{t_{i+1}}, \Delta_i; \theta)|X_{t_i}] = 0$ and $\alpha_j(X_{t_i}, \Delta_i; \theta) \in \mathbb{R}^p$. Estimating functions from $\mathcal{G}_N$ are martingales with respect to the filtration generated by the observations.

2.2.1 Relation between Least Square and Estimating Functions

For the well known least squares estimation technique, estimators are derived from minimization of a criterion function

$$S(\theta; X_{t_0}, \ldots, X_{t_n}) = \sum_{i=0}^{n-1} (X_{t_{i+1}} - E_\theta[X_{t_{i+1}}|X_{t_i}])^2,$$

through differentiating $S(\theta; X_{t_0}, \ldots, X_{t_n})$ w.r.t. θ and solving the estimating equation $\partial_\theta S(\theta; X_{t_0}, \ldots, X_{t_n}) = 0$. Note that $\partial_\theta S(\theta; X_{t_0}, \ldots, X_{t_n})$ corresponds to an estimating function fulfilling Condition 2 and Condition 1.

$$\frac{\partial S(\theta; X_{t_0}, \ldots, X_{t_n})}{\partial \theta} = -2 \sum_{i=0}^{n-1} \frac{\partial E_\theta[X_{t_{i+1}}|X_{t_i}]}{\partial \theta} (X_{t_{i+1}} - E_\theta[X_{t_{i+1}}|X_{t_i}]). \tag{2.16}$$

Observe that the estimating function $\partial_\theta S(\theta; X_{t_0}, \ldots, X_{t_n})$ is within the class $\mathcal{G}_1$ where $h_1(X_{t_{i+1}}, X_{t_i}; \theta) = (X_{t_{i+1}} - E_\theta[X_{t_{i+1}}|X_{t_i}])$ with $\alpha_1(X_{t_i}, \Delta_i; \theta) = \frac{\partial E_\theta[X_{t_{i+1}}|X_{t_i}]}{\partial \theta}$.

Example 7 (Estimating parameters in The Cox-Ingersoll-Ross process) *Consider the Cox-Ingersoll-Ross (CIR) process specified by the stochastic differential equation*

$$dX_t = \kappa(\varphi - X_t)dt + \sigma\sqrt{X_t}dW_t \tag{2.17}$$

where $\kappa > 0, \varphi > 0, \sigma^2 > 0$ *and* $\sigma^2 \leq 2\kappa\varphi$, *for simplicity assume that* σ^2 *is known. It can be shown that the conditional mean of this process is*

$$E_\theta[X_{t_{i+1}}|X_{t_i}] = X_{t_i}e^{-\kappa\Delta_i} + \varphi(1 - e^{-\kappa\Delta_i}) \tag{2.18}$$

with

$$\frac{\partial E_\theta[X_{t_{i+1}}|X_{t_i}]}{\partial\kappa} = -\Delta_i(X_{t_i} - \varphi)e^{-\kappa\Delta_i} \tag{2.19}$$

$$\frac{\partial E_\theta[X_{t_{i+1}}|X_{t_i}]}{\partial\varphi} = (1 - e^{-\kappa\Delta_i}). \tag{2.20}$$

Inserting (2.18), (2.19) and (2.20) in (2.16) results in the estimating equations from where $(\hat{\kappa}, \hat{\varphi})$ *can be found*

$$0 = -\sum_{i=0}^{n-1} \Delta_i(x_{t_i} - \hat{\varphi})e^{-\hat{\kappa}\Delta_i}(x_{t_{i+1}} - x_{t_i}e^{-\hat{\kappa}\Delta_i} + \hat{\varphi}(1 - e^{-\hat{\kappa}\Delta_i})) \tag{2.21}$$

$$0 = \sum_{i=0}^{n-1}(1 - e^{-\hat{\kappa}\Delta_i})(x_{t_{i+1}} - x_{t_i}e^{-\hat{\kappa}\Delta_i} + \hat{\varphi}(1 - e^{-\hat{\kappa}\Delta_i})). \tag{2.22}$$

2.2.2 The Linear and the Quadratic Estimating Functions

The simplest class of estimating functions we will consider is $\mathcal{G}_1$ with $h_1(X_{t_{i+1}}, X_{t_i}, \Delta_i; \theta) = (X_{t_{i+1}} - E_\theta[X_{t_{i+1}}|X_{t_i}])$, this class of estimating functions is referred to as linear estimating functions

$$G_1(\theta; X_{t_0}, \ldots, X_{t_n}) = \sum_{i=0}^{n-1} \alpha_1(X_{t_i}, \Delta_i; \theta)(X_{t_{i+1}} - E_\theta[X_{t_{i+1}}|X_{t_i}]). \tag{2.23}$$

The probably second most common estimating function is from $\mathcal{G}_2$ with $h_1(X_{t_{i+1}}, X_{t_i}, \Delta_i; \theta) = (X_{t_{i+1}} - E_\theta[X_{t_{i+1}}|X_{t_i}])$ and $h_2(X_{t_{i+1}}, X_{t_i}, \Delta_i; \theta) = ((X_{t_{i+1}} - E_\theta[X_{t_{i+1}}|X_{t_i}])^2 - Var_\theta[X_{t_{i+1}}|X_{t_i}])$ called the quadratic class of estimating functions

$$g(X_{t_i}, X_{t_{i+1}}; \theta) = \alpha(X_{t_i}, \Delta_i; \theta) \begin{bmatrix} X_{t_{i+1}} - E_\theta[X_{t_{i+1}}|X_{t_i}] \\ (X_{t_{i+1}} - E_\theta[X_{t_{i+1}}|X_{t_i}])^2 - Var_\theta[X_{t_{i+1}}|X_{t_i}] \end{bmatrix} \tag{2.24}$$

with $\alpha(X_{t_i}, \Delta_i; \theta) = [\alpha_1(X_{t_i}, \Delta_i; \theta), \alpha_2(X_{t_i}, \Delta_i; \theta)]$ which leads to the estimating function

$$\begin{aligned} G_2(\theta; X_{t_0}, \ldots, X_{t_n}) &= \sum_{i=0}^{n-1} \alpha_1(X_{t_i}, \Delta_i; \theta)(X_{t_{i+1}} - E_\theta[X_{t_{i+1}}|X_{t_i}]) \\ &\quad + \alpha_2(X_{t_i}, \Delta_i; \theta)((X_{t_{i+1}} - E_\theta[X_{t_{i+1}}|X_{t_i}])^2 - Var_\theta[X_{t_{i+1}}|X_{t_i}]). \end{aligned}$$

The estimating functions from $\mathcal{G}_1$ and $\mathcal{G}_2$ fulfill the Conditions 1 and 2. $\mathcal{G}_1$ is particularly interesting since it is the simplest class. While $\mathcal{G}_2$ is the simplest natural class to consider which enables estimation of parameters in both the a and the b function.

The topic of the next section is how to chose optimally the weights $\alpha_j(X_{t_i}, \Delta_i; \theta)$ within a certain class $\mathcal{G}_N$.

2.2.3 Optimal Estimating Functions

To start with assume that $p = 1$. As discussed in Section 2.2.1 the idea is to imitate the score function. Godambe introduced the fixed sample size optimality criterion (F-optimality) in [6]

Definition 2.1 The estimating function G_N^* is F-optimal in $\mathcal{G}_N$ if

$$\frac{E_\theta[G_N^2]}{E_\theta^2[\partial_\theta G_N]} \geq \frac{E_\theta[G_N^{*^2}]}{E_\theta^2[\partial_\theta G_N^*]} \tag{2.25}$$

for all $G_N \in \mathcal{G}_N$ and $\theta \in \Theta$, (G_N´s dependency on $(X_{t_0}, \ldots, X_{t_n}; \theta)$ has been dropped for convenience).

The motivation for the F-optimality criterion is that Definition 2.1 is equivalent to maximizing the correlation of G_N with the score function

$$Corr_\theta[U, G_N^*] > Corr_\theta[U, G_N], \forall \theta \in \Theta, \forall G_N \in \mathcal{G}_N, \tag{2.26}$$

which is straightforward to demonstrate. First convince yourselves that $E_\theta[U] = 0$

$$\begin{aligned} E_\theta[U] &= \int \frac{\partial_\theta f(x_{t_0}, \ldots, x_{t_n}; \theta)}{f(x_{t_0}, \ldots, x_{t_n}; \theta)} f(x_{t_0}, \ldots, x_{t_n}; \theta) \mu(dx_{t_1}, \ldots, dx_{t_n}) \\ &= \partial_\theta \int f(x_{t_0}, \ldots, x_{t_n}; \theta) \mu(dx_{t_1}, \ldots, dx_{t_n}) = 0 \end{aligned}$$

with $f(x_{t_0}, \ldots, x_{t_n}; \theta)$ being the density of $(X_{t_1}, \ldots, X_{t_n})$. (when integration and differentiation can be interchanged, assumed throughout this chapter).

Next considering estimating functions fulfilling Condition 1 ($E_\theta[G_N] = 0$).

$$\begin{aligned} Corr_\theta[U, G_N] &= \frac{Cov_\theta[U, G_N]}{\sqrt{Var_\theta[U] Var_\theta[G_N]}} = \frac{E_\theta[UG_N]}{\sqrt{E_\theta[U^2] E_\theta[G_N^2]}} \qquad (2.27) \\ E_\theta[UG_N] &= \int G_N \frac{\partial_\theta f(x_{t_0}, \ldots, x_{t_n}; \theta)}{f(x_{t_0}, \ldots, x_{t_n}; \theta)} f(x_{t_0}, \ldots, x_{t_n}; \theta) \mu(dx_{t_1}, \ldots, dx_{t_n}) \\ &= \underbrace{\partial_\theta E_\theta[G_N]}_{0} - \int \partial_\theta(G_N) f(x_{t_0}, \ldots, x_{t_n}; \theta) \mu(dx_{t_1}, \ldots, dx_{t_n}) \\ &= -E_\theta[\partial_\theta G_N]. \qquad (2.28) \end{aligned}$$

Inserting (2.28) in (2.27) implies that

$$Corr_\theta^2[U, G_N] = \frac{E_\theta^2[\partial_\theta G_N]}{E_\theta[G_N^2] E_\theta[U^2]}. \qquad (2.29)$$

Hence the estimating function $G_N \in \mathcal{G}_N$ which is most correlated with the score function is found be solving the inequality

$$\frac{E_\theta^2[\partial_\theta G_N^*]}{E_\theta[G_N^{*^2}]} > \frac{E_\theta^2[\partial_\theta G_N]}{E_\theta[G_N^2]},$$

equivalent to Definition 2.1.

2.2.3.1 Minimizing the L^2 distance to the score function

It turns out that the F-optimality criterion equivalently can be formulated as

$$E_\theta[(G_N - U)^2] \geq E_\theta[(G_N^* - U)^2], \forall G_N \in \mathcal{G}_N, \forall \theta \in \Theta \qquad (2.30)$$

see [7]. This variant of the F-optimality criterion also applies in the case where G_N is a p-dimensional estimating function. We will now show that the problem stated in (2.30) can be formulated as a Hilbert space minimization problem. Let $X \in \mathcal{X}$ and $Y \in \mathcal{Y}$ with $\mathcal{Y} \subseteq L^2$ and $\mathcal{X} \subseteq L^2$ ($E_\theta[X^2] < \infty$ and $E_\theta[Y^2] < \infty$) and $\mathcal{Y}$ is a linear subspace of $\mathcal{X}$. Define the inner product $< X, Y >= E_\theta[XY]$ and the norm $\|X\|^2 =< X, X >$. In this setting the minimization problem

$$\|X - Y^*\|^2 \leq \|X - Y\|^2 \quad , \forall Y \in \mathcal{Y} \qquad (2.31)$$

can be rewritten as

$$< X - Y^*, X - Y^* > \leq < X - Y, X - Y > \Leftrightarrow \quad (2.32)$$
$$E_\theta[(X - Y^*)(X - Y^*)^T] \leq E_\theta[(X - Y)(X - Y)^T]. \quad (2.33)$$

Hence if we are able to solve the minimization problem sketched in (2.31) the solution to (2.30) is readily found. The solution to (2.31) is well known to be found by making the projection error $X - Y^*$ orthogonal to the space spanning Y, see [11]. Hence, finding the F-optimal estimating function fulfilling Condition 1 and 2 is equivalent to solve

$$< U(\theta; X_{t_0}, \ldots, X_{t_n}) - G_N^*(\theta; X_{t_0}, \ldots, X_{t_n}), h_l(X_{t_{i+1}}, X_{t_i}; \theta) >= 0 \, \forall l, \forall \theta \in \Theta, \forall i = 0, \ldots, n-1. \quad (2.34)$$

When $X_{t_{i+1}}$ is a Markov process most of these terms are 0 simplifying (2.34) to

$$< \frac{\partial_{\theta_i} p(X_{t_{i+1}}, X_{t_i}; \theta)}{p(X_{t_{i+1}}, X_{t_i}; \theta)} - g_l^*(X_{t_{i+1}}, X_{t_i}; \theta), h_l(X_{t_{i+1}}, X_{t_i}; \theta) >= 0, \ \forall \theta \in \Theta, \forall l, \forall i \Leftrightarrow$$
$$< \frac{\partial_{\theta_i} p(X_{t_{i+1}}, X_{t_i}; \theta)}{p(X_{t_{i+1}}, X_{t_i}; \theta)}, h_l(X_{t_{i+1}}, X_{t_i}; \theta) >=$$
$$\sum_{j=1}^{N} \alpha_{lj}^*(X_{t_i}, \Delta_i; \theta) < h_j(X_{t_{i+1}}, X_{t_i}; \theta), h_l(X_{t_{i+1}}, X_{t_i}; \theta) >$$

($g_l^*(X_{t_{i+1}}, X_{t_i}; \theta)$ refers to the i'th element in
$g(X_{t_{i+1}}, X_{t_i}; \theta) = (g_1(X_{t_{i+1}}, X_{t_i}; \theta), \ldots, g_l(X_{t_{i+1}}, X_{t_i}; \theta), \ldots, g_p(X_{t_{i+1}}, X_{t_i}; \theta))^T$ and
$\alpha_{ij}^*(X_{t_i}, \Delta_i; \theta)$ refers to the i element in
$\alpha_j(X_{t_i}, \Delta_i; \theta) = (\alpha_{1j}(X_{t_i}, \Delta_i; \theta), \ldots, \alpha_{ij}(X_{t_i}, \Delta_i; \theta), \ldots \alpha_{pj}(X_{t_i}, \Delta_i; \theta))^T$). Now carrying out equivalent calculations as sketched in (2.28) $< \frac{\partial_{\theta_i} p(X_{t_{i+1}}, X_{t_i}; \theta)}{p(X_{t_{i+1}}, X_{t_i}; \theta)}, h_l(X_{t_{i+1}}, X_{t_i}; \theta) >=$
$\int_\Omega \frac{\partial_{\theta_i} p(X_{t_{i+1}}, X_{t_i}; \theta)}{p(X_{t_{i+1}}, X_{t_i}; \theta)} h_l(X_{t_{i+1}}, X_{t_i}; \theta) p(X_{t_{i+1}}, X_{t_i}; \theta) dx = -E_\theta[\partial_{\theta_i} h_l(X_{t_{i+1}}, X_{t_i}; \theta)]$, we ob-

tain

$$
\begin{aligned}
-E_\theta[\partial_{\theta_1} h_1(X_{t_{i+1}}, X_{t_i};\theta)] &= \alpha^*_{11}(X_{t_i},\Delta_i;\theta)E_\theta[h_1^2(X_{t_{i+1}}, X_{t_i};\theta)] + \cdots \\
&\quad +\alpha^*_{1N}(X_{t_i},\Delta_i;\theta)E_\theta[h_1(X_{t_{i+1}}, X_{t_i};\theta)h_N(X_{t_{i+1}}, X_{t_i};\theta)] \\
&\vdots \\
-E_\theta[\partial_{\theta_1} h_N(X_{t_{i+1}}, X_{t_i};\theta)] &= \alpha^*_{11}(X_{t_i},\Delta_i;\theta)E_\theta[h_N(X_{t_{i+1}}, X_{t_i};\theta)h_1(X_{t_{i+1}}, X_{t_i};\theta)] + \cdots \\
&\quad +\alpha^*_{1N}(X_{t_i},\Delta_i;\theta)E_\theta[h_N^2(X_{t_{i+1}}, X_{t_i};\theta)] \\
&\vdots \\
-E_\theta[\partial_{\theta_p} h_1(X_{t_{i+1}}, X_{t_i};\theta)] &= \alpha^*_{p1}(X_{t_i},\Delta_i;\theta)E_\theta[h_1^2(X_{t_{i+1}}, X_{t_i};\theta)] + \cdots \\
&\quad +\alpha^*_{pN}(X_{t_i},\Delta_i;\theta)E_\theta[h_1(X_{t_{i+1}}, X_{t_i};\theta)h_N(X_{t_{i+1}}, X_{t_i};\theta)] \\
&\vdots \\
-E_\theta[\partial_{\theta_p} h_N(X_{t_{i+1}}, X_{t_i};\theta)] &= \alpha^*_{p1}(X_{t_i},\Delta_i;\theta)E_\theta[h_N(X_{t_{i+1}}, X_{t_i};\theta)h_1(X_{t_{i+1}}, X_{t_i};\theta)] + \cdots \\
&\quad +\alpha^*_{pN}(X_{t_i},\Delta_i;\theta)E_\theta[h_N^2(X_{t_{i+1}}, X_{t_i};\theta)].
\end{aligned}
$$

Isolating $\begin{bmatrix} \alpha^*_1(X_{t_i},\Delta_i;\theta) \\ \vdots \\ \alpha^*_N(X_{t_i},\Delta_i;\theta) \end{bmatrix}^T$ yields

$$
\begin{bmatrix} \alpha^*_1(X_{t_i},\Delta_i;\theta) \\ \vdots \\ \alpha^*_N(X_{t_i},\Delta_i;\theta) \end{bmatrix}^T = -\begin{bmatrix} E_\theta[\partial_\theta h_1(X_{t_{i+1}}, X_{t_i};\theta)] \\ \vdots \\ E_\theta[\partial_\theta h_N(X_{t_{i+1}}, X_{t_i};\theta)] \end{bmatrix}^T
$$
$$
\begin{bmatrix} E_\theta[h_1^2(X_{t_{i+1}}, X_{t_i};\theta)] & \cdots & E_\theta[h_1(X_{t_{i+1}}, X_{t_i};\theta)h_N(X_{t_{i+1}}, X_{t_i};\theta)] \\ \vdots & \ddots & \vdots \\ E_\theta[h_N(X_{t_{i+1}}, X_{t_i};\theta)h_1(X_{t_{i+1}}, X_{t_i};\theta)] & \cdots & E_\theta[h_N^2(X_{t_{i+1}}, X_{t_i};\theta)] \end{bmatrix}^{-1} \quad (2.35)
$$

Hence the F-optimal estimating function is found by the orthogonal projection of U onto the space spanning G_N.

2.2.4 The optimal Linear and the Quadratic Estimating Functions

For the linear estimating function $G_1(\theta; X_{t_0}, \ldots, X_{t_n}) = \sum_{i=0}^{n-1} \alpha_1(X_{t_i};\theta)h_1(X_{t_{i+1}}, X_{t_i};\theta)$ where $h_1(X_{t_{i+1}}, X_{t_i};\theta) = (X_{t_{i+1}} - E_\theta[X_{t_{i+1}}|X_{t_i}])$, the optimal $\alpha^*_1(X_{t_i};\theta)$ is deter-

mined applying (2.35)

$$\alpha_1^*(X_{t_i};\theta) = -\frac{E_\theta[\partial_\theta(X_{t_{i+1}} - E_\theta[X_{t_{i+1}}|X_{t_i}])]}{E_\theta[(X_{t_{i+1}} - E_\theta[X_{t_{i+1}}|X_{t_i}])^2]} = \frac{\partial_\theta E_\theta[X_{t_{i+1}}|X_{t_i}]}{Var_\theta[X_{t_{i+1}}|X_{t_i}]},$$

leading to the expression

$$G_1^*(\theta; X_{t_0}, \ldots, X_{t_n}) = \sum_{i=0}^{n-1} \frac{\partial_\theta E_\theta[X_{t_{i+1}}|X_{t_i}]}{Var_\theta[X_{t_{i+1}}|X_{t_i}]}(X_{t_{i+1}} - E_\theta[X_{t_{i+1}}|X_{t_i}]). \tag{2.36}$$

In $\mathcal{G}_2$ the optimal quadratic estimating function specified by (2.24) equivalently is found by inserting in (2.35)

$$\begin{aligned}
\alpha^*(X_{t_i};\theta) &= -\begin{bmatrix} E_\theta[\partial_\theta(X_{t_{i+1}} - E_\theta[X_{t_{i+1}}|X_{t_i}])] \\ E_\theta[\partial_\theta((X_{t_{i+1}} - E_\theta[X_{t_{i+1}}|X_{t_i}])^2 - Var_\theta[X_{t_{i+1}}|X_{t_i}])] \end{bmatrix}^T \\
&\quad \begin{bmatrix} Var_\theta[X_{t_{i+1}}|X_{t_i}] & \eta(X_{t_i};\theta) \\ \eta(X_{t_i};\theta) & \psi(X_{t_i};\theta) \end{bmatrix}^{-1} \\
&= \frac{\begin{bmatrix} \partial_\theta E_\theta[X_{t_{i+1}}|X_{t_i}]) \\ \partial_\theta Var_\theta[X_{t_{i+1}}|X_{t_i}]) \end{bmatrix}^T \begin{bmatrix} \psi(X_{t_i};\theta) & -\eta(X_{t_i};\theta) \\ -\eta(X_{t_i};\theta) & Var_\theta[X_{t_{i+1}}|X_{t_i}] \end{bmatrix}}{Var_\theta[X_{t_{i+1}}|X_{t_i}]\psi(X_{t_i};\theta) - \eta^2(X_{t_i};\theta)} \Leftrightarrow \\
\alpha_1^*(X_{t_i};\theta) &= \frac{\partial_\theta E_\theta[X_{t_{i+1}}|X_{t_i}]\psi(X_{t_i};\theta) - \partial_\theta Var_\theta[X_{t_{i+1}}|X_{t_i}])\eta(X_{t_i};\theta)}{Var_\theta[X_{t_{i+1}}|X_{t_i}]\psi(X_{t_i};\theta) - \eta^2(X_{t_i};\theta)} \\
\alpha_2^*(X_{t_i};\theta) &= \frac{\partial_\theta Var_\theta[X_{t_{i+1}}|X_{t_i}]Var_\theta[X_{t_{i+1}}|X_{t_i}] - \partial_\theta E_\theta[X_{t_{i+1}}|X_{t_i}])\eta(X_{t_i};\theta)}{Var_\theta[X_{t_{i+1}}|X_{t_i}]\psi(X_{t_i};\theta) - \eta^2(X_{t_i};\theta)}
\end{aligned}$$

with

$$\begin{aligned}
\eta(X_{t_i};\theta) &= E_\theta[(X_{t_{i+1}} - E_\theta[X_{t_{i+1}}])((X_{t_{i+1}} - E_\theta[X_{t_{i+1}}|X_{t_i}])^2 - Var_\theta[X_{t_{i+1}}])|X_{t_{i+1}}] \\
\psi(X_{t_i};\theta) &= E_\theta[((X_{t_{i+1}} - E_\theta[X_{t_{i+1}}|X_{t_i}])^2 - Var_\theta[X_{t_{i+1}}])^2|X_{t_{i+1}}].
\end{aligned}$$

Example 8 (Example 7 continued) *We postulated that the conditional mean for the CIR process was given by (2.18) resulting in the expressions of the derivatives listed in (2.19) and (2.20). Similarly the conditional variance can be computed to be*

$$Var_\theta[X_{t_{i+1}}|X_{t_i}] = \frac{\sigma^2}{2\kappa}(1 - e^{-\kappa\Delta_i})(\varphi(1 - e^{-\kappa\Delta_i}) + 2X_{t_i}e^{-\kappa\Delta_i}). \tag{2.37}$$

Hence the optimal estimating function in $\mathcal{G}_1$, obtained by inserting in (2.36) results in the set of estimating equations (2.38) and (2.39) enabling one to estimate the parameters φ and κ is

$$0 = -\sum_{i=0}^{n-1} \frac{\Delta_i (x_{t_i} - \hat{\varphi}) e^{-\hat{\kappa}\Delta_i} (x_{t_{i+1}} - x_{t_i} e^{-\hat{\kappa}\Delta_i} + \hat{\varphi}(1 - e^{-\hat{\kappa}\Delta_i}))}{(1 - e^{-\hat{\kappa}\Delta_i})(\hat{\varphi}(1 - e^{-\hat{\kappa}\Delta_i}) + 2X_{t_i} e^{-\hat{\kappa}\Delta_i})} \tag{2.38}$$

$$0 = \sum_{i=0}^{n-1} \frac{(1 - e^{-\hat{\kappa}\Delta_i})(x_{t_{i+1}} - x_{t_i} e^{-\hat{\kappa}\Delta_i} + \hat{\varphi}(1 - e^{-\hat{\kappa}\Delta_i}))}{(1 - e^{-\hat{\kappa}\Delta_i})(\hat{\varphi}(1 - e^{-\hat{\kappa}\Delta_i}) + 2X_{t_i} e^{-\hat{\kappa}\Delta_i})}. \tag{2.39}$$

Observe that the set of equations in (2.38) and (2.39) to estimate (φ, κ) are different from the set of equations in (2.21) and (2.22), by simulation it can be shown that the derived estimators from (2.38) and (2.39) are more efficient.

Chapter 3

Acknowledgements

First I would like to thank my two supervisors Henrik Madsen and Mathieu Kessler, for the time and energy they have spent on helping me with the ph.d. project. Henrik Madsen has always supported and believed in me, also when I stubbornly followed my own ways at times contrary his advices. It takes quite a character to allow such an amount of flexibility. Giving me the room to try out my own ideas, does not mean that Henrik hasn't had a keen eye on the process. Further would I like to thank Henrik for finding funding for trips and conferences, during the time where little money was left on the ph.d. budget. Henrik has also given me opportunities to get more involved in the work at IMM, by letting me take part in various activities outside the ph.d. program, for which I am grateful. I would like to thank my Spanish supervisor and dear friend Mathieu Kessler, for his dedication to helping me with the thesis, for many interesting discussions, for his patience with my writing and for all the good time we have had together, the time in Cartagena will always remain sweet memories. It has been a pleasure to work with and learn from such an extraordinary brilliant warm-hearted person.

The list of people I further send my gratitude to includes Michael Stubert Berger for reading parts of the introduction, Paula Inés Aguirre Nolsøe for creating some of the graphics, the staff at IMM especially Rune Overgaard, Christoffer Tornøe and Lasse Christensen for all the good time we have had together. The faculty in Cartagena (Spain) (Juana mari Belchi, Marta Clemente, Juan Carlos Trillo, Sergio Amat, Sonia Busquier, David Javier López, Francisco Periago, Luis Angel Sánchez,

Pablo Carrillo, Manuel Calixto), for welcoming me with open arms, helping me with Spanish and spending time with me, making my stays in Cartagena a great pleasure. The faculty at UBA (Argentina) for interesting discussions, my friends and family for moral support and finally my lovely wife for her endless love and support.

References

[1] Bo Martin Bibby and Michael Sørensen. Martingale estimation functions for discretely observed diffusion processes. *Bernoulli*, 1(1-2):17–39, 1995.

[2] Bo Martin Bibby and Michael Sørensen. Simplified estimating functions for diffusion models with a high-dimensional parameter. *Scand. J. Statist.*, 28 (1):99–112, 2001.

[3] Olivier Cappé, Christian P. Robert, and Tobias Rydén. Manual for ctrjmix. Technical report, Département TSI, Ecole Nationale Supérieure des Télćommunications, 2003. http://www.tsi.enst.fr/~cappe/ctrj_mix/.

[4] Olivier Cappé, Eric Moulines, and Tobias Rydén. *?* Springer Texts in Statistics. Springer-Verlag, forthcoming, New York, 2005.

[5] G. Celeux. Bayesian inference for mixtures, the label-switching problem. In *COMPSTAT 1998*, pages 227–232. Physica, Heidelberg, 1998.

[6] V. P. Godambe. An optimum property of regular maximum likelihood estimation. *Ann. Math. Statist.*, 31:1208–1211, 1960.

[7] V. P. Godambe and C. C. Heyde. Quasi-likelihood and optimal estimation. *Internat. Statist. Rev.*, 55(3):231–244, 1987.

[8] V. P. Godambe and B. K. Kale. Estimating functions: an overview. In *Estimating functions*, volume 7 of *Oxford Statist. Sci. Ser.*, pages 3–20. Oxford Univ. Press, New York, 1991.

[9] Peter J. Green. Reversible jump Markov chain Monte Carlo computation and Bayesian model determination. *Biometrika*, 82(4):711–732, 1995.

[10] Christopher C. Heyde. *Quasi-likelihood and its application*. Springer Series in Statistics. Springer-Verlag, New York, 1997. A general approach to optimal parameter estimation.

[11] Jean Jacod and Philip Protter. *Probability essentials*. Springer, 2. ed. edition, 2003.

[12] Mathieu Kessler. Simple and explicit estimating functions for a discretely observed diffusion process. *Scand. J. Statist.*, 27(1):65–82, 2000.

[13] Mathieu Kessler and Michael Sørensen. Estimating equations based on eigenfunctions for a discretely observed diffusion process. *Bernoulli*, 5(2):299–314, 1999.

[14] P. E. Kloeden and E. Platen. Numerical methods for stochastic differential equations. In *Nonlinear dynamics and stochastic mechanics*, CRC Math. Model. Ser., pages 437–461. CRC, Boca Raton, FL, 1995.

[15] D. L. McLeish and Christopher G. Small. *The theory and applications of statistical inference functions*, volume 44 of *Lecture Notes in Statistics*. Springer-Verlag, New York, 1988.

[16] T.J. Meyer. Chemical approaches to artificial photosynthesis. *Acc. Chem. Res.*, 22:163–170, 1989.

[17] Sylvia Richardson and Peter J. Green. Corrigendum: "On Bayesian analysis of mixtures with an unknown number of components" [J. Roy. Statist. Soc. Ser. B **59** (1997), no. 4, 731–792]. *J. R. Stat. Soc. Ser. B Stat. Methodol.*, 60(3):661, 1998.

[18] Christian P. Robert and George Casella. *Monte Carlo statistical methods*. Springer Texts in Statistics. Springer-Verlag, New York, second edition, 2004.

[19] Michael Sørensen. Prediction-based estimating functions. *Econom. J.*, 3(2): 123–147, 2000.

[20] Matthew Stephens. Dealing with label switching in mixture models. *J. R. Stat. Soc. Ser. B Stat. Methodol.*, 62(4):795–809, 2000.

[21] Matthew Stephens. Bayesian analysis of mixture models with an unknown number of components—an alternative to reversible jump methods. *Ann. Statist.*, 28(1):40–74, 2000.

[22] Rasmus Waagepetersen and Daniel Sorensen. A tutorial on reversible jump MCMC with a view toward applications in QTL-mapping, 2000. URL `citeseer.ist.psu.edu/323227.html`.

[23] M. Zimmer. Molecular mechanics, data and conformational analysis of first-row transition metal complexes in the cambridge strutural database. *Coord. Chem. Rev.*, 212:133–163, 2001.

Papers

I

Paper I

Bayesian conformational analysis of ring molecules through reversible jump MCMC

Published in *Journal of Chemometrics*, **19**(8):412–426 (2005)

JOURNAL OF CHEMOMETRICS
J. Chemometrics in press
Published online in Wiley InterScience (www.interscience.wiley.com). DOI: 10.1002/cem.943

Bayesian conformational analysis of ring molecules through reversible jump MCMC

Kim Nolsøe[1], Mathieu Kessler[2]*, José Pérez[2] and Henrik Madsen[1]

[1]Informatics and Mathematical Modelling, Technical University of Denmark, Lyngby, Denmark
[2]Universidad Politécnica de Cartagena, Paseo Alfonso XII, Cartagena, España, Spain

Received 23 May 2005; Revised 11 August 2005; Accepted 30 September 2005

In this paper, we address the problem of classifying the conformations of *m*-membered rings using experimental observations obtained by crystal structure analysis. We formulate a model for the data generation mechanism that consists in a multidimensional mixture model. We perform inference for the proportions and the components in a Bayesian framework, implementing a Markov chain Monte Carlo (MCMC) reversible jump algorithm to obtain samples of the posterior distributions. The method is illustrated on a simulated data set and on real data corresponding to cyclo-octane structures. Copyright © 2005 John Wiley & Sons, Ltd.

KEYWORDS: cycloalcanes; reversible jump; conformational analysis; mixture model; MCMC

1. INTRODUCTION

For a given compound it is of interest to study what are the preferred geometrical conformations of the corresponding molecules. The conformational classification of structures and, in particular, the understanding of the factors that determine the molecular structure of a particular compound are important, since ideally they would allow for a rational design of complexes with specific and predictable properties; see Reference [1].

On the one hand, molecular mechanics combined with energy considerations allow us to define, for some particular structures, a given number of canonical conformations. For example the ten canonical conformations deduced by Reference [2] for cyclo-octane are represented in Figure 1. However, it is known from experimental data that some of these canonical conformations are almost never observed, and that, in contrast, some new conformations may appear. These new conformations usually appear as deformations of the canonical ones. Statistical descriptive methods have been employed as a complement to molecular mechanics computations, to detect and identify the preferred conformations in a given compound, that is to cluster the observed structures into a number of conformations. A review of different statistical methods for conformational analysis can be found in Reference [3]. These methods generally take a data analysis approach where no model is assumed for the data generation mechanism, and all the conclusions rely on the correlation structure or the similarity structure of the data. Cluster analysis and principal components analysis are examples of such methods.

In this paper, we address the problem of conformational classification of *m*-membered rings, from the observation of crystallographic data consisting in the torsion angles for a number of structures. In contrast to previously proposed methods, an essential step in our approach consists in specifying a probabilistic model for the observed sequences of torsion angles. This probabilistic model is a mixture model with an unknown number of components. We perform a Bayesian analysis by implementing the Reversible Jump Markov chain Monte Carlo (MCMC) methodology proposed by Reference [4], to obtain samples of the posterior distribution of the parameters, and infer on the conformations along with their frequencies of occurrence. We take into consideration, both in the specification of the prior distributions and in the updating steps of the MCMC algorithm, the geometrical restrictions that link the *m* torsion angles of an *m*-membered ring.

Section 2 describes the data. In Section 3, a model is formulated for the data generation mechanism, including the specification of prior distributions for the parameters. Section 4 describes the applied methodology. The results of our method on a simulated dataset and on real a dataset corresponding to cyclo-octane previously investigated by Reference [5] are presented in Section 5. Finally some conclusions are drawn in Section 1 while the Appendix contains a description of the structure of *m*-membered rings used for

*Correspondence to: M. Kessler, Departamento de Matemática Aplicada y Estadística, Universidad Politécnica de Cartagena, Paseo Alfonso XIII, E-30203 Cartagena , España, Spain.
E-mail: Mathieu.Kessler@upct.es
Contract/grant sponsor: European Community's Human Potential Programme; contract/grant number: HPRN-CT-2000-00100, DYNSTOCH.

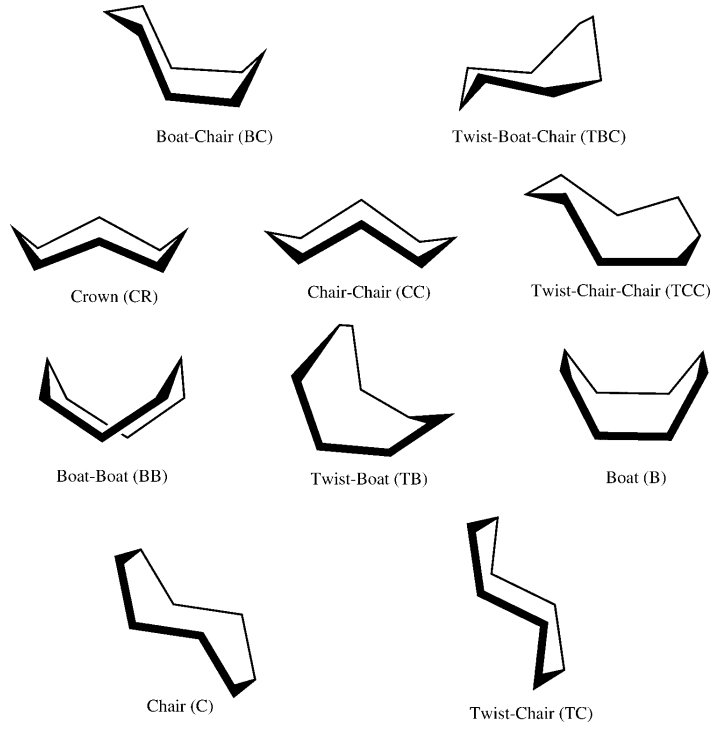

Figure 1. Canonical forms of cyclo-octane.

the MCMC algorithm, together with the expression of the acceptance probabilities associated to the different move types in the reversible jump MCMC algorithm.

2. DESCRIPTION OF THE DATA

The Cambridge Structural Database (CSD) is a powerful tool that provides chemists, access to a large amount of crystallographic structural data. Users of the CSD can retrieve the structures that match a given criterion from the database, for example all the cyclo-octane structures, and can obtain the crystallographic data that characterize each of these structures.

An important set of characteristics associated to a given m-membered ring structure consists in the m-associated torsion angles; see Appendix A.1.1 for a precise definition. These data can be retrieved from the CSD and we will assume that inference is to be made on the conformations and their frequencies of occurrence based on a sample of n structures for each of which we observe the sequence of m torsion angles. In particular, in Section 5, we will carry out the conformational classification of a sample of 31 cyclo-octane structures retrieved from the CSD. This dataset was previously analyzed by means of cluster analysis by Reference [5].

We want to emphasize some important issues related to the data: assume that we retrieve from the CSD the torsion angles corresponding to an $m = 8$ membered ring built of consecutive atoms $A_1, A_2, \ldots, A_8$.

For this single structure, the data consist in the sequence

$$(\mathrm{Tor}(A_1, A_2, A_3, A_4), \mathrm{Tor}(A_2, A_3, A_4, A_5), \ldots \\ \mathrm{Tor}(A_7, A_8, A_1, A_2), \mathrm{Tor}(A_8, A_1, A_2, A_3)) = (\tau_1, \tau_2, \ldots, \tau_7, \tau_8)$$

that is the torsion angles computed from four consecutive atoms, where the starting atom is varying through the whole ring. However, from the retrieved data it is impossible to know what was the atom that was chosen as a starting point to begin measuring the torsion angles. Concretely, this means that, for the same structure, the data could as well be $(\tau_2, \tau_3, \ldots, \tau_8, \tau_1)$, $(\tau_3, \tau_4, \ldots, \tau_1, \tau_2)$ or any of the cyclical translations of $(\tau_1, \tau_2, \ldots, \tau_7, \tau_8)$.

Moreover, the perspective from which the molecule is being measured can either be from above or from below. This implies that, for the same structure, the sequence of torsion angles can be read in a clockwise or counter-clockwise manner.

Finally, if a given conformation is present in the compound, its mirror image can also be found. As a consequence, and as described in Reference [6], the two sequences of torsion angles $(\tau_1, \tau_2, \ldots, \tau_7, \tau_8)$ and $(-\tau_1, -\tau_2, \ldots, -\tau_7, -\tau_8)$ can be met but shall be considered to correspond to equivalent conformations.

These three aspects of the retrieved data will be taken into account when we formulate our model in Section 3.

3. THE INGREDIENTS OF OUR MODEL

3.1. Notations related to vectors

To denote a d-dimensional vector $(v_1, \ldots, v_d)$ we use the notation $v_{1:d}$. If a vector v of length $k \cdot m$ is built up from binding a number k of m-dimensional blocks, we will use the matrix notation $v_{i,j}$ to denote the jth element of the ith block, the notation $v_{i,1:m}$ to denote the ith block and $v = v_{1:k,1:m}$ to denote the whole vector.

3.2. The initial model

Assume that we have retrieved n structures from the CSD, and denote by $\tau^{(1)}, \ldots, \tau^{(n)}$ the n associated m-dimensional vectors of torsion angles. We assume that they correspond to independent and identically distributed realizations from a mixture law with density $\tau \to f(\tau)$, described in Equation (1).

Consider $\tau = \tau_{1:m}$, the m torsion angles that are observed for a given structure. We assume that τ is generated from a mixture of an unknown number k of components. These k components correspond to perturbations of the conformations that can be met for the considered structures. For $c = 1, \ldots, k$, the conformation c is described through an m-dimensional vector of torsion angles $\mu_{c,1:m} = (\mu_{c,1}, \ldots, \mu_{c,m})$ and we denote by w_c its unknown frequency of occurrence for the considered kind of structure.

The observed sequence τ is then generated from the mixture density

$$f(\tau) = \sum_{c=1}^{k} w_c f(\tau, c) \tag{1}$$

where $\tau \to f(\tau, c)$ is the density of τ given the conformation c, which is described in detail below.

We are interested in estimating the number k of conformations present for the structure, the associated torsion angles $\mu_{c,1:m}$ for $c = 1, \ldots, k$, and the frequencies of occurrence $w_1, \ldots, w_k$.

3.2.1. *Description of the density of τ given the conformation $C = c$*

As described in Section 2, the output of the measurement device which yields the observed τ may correspond to a different starting point, a different direction and an opposite sign than the sequence $\mu_{c,1:m}$ associated to the conformation number c.

Consider an m-dimensional vector $\boldsymbol{\mu} = (\mu_1, \ldots, \mu_m)$. The effect of choosing a starting point s in $\{1, \ldots, m\}$, a direction d, which equals 1 if the sequence is read clockwise or -1 if it is read counter-clockwise, and choosing a sign $\delta = \pm 1$, is described through the operator $T^{s,d,\delta}$ which acts on $\boldsymbol{\mu}$ in the following way:

$$T^{s,d,\delta}\boldsymbol{\mu} = \delta \times (\mu_s, \mu_{((s-1+d\times 1) \bmod m)+1}, \ldots, \mu_{((s-1+d\times(m-1)) \bmod m)+1}) \tag{2}$$

where for any integer j, $j \bmod m$ denotes the remainder of the integer division of j by m. Notice in particular that $T^{1,1,1}\boldsymbol{\mu} = \boldsymbol{\mu}$.

As an example, consider the canonical conformation Boat–Chair in Figure 1. As derived in Reference [2], the associated sequence of torsion angles is

$$\mu = (65.0, 44.7, -102.2, 65.0, -65.0, 102.2, 44.7, -65.0)$$

It implies that, for example,

$$T^{2,-1,1}\mu = (44.7, 65.0, -65.0, -44.7, 102.2, -65.0, 65.0, -102.2)$$

Finally, given that the structure was generated from conformation c, the observed sequence τ is obtained, for a given s, d, δ, from $T^{s,d,\delta}\mu_{c,1:m}$ after an additive perturbation $\varepsilon = (\varepsilon_1, \ldots, \varepsilon_m)$, which is assumed to be a Gaussian variable with covariance matrix $\sigma_c^2 \mathbf{I}d_m$.

As a conclusion, the density $\tau \to f(\tau, c)$ in Equation (1), is

$$f(\tau, c) = \frac{1}{4m} \sum_{s=1}^{m} \sum_{d=1,-1} \sum_{\delta=1,-1} f_G(\tau, T^{s,d,\delta}\mu_{c,1:m}, \sigma_c^2 \mathbf{I}d_m) \tag{3}$$

and $\tau \to f_G(\tau, T^{s,d,\delta}\mu_{c,1:m}, \sigma_c^2 \mathbf{I}d_m)$ denotes the density of the m-dimensional Gaussian law with mean $T^{s,d,\delta}\mu_{c,1:m}$ and diagonal covariance matrix $\sigma_c^2 \mathbf{I}d_m$.

3.2.2. *Density of the observations*

To sum up, the density of the observations $\tau^{(1)}, \ldots, \tau^{(n)}$ is given by

$$\prod_{i=1}^{n} \left(\sum_{c=1}^{k} w_c f(\tau^{(i)}, c) \right)$$

where $f(\tau, c)$ is defined in Equation (3).

Remark. The additive perturbation ε may be seen as a measurement error, but our modeling framework is as well inspired by the model-based clustering approach in Reference [7], where mixtures of Gaussian variables are used as a basis for clustering algoritms. In particular, the size and shape of each cluster can be modeled by imposing a given structure for the covariance matrix of the corresponding Gaussian distribution. Assuming, as we do, the covariance matrix of ε to be diagonal but allowing the variance to vary between conformations amounts to considering spherical clusters of possibly different sizes.

3.3. *Extension of the parameter space*

For a given conformation, the parameters $\mu_{c,1:m}$ that enter Equation (3) cannot be freely chosen: for the corresponding ring to be physically coherent, they must satisfy some restrictions. These restrictions are not easy to express, but it is necessary to have a control on them, on the one hand to specify a reasonable prior distribution on $\mu_{c,1:m}$ and on the other hand, since we will need to be able to propose reasonable candidates for $\mu_{c,1:m}$ in the MCMC algorithm.

We can guarantee that the physical restrictions are fulfilled if we extend the parameter space to include as well the bond angles and the atomic lengths of the molecule, and therefore get a complete description of the conformation number c. For a precise definition of torsion angles, bond angles and distances, see Appendix A.1.1.

Consider an m-membered ring with consecutive atoms $A_1, A_2, \ldots, A_m$. As in Appendix A.1.1, we denote by $\tau_{k-2;\,k-1;\,k;\,k+1}$ the torsion angle for the sequence of four points $A_{k-2}, A_{k-1}, A_k, A_{k+1}$, by $b_{k-1;\,k;\,k+1}$ the bond angle for the

points A_{k-1}, A_k, A_{k+1}, and by $d_{k-1;\,k}$ the distance between A_{k-1} and A_k.

For the ring $A_1, A_2, \ldots, A_m$, we can compute m torsion angles $\mu_{1:m}$, m bond angles $b_{1:m}$ and m atomic lengths $d_{1:m}$ as

$$\begin{aligned}\mu_{1:m} =&(\tau_{1;\,2;\,3;\,4}, \ldots, \tau_{m-3;\,m-2;\,m-1;\,m},\\ &\tau_{m-2;\,m-1;\,m;\,1}, \tau_{m-1;\,m;\,1;\,2}, \tau_{m;\,1;\,2;\,3})\end{aligned} \tag{4}$$

$$b_{1:m} = (b_{1;\,2;\,3}, \ldots, b_{m-2;\,m-1;\,m}, b_{m-1;\,m;\,1}, b_{m;\,1;\,2}) \tag{5}$$

$$d_{1:m} = (d_{1;\,2}, \ldots, d_{m-1;\,m}, d_{m;\,1}) \tag{6}$$

These quantities are obviously related. In fact, as described in Appendix A.1, an m-membered ring can be drawn by choosing freely the first $m-3$ torsion angles, $\mu_{1:m-3}$, the first $m-2$ bond angles, $b_{1:m-2}$, and $m-1$ atomic lengths, $d_{1:m-1}$. This fixes fully the relative positions of the m atoms in the ring. The remaining angles and lengths can be uniquely determined through the mapping

$$(\mu_{1:m}, b_{1:m}, d_{1:m}) = F(\mu_{1:m-3}, b_{1:m-2}, d_{1:m-1}) \tag{7}$$

which is described in Appendix A.1.3.

As a conclusion, once we have fixed the number k of components of our mixture model, we will consider the extended parameter to be $w_{1:k}$, $\mu_{1:k,1:m}$, $b_{1:k,1:m}$, $d_{1:k,1:m}$ and $\sigma^2_{1:k}$ although the density of the observed variables τ depends only on $w_{1:k}$, $\mu_{1:k,1:m}$, and $\sigma^2_{1:k}$; see Equations (1) and (3).

3.4. The prior distributions

3.4.1. *The parameters k, $w_{1:k}$ and $\sigma^2_{1:k}$*

For the unknown number of components, the variances of the Gaussian perturbations and the mixture proportions, we follow References [8] and [9], and choose the following priors:

$$k \sim U(1, k_{\max})$$

$\sigma_1^2, \ldots, \sigma_k^2$ are independent and $\sigma_i^2 \sim IG(\alpha_i, \beta_i), \quad i = 1, \ldots, k$

$$(w_1, \ldots, w_k) \sim D(1, \ldots, 1)$$

where $U(1, k_{\max})$ denotes the discrete uniform distribution on the integers between 1 and $k_{\max}$, $IG(\alpha, \beta)$ denotes the Inverse Gamma distribution with parameters (α, β), and $D(\alpha_1, \ldots, \alpha_k)$ denotes the Dirichlet distribution with parameters $(\alpha_1, \ldots, \alpha_k)$.

3.4.2. *The parameters μ, b and d*

Given a value of k, we have to specify our prior distribution on $\mu_{c,1:m}$, $b_{c,1:m}$, and $d_{c,1:m}$ for $c = 1, \ldots, k$ and we want it to charge only physically coherent molecules.

From Subsection 3.3, it is known that this can be done by specifying a prior distribution for $\mu_{c,1:(m-3)}$, $b_{c,1:m-2}$ and $d_{c,1:m-1}$, and deduce the remaining angles and lengths through the mapping F; see Equation (7). We therefore choose, for all $c = 1, \ldots, k$

$$\mu_{c,1:(m-3)} \sim \bigotimes_{1:(m-3)} U(-\pi, \pi) \tag{8}$$

$$b_{c,1:(m-2)} \sim N(\eta^b_{1:m-2}, \kappa^b\, \mathbf{Id}_{m-2}) 1_{[\eta_i^b \pm 2\sqrt{\kappa^b}]} \tag{9}$$

$$d_{c,1:(m-3)} \sim N(\eta^d_{1:m-1}, \kappa^d\, \mathbf{Id}_{m-3}) 1_{[\eta_i^d \pm 2\sqrt{\kappa^d}]} \tag{10}$$

and

$$(\mu_{c,1:m}, b_{c,1:m}, d_{c,1:m}) = F(\mu_{c,1:m-3}, b_{c,1:m-2}, d_{c,1:m-1}) \tag{11}$$

The choice of the prior for μ does not favor any specific conformation. On the contrary, the prior for the bond angles is meant to incorporate chemical knowledge: for the cyclo-octane dataset treated in Section 5 for example, it is known that bond angles for cyclo-octane are centered around 117 degrees, and present little variability; see for example Reference [10], p36. The indicator notation used in the prior distributions for the bond angles and the distances indicate that we truncate the normal distributions and do not consider values for which the distance to the mean is larger than two standard deviations: we discard outliers for bond angles or distances in order to charge only physically reasonable molecules.

The final model is described through the DAG graph in Figure 2.

4. THE METHODOLOGY

4.1. The Reversible Jump algorithm

We use a MCMC algorithm to obtain samples of the posterior distribution of the parameters. Given a target distribution π, such an algorithm allows to simulate trajectories of an ergodic Markov Chain with stationnary distribution π by specifying how to choose the transition of the chain. The Metropolis Hastings algorithm implements a specific way to construct the transition: given a point of the chain, a

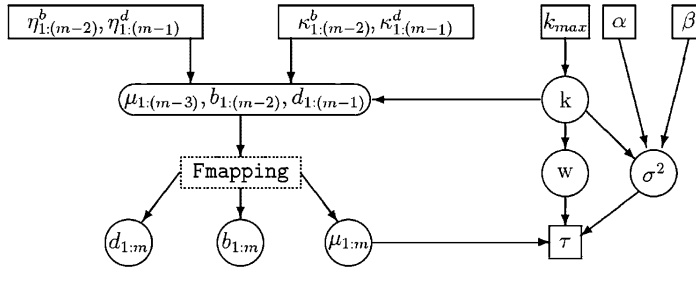

Figure 2. The DAG representation of our model.

candidate is proposed for the next point, from a user-provided candidate distribution and accepted or rejected with a specific probability. For an extensive account on MCMC methods see, for example Reference [11]. The Reversible Jump MCMC was introduced by Reference [4] as a Markov chain algorithm for varying dimension problems. It consists in a random sweep Metropolis-Hastings method adapted for general state space, which is able to jump between spaces of different dimensions. It was applied to carry out Bayesian inference in one-dimensional Gaussian-Mixture models with an unknown number of components in Reference [8] and later in Reference [9], to which we refer for more details about the implementation of the algorithm.

A complete sweep of the algorithm consists in a scanning of the following move types:

(a) updating the weights w
(b) updating the parameters $(\mu_{1:m}, b_{1:m}, d_{1:m})$
(c) updating the variance parameters $\sigma^2_{1:k}$
(d) the birth or death of a component

Notice that the dimension changing move types used for this application consist only in birth/death moves (d), and do not include the split/merge moves considered in Reference [8]. This last kind of move is not easy to implement efficiently in a multidimensional setting, we obtained rather low acceptance rates and decided to discard them in our final analysis. See [12] for a suggestion on how to implement split/merge moves for multivariate mixtures.

At each iteration of the algorithm we either perform the three fixed-k moves (a), (b), and (c) altogether or the birth/death move (d). Each of these two possibilities is decided upon with probability 0.5. Moreover, if we decide to perform move type (d), we choose either birth or death of a component with probability 0.5.

As for move types (a) and (c), we follow Reference [9] and choose multiplicative lognormal random walks for updating the weights and the variances parameters, see also Reference [13] for a detailed description.

In the following Subsection we describe in more detail the updating of the parameters $(\mu_{1:m}, b_{1:m}, d_{1:m})$ in move type (b), which requires involved computations in order to ensure that the proposed parameters correspond to a physically coherent molecule.

4.2. Updating the parameters $(\mu_{1:m}, b_{1:m}, d_{1:m})$

Assume that the previous sample was $(\mu_{1:m}, b_{1:m}, d_{1:m})$, we propose the candidate $(\mu^*_{1:m}, b^*_{1:m}, d^*_{1:m})$, ensuring that it is associated to a physically coherent m-membered ring. To do so, we update $(\mu_{1:m-3}, b_{1:m-2}, d_{1:m-1})$ following a Gaussian Random Walk proposal,

$$\mu^*_{1:m-3} \sim N(\mu_{1:m-3}, \sigma^2_{\epsilon_\mu} \mathbf{I}d_{m-3}) \tag{12}$$

$$b^*_{1:m-2} \sim N(b_{1:m-2}, \sigma^2_{\epsilon_b} \mathbf{I}d_{m-2}) \tag{13}$$

$$d^*_{1:m-1} \sim N(d_{1:m-1}, \sigma^2_{\epsilon_d} \mathbf{I}d_{m-1}) \tag{14}$$

and deduce the remaining parameters $\mu^*_{m-2:m}$, $b^*_{m-1:m}$ and d^*_m using the F mapping described in Appendix A.1.3,

$$(\mu^*_{1:m}, b^*_{1:m}, d^*_{1:m}) = F(\mu^*_{1:m-3}, b^*_{1:m-2}, d^*_{1:m-1})$$

Following the Metropolis Hastings algorithm, we then accept the candidate with probability ρ described in Appendix A.2.

4.3. Birth and death move

We choose with probability 0.5 between the birth or the death of a component. The birth move consists in creating a new component, by first drawing $w^*_{k+1} \sim Be(1, k)$. The candidate weights are then deduced through, for $j = 1, \ldots, k$, $w^*_j = w_j(1 - w^*_{k+1})$. The remaining parameters for the new component $(\mu^*_{k+1,1:m}, b^*_{k+1,1:m}, d^*_{k+1,1:m})$ and $\sigma^{2^*}_{k+1}$ are drawn from their prior distributions, see the Appendix A.2 for details, and appended to the current state parameters.

Finally the death move consists in choosing randomly a component and deleting it from the current state, and renormalizing the weights.

The expression for the acceptance probability for these moves can be found in Subsection A.2.2.

4.4. Post processing of the output

As described in References, for example [14], [15] or [16], the invariance of the likelihood under arbitrary relabeling of the mixture components leads to symmetries in the posterior distributions of the parameters, which are therefore difficult to summarize. In particular, the posterior marginal distributions are, for permutation invariant priors, indistinguishable. One of the proposed solutions consists in imposing identifiability constraints on the parameter space through an ordering specification in the prior, for example on the weights $w_1 < \cdots < w_k$ or in the case of one-dimensional mixtures on the components means; see Reference [8]. However the choice of the identifiability constraints is not unique and, more importantly, this approach does not guarantee an acceptable solution, since the chosen identifiability constraints may not break the symmetry of the likelihood efficiently. Alternatively, post-processing algorithms of the output of the MCMC trajectories, which involve a relabeling of the mixture components, have been investigated; see References [15] or [17].

We follow a post-processing algorithm proposed by Reference [18], which intends to carry out, for each value of the parameters provided by the sampler, a relabeling of the components so that the relabeled sample *points all agree* well with each other. More concretely, if $\theta^{(1)}, \ldots, \theta^{(N)}$ are the N samples of the posterior distributions of the parameters provided by the MCMC algorithm, the aim is to find N permutations $\nu_1, \ldots, \nu_N$ which operate a relabeling of each $\theta^{(1)}, \ldots, \theta^{(N)}$ such that the permuted parameters $\nu_1(\theta^{(1)}), \ldots, \nu_N(\theta^{(N)})$ present the same ordering of the components.

The general algorithm suggested by Stephens requires the definition of a divergence $D(\theta^{(1)} \| \theta^{(2)})$ between two parameters $\theta^{(1)}$ and $\theta^{(2)}$, designed to be small when these are labeled 'the same way'. The algorithm (see Algorithm 3.1, p47, [18]), then consists, starting with some initial values for $\nu_1, \ldots, \nu_N$, in iterating the following steps until a fixed point is reached

Step 1: Choose $\hat{\theta}$ to minimize

$$\sum_{t=1}^{N} D(\nu_t(\theta^{(t)}) \| \hat{\theta})$$

Step 2: For $t = 1, \ldots, N$ choose ν_t to minimize

$$D(\nu_t(\theta^{(t)}) \| \hat{\theta})$$

Stephens suggests the following measure of divergence:

$$D(\theta^{(1)} \| \theta^{(2)}) = \sum_{i=1}^{k} \Delta\left[w_i^{(1)} N\left(.; \mu_i^{(1)}, \Sigma^{(1)}\right) \| w_i^{(2)} N\left(.; \mu_i^{(2)}, \Sigma^{(2)}\right)\right]$$

where Δ is a measure of divergence between two weighted density functions based on the Kulback Leibler divergence. In this case the two minimizations in Steps 1 and 2 above can be carried out explicitly and yield the Algorithm 3.2, p49, in Reference [18].

Notice that in our case, we have to adapt the general algorithm above in order to take into account the possibly arbitrary starting point, direction and sign of each component mean. Our algorithm therefore aims at finding, on the one hand, for each $\theta^{(t)}, t = 1, \ldots, N$, an 'optimal' permutation of the components labels, ν_t and, on the other hand, for each component mean, 'optimal' starting points $s_{t,1}, \ldots, s_{t,k}$ in $\{1, \ldots, m\}$, directions $d_{t,1}, \ldots, d_{t,k}$ in $\{-1, 1\}$ and signs $\delta_{t,1}, \ldots, \delta_{t,k}$ in $\{-1, 1\}$. Consider, therefore, the associated operators $T_{t,1} = T^{s_{t,1}, d_{t,1}, \delta_{t,1}}, \ldots, T_{t,k} = T^{s_{t,k}, d_{t,k}, \delta_{t,k}}$, see Equation (2), we form the global operator $T_{t,1:k} = (T_{t,1}, \ldots, T_{t,k})$ which acts block-wise on a vector $\mu_{1:k,1:m}$ of length $k \cdot m$,

$$T_{t,1:k}(\boldsymbol{\mu}_{1:k,1:m}) = (T_{t,1}\boldsymbol{\mu}_{1,1:m}, \ldots, T_{t,k}\boldsymbol{\mu}_{k,1:m})$$

The output of the post-processing algorithm is thus N relabeled samples, where a change is allowed for in the starting points, directions and signs of each conformation; see Section 2 and in particular Equation (2)

$$\theta_*^{(1)} = \left(\nu_1\left(w_{1:k}^{(1)}\right), \nu_1\left(\sigma_{1:k}^{2,(1)}\right), \nu_1\left(T_{1,1:k}\left(\boldsymbol{\mu}_{1:k,1:m}^{(1)}\right)\right)\right)$$

$$\theta_*^{(N)} = \left(\nu_N\left(w_{1:k}^{(N)}\right), \nu_N\left(\sigma_{1:k}^{2,(N)}\right), \nu_N(T_{N,1:k}\left(\boldsymbol{\mu}_{1:k,1:m}^{(N)}\right)\right)\right)$$

Notice that the permutations operators ν_t, $t = 1, \ldots, N$ act on a k-dimensional vector $\boldsymbol{v}_{1:k}$. However, the same notation is used for the operators that permute the k blocks of a $(k \cdot m)$-dimensional vector $\boldsymbol{v}_{1:k;1:m}$: $\mathbf{v}_t(v_{1:k;1:m}) = v_{\nu_t(1:k);1:m}$.

Before describing the post-processing algorithm, we introduce a last notation; for $i = 1, \ldots, k$, consider the operator p_i that picks up the ith m-dimensional block, in a $(k \cdot m)$-dimensional vector $\boldsymbol{\mu}_{1:k,1:m}$:

$$p_i(\boldsymbol{\mu}_{1:k,1:m}) = (\boldsymbol{\mu}_{i,1:m})$$

To sum up, notice in particular that $p_i(\nu_t(T_{t,1:k}(\boldsymbol{\mu}_{1:k,1:m}^{(t)})))$ is the mean of the ith -component in the relabeled $\theta^{(t)}$, where the starting point, direction and sign have been changed according to $T_{t,i}$.

Algorithm 1 below is summarizing the suggested post-processing algorithm, inspired by Reference [18], p49.

5. RESULTS

5.1. Simulated data

In this subsection, we test the performance of our method on a simulated dataset. Concretely, a three components dataset is simulated, where the three eight-membered conformations correspond to the CR, BB and TC conformations (see Figure 1) present for cyclo-octane, for which we can find the torsion angles in Reference [2]. The dataset was generated from model Equation (1) (see also Equation (3)), where the standard deviations of the perturbations were assumed to be $\sigma_1 = \sigma_2 = \sigma_3 = 10$ degrees. The total number of structures in the dataset is 60, with 10 CR structures, 20 BC structures and 30 TC structures.

In order to evaluate the benefit of taking into account the physical restrictions, through the extension of the parameter space as described in Subsection 3.3, we have also

---

Algorithm 1 Relabeling the N samples associated to k components mixture

1: Set all permutations $\nu_1, \ldots, \nu_N$ to be identity permutations and operators $T_{1,1:k}, \ldots, T_{N,1:k}$ to be identity operators.

2: Set

$$\text{for all } 1 \le i \le k, \quad \hat{\boldsymbol{w}}_i = \frac{1}{N}\sum_{t=1}^{N} \nu_t\left(w_{1:k}^{(t)}\right)[i]$$

$$\text{for all } 1 \le i \le k \quad \hat{\boldsymbol{\mu}}_{i,1:m} = \frac{\sum_{t=1}^{N} \nu_t\left(w_{1:k}^{(t)}\right)[i] p_i\left(\nu_t\left(T_{t,1:k}\left(\boldsymbol{\mu}_{1:k,1:m}^{(t)}\right)\right)\right)}{\sum_{t=1}^{N} \nu_t(w_{1:k}^{(t)})[i]}$$

$$\text{for all } 1 \le i \le k, \quad \hat{\sigma}_i^2 = \frac{\sum_{t=1}^{N} \nu_t\left(w_{1:k}^{(t)}\right)[i]\left(m\left(\sigma_{\nu_t[i]}^{(t)}\right)^2 + \|p_i\left(\nu_t\left(T_{t,1:k}\left(\boldsymbol{\mu}_{1:k,1:m}^{(t)}\right)\right)\right) - \hat{\boldsymbol{\mu}}_{i,1:m}\|^2\right)}{m\sum_{t=1}^{N} \nu_t(w_{1:k}^{(t)})[i]}$$

3: For each $t = 1, \ldots, N$ choose the optimal permutation ν_t and the optimal operator T_t of the form Equation (2), minimizing

$$\begin{aligned} &\sum_{i=1}^{k} \Big\{ -\nu_t(w_{1:k})[i]\log(\hat{\boldsymbol{w}}_i) - (1 - \nu_t(w_{1:k})[i])\log(1 - \hat{\boldsymbol{w}}_i) \\ &+ \nu_t(w_{1:k})[i]\frac{m}{2}\log(\hat{\sigma}_i^2). + \frac{w_{\nu_t[i]}}{2\hat{\sigma}_i^2}\left(m\sigma_{\nu_t[i]}^2 + \|p_i(\nu_t(T_{t,1:k}(\boldsymbol{\mu}_{1:k,1:m}))) - \hat{\boldsymbol{\mu}}_{i,1:m}\|^2\right)\Big\} \end{aligned} \tag{15}$$

4: Stop when a fix point is reached, otherwise return to step (2).

implemented the naive model that would consist in ignoring these physical restrictions and the relations between the eight torsion angles and, in the MCMC algorithm, simply update $\mu_{1:m}$ following a Gaussian Random Walk proposal,

$$\mu^*_{1:m} \sim N(\mu_{1:m}, \sigma^2_{\epsilon_\mu} \mathbf{I}d_m) \tag{16}$$

as opposed to Equations (12)–(14).

As for the prior distributions, both models share the specification for parameters k, $\sigma^2_{1:k}$ and $w_{1:k}$; see Subsection 3.4.1. More concretely, $k_{\max} = 15$, $\sigma^2_1, \ldots, \sigma^2_k$ are i.i.d IG$(2, 40)$ which centers σ_i around 10 degrees. However, they differ in the specification of the prior for $\mu_{1:m}$.

For the full model, as described in Subsection 3.4.2, we have chosen $\mu_{1:(m-3)} \sim \otimes_{1:(m-3)} U(-\pi, \pi)$, which does not favor any conformation. The prior distribution for the bond angles was based on chemical knowledge; see Reference [10], p36, $b_{1:(m-2)} \sim \otimes_{1:(m-2)} N(117, 3^2)$. Finally we know that all atoms in the chain are the same, and we therefore assume that the distances are basically equal: $d_{1:(m-1)} \sim \otimes_{1:(m-1)} N(1, .1^2)$.

For the naive model, we have simply specified $\mu_{1:m} \sim \otimes_{1:m} U(-\pi, \pi)$, it is a prior distribution that charges also non-physically drawable molecules.

The MCMC Reversible Jump algorithm was run for 2 02 000 iterations and we kept the last 2000 points for inference. The value of the constants involved in the proposal steps were tuned so that we obtained the following reasonable acceptance rates for the different move types: for the fixed-dimension moves (a), (b), and (c) in Subsection 4.1, the acceptance rate was close to 0.5, while the birth or death moves presented an acceptance rate of approximately 6%. The mixing of the chain was satisfactory and a shorter burn-period could as well have been chosen. Our attempts with a shorter burn-in period yielded in fact similar results.

The posterior distribution for k, the number of components in the mixture, is presented in Figure 3. They both clearly favor three components in the mixture.

In Table I, the first rows contain the true values of the parameters of interest for the simulated dataset: N_c is the number of structures simulated from each conformation, w are the corresponding proportions, σ represents the standard deviation of the perturbation, while $\mu_1, \ldots, \mu_8$ are the theoretical torsion angles for the CR, BR, and TC conformations reported in Reference [2].

The estimation results for the full model, which take into account the physical restrictions through the F-mapping, as described in Subsection 4.2, are presented in the middle of the table, where the medians of the posterior distributions of the parameters $w_{1:3}$, $\sigma_{1:3}$ and $\mu_{1:3,1:8}$ are reported. Finally, the same summary for the naive model, which does not take into account the physical restrictions but uses the proposal (16), is presented in the bottom of Table I.

Figures 4 and 5 present box plot-like diagrams for the posterior distributions of the parameters of interest for both methods. Seven horizontal lines are drawn for each box, representing the percentiles 10, 15, 25, 50, 75, 85, 90. Moreover wider, thicker horizontal lines are drawn for the values of the parameter that were used to generate the simulated dataset.

As a conclusion, on this simulated dataset, the results for the full model described in this paper are very satisfying. The three components are detected and correctly estimated. On the other hand, the results are significantly better for the full model than for the naive model: the standard deviations are much better estimated and the dispersion for the posterior distribution of the means is smaller. We conclude that, even if the full model requires more involved computations, because of the evaluation of the F mapping, the improvement is worth the increase in sophistication.

5.2. Cyclo-octane dataset

In Reference [5] measurements of torsion angles for cyclo-octane were retrieved from the CSD and principal component analysis and cluster analysis were carried out. They consider in particular a dataset, labeled 8C1 in their

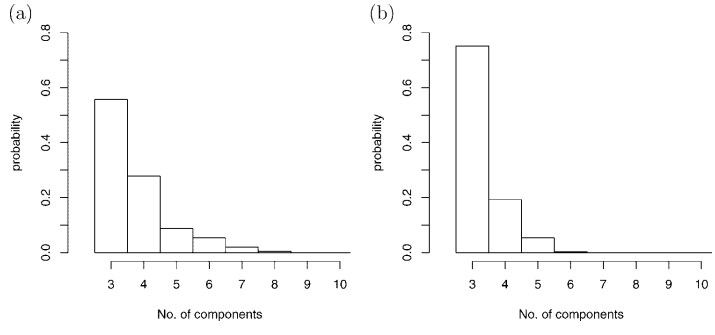

Figure 3. Posterior distribution for k, the number of components for the simulated dataset of Subsection 5.1. (a) and (b) correspond respectively to the full and naive model, that is with/without the F mapping and the physical restrictions.

Table I. True values of the parameters, and estimation results for the simulated dataset of Subsection 5.1.

N_c	w_c	σ_c	Identifiers	$\mu_{c,1}$	$\mu_{c,2}$	$\mu_{c,3}$	$\mu_{c,4}$	$\mu_{c,5}$	$\mu_{c,6}$	$\mu_{c,7}$	$\mu_{c,8}$
True values of the parameters used in the simulation of the dataset											
30	0.5	10	TC	37.3	−109.3	109.3	−37.3	−37.3	109.3	−109.3	37.3
20	0.333	10	BB	52.5	52.5	−52.5	−52.5	52.5	52.5	−52.5	−52.5
10	0.167	10	CR	87.5	−87.5	87.5	−87.5	87.5	−87.5	87.5	−87.5
Estimation results for the full model which involves the F mapping to take into account the physical restrictions											
	0.49	16.61	TC	31.67	−108.48	110.61	−36.54	−35.55	106.10	−107.96	40.62
	0.34	11.71	BB	48.46	57.55	−53.30	−53.65	53.21	58.01	−57.56	−49.41
	0.16	21.5	CR	80.94	−77.00	87.22	−95.77	90.13	−83.93	86.97	−86.60
Estimation results for the 'naive' model, that does not take into account the physical restrictions											
	0.49	34.67	TC	41.01	−109.55	108.76	−39.50	−36.55	107.60	−111.82	33.90
	0.33	42.09	BB	52.92	46.60	−59.44	−46.29	49.08	56.51	−48.31	−49.96
	0.18	61.02	CR	94.67	−71.32	107.79	−78.33	101.15	−98.18	75.83	−76.00

The upper part of the table contains the values of the parameters that were used to simulate the dataset. The column labeled N_c contains the number of structures that were simulated for each cluster, while w_c denotes the corresponding proportion. The dataset was simulated from a mixture of three conformations TC (Twisted-Chair), BB (Boat–Boat) and CR (Crown). The corresponding torsion angles are reported in the columns $\mu_{c,1}$ to $\mu_{c,8}$, while σ_c denotes the standard deviation associated to each cluster. The middle part of the table contains the medians of the posterior distributions of the parameters of interest, when the full model is used and the physical restrictions are taken into account. The bottom part of the table contains the medians of the posterior distributions of the parameters when the simple, 'naive' is used, and the physical restrictions are not taken into account

paper, consisting of 31 observations, of which 12 were classified as Boat–Chair (BC), 10 as two different components both identified as 'deformed' BC, (in between BC and Twist–Boat–Chair (TBC)) and finally 2 observations were classified as respectively Crown (CR) and Twist–Chair–Chair (TCC); 7 observations were not classified. The standard deviations within the clusters seem to be centered around 15 degrees. The results from Reference [5] are reported in Table 2: the first column contains the index of the cluster, the second column the number of elements in each cluster, the Refcode is the reference code of the structure chosen as most representative of the cluster, while the identifier column contains the kind of conformation associated to the cluster by the authors. Finally the columns $\mu_{c,1}, \ldots, \mu_{c,8}$ contain the torsion angles of the representative member of the cluster, that is the structure corresponding to the Refcode of the third column.

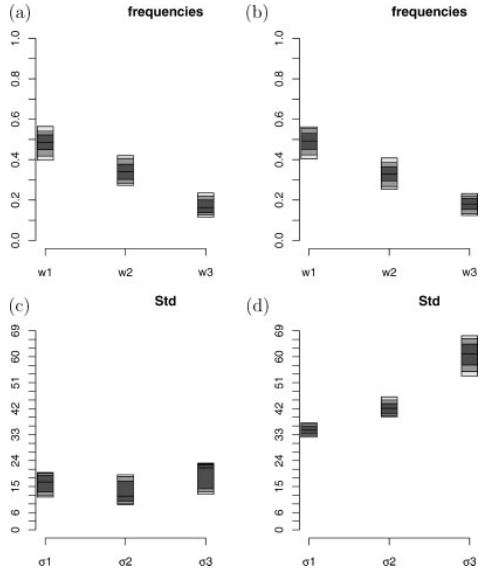

Figure 4. Simulated dataset of Subsection 5.1: Box plot-like diagrams of the posterior distributions of the proportions $w_{1:3}$ and the standard deviations $\sigma_{1:3}$ associated to the $k = 3$ detected components. The plots (a) and (c) correspond to the case when the full model is used, while the plots (b) and (d) to the case when the 'naive' model is used. Seven horizontal lines are drawn for each box, representing the percentiles 10, 15, 25, 50, 75, 85, 90.

These results will now be compared to the ones obtained by applying the method described in this paper. The prior distributions for the parameters were the same as in the previous subsection for the simulated dataset (full model), and the constants needed in the updating steps of the MCMC algorithm were tuned to obtain similar acceptance rates.

The posterior distribution for the number k of components in the mixture is presented in Figure 6 from which we deduce that $k = 6$ or $k = 7$ is the most likely value. The post-processing algorithm was therefore carried out for both values of k and no significant differences were found concerning the main groups. We present here the results obtained with $k = 7$.

In Table III the mean values are listed for comparison with Table II and in Figure 7 box plots of the posterior distributions are presented, where the 10, 15, 25, 50, 75, 85 and 90 percentiles are indicated. In the box plots where the conformations are identified as being equivalent to a conformation obtained by Reference [5] (see Table II) a horizontal black wide line has been drawn, which represents the value of a representative member of the corresponding cluster according to these authors.

Our results coincide basically with Reference [5]: the preferred BC conformation is clearly identified (component

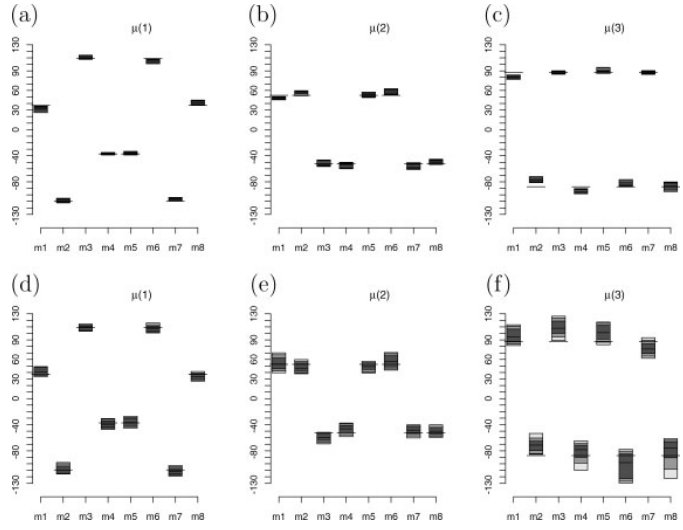

Figure 5. Simulated dataset of Subsection 5.1: Box plot-like diagrams of the posterior distributions of the components means $\mu_{c,1:8}$, for $c = 1, 2, 3$. The plots (a), (b) and (c) correspond to the case when the full model is used, while the plots (d), (e) and (f) to the case when the 'naive' model is used. Seven horizontal lines are drawn for each box, representing the percentiles 10, 15, 25, 50, 75, 85, 90. Moreover wider, thicker horizontal lines are drawn for the values of the parameter that were used to generate the simulated dataset.

Table II. Results reported in Reference [5], for the cyclo-octane dataset under study.

c	N_c	w_c	Refcode	Identifiers	$\mu_{c,1}$	$\mu_{c,2}$	$\mu_{c,3}$	$\mu_{c,4}$	$\mu_{c,5}$	$\mu_{c,6}$	$\mu_{c,7}$	$\mu_{c,8}$
1	12	0.39	BAGPII	BC	−100.9 (10)	43.2 (11)	65.0 (8)	−65.0 (8)	−43.2 (11)	100.9 (10)	−66.8 (10)	66.8 (10)
2	6	0.19	COVLUU	BC/TBC	−91.0 (9)	24.3 (18)	77.2 (10)	−57.3 (10)	−53.4 (7)	103.1 (13)	−65.3 (12)	68.9 (8)
3	4	0.13	SPTZBN	BC/TBC	−79.5 (4)	0.5 (21)	89.6 (24)	−52.4 (7)	−56.4 (13)	102.6 (32)	−71.2 (15)	76.3 (36)
4	1	0.03	DEZPUT	CR	70.4	−83.2	92.3	−73.3	63.8	−82.3	96.5	−82.0
5	1	0.03	EOCNON10	TCC	47.7	−84.7	134.4	−85.3	48.7	−82.4	124.9	−80.7

For each component index c, the number N_c of structures assigned to the component c and the corresponding proportion w_c are given. The refcode of the most representative structure of the cluster is reported, together with its observed torsion angles in the columns labeled $\mu_{c,1}$–$\mu_{c,8}$. The identifiers column represents which kind of conformation present the structures in the cluster. The number in parenthesis for the first three components represent the empirical standard deviations for each cluster

Table III. Cyclo-octane dataset of Subsection 5.2: medians of the posterior distributions for the proportions w_c, the standard deviations σ_c and the components means $\mu_{c,1}$–$\mu_{c,8}$ when $k = 7$ components are chosen

c	w_c	σ_c	Identifiers	$\mu_{c,1}$	$\mu_{c,2}$	$\mu_{c,3}$	$\mu_{c,4}$	$\mu_{c,5}$	$\mu_{c,6}$	$\mu_{c,7}$	$\mu_{c,8}$
1	0.49	9.82	BC	−98.9	39.3	67.8	−63.2	−46.0	100.8	−66.0	66.7
2	0.06	9.07	BC/TBC	−97.5	54.9	53.6	−82.4	−8.1	81.1	−71.3	66.8
3	0.11	9.26	BC/TBC	−82.5	5.1	85.8	−53.9	−57.7	100.8	−69.6	72.3
4	0.08	11.03	Crown	73.5	−94.4	92.6	−70.2	69.9	−87.2	87.7	−68.7
5	0.04	12.51	TCC	68.6	−101.0	87.5	−49.1	54.0	−93.7	89.1	−57.4
6	0.10	12.52		1.7	−61.9	101.8	−67.3	60.3	−101.0	83.8	−5.8
7	0.07	12.13		88.5	3.6	−74.5	89.8	−88.1	70.8	−4.9	−88.5

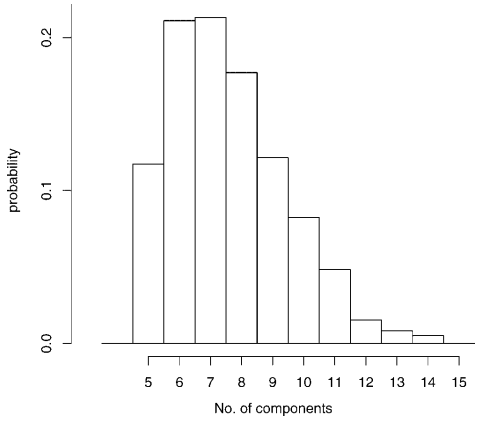

Figure 6. Cyclo-octane dataset of Subsection 5.2: posterior distribution for k the number of components.

1 in our results), and our conformations 2, 3, and 4 are similar to their clusters with refcodes COVLUU, SPTZBN, and DEZPUT (see Table II). As for the three remaining components the high dispersion of the posterior distribution for the standard deviations and the corresponding low frequencies lead us to be cautious as for their interpretation. Component no. 5, however, is somehow similar to TCC identified in Reference [5]. Notice that this dataset is particularly difficult to process since there are few observations and some of the clusters only contain one observation.

6. CONCLUSION

In this work a full Bayesian approach to conformational classification of m-membered rings is proposed, based on torsion angles measurements. We have proposed a multivariate mixture model for the data generation mechanism. We can see several advantages of a full Baye-

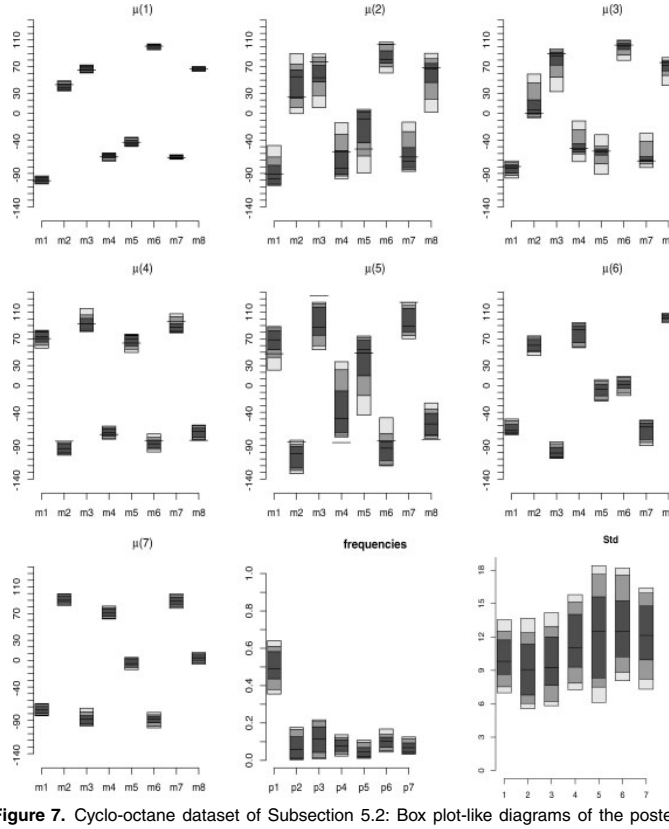

Figure 7. Cyclo-octane dataset of Subsection 5.2: Box plot-like diagrams of the posterior distributions of the means, frequencies and standard deviations associated to $k = 7$ components. For comparison with the results reported in Reference [5], see Table 2, when appropiate, a horizontal black wide line has been drawn, which represents the value of a representative member of the corresponding cluster according to these authors.

sian approach to this applied problem: on the one hand, it easily allows to take into account, through an extension of the parameter space, the physical restrictions and the intricate relations these imply between the torsion angles. On the other hand, we have been able to include chemical knowledge as part of the prior specification. Moreover, the output includes a measure of the uncertainty linked to the inference procedure, which represents a useful information for chemists.

The implementation of the Reversible Jump algorithm, combined with a post-processing of the sampler output, provided quite satisfying results both for a simulated dataset and for a real dataset of cyclo-octane structures, though we did not consider a split/merge move as in Reference [8], since it turned out to be difficult to implement.

Acknowledgements

This work was supported in part by the European Community's Human Potential Programme under contract HPRN-CT-2000-00100, DYNSTOCH. The authors are grateful to Tobias Rydén for helpful discussions.

APPENDIX

A.1. Relations between torsion angles, bond angles and distances in an *m*-membered ring

A chemical structure can be described in terms of (xyz) positions of its atoms in a Cartesian coordinate system. This description is, however, not particularly useful since the absolute coordinates are irrelevant from a chemical point of view, and instead, a description in terms of distances, bond- and torsion-angles is preferred, which moreover has the property of being invariant under rotations and translations of the structure. However for a structure consisting of m atoms, an arbitrary specification of m distances $d_{1:m}$, m bond angles $b_{1:m}$ and m torsion angles $\mu_{1:m}$ may lead to a structure with inner conflicts since the structure is uniquely described with fewer parameters.

The aim of this subsection is to describe the relations between torsion angles, bond angles and distances for an m-membered ring. An understanding of these relations allow us to suggest priors on $(\mu_{1:m}, b_{1:m}, d_{1:m})$, see Subsection 3.4.2, that only charge physically coherent molecules, or to produce samples of these parameters that fulfill the physical restrictions, see Subsection 4.2.

Some background and definitions are needed. We begin in Subsection A.1.1 by defining the concept of torsion and bond angles. In Subsection A.1.2, we explain what are the angles and distances required to build sequentially an m-membered ring. In Subsection A.1.3 we deduce an sequential procedure that expresses the coordinates, in one reference Cartesian system, of all m atoms in terms of the torsion angles, bond angles and distances and obtain in that way an operational description of the mapping F introduced in Equation (7).

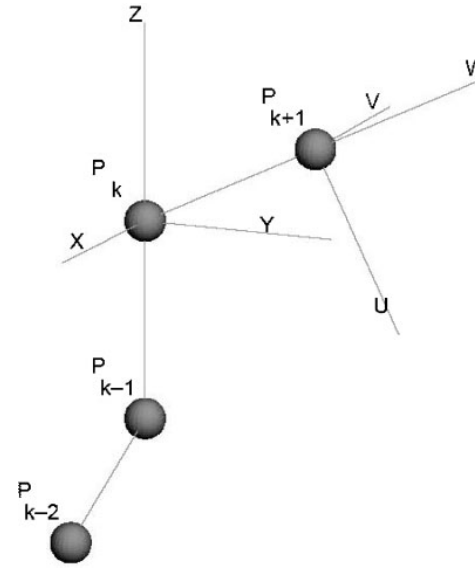

Figure 8. Two local Cartesian coordinate system are displayed. System $\Im_k$ determined by P_{k-2}, P_{k-1} and P_k and system $\Im_{k+1}$ determined by P_{k-1}, P_k and P_{k+1}.

A.1.1. Definitions and notation

Consider, for a given Cartesian system, four distinct points $P_{k-2}, P_{k-1}, P_k, P_{k+1} \in \mathbb{R}^3$. Introduce the vectors $\vec{a}, \vec{b}$ and $\vec{c}$

$$\vec{a} = \frac{P_{k-1} - P_{k-2}}{\|P_{k-1} - P_{k-2}\|}$$
$$\vec{b} = \frac{P_k - P_{k-1}}{\|P_k - P_{k-1}\|}$$
$$\vec{c} = \frac{P_{k+1} - P_k}{\|P_{k+1} - P_k\|}$$

see Figure 8.

DEFINITION A.1. *The torsion angle or dihedral angle* $\mathrm{Tor}(P_{k-2}, P_{k-1}, P_k, P_{k+1})$ *for a sequence of four points* $P_{k-2}, P_{k-1}, P_k, P_{k+1}$ *is, expressed in terms of* $\vec{a}, \vec{b}$ *and* $\vec{c}$,

$$\mathrm{Tor}(P_{k-2}, P_{k-1}, P_k, P_{k+1}) = \arg\left(\begin{pmatrix} -\vec{a}\cdot\vec{c} + (\vec{a}\cdot\vec{b})(\vec{b}\cdot\vec{c}) \\ \vec{a}\cdot(\vec{b}\times\vec{c}) \end{pmatrix}, \begin{pmatrix} 1 \\ 0 \end{pmatrix} \right)$$

where the arg *function denotes the planar angle between two vectors and takes its values in* $(-\pi, \pi]$. *In this Appendix, we will use the shorter notation* $\tau_{k-2;\,k-1;\,k;\,k+1}$ *for* $Tor(P_{k-2}, P_{k-1}, P_k, P_{k+1})$.

Note that the torsion angle between $\vec{a}, \vec{b}$ and $\vec{c}$ is undefined if ($\vec{b}$ and $\vec{c}$) or ($\vec{a}$ and $\vec{b}$) are parallel.

For an intuitive geometric interpretation of the torsion angle $\tau_{k-2;\,k-1;\,k;\,k+1}$ consider two planes A and B spanned by respectively P_{k-2}, P_{k-1}, P_k and P_{k-1}, P_k, P_{k+1}, the torsion angle

$\tau_{k-2;\,k-1;\,k;\,k+1}$ unites the two planes by rotating the plane A around $\vec{b}$ by an angle $\tau_{k-2;\,k-1;\,k;\,k+1} \in (-\pi;\,\pi]$.

DEFINITION A.2. *The bond angle $b_{k-1;\,k;\,k+1}$ between P_{k-1}, P_k, P_{k+1} is the numerical value of the planar angle $\angle_{P_{k-1}P_kP_{k+1}}$, which expressed in terms of $\vec{b}$ and $\vec{c}$ is*

$$b_{k-1;\,k;\,k+1} = \mathrm{Bind}(P_{k-1}, P_k, P_{k+1}) = |\arg\left(\vec{b}, \vec{c}\right)|$$

DEFINITION A.3. *The distance $d_{k-1;\,k}$ between P_{k-1}, P_k is the euclidian distance $\|P_k - P_{k-1}\|$.*

A.1.2. Sequential specification of a molecule through torsion angles, bond angles and distances

Assume we want to build an m-membered ring, how many torsion angles, bond angles and distances do we have to specify? To define the relative positions of the first two atoms, it is enough to specify the distance $d_{1;\,2}$. The position of the third atom will be fixed if we specify further $d_{2;\,3}$ and the bond angle $b_{1;\,2;\,3}$, while to position the fourth atom we will need $d_{2;\,4}$, $b_{2;\,3;\,4}$ and the torsion angle $\tau_{1;\,2;\,3;\,4}$. From there on, an additional atom requires the specification of one more distance, one more bond angle and one more torsion angle. The procedure is summarized in

$$P_1 \xrightarrow{d_{1;\,2}} P_2 \xrightarrow{d_{2;\,3},\, b_{1;\,2;\,3}} P_3 \xrightarrow[[\tau_{1;\,2;\,3;\,4}]]{d_{3;\,4},\, b_{2;\,3;\,4}} P_4 \rightarrow \ldots \xrightarrow[[\tau_{k-3;\,k-2;\,k-1;\,k}]]{d_{k-1;\,k},\, b_{k-2;\,k-1;\,k}} P_k \rightarrow \ldots$$

As a conclusion, we can build sequentially an m-membered ring if we specify the first $m-1$ distances, $m-2$ bond angles and $m-3$ torsion angles.

A.1.3. Description of the F mapping

The goal of this subsection is to obtain a description of the F mapping that relates the torsion angles, bond angles and distances of an m-membered ring through

$$(\tau_{1:m}, b_{1:m}, d_{1:m}) = F(\tau_{1:m-3}, b_{1:m-2}, d_{1:m-1})$$

For any $k = 3, \ldots, m$, we associate to the sequence of three points P_{k-2}, P_{k-1} and P_k, the local Cartesian system $\mathfrak{S}_k$, with an orthonormal basis $\vec{x}^{\mathfrak{S}_k}$, $\vec{y}^{\mathfrak{S}_k}$ and $\vec{z}^{\mathfrak{S}_k}$, such that the origin is in P_k, the vectors $\overrightarrow{P_{k-1}P_k}$ and $\vec{z}^{\mathfrak{S}_k}$ are parallel and pointing in the same direction, and such that $(\overrightarrow{P_{k-2}P_{k-1}} \times \overrightarrow{P_{k-1}P_k})$ and $\vec{y}^{\mathfrak{S}_k}$ are parallel and pointing in the same direction. In Figure 8 the local Cartesian coordinate system $\mathfrak{S}_k$ is specified by (X, Y, Z).

The description of F will involve the characterization of the coordinates of the m atoms of the ring in $\mathfrak{S}_m$, in terms of the first $m-1$ distances, $m-2$ bond angles and $m-3$ torsion angles.

PROPOSITION A.1. *The coordinates of $P_1, \ldots, P_m$ in $\mathfrak{S}_m$ can be obtained sequentially by the following algorithm*

Initialization: *Consider the coordinates of P_1, P_2 and P_3 in $\mathfrak{S}_3$:*

$$P_1^{\mathfrak{S}_3} = \left(d_{1;\,2}\sin\left(b_{1;\,2;\,3}\right),\ 0,\ d_{1;\,2}\cos\left(b_{1;\,2;\,3}\right) - d_{2;\,3}\right)'$$
$$P_2^{\mathfrak{S}_3} = \left(0,\ 0,\ -d_{2;\,3}\right)'$$
$$P_3^{\mathfrak{S}_3} = (0,\ 0,\ 0)'$$

For $k = 3$ **to** $m-1$, **do:**] *From the coordinates $(P_1^{\mathfrak{S}_k}, \ldots, P_k^{\mathfrak{S}_k})$ of $P_1, \ldots, P_k$ in $\mathfrak{S}_k$, deduce the coordinates $(P_1^{\mathfrak{S}_{k+1}}, \ldots, P_k^{\mathfrak{S}_{k+1}})$ of $P_1, \ldots, P_k$ in $\mathfrak{S}_{k+1}$, through the relation, for $i = 1, \ldots, k$,*

$$P_i^{\mathfrak{S}_{k+1}} = \mathfrak{T}_{\mathfrak{S}_k, \mathfrak{S}_{k+1}}\left(P_i^{\mathfrak{S}_k}\right) = B_{b_{k-1;\,k;\,k+1}} A_{\tau_{k-2;\,k-1;\,k;\,k+1}} P_i^{\mathfrak{S}_k} + C_{d_{k;\,k+1}} \tag{17}$$

with

$$A_{\tau_{k-2;\,k-1;\,k;\,k+1}} = \begin{bmatrix} \cos\left(\tau_{k-2;\,k-1;\,k;\,k+1}\right) & -\sin\left(\tau_{k-2;\,k-1;\,k;\,k+1}\right) & 0 \\ \sin\left(\tau_{k-2;\,k-1;\,k;\,k+1}\right) & \cos\left(\tau_{k-2;\,k-1;\,k;\,k+1}\right) & 0 \\ 0 & 0 & 1 \end{bmatrix}$$

whereas

$$B_{b_{k-1;\,k;\,k+1}} = \begin{bmatrix} -\cos\left(b_{k-1;\,k;\,k+1}\right) & 0 & -\sin\left(b_{k-1;\,k;\,k+1}\right) \\ 0 & 1 & 0 \\ \sin\left(b_{k-1;\,k;\,k+1}\right) & 0 & -\cos\left(b_{k-1;\,k;\,k+1}\right) \end{bmatrix}$$

and $C_{d_{k;\,k+1}} = (0,\ 0,\ -d_{k;\,k+1})'$. Moreover set $P_{k+1}^{\mathfrak{S}_{k+1}} = (0,0,0)'$.

Proof. Proposition A.1 is easily deduced from the following lemma:

LEMMA A.2. *Let P a point of $\mathbb{R}^3$, its coordinates in $\mathfrak{S}_k$ and $\mathfrak{S}_{k+1}$ are related through*

$$P^{\mathfrak{S}_{k+1}} = \mathfrak{T}_{\mathfrak{S}_k, \mathfrak{S}_{k+1}}\left(P^{\mathfrak{S}_k}\right) = B_{b_{k-1;\,k;\,k+1}} A_{\tau_{k-2;\,k-1;\,k;\,k+1}} P_i^{\mathfrak{S}_k} + C_{d_{k;\,k+1}} \tag{18}$$

where $A_{\tau_{k-2;\,k-1;\,k;\,k+1}}$, $B_{b_{k-1;\,k;\,k+1}}$ and $C_{d_{k;\,k+1}}$ are defined in Proposition A.1.

Proof. From the definition of $\mathfrak{S}_k$ and $\mathfrak{S}_{k+1}$ it is easily checked that

$$\begin{aligned} \arg\left(\vec{z}^{\mathfrak{S}_k}, \vec{z}^{\mathfrak{S}_{k+1}}\right) &= \pi - b_{k-1;\,k;\,k+1} \\ \arg\left(\vec{y}^{\mathfrak{S}_k}, \vec{y}^{\mathfrak{S}_{k+1}}\right) &= \tau_{k-2;\,k-1;\,k;\,k+1} \end{aligned},$$

see Figure 8, where $\mathfrak{S}_k$ is indicated with X, Y, Z and $\mathfrak{S}_{k+1}$ indicated with U, V, W. Hence we can transform $\mathfrak{S}_{k+1}$ into $\mathfrak{S}_k$, by the rotation of angle $-\tau_{k-2;\,k-1;\,k;\,k+1}$ around $\vec{z}^{\mathfrak{S}_k}$, next by the rotation of angle $-(\pi - b_{k-1;\,k;\,k+1})$ around $\vec{y}^{\mathfrak{S}_k}$ and finally by the translation of vector $(0, 0, -d_{k;\,k+1})'$. These transformations are presented graphically in Figure 9. Let us denote by $\mathfrak{T}_{\mathfrak{S}_k, \mathfrak{S}_{k+1}}$ the resulting transformation, composition of the two rotations and the translation. It is easy to check that, since the angles and distances are preserved by rotations and translations, the coordinates of a given point P in $\mathfrak{S}_{k+1}$ are equal to the coordinates of its image $\mathfrak{T}_{\mathfrak{S}_k, \mathfrak{S}_{k+1}}(P)$ in $\mathfrak{S}_k$. We deduce Equation (18) after checking that $A_{\tau_{k-2;\,k-1;\,k;\,k+1}}$, $B_{b_{k-1;\,k;\,k+1}}$ and $C_{d_{k;\,k+1}}$ are the matrices of the involved rotations and translation.

We are now able to provide an operational description of F which will suit our purposes:

Starting from the first $m-3$ torsion angles $\mu_{1:m-3}$, the first $m-2$ bond angles $b_{1:m-2}$ and the first $m-1$ distances $d_{1:m-1}$ that define a ring $A_1, A_2, \ldots, A_m$ (the convention used to number the torsion-, bond angles and distances in such a ring is described in (4)–(6)), use the algorithm described in Proposition A.1 to obtain the coordinates of the m atoms $A_1, A_2, \ldots, A_m$ in $\mathfrak{S}_m$. Deduce from these coordinates the remaining

$$\begin{aligned} \mu_{m-2:m} &= \left(\tau_{m-2;\,m-1;\,m;\,1}, \tau_{m-1;\,m;\,1;\,2}, \tau_{m;\,1;\,2;\,3}\right) \\ b_{m-1:m} &= \left(b_{m-1;\,m;\,1}, b_{m;\,1;\,2}\right) d_m = d_{m;\,1} \end{aligned}$$

This provides

$$(\mu_{1:m}, b_{1:m}, d_{1:m}) = F(\mu_{1:m-3}, b_{1:m-2}, d_{1:m-1}) \tag{19}$$

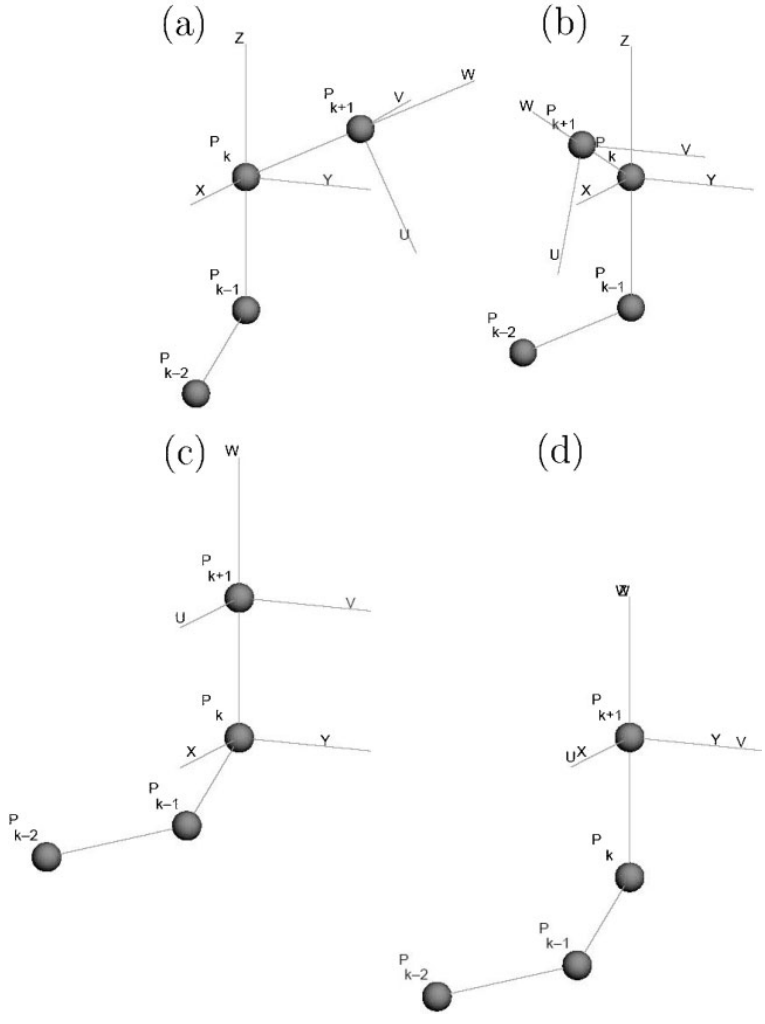

Figure 9. The decomposition of the transformation $\mathfrak{T}_{\Xi}k, \Xi_{k+1}$ of a structure $P_{k-2}, P_{k-1}, P_k, P_{k+1}$, described in the proof of Lemma A.2: starting from (a), the structure is rotated around $\vec{z}^{\Xi_k}$ by $-\tau_{k-2;\,k-1;\,k;\,k+1}$, resulting in (b), next rotated by angle $-(\pi - b_{k-1;\,k;\,k+1})$ around $\vec{y}^{\Xi_k}$ resulting in (c) and finally translated to the origin of S_k, (d).

A.2. Acceptance probabilities

We present the log acceptance probabilities $\log(\rho)$ for the different move-types in the Reversible Jump implementation for the m-membered ring structures application. The expressions follow to some extent the presentation from Reference [13].

Let l, p and f denote the likelihood, the prior- and proposal-distributions respectively. θ^* indicates the proposed state and θ is the current state of the sampler. The probability of accepting the value θ^* given that we are currently in the state θ is given by $\rho = \min(r, 1)$, where

$$\begin{aligned}\log(r) = {} & \log l(\tau_{1:n} \mid \theta^*) + \log(p(\theta^*)) - \log(f(\theta^* \mid \theta)) \\ & - \log l(\tau_{1:n} \mid \theta) - \log(p(\theta)) + \log(f(\theta \mid \theta^*))\end{aligned} \tag{20}$$

The Subsections A.2.1 and A.2.2 contain descriptions of the proposal distributions and the deduced expressions for $\log(r)$ for the fixed k moves and the birth/death moves.

A.2.1. Fixed k moves

For $w_{1:k}$:

(a) Proposal: Normalized multiplicative perturbation $\otimes$Log normal$(0,\eta)$, for details, see Reference 13,

$$\log\big(f(w_{1:k} \mid w^*_{1:k})\big) - \log\big(f(w^*_{1:k} \mid w_{1:k})\big) = \sum_{i=1}^{k} \log\left(\frac{w^*_i}{w_i}\right)$$

(b) Prior: Dirichlet $(\mathfrak{D}(\delta)$ with $\delta_{1:k-1} = 1)$

$$\log\big(p(w^*_{1:k})\big) - \log(p(w_{1:k})) = \sum_{i=1}^{k} (\delta_i - 1)\log\left(\frac{w^*_i}{w_i}\right) = 0$$

(c) $\log(r)$:

$$\log(r) = \log l(\tau_{1:n} \mid \theta^*) - \log l(\tau_{1:n} \mid \theta) + \sum_{i=1}^{k} \log\left(\frac{w^*_i}{w_i}\right)$$

For $(\mu_{1:k,1:m}, b_{1:k,1:m}, d_{1:k,1:m})$:

(a) Proposal: For $(\mu_{1:k,1:m-3}, b_{1:k,1:m-2}, d_{1:k,1:m-1})$, normal perturbation

$$\underset{1:k}{\otimes} \underset{1:(m-3)}{\otimes} \mathcal{N}\Big(0, \sigma^2_{\epsilon_\mu}\Big) \underset{1:k}{\otimes} \underset{1:(m-2)}{\otimes} \mathcal{N}\Big(0, \sigma^2_{\epsilon_b}\Big) \underset{1:k}{\otimes} \underset{1:(m-1)}{\otimes} \mathcal{N}\Big(0, \sigma^2_{\epsilon_d}\Big)$$

As for the remaining $(\mu^*_{1:k,m-2:m}, b^*_{1:k,m-1:m}, d^*_{1:k,m})$, they are computed from the deterministic mapping, for all $1 \le c \le k$,

$$\Big(\mu^*_{c,1:m}, b^*_{c,1:m}, d^*_{c,1:m}\Big) = F\Big(\mu^*_{c,1:m-3}, b^*_{c,1:m-2}, d^*_{c,1:m-1}\Big), \qquad (21)$$

described in Subsection A.1.3.
Moreover we add, as described in Subsection 4.2, an additional restriction on the candidate, namely it should satisfy, for all $c = 1, \ldots, k$ and $i = 1, \ldots, m$,

$$b^*_{c,i} \in \Big[\eta^b_i \pm 2\sqrt{\kappa^b}\Big] \quad d^*_{c,i} \in \Big[\eta^d_i \pm 2\sqrt{\kappa^d}\Big]$$

For candidates that satisfy Equation (21), it is easy to prove that

$$\begin{aligned} &f\Big(\mu^*_{1:k,1:m}, b^*_{1:k,1:m}, d^*_{1:k,1:m} \mid \mu_{1:k,1:m}, b_{1:k,1:m}, d_{1:k,1:m}\Big) \\ &= f\Big(\mu^*_{1:k,1:m-3}, b^*_{1:k,1:m-2}, d^*_{1:k,1:m-1} \mid \mu_{1:k,1:m-3}, b_{1:k,1:m-2}, d_{1:k,1:m-1}\Big) \end{aligned} \qquad (22)$$

Moreover,

$$\begin{aligned} &\log\big(f(\mu^*_{1:k,1:(m-3)}, b^*_{1:k,1:(m-2)}, d^*_{1:k,1:(m-1)} \mid \\ &\quad \mu_{1:k,1:(m-3)}, b_{1:k,1:(m-2)}, d_{1:k,1:(m-1)})\big) \\ &- \log\big(f(\mu_{1:k,1:(m-3)}, b_{1:k,1:(m-2)}, d_{1:k,1:(m-1)} \mid \\ &\mu^*_{1:k,1:(m-3)}, b^*_{1:k,1:(m-2)}, d^*_{1:k,1:(m-1)})\big) = 0 \end{aligned}$$

(b) Prior: for $(\mu_{1:k,1:m-3}, b_{1:k,1:m-2}, d_{1:k,1:m-1})$

$$\begin{aligned} \underset{1:k}{\otimes} \underset{1:(m-3)}{\otimes} U(-\pi,\pi) &\underset{1:k}{\otimes} \mathcal{N}\Big(\eta^b_{1:(m-2)}, \kappa^b \mathbf{I}d_{m-2}\Big) \\ &\underset{1:k}{\otimes} \mathcal{N}\Big(\eta^d_{1:(m-1)}, \kappa^d \mathbf{I}d_{m-1}\Big) \end{aligned}$$

As for the remaining $(\mu_{1:k,m-2:m}, b_{1:k,m-1:m}, d_{1:k,m})$, they are deduced from the deterministic mapping, for all $1 \le c \le k$,

$$\Big(\mu^*_{c,1:m}, b^*_{c,1:m}, d^*_{c,1:m}\Big) = F\Big(\mu^*_{c,1:m-3}, b^*_{c,1:m-2}, d^*_{c,1:m-1}\Big)$$

described in Subsection A.1.3.

As a consequence,

$$\begin{aligned} &\log\big(p(\mu^*_{1:k,1:(m-3)}, b^*_{1:k,1:(m-2)}, d^*_{1:k,1:(m-1)})\big) \\ &- \log\big(p(\mu_{1:k,1:(m-3)}, b_{1:k,1:(m-2)}, d_{1:k,1:(m-1)})\big) \\ &= \sum_{c=1}^{k} \Bigg[\sum_{i=1}^{m-2} \frac{b^2_{ci} - b^{*2}_{ci} - 2\eta^b_i(b_{ci} - b^*_{ci})}{2\kappa^b} \\ &\quad + \sum_{i=1}^{m-1} \frac{d^2_{ci} - d^{*2}_i - 2\eta^d_i(d_{ci} - d^*_{ci})}{2\kappa^d}\Bigg] \end{aligned}$$

(c) $\log(r)$:

$$\begin{aligned} \log(r) = \log l(\tau_{1:n} \mid \theta^*) &- \log l(\tau_{1:n} \mid \theta) \\ &+ \sum_{c=1}^{k} \Bigg[\sum_{i=1}^{m-2} \frac{b^2_{ci} - b^{*2}_{ci} - 2\eta^b_i(b_{ci} - b^*_{ci})}{2\kappa^b} \\ &+ \sum_{i=1}^{m-1} \frac{d^2_{ci} - d^{*2}_{ci} - 2\eta^d_i(d_{ci} - d^*_{ci})}{2\kappa^d}\Bigg] \end{aligned}$$

For $\sigma^2_{1:k}$:

(a) Proposal: Normalized multiplicative distribution $\otimes$Log normal$(0,\nu)$

$$\log\Big(f\Big(\sigma^2_{1:k} \mid \sigma^{2*}_{1:k}\Big)\Big) - \log\Big(f\Big(\sigma^{2*}_{1:k} \mid \sigma^2_{1:k}\Big)\Big) = \sum_{c=1}^{k} \log\left(\frac{\sigma^{2*}_c}{\sigma^2_c}\right)$$

(b) Prior: Inverse Gamma $(\mathfrak{IG}(\alpha,\beta))$

$$\begin{aligned} \log\big(p(\sigma^{2*}_{1:k})\big) - \log\big(p(\sigma^2_{1:k})\big) &= (\alpha+1)\sum_{c=1}^{k} \log\left(\frac{\sigma^2_c}{\sigma^{2*}_c}\right) \\ &+ \frac{1}{\beta}\sum_{c=1}^{k}\left(\frac{1}{\sigma^2_c} - \frac{1}{\sigma^{2*}_c}\right) \end{aligned}$$

(c) $\log(r)$:

$$\begin{aligned} \log(r) = \log l(\tau_{1:n} \mid \theta^*) &- \log l(\tau_{1:n} \mid \theta) \\ &+ \alpha\sum_{c=1}^{k} \log\left(\frac{\sigma^2_c}{\sigma^{2*}_c}\right) + \frac{1}{\beta}\sum_{c=1}^{k}\left(\frac{1}{\sigma^2_c} - \frac{1}{\sigma^{2*}_c}\right) \end{aligned}$$

A.2.2. Birth or death moves

Birth: For k components, the proposal for the $k+1$-th component is constructed by drawing respectively

1. $w^*_{k+1} \sim Be(1,k)$ followed by a re-normalization $w^*_{1:k+1} = ((1 - w^*_{k+1})w_{1:k}, w^*_{k+1})$.
2. For $(\mu_{k+1,1:m-3}, b_{k+1,1:m-2}, d_{k+1,1:m-1})$,

$$\underset{1:(m-3)}{\otimes} U(-\pi,\pi) \otimes \mathcal{N}\Big(\eta^b_{1:(m-2)}, \kappa^b \mathbf{I}d_{m-2}\Big) \otimes \mathcal{N}\Big(\eta^d_{1:(m-1)}, \kappa^d \mathbf{I}d_{m-1}\Big)$$

As for the remaining $(\mu_{k+1,m-2:m}, b_{k+1,m-1:m}, d_{k+1,m})$, they are deduced from the deterministic mapping,

$$\Big(\mu^*_{k+1,1:m}, b^*_{k+1,1:m}, d^*_{k+1,1:m}\Big) = F\Big(\mu^*_{k+1,1:m-3}, b^*_{k+1,1:m-2}, d^*_{k+1,1:m-1}\Big)$$

described in Subsection A.1.3.
3. $\sigma^{2*}_{k+1} \sim \mathfrak{IG}(\alpha,\beta)$.

The expression of the acceptance probability for the birth-death move is deduced as in Reference [9], $P_d(k+1)$ and $P_b(k)$ respectively being the death probability in space $k+1$ and the birth probability in space k. $P_d(k+1)$ and $P_b(k)$ were

chosen such that $P_d(k+1) = P_b(k) = c$ for $k = 1, \ldots, k_{\max}$ otherwise $P_d(1) = 0$ and $P_b(k_{\max}) = 0$

$$\begin{aligned} r &= \frac{(k+1)!l(\tau_{1:n} \mid \theta_{1:k+1})p(\theta_{1:k+1})}{k!l(\tau_{1:n} \mid \theta_{1:k})p(\theta_{1:k})} \frac{\frac{P_d(k+1)}{k+1}}{P_b(k)} \frac{1}{p(u)} \\ &= \frac{l(\tau_{1:n} \mid \theta_{1:k+1})}{l(\tau_{1:n} \mid \theta_{1:k})} \frac{P_d(k+1)}{P_b(k)} \frac{p(\theta_{1:k+1})}{p(\theta_{1:k})p(u)} \\ &= \frac{l(\tau_{1:n} \mid \theta_{1:k+1})}{l(\tau_{1:n} \mid \theta_{1:k})} \frac{P_d(k+1)}{P_b(k)} \end{aligned}$$

As for the death move, a component is chosen randomly among the existing components and is killed with probability $1/r$, where r is given above.

REFERENCES

1. Meyer TJ. Chemical approaches to artificial photosynthesis. *Acc. Chem. Res.* 1989; **22**: 163–170.
2. Hendrickson JB. Molecular geometry. vii. Modes of interconversion in the medium rings. *J. Am. Chem. Soc.* 1967; **89**: 7047–7054.
3. Zimmer M. Molecular mechanics, data and conformational analysis of first-row transition metal complexes in the cambridge strutural database. *Coord. Chem. Rev.* 2001; **212**: 133–163.
4. Green PJ. Reversible jump Markov chain Monte Carlo computation and Bayesian model determination. *Biometrika* 1995; **82**: 711–732.
5. Allen FH, Howard JAK, Pitchford NA. Symmetry-modified conformational mapping and classification of the medium rings from crystallographic data. iv. cyclooctane and related eight-membered rings. *Acta Cryst.* 1996; **B52**: 882–891.
6. Mass W. *Crystal Structure Determination*. Springer-Verlag: Berlin (second edition), 2004.
7. Banfield JD, Raftery AE. Model-based Gaussian and non-Gaussian clustering. *Biometrics* 1993; **49**: 803–821.
8. Richardson S, Green PJ. Corrigendum: on Bayesian analysis of mixtures with an unknown number of components. *J. Roy. Statist. Soc. Ser. B* 1997; **59**: 731–792. *J. R. Stat. Soc. Ser. B Stat. Methodol.* 1998; **60**: 661.
9. Cappé O, Robert CP, Rydén T. Reversible jump, birth-and-death and more general continuous time Markov chain Monte Carlo samplers. *J. R. Stat. Soc. Ser. B. Stat. Methodol.* 2003; **65**: 679–700.
10. Dunitz JD. Conformations of medium rings. In *Perspectives in Structural Chemistry*, Vol II, Dunitz JD, Ibers JA (eds). John Wiley: New York, 1968.
11. Robert CP, Casella G. *Monte Carlo statistical methods*. Springer texts in statistics (second edition). Springer-Verlag: New York, 2004.
12. Dellaportas P, Papageorgiou I. Multivariate mixtures of normals with unknown number of components. Technical report, Department of Statitics, Athens University of Economics and Finance, 2004.
13. Cappé O, Robert CP, Rydén T. Manual for ctrjmix. Technical report, Département TSI, Ecole Nationale Supérieure des Télćommunications, 2003. http://www.tsi.enst.fr/∼cappe/ctrj_mix/
14. Celeux G, Hurn M, Robert CP. Computational and inferential difficulties with mixture posterior distributions. *J. Amer. Statist. Assoc.* 2000; **95**: 957–970.
15. Stephens M. Dealing with label switching in mixture models. *J. R. Stat. Soc. Ser. B Stat. Methodol.* 2000; **62**: 795–809.
16. Cappé O, Moulines E, Rydén T. *Inference in Hidden Markov Models*. Springer texts in statistics. Springer-Verlag: New York, 2005.
17. Celeux G. Bayesian inference for mixtures, the label-switching problem. In *COMPSTAT 1998* 1998; Physica, Heidelberg, 227–232.
18. Stephens M. *Bayesian Inference for Mixtures of Normal Distributions*. PhD dissertation, Oxford, 1997.

Paper II

II

Bayesian methods for the conformational classification of eight-membered rings

Published in *Acta Crystallographica Section B*, **61**(5):585-594 (2005)

electronic reprint

Acta Crystallographica Section B
Structural Science
ISSN 0108-7681
Editor: **Carolyn P. Brock**

Bayesian methods for the conformational classification of eight-membered rings

J. Pérez, K. Nolsøe, M. Kessler, L. García, E. Pérez and J. L. Serrano

research papers

Acta Crystallographica Section B
Structural Science
ISSN 0108-7681

Bayesian methods for the conformational classification of eight-membered rings

J. Pérez,[a]* K. Nolsøe,[b] M. Kessler,[b]* L. García,[a] E. Pérez[a] and J. L. Serrano[a]

[a]Departamento de Ingeniería Minera, Geológica y Cartográfica, Área de Química Inorgánica, Universidad Politécnica de Cartagena, Spain, and [b]Departamento de Matemática Aplicada y Estadística, Universidad Politécnica de Cartagena, Spain

Correspondence e-mail: jose.pperez@upct.es, mathieu.kessler@upct.es

Received 13 May 2005
Accepted 26 July 2005

Two methods for the classification of eight-membered rings based on a Bayesian analysis are presented. The two methods share the same probabilistic model for the measurement of torsion angles, but while the first method uses the canonical forms of cyclooctane and, given an empirical sequence of eight torsion angles, yields the probability that the associated structure corresponds to each of the ten canonical conformations, the second method does not assume previous knowledge of existing conformations and yields a clustering classification of a data set, allowing new conformations to be detected. Both methods have been tested using the conformational classification of Csp^3 eight-membered rings described in the literature. The methods have also been employed to classify the solid-state conformation in Csp^3 eight-membered rings using data retrieved from an updated version of the Cambridge Structural Database (CSD).

1. Introduction

The conformational analysis of organic (Allen & Motherwell, 2002) and metallic complexes (Zimmer, 2001) is an active research area, the CSD being a powerful tool in this kind of study (Allen & Taylor, 2004; Orpen, 1993). Despite the large amount of structural data available, a full understanding of the factors that determine the molecular structure of a particular compound has not yet been achieved. In coordination and organometallic chemistry the manner in which a ligand controls the properties of the complex depends on a combination of steric, electronic and conformational factors. Detailed knowledge of these effects will allow a rational design of complexes with specific and predictable properties (Meyer, 1989).

A review of the different statistical methods for conformation analysis can be found in Zimmer (2001). Reviews such as this generally take a data-analysis approach where no model is assumed for the data generation mechanism, and all the conclusions rely on the correlation structure of the data or their similarities. Cluster analysis and principal-component analysis are examples of such methods. In contrast, an essential step in our approach consists of specifying a probabilistic model for the observed sequences of torsion angles. This model is mainly based on assuming that the sequences of torsion angles are generated, after a perturbation that takes into account measurement errors, from a number k of 'preferred' conformations. Two levels of generality can then be chosen: either the 'preferred' conformations are assumed to be provided, *a priori*, by the user; for example, they could consist of the ten canonical conformations for cyclooctane, as described in Hendrickson (1967) and shown in Fig. 1; or no assumption is made about the 'preferred' conformations nor

research papers

about their number. Associated with these two levels of generality, we propose the following two methods:

(i) First level of generality: the 'preferred' conformations are provided by the user: an individual classification of the observed structures is performed. Based on the eight values of the torsion angles for a structure, it is possible, through Bayes' rule, to compute the posterior probability that the structure comes from each of the preferred conformations. These probabilities provide more information than only a classification: their relative order of magnitude indicates, in particular, the strength of the evidence in the data in favour of a given conformation. Likewise, similarities between conformations can be detected. We will refer to this method as the '*Classification method*'.

(ii) Second level of generality: no previous knowledge of the 'preferred' conformations is assumed: Bayesian inference on the number of conformations, the conformations themselves, their frequencies of occurrence, as well as the standard deviations associated to each conformation were determined. As a result of the Bayesian approach, a posterior distribution for each of the parameters of interest can be obtained. The structures in each of the obtained conformations can also be classified. We will refer to this method as the '*Full Bayesian Analysis method*'.

Notice that the Classification method performs the individual classification of structures but requires *a priori* specification of the 'preferred' conformations. The Full Bayesian Analysis applies to a set of structures but allows for the detection of new conformations and is not dependent on theoretical canonical conformations.

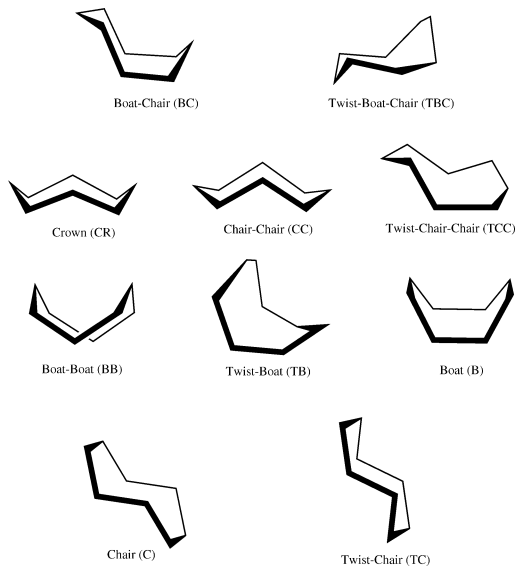

Figure 1
Canonical forms of cyclooctane.

In order to test the methods described in this article we have studied the data of the Csp^3 eight-membered rings analyzed by Allen and co-workers (Allen *et al.*, 1996) using cluster and principal components techniques. We have also studied the data of Csp^3 eight-membered rings extracted from an updated CSD version. It is to be stressed that the proposed methods can easily be extended to rings with differing numbers of atoms.

2. Theory

2.1. The model

The eight torsion angles observed for a given structure retrieved from the CSD are denoted by $\boldsymbol{\tau} = (\tau_1, \tau_2, \tau_3, \tau_4, \tau_5, \tau_6, \tau_7, \tau_8)$. The model we assume for the data-generation mechanism resulting in a realisation of $\boldsymbol{\tau}$ is built up in three steps:

(i) Randomly choose one of the k 'preferred' conformations, according to the probabilities $p_1, p_2, \ldots, p_k$. These probabilities are unknown parameters that correspond to the natural frequency of occurrence of each 'preferred' conformation. We denote by C the index of the chosen conformation (C thus ranges from 1 to k).

(ii) Let $\boldsymbol{\mu}(C) = (\mu_{C,1}, \mu_{C,2}, \mu_{C,3}, \mu_{C,4}, \mu_{C,5}, \mu_{C,6}, \mu_{C,7}, \mu_{C,8})$ be the sequence of torsion angles associated with conformation C. The observed values of the torsion angles in τ may correspond to a different starting point in the structure than that in the canonical sequence $\boldsymbol{\mu}(C)$. To take this fact into account, a starting point v between 1 and 8 was randomly chosen, with equal probabilities and the cyclically translated sequence

$$\mu(C, v) = (\mu_{C,v}, \mu_{C,((v) \bmod 8+1)}, \mu_{C,(v+1) \bmod 8+1}, \ldots, \mu_{C,(v+6) \bmod 8+1})$$

was constructed, where, for any integer j, j mod 8 denotes j modulo 8, *i.e.* the remainder of the integer division of j by 8. Moreover, the sequence of torsion angles can be read in a clockwise or counter-clockwise manner. The counter-clockwise version of $\boldsymbol{\mu}(\mathrm{C},v)$ is readily obtained as

$$\mu(C, v) = (\mu_{C,v}, \mu_{C,(v+6) \bmod 8+1}, \mu_{C,(v+5) \bmod 8+1}, \ldots, \mu_{C,(v \bmod 8+1)}).$$

Let us now introduce the variable d which takes the values 1 or -1 according to whether the direction of the rotation is clockwise or counter-clockwise. The two previous formulae can now be summarized as

$$\mu(C, v, d) = (\mu_{C,v,\mu C,(v-1+d\times 1) \bmod 8+1}, \mu_{C,(v-1+d\times 2) \bmod 8+1}, \ldots, \mu_{C,(v-1+d\times 7) \bmod 8+1}).$$

It is also necessary to consider the coordinate inversions from which sequences of torsion angles are readily obtained by a change of sign. We therefore introduce the random variable δ which can take either the value 1 or -1 with equal probabilities and

$$\mu(C, v, d, \delta) = \delta \times (\mu_{C,v,\mu C,(v-1+d\times 1) \bmod 8+1}, \mu_{C,(v-1+d\times 2) \bmod 8+1}, \ldots, \mu_{C,(v-1+d\times 7) \bmod 8+1}).$$

As an example, consider conformation BC, index C = 1 in *Appendix A*, we have

$$\mu(1, 2, -1, 1) = (44.7, 65.0, -65.0, -44.7, 102.2, -65.0, 65.0, -102.2).$$

(iii) Finally, we consider that the observed sequence is obtained from $\mu(C, \nu, d, \delta)$ after an additive perturbation $\boldsymbol{\varepsilon} = (\varepsilon_1, \varepsilon_2, \varepsilon_3, \varepsilon_4, \varepsilon_5, \varepsilon_6, \varepsilon_7, \varepsilon_8)$, that is

$$\tau = \mu(C, \nu, d, \delta) + \varepsilon,$$

where the perturbation's components $\varepsilon_1, \varepsilon_2, \varepsilon_3, \varepsilon_4, \varepsilon_5, \varepsilon_6, \varepsilon_7, \varepsilon_8$ are assumed to be independent Gaussian random variables with a zero mean and then unknown variance parameter σ_c^2, which may depend on the conformation C.

As a conclusion, from the relation between $\boldsymbol{\tau}, \boldsymbol{\mu}(C, \nu, \delta)$ and ε, in step (iii) we deduce that the density $(\tau_1, \tau_2, \tau_3, \tau_4, \tau_5, \tau_6, \tau_7, \tau_8) \rightarrow f(\tau_1, \tau_2, \tau_3, \tau_4, \tau_5, \tau_6, \tau_7, \tau_8)$ of the random variable τ is easily computable: it is a mixture of multivariate laws

$$f(\tau) = \sum_{c=1,\ldots,k} p_c f(\tau, c),$$

where $f(\boldsymbol{\tau}, \mathbf{c})$ are themselves mixtures of multivariate Gaussian laws

$$f(\tau, c) = \sum_{\nu=1,\ldots,8} \sum_{d=-1,1} \sum_{\delta=-1,1} f_G\left(\tau, \mu(c, \nu, d, \delta), \sigma_c^2\right),$$

$\boldsymbol{\tau} \rightarrow f_G\,(\boldsymbol{\tau}, \boldsymbol{\mu}(c, \nu, d, \delta), \sigma_c^2)$ denoting the density of the eight-dimensional Gaussian law with mean $\mu(c, \nu, d, \delta)$ and diagonal covariance matrix $\sigma_c^2 Id$.

When analysing torsion angle data, the symmetry of the conformation space has to be taken into account. In particular, to be able to apply the principal-component analysis, for example, the initial torsion angle data have to be expanded by symmetry. In our paper, we avoid expanding the data by incorporating the symmetries in the model formulation through the starting point, rotation direction and sign of the torsion angles, as described above.

3. The Classification method

As explained in §1, the Classification method assumes the first level of generality for the model: the 'preferred' conformations are supplied by the user. In the following these will be taken to be the ten canonical conformations crown (D_{4d}), twist-boat (S_4), boat–boat (D_{2d}), boat (D_{2d}), twist-chair–chair (D_2), chair–chair (C_{2v}), chair (C_{2h}), twist-chair (C_{2h}), twist-boat–chair (C_2) and boat–chair (C_s), as described in Allen *et al.* (1996), for example. The table in *Appendix A* contains the torsion angles corresponding to these canonical conformations.

Using Bayes' rule we are able to compute, given an observed sequence $(\tau_1, \tau_2, \tau_3, \tau_4, \tau_5, \tau_6, \tau_7, \tau_8)$, the probability that it was generated from the conformation c:

$$P(C = c|\tau = (\tau 1, \tau 2, \tau 3, \tau 4, \tau 5, \tau 6, \tau 7, \tau 8)) = pc\, f(\tau, c) \Big/ \left(\sum_{c'=1,\ldots,10} pc\, f(\tau, c') \right).$$

The computation of these probabilities requires the specification of a prior distribution both for $(p1, p2, p3, p4, p5, p6, p7, p8, p9, p10)$ and for σ_c, the standard deviation of the perturbations ε, which are to reflect our prior knowledge, if any, about these quantities. As for the proportions, we make the choice $pc = 1/10$, for $c = 1, \ldots, 10$, which means that we do not favour *a priori* any particular canonical conformation. For σ_c, if we choose $\sigma_c = 10^\circ$, from the well known property of the Gaussian law, 95% of the values taken by the perturbations will lie between -20 and 20°, which seems a reasonable range of values. We recommend repeating the analysis for different values of σ_c, in order to check that the classification results are not too sensitive to changes in values of σ_c.

For an illustration, we finish this section by applying the Classification method to the YOPPIC structure (Villar *et al.*, 1995), retrieved from the CSD containing two molecules in the asymmetric unit with torsion angles: $\boldsymbol{\tau}(a)$ = (44.93, −47.95, 98.13, −53.31, −57.89, 81.61, 13.77, −72.05) and $\boldsymbol{\tau}(b)$ = (4.58, 21.13, −89.86, 55.43, 55.75, −89.68, 15.40, 18.44). Fig. 2 illustrates the posterior probabilities of each of the 10 canonical conformations in the case of $\sigma = 10^\circ$. For both molecules the boat–chair (BC) conformation is the most likely one. In the case of YOPPIC1, the posterior probability of the BC conformation is almost one, while for YOPPIC2 a posterior probability of 0.21 is assigned to the boat–boat (BB) conformation and a posterior probability of approximately 0.79 to the BC conformation, indicating that the structure is intermediate between the BB and BC conformations.

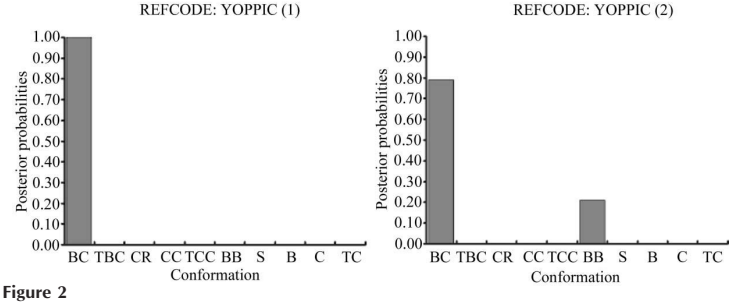

Figure 2
Posterior probabilities for the two molecules in the asymmetric unit of YOPPIC.

4. The Full Bayesian Analysis method

For this method no previous knowledge of the 'preferred' conformations is assumed, in particular, the number of these 'preferred' conformations is unknown. The parameters of the statistical model we consider are therefore: the number k of 'preferred' conformations, the k

research papers

Table 1
Conformational analysis of Csp^3 eight-membered rings in Allen *et al.* (1996) according to the methods described in this paper.

	Classification Method		Full Bayesian method
	$\sigma = 10^\circ$	$\sigma = 20^\circ$	
AMCOCA	1.00 BC	1.00 BC	$\mu(1)$
BAGPII	1.00 BC	1.00 BC	$\mu(1)$
BCOCTB	1.00 BC	1.00 BC	$\mu(1)$
CLCOCT	1.00 BC	1.00 BC	$\mu(1)$
COCOAC	1.00 BC	1.00 BC	$\mu(1)$
COCOXA10	1.00 BC	1.00 BC	$\mu(1)$
COVLUU	1.00 BC	0.99 BC; 0.01 TBC	$\mu(2)$
CURBIA	1.00 BC	1.00 BC	$\mu(1)$
CUVZEY	1.00 BC	1.00 BC	$\mu(1)$
CYOCDL	1.00 BC	1.00 BC	$\mu(1)$
DEZPUT	0.73 CR; 0.03 CC; 0.24 TCC	0.67 CR; 0.15 CC; 0.19 TCC	$\mu(4)$
ECOTDA	0.90 BC; 0.10 TBC	0.51 BC; 0.49 TBC	$\mu(3)$
EOCNON10	1.00 TCC	0.06 CC; 0.94 TCC	$\mu(5)$
GATRAU	1.00 BC	1.00 BC	$\mu(1)$
GIVBAO	1.00 BC	1.00 BC	$\mu(1)$
HOXTHD	1.00 BC	0.98 BC; 0.02 TBC	$\mu(2)$
HUMULB10	0.12 BC; 0.88 TBC	0.27 BC; 0.73 TBC	$\mu(3)$
KESVIN	1.00 BC	0.98 BC; 0.02 TBC	$\mu(2)$
OCSHYD	1.00 BC	1.00 BC	$\mu(1)$
PCDODO	1.00 BC	0.78 BC; 0.22 TBC	$\mu(3)$
SATKIH (1)	0.41 CC; 0.59 TCC	0.47 CC; 0.52 TCC	$\mu(6)$
SATKIH (2)	0.08 CC; 0.92 TCC	0.35 CC; 0.65 TCC	$\mu(6)$
SATKIH (3)	0.95 CC; 0.05 TCC	0.01 CR; 0.65 CC; 0.34 TCC	$\mu(6)$
SATKIH (4)	0.21 CR; 0.04 CC; 0.75 TCC	0.55 CR; 0.18 CC; 0.27 TCC	$\mu(4)$
SEJFIW (1)	0.89 BC; 0.08 TBC; 0.03 TC	0.38 BC; 0.33 TBC; 0.29 TC	$\mu(7)$
SEJFIW (2)	0.79 BC; 0.19 TBC; 0.02 TC	0.35 BC; 0.35 TBC; 0.30 TC	$\mu(7)$
SPOCTC10	1.00 BC	1.00 BC	$\mu(1)$
SPTZBN	0.88 BC; 0.12 TBC	0.49 BC; 0.51 TBC	$\mu(3)$
VALGOE (1)	1.00 BC	0.99 BC; 0.01 TBC	$\mu(1)$
VALGOE (2)	1.00 BC	0.99 BC; 0.01 TBC	$\mu(1)$
VASWOB	1.00 BC	0.97 BC; 0.03 TBC	$\mu(2)$

sequences of torsion angles corresponding to these conformations, $\boldsymbol{\mu}(1), \ldots, \boldsymbol{\mu}(k)$, their corresponding frequencies of occurrence $p1, \ldots, pk$, and the associated standard deviations $\sigma_1, \ldots, \sigma_k$. The Bayesian approach consists of first providing *prior distributions* for these parameters and updating these distributions with the information provided by the observed data through Bayes' rule, to finally compute the *posterior distributions* of the parameters. As mentioned in §2.1 we describe the data by a multivariate mixture model. The problem of Bayesian inference in mixture models has been extensively studied in the last decade. Useful reviews can be found in Robert & Casella (2005) or Robert (1996). As described in these reviews, no analytically tractable form for the posterior distributions of the parameters is available. It is, however, possible to simulate as many samples of these posterior distributions as desired using a Markov Chain Monte Carlo algorithm, for a simple introduction see Robert & Casella (2005) and for a description of the application to mixture models see Robert (1996). From the samples it is then possible to obtain approximations of any quantity of interest related to the posterior distribution: a histogram of the draws for example can provide an approximation to the density. The case when the number of components in the mixture is itself a parameter requires a somehow more sophisticated Markov Chain Monte Carlo algorithm called Reversible-Jump algorithm, which has been described in Richardson & Green (1997). A detailed description of the mathematical aspects of the 'Full Bayesian Analysis' method we have implemented can be found in Nolsøe *et al.* (2005), which is available from the authors upon request.

The output of the 'Full Bayesian Analysis' method consists of, on one hand, a histogram of the number of 'preferred' conformations after the structures have been analyzed, providing probabilities that the data have been generated from a one-, two-, three- *etc* conformations mixture. For each of the possible estimated number of conformations, one obtains as well histograms of the posterior distributions of the 'preferred' conformations torsion angles, of their frequencies and their associated standard deviations.

5. Experimental

5.1. Structural analysis

The Cambridge Structural Database (Allen, 2002), Version 5.25, was searched for all the structures containing Csp^3 eight-membered rings in organic structures. A total of 95 refcodes matched the search, the total number of fragments was 115. Torsion angles were tabulated and transferred to Excel for statistical analysis, these data are included in the supplementary material.[1]

The Classification method is very simple to implement and was programmed in Visual Basic and incorporated as a macro in *Excel*. The Full Bayesian Analysis method is not so straightforward to implement and was programmed in *Java*.

6. Results and discussion

6.1. Conformational analysis of Csp^3 eight-membered rings in Allen *et al.* (1996).

6.1.1. Classification method: the preferred conformations are assumed to be the canonical conformations. In order to test the conformational classification method described above we employed Csp^3 eight-membered rings. We chose this system because the conformations of cyclooctane and related eight-membered rings have been widely studied, both theoretically (Hendrickson, 1967) and experimentally (Allen *et al.*, 1996; Evans & Boeyens, 1988). Table 1 shows the most likely canonical conformations, together with the associated probabilities, that were deduced from the computation of the posterior probabilities with the Classification method, for the

[1] Supplementary data for this paper are available from the IUCr electronic archives (Reference: BS5019). Services for accessing these data are described at the back of the journal.

rings with Csp^3 atoms analyzed by Allen and co-workers (Allen *et al.*, 1996).

As can be seen in Table 1 the most frequent conformation is boat–chair (BC), this is the most likely conformation in 23 of the 31 data analyzed. The twist-boat–chair (TBC) and twist-chair–chair (TCC) conformations often exhibited a significant probability in the structures reviewed in Table 1. These conformations (BC, TBC and TCC) in cyclooctane have been identified as energy minima with respect to all the small distortions (Anet & Krane, 1973), with BC being the most stable conformation.

In Table 1, 13 structures have a probability of 1 for the BC conformation with σ = 10 or 20°. These structures exhibit torsion angles similar to those of the ideal BC conformation and can be identified as free (non-fused) cyclooctane rings in accordance with the results of Allen and co-workers (Allen *et al.*, 1996). Interestingly, the appearance of a non-zero probability for more than one ideal conformation can be used to identify a structure as intermediate between two or more theoretical conformations. Thus, some structures in Table 1 show a small probability (0.01–0.02) for the TBC conformation, but only in the case of $\sigma = 20°$. All the structures show a similar trend in the deviation from the ideal BC conformation: the ideal BC angles of 44.7 and −102° (see *Appendix A*) show absolute value ranges of 19–30 and 88–94°. These structures correspond to the cluster BC/TBC described by Allen and co-workers (Allen *et al.*, 1996). Significantly, a value of $\sigma = 20°$ was necessary to detect this conformational feature; the advantage of using $\sigma = 20°$ rather than $\sigma = 10°$ in order to detect the intermediate character of a conformation can be observed throughout Table 1.

In some cases the deviation from the BC conformation is larger (ECOTDA, HUMULB10, SPTZBN) and a significant probability for TBC conformation appears even with $\sigma = 10°$. This corresponds to the second BC/TBC cluster identified by Allen and co-workers (Allen *et al.*, 1996). The remaining structures are distorted conformations with significant probabilities for CR/CC/TCC or BC/TBC/TC conformations.

6.1.2. Full Bayesian Analysis method: no previous knowledge of preferred conformations assumed. We have also studied the set of data analyzed by Allen and co-workers (Allen *et al.*, 1996) by the Full Bayesian method without *a priori* knowledge of the ideal conformations described previously. A histogram for the posterior distribution of k, the number of detected conformations, is given in Fig. 3.

Six or seven clusters are found to be most likely. In Fig. 4, box-plot-like diagrams are presented for the posterior distributions of the detected conformational sequences of torsion angles $\boldsymbol{\mu}(1), \ldots, \boldsymbol{\mu}(7)$, their corresponding frequencies of occurrence $p1, \ldots, p7$, and the associated standard deviations $\sigma_1, \ldots, \sigma_7$, when seven clusters are chosen. Eight horizontal lines were drawn for each box, representing the percentiles 10, 15, 25, 50, 75, 85 and 90% of the distribution. Moreover, in the case of the conformations $\boldsymbol{\mu}(1), \ldots, \boldsymbol{\mu}(5)$, a wider horizontal black line was drawn which represents the torsion angles of the representative member of clusters detected by Allen *et al.* (1996). The torsion angles of the centroids for the seven clusters are presented in Table 2.

Table 2
Torsion angles (°) for the centroids of the clusters obtained by the Full Bayesian Analysis method applied to the Csp^3 eight-membered rings of Allen *et al.* (1996).

Cluster	τ_1	τ_2	τ_3	τ_4	τ_5	τ_6	τ_7	τ_8	Cluster type	Data
$\mu(1)$	−98.9	39.3	67.8	−63.2	−46.0	100.8	−66.0	66.7	BC	15
$\mu(2)$	−97.5	54.9	53.6	−82.4	−8.1	81.1	−71.3	66.8	BC/TBC	4
$\mu(3)$	−82.5	5.1	85.8	−53.9	−57.7	100.8	−69.6	72.3	BC/TBC	4
$\mu(4)$	73.5	−94.4	92.6	−70.2	69.9	−87.2	87.7	−68.7	–	–
$\mu(5)$	68.6	−101.0	87.5	−49.1	54.0	−93.7	89.1	−57.4	–	–
$\mu(6)$	1.7	61.9	101.8	−67.3	60.3	101.0	83.8	−5.8	–	–
$\mu(7)$	88.5	3.6	−74.5	89.8	−88.1	70.8	−4.9	−88.5	–	–

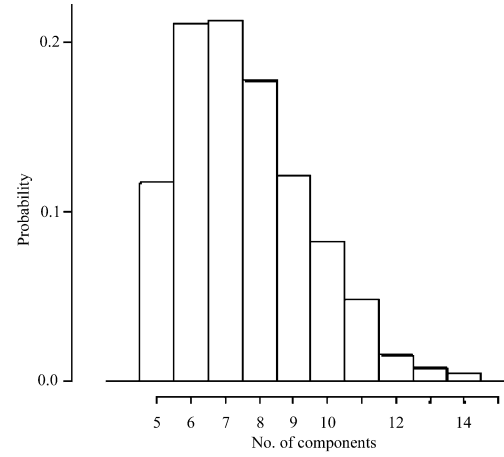

Figure 3
Probabilities for the number of conformations.

In Table 1 the last column indicates to which of the detected clusters is each individual structure in the dataset assigned. The detected clusters are interpreted as follows.

Cluster $\mu(1)$: This is the most populated cluster, it includes 15 data. The torsion angles of the centroids of the clusters (Table 2) are close to those of the boat–chair conformation. This cluster essentially agreres with the BC cluster reported by Allen and co-workers (Allen *et al.*, 1996). The structures correspond to free (non-fused) cyclooctane rings and it is the expected conformation according to energy (Hendrickson, 1967; Anet & Krane, 1973).

Cluster $\mu(2)$: As can be seen in Table 1 this cluster includes 4 data. The torsion angles in this structures are close to those of the ideal boat–chair (BC), but there are some differences: the ideal BC angles of 44.7 and −102° (see the supplementary material) show absolute value ranges of 19–30 and 88–94°; this means a flattening of the BC structure towards the twist-boat–chair (TBC) conformation. In addition, BC and TBC confor-

research papers

mations can interconvert by a pseudorotation pathway (Allen *et al.*, 1996).

Cluster μ(3): This cluster includes 4 data. When the torsion angles for the centroid of this cluster are analyzed by the Classification method significant probabilities for the BC and TBC conformations are obtained. In fact, this corresponds to the BC/TBC cluster proposed by Allen and co-workers (Allen *et al.*, 1996).

The remaining clusters are less populated (Table 1) and they correspond to distorted structures between the ideal conformations. The torsion angles of the centroids are shown in Table 2. Notice that the distribution for the corresponding

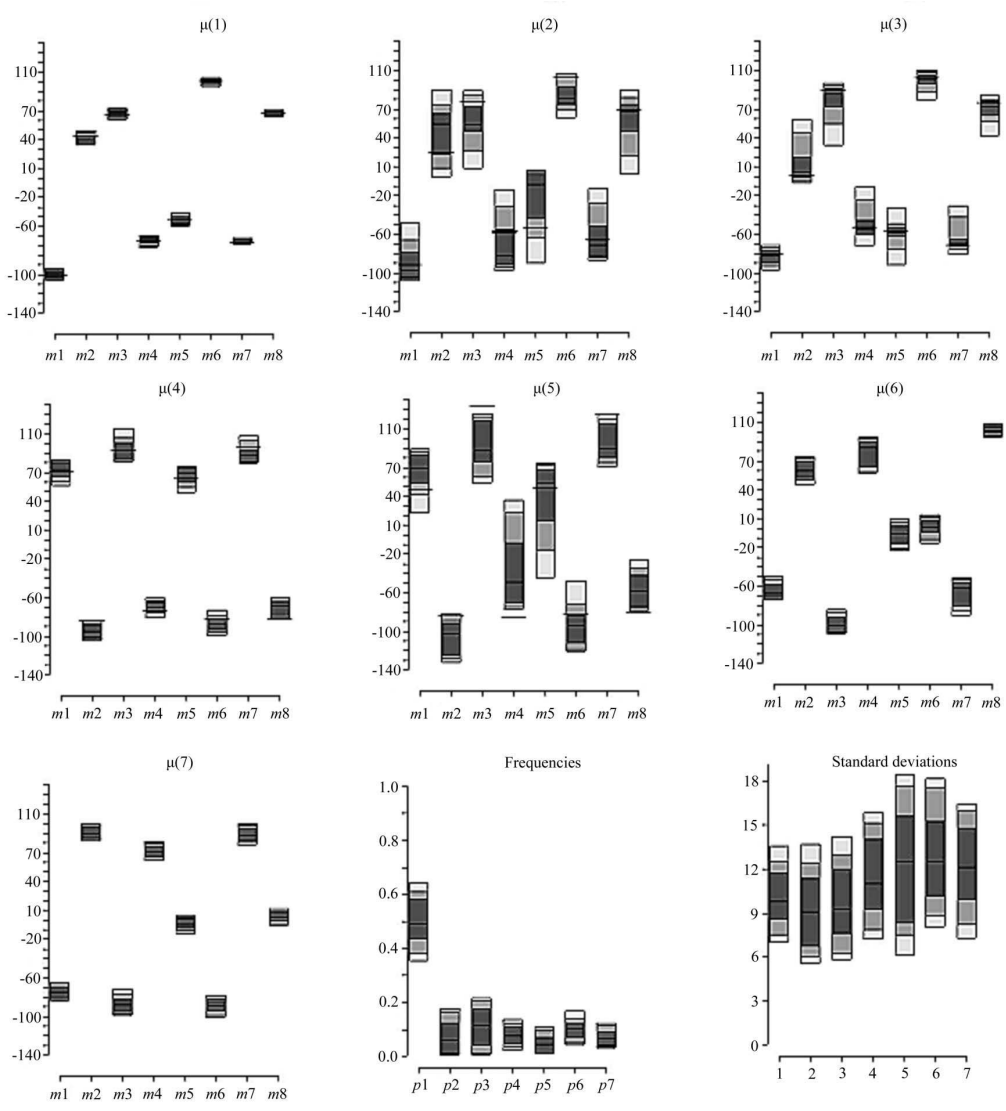

Figure 4
Box-plot type representations of the posterior distributions of the conformations detected, frequencies and standard deviations of Csp^3 eight-membered rings in Allen *et al.* (1996). Eight horizontal lines were drawn for each box, representing the 10, 15, 25, 50, 75, 85 and 90% percentiles of the distribution.

Table 3
Conformational classification of Csp^3 eight-membered rings in the CSD, Version 5.25, according to the methods described in this paper.

	Classification method		Full Bayesian method
	$\sigma = 10^\circ$	$\sigma = 20^\circ$	
BAJQIN	1.00 BC	0.90 BC; 0.10 TBC	$\mu(2)$
BAJQOT	1.00 BC	0.77 BC; 0.23 TBC	$\mu(2)$
BAJQUZ	1.00 BC	1.00 BC	$\mu(1)$
BEYPAW	1.00 BC	1.00 BC	$\mu(1)$
DUVFUV03 (1)	1.00 BC	1.00 BC	$\mu(1)$
DUVFUV03 (2)	1.00 BC	1.00 BC	$\mu(1)$
FADTAG	1.00 BC	1.00 BC	$\mu(1)$
GIPPAW	1.00 B	1.00 B	$\mu(6)$
GIQRUT	1.00 BC	1.00 BC	$\mu(1)$
HABXEN (1)	1.00 TCC	0.07 CR; 0.17 CC; 0.76 TCC	$\mu(4)$
HABXEN (2)	1.00 BC	1.00 BC	$\mu(1)$
HAVGOA	1.00 C	1.00 C	$\mu(5)$
HAVGUG	1.00 C	1.00 C	$\mu(5)$
HEMTIC (1)	1.00 BC	0.70 BC; 0.30 TBC	$\mu(2)$
HEMTIC (2)	1.00 BC	0.72 BC; 0.28 TBC	$\mu(2)$
HEMTIC (3)	0.93 BC; 0.07 TBC	0.53 BC; 0.47 TBC	$\mu(2)$
HEMTIC (4)	1.00 BC	0.81 BC; 0.19 TBC	$\mu(2)$
IFOKOD	1.00 BC	1.00 BC	$\mu(1)$
IGARUD	1.00 BC	0.98 BC; 0.02 TBC	$\mu(2)$
JAGQIR	0.08 CR; 0.12 CC; 0.80 TCC	0.47 CR; 0.22 CC; 0.31 TCC	$\mu(4)$
JITNIJ	1.00 C	1.00 C	$\mu(5)$
JIWWUH (1)	1.00 BC	1.00 BC	$\mu(1)$
JIWWUH (2)	1.00 BC	1.00 BC	$\mu(1)$
JOQMIL (1)	0.98 BC; 0.02 TBC	0.61 BC; 0.39 TBC	$\mu(2)$
JOQMIL (2)	1.00 BC	0.48 BC; 0.52 TBC	$\mu(2)$
JOQMIL01 (1)	1.00 BC	0.59 BC; 0.41 TBC	$\mu(2)$
JOQMIL01 (2)	0.85 BC; 0.15 TBC	0.48 BC; 0.52 TBC	$\mu(2)$
KIKWAC	1.00 C	1.00 C	$\mu(5)$
KOJDIW	0.75 BC; 0.25 TBC	0.44 BC; 0.56 TBC	$\mu(2)$
KOJDOC	1.00 BC	0.97 BC; 0.03 TBC	$\mu(2)$
KOJNUS	1.00 B	1.00 B	$\mu(6)$
KOJPAA (1)	1.00 C	1.00 C	$\mu(5)$
KOJPAA (2)	1.00 C	1.00 C	$\mu(5)$
MOZSAV	1.00 C	1.00 C	$\mu(5)$
NACGAZ	1.00 BC	1.00 BC	$\mu(1)$
NADCOK	1.00 S	0.20 BB; 0.78 S; 0.02 B	$\mu(6)$
NADNAH	0.48 BC; 0.52 TBC	0.37 BC; 0.63 TBC	$\mu(2)$
NUJHUV	1.00 BC	1.00 BC	$\mu(1)$
NUWMIB	1.00 BC	0.86 BC; 0.14 TBC	$\mu(2)$
NUZDER	1.00 BC	0.97 BC; 0.03 TBC	$\mu(2)$
PAPWAE (1)	1.00 C	1.00 C	$\mu(5)$
PAPWAE (2)	1.00 C	1.00 C	$\mu(5)$
PAZJEF	1.00 BC	1.00 BC	$\mu(1)$
PETFOJ	0.04 BC; 0.96 TBC	0.21 BC; 0.79 TBC	$\mu(3)$
PIVWEW	1.00 BC	1.00 BC	$\mu(1)$
POYJOC (1)	1.00 BC	1.00 BC	$\mu(1)$
POYJOC (2)	1.00 BC	1.00 BC	$\mu(1)$
QADNEP	1.00 BC	0.97 BC; 0.03 TBC	$\mu(2)$
QETVUG	1.00 TBC	1.00 TBC	$\mu(3)$
QOTGEL	1.00 BC	1.00 BC	$\mu(1)$
QOTGEL01	1.00 BC	0.99 BC; 0.01 TBC	$\mu(2)$
RECFOU	1.00 BC	1.00 BC	$\mu(1)$
RECPUK	1.00 BC	1.00 BC	$\mu(1)$
RILWIS (1)	1.00 BC	0.75 BC; 0.25 TBC	$\mu(2)$
RILWIS (2)	1.00 BC	0.72 BC; 0.28 TBC	$\mu(2)$
RIZCUY	0.96 BC; 0.04 TBC	0.56 BC; 0.44 TBC	$\mu(2)$
RULMAM	0.91 BC; 0.09 TBC	0.52 BC; 0.48 TBC	$\mu(2)$
SORDAE	1.00 C	1.00 C	$\mu(5)$
VIDNAX	1.00 C	1.00 C	$\mu(5)$
VIDNAX01 (1)	0.01 S; 0.99 B	0.14 S; 0.86 B	$\mu(6)$
VIDNAX01 (2)	0.27 S; 0.73 B	0.32 S; 0.68 B	$\mu(6)$
VIDNEB	1.00 C	1.00 C	$\mu(5)$
WAHRAY	1.00 B	1.00 B	$\mu(6)$
WIDSEH	0.02 BC; 0.98 TBC	0.19 BC; 0.81 TBC	$\mu(3)$
WIRPAO	1.00 BC	1.00 BC	$\mu(3)$
WOQKUI	1.00 BC	0.97 BC; 0.03 TBC	$\mu(2)$
XENREN	0.97 BC; 0.03 TBC	0.58 BC; 0.42 TBC	$\mu(2)$
XEPWUK	1.00 BC	1.00 BC	$\mu(1)$

standard deviations presents a higher dispersion (Fig. 4), which can be explained by the fact that only very few observations belong to these clusters.

6.2. Conformational analysis of Csp^3 eight-membered rings in the CSD

In order to complete the conformational analysis described above we have studied the Csp^3 eight-membered rings included in the CSD, Version 5.25. The refcodes of the structures and the results obtained by the Classification method and the full Bayesian Analysis method are shown in Table 3 (the results of the refcodes analyzed in §6.1 have been omitted for clarity).

The BC/TBC pseudorotation pathway is clearly visible from the results in Table 3 for the Classification method: 30 data show a probability of 1.00 for BC, 19 data exhibit a small distortion from the BC to the TBC conformation (a significant probability appears only when $\sigma = 20^\circ$), 12 data show a larger deviation from BC and two structures even show a probability of 1.00 for the TBC conformation.

An accessible deformation of the BC conformation towards the TBC conformation can also be inferred from the probabilities of the structures QOTGEL, HEMTIC or JOQMIL, where chemically indistinguishable fragments show different probabilities for BC and TBC conformations.

In Table 3, 12 data sets are assigned to the chair (C) conformation, but all of them have fused rings in the 1,2 and 5,6 positions, most being chemically very similar. There are also 3 data with a probability of 1 (using both $\sigma =$ 10 or 20°) for the boat (B) conformation having a variable number of fused rings to the Csp^3 eight-membered ring.

When data are analyzed by the Full Bayesian method the histogram of the posterior distribution for k indicates that seven clusters are found to be most likely. In Fig. 5, box-plot-like diagrams are presented for the

research papers

Table 3 (continued)

	Classification method		Full Bayesian method
	$\sigma = 10^\circ$	$\sigma = 20^\circ$	
XOLYEC	0.99 BC; 0.01 TBC	0.67 BC; 0.33 TBC	$\mu(2)$
XUDWEY	1.00 BC	1.00 BC	$\mu(1)$
XUDWIC	1.00 BC	1.00 BC	$\mu(1)$
XUDWOI	1.00 BC	1.00 BC	$\mu(1)$
XULROL	1.00 TBC	1.00 TBC	$\mu(5)$
YAFLAS	1.00 BC	1.00 BC	$\mu(1)$
YOPPEY (1)	1.00 BC	1.00 BC	$\mu(1)$
YOPPEY (2)	1.00 BC	1.00 BC	$\mu(1)$
YOPPIC (1)	1.00 BC	0.98 BC; 0.02 TBC	$\mu(2)$
YOPPIC (2)	0.79 BC; 0.21 BB	0.18 BC; 0.08 TBC; 0.60 BB; 0.15 S	$\mu(2)$
ZAVRET	1.00 BC	1.00 BC	$\mu(1)$
ZAYPEU	1.00 BC	0.95 BC; 0.05 TBC	$\mu(2)$
ZAYPIY	1.00 BC	0.98 BC; 0.02 TBC	$\mu(1)$
AHOQOD	1.00 BC	1.00 BC	$\mu(1)$
BEHNEI	1.00 BC	1.00 BC	$\mu(1)$
UMIJIJ	0.86 BC; 0.14 TBC	0.49 BC; 0.51 TBC	$\mu(3)$

Table 4
Torsion angles (°) for the centroids of the clusters obtained by the Full Bayesian Analysis method applied to Csp^3 eight-membered in the CSD, Version 5.25.

Cluster	τ_1	τ_2	τ_3	τ_4	τ_5	τ_6	τ_7	τ_8	Cluster type	Data
$\mu(1)$	−97.5	38.9	65.6	−63.4	−45.5	98.7	−66.6	67.8	BC	47
$\mu(2)$	−90.3	48.9	55.8	−81.0	−10.1	78.3	−72.6	69.1	BC/TBC	34
$\mu(3)$	−75.3	−0.5	89.3	−56.6	−49.6	83.8	−75.9	77.2	TBC/BC	7
$\mu(4)$	75.5	−67.0	97.3	−94.9	61.8	−56.7	84.6	100.0	CC/TCC	5
$\mu(5)$	115.9	−79.7	4.7	76.7	−120.0	67.8	5.2	−74.3	C	13
$\mu(6)$	−65.1	7.4	75.8	−11.7	−73.5	17.2	68.5	−11.1	B	6
$\mu(7)$	−96.3	64.8	−65.3	94.3	−75.1	2.3	3.1	74.7	–	–

posterior distributions of the conformational sequences of torsion angles detected, their corresponding frequencies of occurrence and the associated standard deviations. The torsion angles of the centroids are presented in Table 4. In clusters $\mu(1)$, $\mu(2)$ and $\mu(3)$ the torsion angles for the centroids are similar to those found in the three most populated clusters obtained in §6.1, corresponding to the BC or BC/TBC conformations.

The most significant differences with data analyzed in §6.1 are clusters $\mu(5)$ and $\mu(6)$. Cluster $\mu(5)$ includes structures having the chair (C) conformation. For $\mu(5)$ in Fig. 5 a wider horizontal black line is drawn which represents the torsion angles of the ideal chair conformation. According to the torsion angles of its centroid (Table 4) cluster $\mu(6)$ corresponds to structures having a boat (B) conformation, which is in agreement with the results obtained by the Classification method.

6.3. Features of the methods described and differences with PCA

When studying the conformations of ring systems using familiar intramolecular parameters such as torsion angles, the exploration and classification of the data are made difficult by the large number of variables for each observed structure: for an eight-membered ring, for example, the data observed lie in an eight-dimensional space, even if it is well known that there are only five degrees of conformational freedom. One way around the problem is to achieve a dimension reduction in order to be able to display the data in a two- or three-dimensional space and visually detect groups of molecules. This is the method used in the principal component analysis: for example, the direction given by the first principal component (pc1) is the direction along which the data present more variability and therefore the possible groups of structures can be distinguished.

The two methods described in this paper do not perform any kind of dimension reduction, but are designed to deal directly with grouping in multivariate data. The purpose and the output of the 'Classification method' and the 'Full Bayesian Analysis method' are different but, in our experience, both provide useful information for the conformational analysis of structures. We would like to emphasize the following facts:

(i) Both methods share the same underlying probabilistic model to explain the observed torsion angles. In particular, treatment of the symmetry of the parameter space, the enantiomers *etc.* is taken into account in the modelling step, which, in contrast to the pca method, allows the symmetry expansion of the initial set of torsion angles to be avoided.

(ii) The 'similarity' between two structures can be understood in terms of the underlying probabilistic model: two structures will be found to be close if their merging in the same group yields a high corresponding likelihood.

(iii) The 'Classification method' requires as input prior knowledge of the preferred conformations. This is, of course, a real restriction to its applicability, since for many practical cases no sound energy-based starting point may be available. However, we would like to stress its simplicity: it is a straightforward sub-product of the model formulation; its implementation only requires a few lines of code and it is able to perform the classification of an individual structure into one of any collection of preferred conformations of interest to the user. Moreover, as illustrated in the experimental study, significant classification probabilities for several preferred conformations give hints about the interconversion pathways that connect some of these conformations. This is also one of the acceptable by-products of the pca method.

(iv) The 'Full Bayesian Analysis' method detects groups without requiring either knowledge of the preferred confor-

mations or of their number. It consists of an implementation of the Bayesian paradigm for the case where the number of preferred conformations, the preferred conformations themselves, their relative frequencies of occurrence and the standard deviations of the perturbations are the unknown parameters of interest. Since the number of preferred conformations is itself a parameter to be inferred, the output of the method includes the posterior probability of each possible conformation. The implementation of the 'Full Bayesian Analysis' method was carried out using the Reversible-Jump Markov Chain Monte Carlo (MCMC) algorithm. We developed our code based on the available code as described in Cappé *et al.* (2003). As with any MCMC algorithm, it is on one hand computationally demanding and on the other hand requires tuning of the parameters to ensure the convergence of the algorithm. In that sense, some experience is needed to run the code.

(v) Finally, even if we have chosen to present the methods using eight-membered rings, they extend to *m*-membered rings in a straightforward manner. The only difference lies in

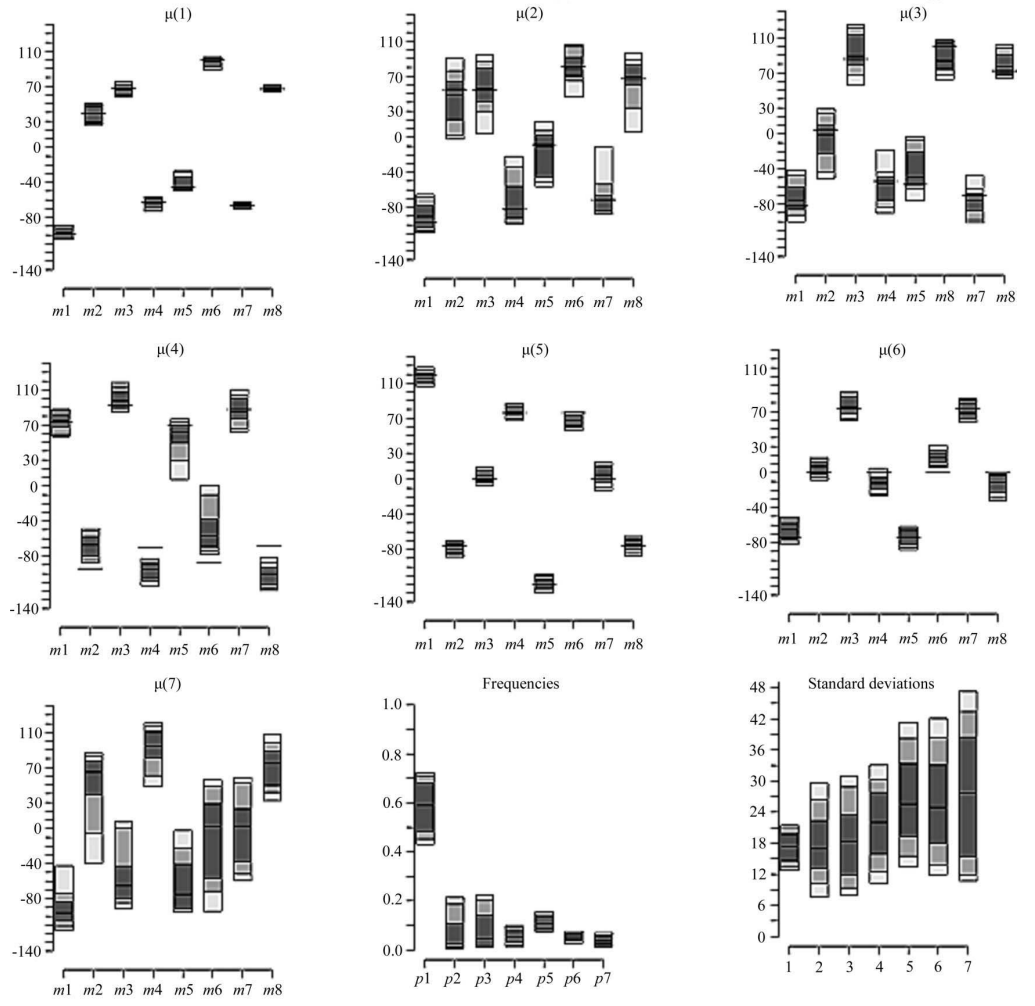

Figure 5
Posterior distribution of the detected conformations, frequencies and standard deviations of Csp^3 eight-membered rings in the CSD, Version 5.25. Eight horizontal lines were drawn for each box, representing the 10, 15, 25, 50, 75, 85 and 90% percentiles of the distribution.

research papers

the formulation of the model: the expression of the density functions $f(\tau,c)$ in §2.1 is now

$$f(\tau, c) = \sum_{v=1,\ldots,m} \sum_{d=-1,1} \sum_{\delta=-1,1} f_G\big(\tau, \mu(c, v, d, \delta), \sigma_c^2\big),$$

with $\boldsymbol{\tau} \rightarrow f_G(\boldsymbol{\tau}, \boldsymbol{\mu}(c, v, d, \delta), \sigma_c^2)$ denoting the density of the m-dimensional Gaussian law with the mean $\mu(c, v, d, \delta)$ given by

$$\delta\times(\mu C, v, \mu_{C,(v-1+d\times 1) \bmod m+1}, \mu_{C,(v-1+d\times 2) \bmod m+1}, \ldots, \mu_{C,(v-1+d\times(m-1)) \bmod m+1}).$$

7. Conclusions

(i) The Classification method that uses the canonical conformations described in this article allows the closest ideal conformation for an individual eight-membered ring to be established using the eight torsion angles in the ring. Moreover, the method can easily be extended to rings with different numbers of atoms or when choosing different canonical conformations.

(ii) In the output of the Classification method for an individual structure, the appearance of non-zero probabilities for different theoretical conformations indicates that the structure is an intermediate between theoretical conformations. In addition, the relative value of the probability indicates the proximity to the ideal conformation.

(iii) It is convenient to allow large values for the deviations from the ideal torsion angles (*e.g.* $\sigma = 20^\circ$) in order to detect small deviations from the ideal conformations. We recommend checking the sensitivity of the results to different values of σ.

(iv) The Full Bayesian method does not assume any previous knowledge on the preferred conformations. It allows on one hand a decision about the most likely number of clusters and, on the other hand, provides details of the centroids of the clusters, their frequencies and the estimated standard deviations.

(v) The combined use of both methods draws significant chemical conclusions.

APPENDIX *A*

Torsion angles (°) for the canonical conformations of cyclooctane, *i.e.* the 'preferred' conformations for the Classification method are shown in the table below.

Conf.	C	$\mu_{C,1}$	$\mu_{C,2}$	$\mu_{C,3}$	$\mu_{C,4}$	$\mu_{C,5}$	$\mu_{C,6}$	$\mu_{C,7}$	$\mu_{C,8}$
BC	1	65.0	44.7	−102.2	65.0	−65.0	102.2	−44.7	−65.0
TBC	2	88.0	−93.2	51.9	44.8	−115.6	44.8	51.9	−93.2
CR	3	87.5	−87.5	87.5	−87.5	87.5	−87.5	87.5	−87.5
CC	4	66.0	−105.2	105.2	−66.0	66.0	−105.2	105.2	−66.0
TCC	5	56.2	−82.4	114.6	−82.4	56.2	−82.4	114.6	−82.4
BB	6	52.5	52.5	−52.5	−52.5	52.5	52.5	−52.5	−52.5
S	7	64.9	37.6	−64.9	−37.6	64.9	37.6	−64.9	−37.6
C	8	119.9	−76.2	0.0	76.2	−119.9	76.2	0.0	−76.2
B	9	−73.5	0.0	73.5	0.0	−73.5	0.0	73.5	0.0
TC	10	37.3	−109.3	109.3	−37.3	−37.3	109.3	−109.3	37.3

This work was supported in part by the European Community's Human Potential Programme under contract HPRN-CT-2000-00100, DYNSTOCH, and was developed using the computing facilities of the SAIT, Universidad Politécnica de Cartagena.

References

Allen, F. H. (2002). *Acta Cryst.* B**58**, 380–388.
Allen, F. H., Howard, J. A. K. & Pitchford, N. A. (1996). *Acta Cryst.* B**52**, 882–891.
Allen, F. H. & Motherwell, W. D. S. (2002). *Acta Cryst.* B**58**, 407–422.
Allen, F. H. & Taylor, R. (2004). *Chem. Soc. Rev.* **33**, 463–475.
Anet, F. A. L. & Krane, J. (1973). *Tetrahedron Lett.* **50**, 5029–5032.
Cappé, O., Robert, C. P. & Rydén, T. (2003). *J. R. Stat. Soc. Ser. B Stat. Methodol.* **65**, 679–700.
Evans, D. G. & Boeyens, J. C. A. (1988). *Acta Cryst.* B**44**, 663–671.
Hendrickson, J. B. (1967). *J. Am. Chem. Soc.* **89**, 7047–7061.
Meyer, T. J. (1989). *Acc. Chem. Res.* **22**, 163.
Nolsøe, K., Kessler, M., Pérez, J. & Madsen, H. (2005). Technical report.
Orpen, A. G. (1993). *Chem. Soc. Rev.* pp. 191–197.
Richardson, S. & Green, P. J. (1997). *J. R. Stat. Soc. Ser. B*, **59**, 731–792.
Robert, C. (1996). *Interdisciplinary Statistics*, pp. 441–464. London: Chapman and Hall.
Robert, C. P. & Casella, C. (2005). *Monte Carlo Statistical Methods*, 2nd ed. Berlin: Springer Verlag.
Villar, J. M., Delgado, A., Llebaria, A. & Moreto, J. M. (1995). *Tetrahedron Asymm.* **6**, 665–668.
Zimmer, M. (2001). *Coord. Chem. Rev.* **212**, 133–163.

Paper III

Solid state conformational classification of eight-membered rings in copper complexes double bridged by phosphate, phosphonate or phosphinate ligands

Published in *Inorganica Chimica Acta*, **358**:2432-2436 (2005)

Available online at www.sciencedirect.com
SCIENCE DIRECT®
Inorganica Chimica Acta 358 (2005) 2432–2436
Inorganica Chimica Acta
www.elsevier.com/locate/ica

Note

Solid state conformational classification of eight-membered rings in copper complexes double bridged by phosphate, phosphonate or phosphinate ligands

J. Pérez [a,*], L. García [a], M. Kessler [b], K. Nolsøe [b], E. Pérez [a], J.L. Serrano [a], J.F. Martínez [a], R. Carrascosa [a]

[a] Departamento de Ingeniería Minera, Geológica y Cartográfica Área de Química Inorgánica, Universidad Politécnica de Cartagena, 30203, Cartagena, Murcia, Spain
[b] Departamento de Matemática Aplicada y Estadística, Universidad Politécnica de Cartagena, 30203, Cartagena, Murcia, Spain

Received 21 October 2004; accepted 21 January 2005

Abstract

A statistical classification of the solid state conformation in the title complexes using data retrieved from the Cambridge Structural Database (CSD) has been made. Phosphate and phosphinate complexes show a *chair* conformation preferably. In phosphonate complexes, the most frequent conformations are found to be *boat–chair*, *chair* and *boat–boat*; in all the *boat–chair* cases, the phosphorus atoms appear connected by a bridging carbon atom.

Keywords: Copper; CSD; Conformatiion analysis

1. Introduction

The conformational analysis of metallic complexes is an active research area [1], the CSD being a powerful tool in this kind of study [2]. Despite the large amount of available structural data, a full understanding of the factors that determine the molecular structure of a particular compound has not been achieved yet. The manner in which a ligand controls the properties of the complex depends on a combination of steric, electronic and conformational factors. A detailed knowledge of these effects will allow a rational design of complexes with specific and predictable properties [3]. Moreover, the conformational preferences in complexes double bridged by phosphate or phosphinate ligands play an important role in their magnetic properties or as biological models [4].

The conformation of cyclooctane and related eight-membered rings has been thoroughly analyzed, both theoretically [5] and experimentally [6] and methods for their conformational classification have been reported [6–8]. However, much less attention has been paid to rings having transition metal atoms. Ten symmetrical conformations have been established [7] for eight-membered cyclic fragments (see Fig. 1): *crown* (D_{4d}), *twist–boat* (S_4), *boat–boat* (D_{2d}), *boat* (D_{2d}), *twist-chair–chair* (D_2), *chair–chair* (C_{2v}), *chair* (C_{2h}), *twist-chair* (C_{2h}), *twist-boat–chair* (C_2) and *boat–chair* (C_s).

In this paper, we classify individually the observed structures by evaluating the probabilities that the associated sequence of torsion angles was generated as a perturbation of each of these 10 canonical conformations.

* Corresponding author. Tel.: +34968326420; fax: +34968325420.
E-mail address: jose.pperez@upct.es (J. Pérez).

0020-1693/$ - see front matter © 2005 Elsevier B.V. All rights reserved.
doi:10.1016/j.ica.2005.01.011

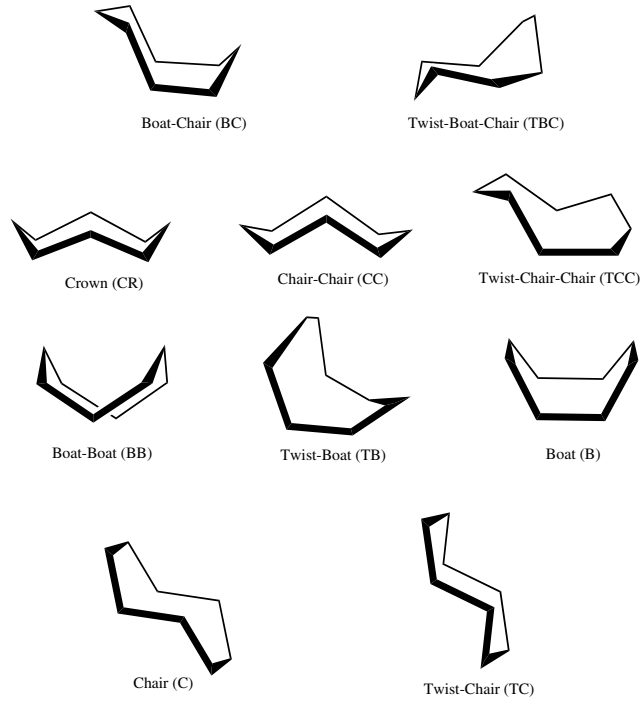

Fig. 1. Canonical forms of cyclooctane.

2. Experimental

2.1. Structural analysis

The Cambridge Structural Database [9] (CSD) V. 5.24 together with February, April and July 2003 updates was searched for all the structures containing the fragment shown in Fig. 2. A total of 60 *refcodes* (Table 1) matched the search, the Cu···X distance and the intra-ring torsion angles were tabulated for statistical analysis.

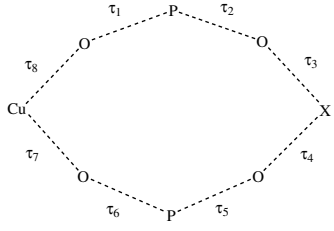

Fig. 2. Substructure used in the CSD search. X denotes any kind of atom.

2.2. Statistical analysis

We begin by formulating a model for the observed sequence of torsion angles: it is assumed to be generated as a perturbation of one of the 10 canonical conformations. We have moreover taken into account that the observed values of the torsion angles may correspond to a different starting point, the sequence of torsion angles can be read in a clockwise or counter clockwise manner and the possibility of coordinate inversions. Based on the eight values of the torsion angles for a structure, through the Bayes rule [10], we have computed the probability that the structure comes from each of the canonical conformations. The observed sequence of torsion angles is obtained from the theoretical one after an additive perturbation where the perturbation's components are assumed to be Gaussian random variables with zero mean. By the Bayes rule, we are able to compute, given an observed sequence the probability that it was generated from the theoretical conformation. We do not favor a priori any particular canonical conformation and the value for the standard deviation of the perturbations was 10. The computed probabilities for the most likely canonical conformation are shown in Table 1.

Table 1
Refcodes for the structures retrieved from the CSD, crystallographic *R*-factor (%) value and the probabilities for the two most likely conformations[a]

Phosphates	Phosphonates	Phosphinates
AGOKEM, 3.59, 0.998 (TC) 0.003 (C)	COYHAZ, 4.35, 1.000 (BC)	BIRFAJ, 2.50, 1.000 (C)
AMPPCU, 4.60	COYLOR, 5.27, 1.000 (BC)	BOXBIZ, 5.80, 1.000 (C)
ATPLCU, 6.90	COYNIN, 2.97, 1.000 (BC)	DBUPCU, 6.10, 1.000 (C)
BONTAZ, 6.00, 1.000 (BC)	DEGDAU10, 6.80, 1.000 (C)	FEPBEH, 4.87, 0.783 (C) 0.217 (TC)
CUCMPA, 10.30, 1.000 (C)	ECOKIQ, 4.68, 1.000 (BC)	GAWZAF, 7.77, 1.000 (C)
EBARII[b], 5.19, 1.000 (BC)	EFUNAU[b], 6.86, 0.999 (BB) 0.001 (S)	GIRRAA, 8.10, 0.999 (CC) 0.001 (TCC)
EBAROO[b], 3.50, 1.000 (B)	HOWFEE, 2.45, 1.000 (TC)	LOXSEW, 2.44, 1.000 (C)
FEBYOA20, 10.00, 1.000 (C)	HOWFII, 5.28, 1.000 (TC)	MEFKAJ, 3.42, 0.881 (BB) 0.119 (S)
GADZOA	HUXGOW, 3.26, 1.000 (BC)	MEFKEN, 7.35, 0.997 (S) 0.003 (BB)
GMPCUP, 6.10, 1.000 (C)	ICISOC, 2.95, 1.000 (BB)	QEDKAL, 6.86, 0.984 (C) 0.016 (TC)
JAGRUE, 8.50, 0.999 (C) 0.001 (TC)	ICISUI, 2.76, 0.999 (BB) 0.001(S)	RUQHUG, 2.90, 1.000 (B)
JAGSAL, 11.60, 1.000 (C)	LOFGAO, 5.87, 0.984 (BB) 0.015 (S) 0.879 (BB) 0.115 (BC)	TIRXUN, 11.17, 1.000 (C)
JAGSEP, 8.40, 1.000 (C)	MANHAK, 5.21, 1.000 (TC)	YOMDOT, 3.60, 0.997 (TC) 0.003 (C)
LULGII, 6.22, 1.000 (TC)	NAVYEO, 3.40, 0.997 (BB) 0.003 (S)	ZUHCAG, 2.90, 1.000 (C)
MEJVEC[b], 5.20, 1.000 (BB)	OCAGII[b], 3.99, 1.000 (CC)	
QIWDOP, 4.82, 1.000 (BC)	OFISAX, 13.50, 0.999 (CC) 0.001 (TCC)	
RECROG, 4.96, 1.000 (C)	PORROD, 5.42, 0.518 (C) 0.482 (TC)	
	QINLOO[b], 3.64, 1.000 (BC)	
	UBEXAA[b], 4.85, 1.000 (BC)	
	UGARAV, 5.11, 1.000 (BB)	
	WAJHIY, 7.90, 1.000 (BC)	
	WIHNOQ, 7.21, 1.000 (C) 1.000 (C) 1.000 (B)	
	WUTLIG, 6.65, 1.000 (BC)	
	WUTLOM, 3.44, 1.000 (CC)	
	WUTLUS, 3.05, 1.000 (S)	
	WUTMAZ, 2.93, 1.000 (CC) 0.635 (CC) 0.365 (TCC)	
	WUVGOJ, 3.31, 1.000 (BC)	
	WUVGUP, 4.84, 1.000 (BC)	
	XONCUY, 4.73, 1.000 (BC) 1.000 (BC)	

[a] In structures with several fragments it appears the probabilities for each one of them.
[b] Heterodinuclear compounds.

3. Results and discussion

A total of 60 structures having the fragment defined in Fig. 2 were found in the CSD. The total number of fragments was 68. Most of the structures correspond to Cu(II); only four of them contain Cu(I) according to the chemical information supplied by the CSD. We have found 17 structures incorporating various types of phosphate moieties (hereafter referred to as phosphates), 29 bis(phosphonate) or bis(phosphonate ester) complexes (hereafter referred to as phosphonates), and 14 bis(phosphinate)complexes (hereafter referred to as phosphinates). Scheme 1 shows the kind of ligands included in these structures and the refcodes are shown in Table 1. Four structures contain a vanadium atom in the ring (two phosphate-complexes and two phosphonate-complexes); two structures possess a molybdenum atom (phosphonate-complexes) and one structure has a boron atom (phosphate-complexes).

In overall the mean distance Cu···Cu is 4.759(572) Å, ranging from 2.907 to 5.483 Å. We have employed the

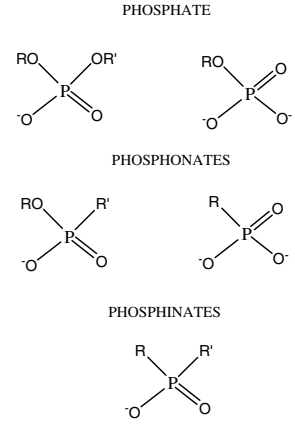

Scheme 1.

above 10 canonical conformations to map the rings studied in this paper. The statistical analysis of the phosphate, phosphonate and phosphinate data sets has yielded the conclusion that the most frequent conformations in the compounds studied in this paper are *chair* and *boat–chair*, however differences have been found according to the bridging ligand.

3.1. Double bridged phosphate-complexes

The structural results in eight-membered rings containing two copper atoms double bridged by phosphate ligands are shown in Fig. 3, the graphic shows the coordination number around the copper atoms and the closest symmetrical conformation. All the compounds have Cu(II) atoms and nearly all phosphate-complexes exhibit pentacoordinated coordination (only one complex exhibits tetracoordinated Cu atoms and only one complex exhibits hexacoordinated metal atoms).

As can be seen in Fig. 3, the ring conformation found is mostly *chair* (C), the *boat–chair* (BC) and *twist-chair* (TC) are also present in some cases. According to Hendrickson [5], there is an accessible path for the interconversion between C, BC and TC conformations in eight-membered carbon rings. The BC and TC conformations can interconvert by an *asymmetrical mode*, in this mode only one side of a symmetrical ring is allowed to change, as in a wagging of a single atom which in general will invert the signs of the two dihedral angles directly adjacent to it. TC and C conformations can interconvert by a *pseudorotation*, this is a concerted, continuous change of dihedral angles such that each ring atom sequentially takes up each of the possible ring positions; moreover, TC and C conformations in cyc-

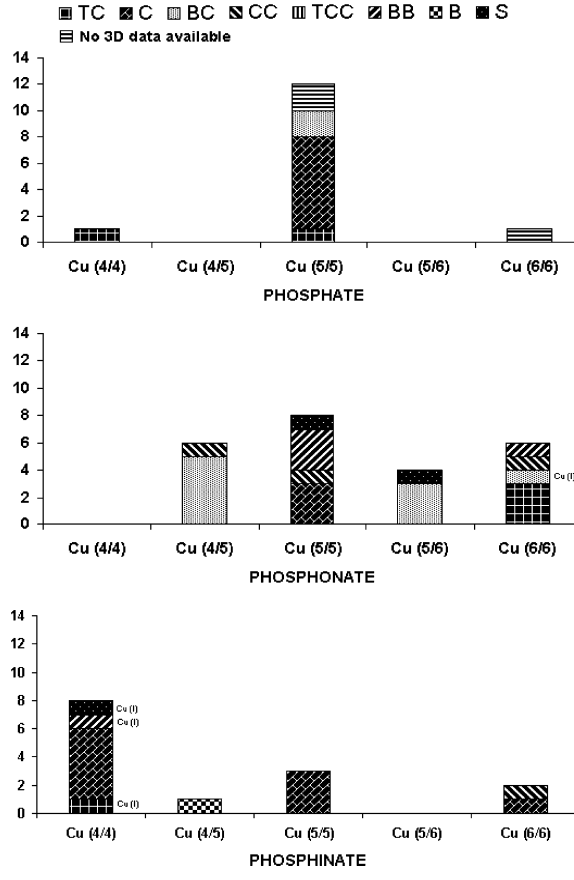

Fig. 3. Coordination number and conformation in dinuclear copper-complexes.

looctane have been grouped in the same family [11] with similar strain energies. Studies about the relative energies in the system analyzed in this paper are in progress. In addition, this ring contains several kinds of atoms (namely Cu, O and P) and the *chair* conformations found are different because the atomic positions in the ring are not the same. The Cu···Cu distance in structures adopting the *chair* conformation ranges from 5.050 to 5.157 Å (mean value of 5.109(43) Å), the structure of bis(μ_2-phenylphosphato)-aqua-(6,6′-bis(3-dimethylaminopropynyl)-2,2′-bipyridine)-copper(II) tetranitrate (refcode: RECROG [12]) shows a *chair* conformation too but the value for the Cu···Cu distance is shorter, 4.455 Å, because of the different positions of atoms in the ring.

Rings having Cu and V atoms exhibit BC (Cu···V distance of 4.605 Å) and B (Cu···V distance of 3.324 Å) conformations. Complex containing Cu and B atoms shows a BB conformation (Cu···B distance of 3.090 Å).

3.2. Double bridged phosphonate-complexes

The phosphonate complexes exhibit more variety in the coordination number than the phosphate or phosphinate as can be seen in Fig. 3; in the case of phosphonate, there are a significant number of structures having Cu atoms with mixed coordination number (^{4}Cu/^{5}Cu and ^{5}Cu/^{6}Cu). Only one of the structures found in the CSD contains Cu(I). The most frequent conformation in these complexes is the *boat–chair*, but all the BC cases show the phosphorus atoms connected by a bridging carbon atom, this P–C–P connection probably constrains the conformation of the eight-membered ring as it has been reported in other conformational studies [13]. The phosphonate-complexes exhibit a high variety in the solid-state conformation of the double bridged ring. As can be seen in Fig. 3(a), representative number of structures show the *chair*, *twist-chair* and *boat–boat* conformations. One of the fragments in the structure of catena-(tetra-sodium bis(μ_3-methylenediphosphonato)-di-copper(II) dehydrate) (refcode: WUTMAZ [14]) shows a probability of 0.635 for the *chair–chair* (CC) conformation and 0.365 for the *twist-chair–chair* (TCC) one; the torsion angles being intermediates between the two ideal conformations.

The Cu···Cu distances also exhibit a higher variability than the phosphate-complexes ranging from 2.907 to 5.363 Å (mean value of 4.610 (674) Å). It has not been possible to establish any correlation with the coordination number or the ring conformation.

Heterodinuclear complexes having Cu and Mo atoms exhibit *boat–boat* (BB) (Cu···Mo distance of 3.731 Å) and BC (Cu···Mo distance of 5.067 Å) conformations. Complexes containing Cu and V atoms show CC and BC conformations (Cu···V distances of 5.042 and 4.702 Å, respectively).

3.3. Double bridged phosphinate-complexes

In this case, there are less data available in the CSD than for phosphate or phosphonate. As can be seen in Fig. 3, in the phosphinate-complexes the most frequent coordination number is four (three structures showing Cu(I)). The most frequent conformation is *chair* (as it happens in phosphate-complexes). The Cu···Cu distance in these *chair* structures shows a narrow range (from 4.938 to 5.483 Å with a mean value of 5.099(150) Å). The complex having a CC conformation possesses an intraring bridging atom that could constrain the conformation of the ring.

As can be seen in Table 1, there are some structures with *chair* (C) and *twist-chair* (TC) having the highest probabilities, this happens too in phosphate- and phosphonate-complexes. Also, there are some structures with *boat–boat* (BB) and *twist-boat* (S) as the most likely conformations, the same applies to phosphonate-complexes. The C/TC and BB/S pseudo-rotational pathways have been described in carbon eight-membered rings [6].

Acknowledgments

Financial support from the Centro de Coordinación de la Investigación de la Región de Murcia (Project PI-61/00813/FS/01), Spain, is gratefully acknowledged. M. Kessler and K. Nolsøe acknowledge the financial support provided through the European Community's Human Potential Programme under contract No. HPRN-CT-2000-00100, DYNSTOCH.

References

[1] M. Zimmer, Coord. Chem. Rev. 212 (2001) 133.
[2] A.G. Orpen, Chem. Soc. Rev. (1993) 191.
[3] T.J. Meyer, Acc. Chem. Res. 22 (1989) 163.
[4] M.D. Santana, G. García, A. Lozano, G. López, J. Tudela, J. Pérez, L. García, L. Lezama, T. Rojo, Chem. Eur. J. 10 (7) (2004) 1738.
[5] J.B. Hendrickson, J. Am. Chem. Soc. 89 (1967) 7047.
[6] F.H. Allen, J.A.K. Howard, N.A. Pitchford, Acta Crystallogr. B52 (1996) 882.
[7] D.G. Evans, J.C.A. Boeyens, Acta Crystallogr. B44 (1988) 663.
[8] D. Conklin, S. Fortier, J.I. Glasgow, F.H. Allen, Acta Crystallogr. B52 (1996) 535.
[9] F.H. Allen, O. Kennard, Chem. Des. Autom. News 8 (1) (1993) 31.
[10] K.V. Mardia, J.T. Kent, J.M. BibbyMultivariate Analysis, Academic Press, 1979, chapter 11.
[11] F.A.L. Anet, J. Krane, Tetrahedron Lett. 50 (1973) 5029.
[12] E. Kovari, R. Kramer, J. Am. Chem. Soc. 118 (1996) 12704.
[13] K.M. Norenberg, C.M. Shoemaker, M. Zimmer, J. Chem. Soc., Dalton Trans. (1997) 1521.
[14] K. Barthelet, M. Nogues, D. Riou, G. Feray, Chem. Mater. 14 (2002) 4910.

Paper IV

Model Based Conformational Analysis of Ring Molecules

IV

Submitted to *Chemometrics and Intelligent Laboratory Systems*

Model Based Conformational Analysis of Ring Molecules

Mathieu Kessler[1], Kim Nolsøe[2], María C. Bueso[1] and José Pérez[1]
[1] *Universidad Politécnica de Cartagena, Spain* [2] *Denmark Technical University*

Short Title : Model Based Conformational Classification.

Corresponding Author:
Mathieu Kessler, Departamento de Matemática Aplicada y Estadística, Universidad Politécnica de Cartagena, Paseo Alfonso XIII, E-30203 Cartagena, España, tel = +34 968 325662, Mathieu.Kessler@upct.es, fax = +34 968 325694.

Abstract

In this paper we address the problem of classifying the conformations of m-membered rings using experimental observations obtained by crystal structure analysis. We formulate a model for the data generation mechanism that consists in a multidimensional mixture model. We propose two methods to perform inference for the proportions and the components: the first method consists in a full Bayesian analysis, implementing an MCMC Reversible Jump Algorithm to obtain samples of the posterior distributions, while the second method is an adaptation of the model based clustering algorithms suggested by [1]. Both methods are illustrated on a real dataset corresponding to cyclo-octane structures.
Keywords: Cycloalkanes, Reversible Jump, Conformational Analysis, Mixture Model, MCMC, Clustering Algorithms.

1 Introduction

For a given compound it is of interest to study what are the preferred geometrical conformations of the corresponding molecules. The conformational classification of structures and in particular, the understanding of the factors that determine the molecular structure of a particular compound is important, since ideally it would allow for a rational design of complexes with specific and predictable properties.

A first approach to conformational analysis consists in theoretical computations: molecular mechanics combined with energy considerations allow to define, for some particular structures, a given number of theoretical canonical conformations. However it is known from experimental data that some of these canonical conformations are almost never observed, and that, in contrast, some new conformations may appear, which usually are deformations of the canonical ones. As a consequence, statistical descriptive methods have been employed as a complement to molecular mechanics computations, to detect and identify the preferred conformations in a given compound, that is to cluster the observed structures into a number of conformations. A review of different statistical methods for conformational analysis can be found in [2]. These methods generally take a data analysis approach where no model is assumed for the data generation mechanism, and all the conclusions rely on the correlation structure or the similarity structure of the data. Cluster analysis and principal components analysis are examples of such methods.

In this paper, we address the problem of conformational classification of m-membered rings, from the observation of crystallographic data consisting in the torsion angles for a number of structures. In contrast to previously proposed methods, an essential step in our approach specifies a probabilistic model for the observed sequences of torsion angles. This probabilistic model is a mixture model with an unknown number of components. We then suggest two methods to perform inference on the parameters of interest: the first method consists in a full Bayesian analysis, which includes prior specification and the implementation of the Reversible Jump MCMC methodology proposed by [3] to obtain samples of the posterior distribution of the parameters, while the second method consists in a model-based clustering algorithm derived by [1].

Section 2 describes the data and specifies the model. In Section 3, the full Bayesian analysis method is presented while the model-based clustering algorithm is described in Section 4. The results of both methods on a real dataset corresponding to cyclo-octane previously investigated by [4] are presented in Section 5. Finally some conclusions are drawn in Section 6.

2 The model

2.1 Description of the data

The Cambridge Structural Database (CSD) is a powerful tool that provides chemists access to a large amount of crystallographic structural data. Users of the CSD can retrieve the structures that match a given criterion from the database, for example all the cyclo-octane structures, and obtain the associated crystallographic data.

Consider an m-membered ring built-up from m consecutive atoms $A_1, A_2, \ldots, A_m$. The crystallographic data that can be used to characterize the structure consist in

1. The sequence of m atomic lengths $d_{1;\,2}, d_{2;\,3}, \ldots, d_{m-1;\,m}, d_{m;\,1}$, where $d_{k;\,k+1}$ denotes the distance between atom A_k and atom A_{k+1}.

2. The sequence of m bond angles $b_{1;\,2;\,3}$, $\ldots$ $b_{k-1;\,k;\,k+1}, \ldots, b_{m;1;2}$, where $b_{k-1;\,k;\,k+1}$ denotes the angle $A_{k-1}\widehat{A_kA_{k+1}}$ which is taken to belong to $[0, 180[$ degrees.

3. The sequence of m torsion angles $\tau_{1;\,2;\,3;\,4}$, $\ldots$, $\tau_{k-2;\,k-1;\,k;\,k+1}$, $\ldots$ $\tau_{m;\,1;\,2;\,3}$, where $\tau_{k-2;\,k-1;\,k;\,k+1}$ denotes the torsion - or dihedral angle - between the atoms A_{k-2}, A_{k-1}, A_k and A_{k+1}. This torsion angle can be seen as the angle between the plane that contains A_{k-2}, A_{k-1} and A_k and the plane that contains A_{k-1}, A_k and A_{k+1}. More concretely, the torsion angle (or angle of twist) about the bond B–C in a series of bonded atoms A–B–C–D is defined as the angle of rotation needed to make the projection of the line B–A coincide with the projection of the line C–D, when viewed along the B–C direction. The positive sense is clockwise.

For a precise definition of these quantities, see [5], p 161. The bond angles and distances present little variability between conformations corresponding to the same kind of structures. Therefore, as for geometrical conformation is concerned, the most informative set of characteristics associated to a given m-membered ring structure consists in the m associated torsion angles. These data can be retrieved from the CSD and we will assume that inference is to be made on the conformations and their frequencies of occurrence based on a sample of n structures for each of which we observe the sequence of m torsion angles. In particular, in Section 5, we will carry out the conformational classification of a sample of 31 cyclo-octane structures retrieved from the CSD. This dataset was previously analyzed by means of cluster analysis by [4].

We want to emphasize some important issues related to the data: assume that we retrieve from the CSD the torsion angles corresponding to an $m = 8$ membered ring built of consecutive atoms $A_1, A_2, \ldots,\ A_8$.

For this single structure, the data consist in the sequence

$$(Tor(A_1, A_2, A_3, A_4), Tor(A_2, A_3, A_4, A_5), \ldots \\ Tor(A_7, A_8, A_1, A_2), Tor(A_8, A_1, A_2, A_3)) = (\tau_1, \tau_2, \ldots, \tau_7, \tau_8),$$

i.e. the torsion angles computed from 4 consecutive atoms, where the starting atom is varying through the whole ring. However from the retrieved data it is impossible to know what was the atom that was chosen as a starting point to begin measuring the torsion angles. Concretely, this means that, for the same structure, the data could as well be $(\tau_2, \tau_3, \ldots, \tau_8, \tau_1)$, $(\tau_3, \tau_4, \ldots, \tau_1, \tau_2)$ or any of the cyclical translations of $(\tau_1, \tau_2, \ldots, \tau_7, \tau_8)$.

Moreover, the perspective from which the molecule is being measured can either be from above or from below. This implies that, for the same structure, the sequence of torsion angles can be read in a clockwise or counter clockwise manner.

Finally, if a given conformation is present in the compound, its mirror image can also be found. As a consequence, and as described in [5] p 49, the two sequences of torsion angles $(\tau_1, \tau_2, \ldots, \tau_7, \tau_8)$ and $(-\tau_1, -\tau_2, \ldots, -\tau_7, -\tau_8)$ can be met but shall be considered to correspond to equivalent conformations.

To sum up, consider an m-dimensional vector $\mu = (\mu_1, \ldots, \mu_m)$. The effect of choosing a starting point s in $\{1, \ldots, m\}$, a direction d, which equals 1 if the sequence is read clockwise or -1 if it is read counter-clockwise, and choosing a sign $\delta = \pm 1$, is described through the operator $T^{s,d,\delta}$ which acts on μ in the following way

$$T^{s,d,\delta}\mu = \delta \times (\mu_s, \mu_{((s-1+d\times 1) mod\ m)+1}, \ldots, \mu_{((s-1+d\times(m-1)) mod\ m)+1}), \tag{1}$$

where for any integer j, $j\ mod\ m$ denotes the remainder of the integer division of j by m. Notice in particular that $T^{1,1,1}\mu = \mu$. For any $1 \leq s \leq m$, $d = \pm 1$, $\delta = \pm 1$, the data $T^{s,d,\delta}\tau$ should be considered to be equivalent to τ.

These three aspects of the retrieved data will be taken into account when we formulate our model in Subsection 2.2.

In the sequel we will repeatedly use the notation $\mu_{1:m}$ to denote a m-dimensional vector $\mu = (\mu_1, \ldots, \mu_m)$.

2.2 The formulation of the model

Assume that we have retrieved n structures from the CSD, and denote by $\tau^{(1)}, \ldots, \tau^{(n)}$ the n associated m-dimensional vectors of torsion angles. We assume that they correspond to independent and identically distributed realizations from a mixture law with density

$$f(\tau) = \sum_{c=1}^{k} w_c f(\tau, c). \tag{2}$$

We would like to specify each density $\tau \mapsto f(\tau, c)$ to be multivariate normal with mean vector $\mu_{c,1:m}$ and diagonal covariance matrix $\sigma_c^2 Id_m$, but we have to take into

account the aspects of the data described in the previous Subsection: for any $1 \leq s \leq m$, $d = \pm 1$, $\delta = \pm 1$, the two vectors τ and $T^{s,d,\delta}\tau$ - see (1) - are equivalent in the sense that they yield the same density value. Concretely, this means that $\tau \mapsto f(\tau, c)$ is itself a mixture with $m \times 2 \times 2$ components, each of which correspond to a given equivalent version $T^{s,d,\delta}\tau$ of τ. To sum up, the likelihood is, for a number k of components,

$$\prod_{i=1}^{n} \left(\sum_{c=1}^{k} w_c \cdot \sum_{\substack{1 \leq s \leq m \\ d=\pm 1, \delta=\pm 1}} \frac{1}{4m} f_G(\tau, T^{s,d,\delta}\mu_{c,1:m}, \sigma_c^2 Id_m) \right), \tag{3}$$

and $\tau \mapsto f_G(\tau, T^{s,d,\delta}\mu_{c,1:m}, \sigma_c^2 Id_m)$ denotes the density of the m-dimensional Gaussian law with mean $T^{s,d,\delta}\mu_{c,1:m}$ and diagonal covariance matrix $\sigma_c^2 Id_m$.

From the observation of n sequences of m torsion angles $\tau^{(1)}, \ldots, \tau^{(n)}$, the parameters we want to infer about are: the number k of components, the components weights $w_{1:k}$, the components means $\mu_{1,1:m}$, ..., $\mu_{k,1:m}$ and the variances $\sigma_1^2, \ldots \sigma_k^2$.

3 The full Bayesian analysis

The full Bayesian analysis proceeds by specifying prior distributions for the parameters of interest (including the number of components k) and update, through the Bayes rule, this prior information to obtain the posterior distributions. No tractable expressions are available for the latter and we set up an MCMC algorithm to simulate samples from the posterior distributions, from which we extract the main characteristics. Notice that, since the number of components is itself a parameter, the constructed chain shall be able to jump between spaces of varying dimensions.

3.1 Extension of the parameter space

Since we need in particular to specify distributions for the torsion angles both for the prior elicitation and for the sampling steps in the MCMC algorithm, we shall be aware that, for a given structure, the m torsion angles cannot be choosen arbitrarily. Assume we want to build an m-membered ring, how many torsion angles, bond angles and distances do we have to specify? To define the relative positions of the first two atoms, it is enough to specify the distance $d_{1;\,2}$. The position of the third atom will be fixed if we specify further $d_{2;\,3}$ and the bond angle $b_{1;\,2;\,3}$, while to position the fourth atom we will need $d_{2;\,4}$, $b_{2;\,3;\,4}$ and the torsion angle $\tau_{1;\,2;\,3;\,4}$. From there on, an additional atom requires the specification of one more distance, one more bond angle and one more torsion angle. The procedure is summarized in

$$A_1 \xrightarrow{d_{1;\,2}} A_2 \xrightarrow{d_{2;\,3},\ b_{1;\,2;\,3}} A_3 \xrightarrow[\tau_{1;\,2;\,3;\,4}]{d_{3;\,4},\ b_{2;\,3;\,4}} A_4 \rightarrow \ldots \xrightarrow[\tau_{k-3;\,k-2;\,k-1;\,k}]{d_{k-1;\,k},\ b_{k-2;\,k-1;\,k}} A_k \rightarrow \ldots$$

As a conclusion, we can build sequentially an m-membered ring if we specify the first $m-1$ distances, $m-2$ bond angles and $m-3$ torsion angles.

We will denote by F the mapping that relates the torsion angles, bond angles and distances of an m-membered ring through

$$(\tau_{1:m}, b_{1:m}, d_{1:m}) = F(\tau_{1:m-3}, b_{1:m-2}, d_{1:m-1}). \tag{4}$$

It is possible to obtain an operational, though not straightforward, description of the mapping F, by using appropiate change of coordinates.

3.2 The prior distributions

For the unknown number of components, the variances of the Gaussian perturbations and the mixture proportions, we follow [6] and [7], and choose the following priors:

$$\begin{array}{rcll} k & \sim & U(1, k_{max}), & \\ \sigma_1^2, \ldots, \sigma_k^2 \text{ are independent and } \sigma_i^2 & \sim & \mathfrak{IG}(\alpha_i, \beta_i), & i = 1, \ldots, k, \\ (w_1, \ldots, w_k) & \sim & \mathfrak{D}(1, \ldots, 1), & \end{array}$$

where $U(1, k_{max})$ denotes the discrete uniform distribution on the integers between 1 and k_{max}, $\mathfrak{IG}(\alpha, \beta)$ denotes the Inverse Gamma distribution with parameters (α, β), and $\mathfrak{D}(\alpha_1, \ldots, \alpha_k)$ denotes the Dirichlet distribution with parameters $(\alpha_1, \ldots, \alpha_k)$.

On the other hand, we have to specify our prior distribution on $\mu_{c,1:m}$, $b_{c,1:m}$ and $d_{c,1:m}$ for $c = 1, \ldots, k$ and we want it to charge only physically coherent molecules.

From Subsection 3.1, it is known that this can be done by specifying a prior distribution for $\mu_{c,1:(m-3)}$, $b_{c,1:m-2}$ and $d_{c,1:m-1}$, and deduce the remaining angles and lengths through the mapping F, see (4). We therefore choose, for all $c = 1, \ldots, k$

$$\mu_{c,1:(m-3)} \sim \bigotimes_{1:(m-3)} U(-\pi, \pi), \tag{5}$$

$$b_{c,1:(m-2)} \sim N(\eta^b_{1:m-2}, \kappa^b \, Id_{m-2}), \tag{6}$$

$$d_{c,1:(m-3)} \sim N(\eta^d_{1:m-1}, \kappa^d \, Id_{m-3}). \tag{7}$$

and

$$(\mu_{c,1:m}, b_{c,1:m}, d_{c,1:m}) = F(\mu_{c,1:m-3}, b_{c,1:m-2}, d_{c,1:m-1}). \tag{8}$$

The choice of the prior for μ does not favor any specific conformation. On the contrary, the prior for the bond angles is meant to incorporate chemical knowledge: for the cyclo-octane dataset treated in Section 5 for example, it is known that bond angles for cyclo-octane are centered around 117 degrees, and present little variability, see *e.g.* [8], p 36.

3.3 The Reversible Jump MCMC algorithm

We use a Markov Chain Monte Carlo (MCMC) algorithm to obtain samples of the posterior distribution of the parameters. Given a target distribution π, such an algorithm allows to simulate trajectories of an ergodic Markov Chain with stationnary distribution

π by specifying how to choose the transition of the chain. The Metropolis Hastings algorithm implements a specific way to construct the transition: given a point of the chain, a candidate is proposed for the next point, from a user-provided candidate distribution and accepted or rejected with a specific probability. For an extensive account on MCMC methods see e.g. [9]. The Reversible Jump MCMC was introduced by [3] as a Markov chain algorithm for varying dimension problems. It consists in a random sweep Metropolis-Hastings method adapted for general state space, which is able to jump between spaces of different dimensions. It was applied to carry out Bayesian inference in one-dimensional Gaussian-Mixture models with an unknown number of components in [6] and later in [7], to which we refer for more details about the implementation of the algorithm.

A complete sweep of the algorithm consists in a scanning of the following move types:

(a) updating the weights w,

(b) updating the parameters $(\mu_{1:m}, b_{1:m}, d_{1:m})$,

(c) updating the variance parameters $\sigma^2_{1:k}$,

(d) the birth or death of a component.

At each iteration of the algorithm we either perform the three fixed-k moves (a), (b) and (c) altogether or the birth/death move (d). Each of these two possibilities is decided upon with probability 0.5. Moreover, if we decide to perform move type (d), we choose either birth or death of a component with probability 0.5.

As for move types (a) and (c), we follow [7] and choose multiplicative Lognormal random walks for updating the weights and the variances parameters. As for the move type (b), given the previous sample $(\mu_{1:m}, b_{1:m}, d_{1:m})$, we propose the candidate $(\mu^*_{1:m}, b^*_{1:m}, d^*_{1:m})$, ensuring that it is associated to a physically coherent m-membered ring, by updating $(\mu_{1:m-3}, b_{1:m-2}, d_{1:m-1})$ following a Gaussian Random Walk proposal, and deduce the remaining parameters $\mu^*_{m-2:m}$, $b^*_{m-1:m}$ and d^*_m using the F mapping described in Subsection 3.1.

Finally, as for the move type (d), the birth move consists in creating a new component, by first drawing $w^*_{k+1} \sim \mathcal{B}e(1, k)$. The candidate weights are then deduced through, for $j = 1, \ldots, k$, $w^*_j = w_j(1 - w^*_{k+1})$. The remaining parameters for the new component $(\mu^*_{k+1,1:m}, b^*_{k+1,1:m}, d^*_{k+1,1:m})$ and $\sigma^{2^*}_{k+1}$ are drawn from their prior distributions, and appended to the current state parameters.

3.4 Post processing of the output

As described in, for example, [10], the invariance of the likelihood under arbitrary relabeling of the mixture components leads to symmetries in the posterior distributions of the parameters, which are therefore difficult to summarize. In particular the posterior marginal distributions are, for permutation invariant priors, indistinguishable. One of the proposed solutions consists in imposing identifiability constraints on the parameter space through an ordering specification in the prior. Alternatively, post processing

algorithms of the output of the MCMC trajectories, which involve a relabeling of the mixture components, have been investigated, see [10].

We follow a post processing algorithm proposed by [10], which intends to carry out, for each value of the parameters provided by the sampler, a relabeling of the components so that the relabeled sample points all agree well with each other. More concretely, if $\theta^{(1)}, \ldots, \theta^{(N)}$ are the N samples of the posterior distributions of the parameters provided by the MCMC algorithm, the aim is to find N permutations $\nu_1, \ldots, \nu_N$ which operate a relabeling of each $\theta^{(1)}, \ldots, \theta^{(N)}$ such that the permuted parameters $\nu_1(\theta^{(1)}), \ldots, \nu_N(\theta^{(N)})$ present the same ordering of the components.

4 Model-based clustering algorithm

A number of new clustering methods have arisen from the premise that clustering analysis can be based on probabilistic models. These approaches allow in particular to restate the basic questions in an inferential context and get insight about when a particular method is expected to work well. We have adapted one of these approaches, the `mclust` algorithm suggested by [1], to take into account the characteristics of the torsion angle data that were described in Subsection 2.1 and deal with the finite mixture model of equation (3). The `mclust` algorithm builds upon two methods: hierarchical agglomeration based on the classification likelihood and the EM algorithm for maximum likelihood estimation of multivariate mixture models.

4.1 Hierarchical agglomeration algorithm

Given the data $\tau^{(1)}, \ldots, \tau^{(n)}$, introduce the labels $\gamma_1, \ldots, \gamma_n$, where $\gamma_i = c$ if the data $\tau^{(i)}$ was generated from the conformation number c. In the classification likelihood approach to clustering, the choice of the unknown parameters θ and the labels $\gamma_{1:n}$ is made so as to maximize the classification likelihood:

$$l_{clas}(\theta; \gamma_{1:n}) = \prod_{i=1}^{n} f(\tau^{(i)}, \gamma_i),$$

where $\tau \mapsto f(\tau, c)$ corresponds to the density of the c-th component, see Subsection 2.2.

Since there is only a finite number of possibilities for the labels $\gamma_1, \ldots, \gamma_n$, the maximum is obtained by first maximizing the classication likelihood with respect to θ for a fixed $\gamma_{1:n}$ and then find the optimal labels. Using the normality assumption, the first maximization can be carried out explicitely, and the second step can then be expressed as follows.

Assuming a partition in k groups, the optimal labels $\gamma_{1:n}$ minimize the criterion:

$$\sum_{c=1}^{k} n_c \log \left[tr\left(\frac{W_c}{n_c}\right)\right], \tag{9}$$

where n_c denotes the number of members in cluster c, and $W_c = \sum_{\gamma_i=c}(\tau^{(i)} - \bar{\tau}_k)(\tau^{(i)} - \bar{\tau}_k)^T$ denotes the sample cross-product matrix for the k-th group.

In fact, due to the characteristics of the cristallographic data, not only the optimal labels should be found, but also the optimal choices for the starting point s_i, the direction d_i and the sign δ_i for each data $\tau^{(i)}$. It is possible to prove that, for a given partition in groups, this is achieved by fixing a representative member in each group, and for each data $\tau^{(i)}$, choose T^{s_i,d_i,δ_i} such that the euclidean distance from $T^{s_i,d_i,\delta_i}\tau^{(i)}$ to its group representative is minimum.

Finally, the agglomerative hierarchical clustering algorithm consists in a stagewise procedure in which optimal pairs of clusters are sucessively merged. At a given stage, two clusters are said to be optimal if their merging leads to the minimum increase of the quantity in (9).

The resulting agglomerative algorithm can be used to build a hierarchical classification of the structures. However, it does not provide a way to decide the number of preferred conformations. The `mclust` algorithm uses the output of the hierarchical classification as input to an EM algorithm and computes the BIC criterion to assess the number of clusters.

4.2 EM algorithm

Given our model, the EM algorithm can be straightforwardly implemented if we complete the data $\tau^{(1)}, \ldots, \tau^{(n)}$ by considering, for any $i = 1, \ldots, n$, $c = 1, \ldots, k$, $s = 1, \ldots, m$, $d = \pm 1$, $\delta = \pm 1$,

$$R_{icsd\delta} = \begin{cases} 1 & \text{if } x_i \text{ was generated from } f(\cdot, c), \text{ with the starting point } s, \\ & \text{the direction } d \text{ and the sign } \delta \\ 0 & \text{otherwise} \end{cases}$$

The r-th iteration of the algorithm consists then in the following steps:

E-Step Compute the conditional expectation

$$R^{(r)}_{icsd\delta} = E\left[R_{icsd\delta} | \tau^{(1)} \ldots \tau^{(n)}, \theta^{(r)}\right] = \frac{w_c^{(r)} f_G(\tau^{(i)}, T^{s,d,\delta}\mu^{(r)}_{c,1:m}, \sigma_c^{2(r)} Id_m)}{\sum_{j,h,s,\varepsilon} w_j^{(r)} f_G(\tau^{(j)}, T^{h,s,\varepsilon}\mu^{(r)}_{j,1:m}, \sigma_j^{2(r)} Id_m)},$$

where f_G is defined in Subsection 2.2.

M-step Update the estimates for the parameters by

$$w_c^{(r+1)} = \frac{\sum_{i,s,d,\delta} R_{icsd\delta}^{(r)}}{n}, \quad \mu_{c,1:m}^{(r+1)} = \frac{\sum_{i,s,d,\delta} R_{icsd\delta}^{(r)} \left(T^{s,d,\delta}\right)^{-1} \tau^{(i)}}{\sum_{i,s,d,\delta} R_{icsd\delta}^{(r)}},$$

$$\sigma_c^{2(r+1)} = \frac{\sum_{i,s,d,\delta} R_{icsd\delta}^{(r)} (\tau^{(i)} - T^{s,d,\delta}\mu_{c,1:m}^{(r+1)})^T (\tau^{(i)} - T^{s,d,\delta}\mu_{c,1:m}^{(r+1)})}{m \sum_{i,s,d,\delta} R_{icsd\delta}^{(r)}},$$

for $c = 1, \ldots, k$.

5 Results

In [4] measurements of torsion angles for cyclo-octane were retrieved from the Cambridge Structural Database and principal component analysis and cluster analysis were carried out. The authors considered in particular a dataset, labeled 8C1 in their paper, consisting of 31 observations, of which 12 were classified as Boat-Chair (BC), 10 as two different components both identified as "deformed" BC, (in between BC and Twist-Boat-Chair (TBC)) and finally 2 observations were classified as respectively Crown (CR) and Twist-Chair-Chair (TCC), 7 observations were not classified. The standard deviations within the clusters seem to be centered around 15 degrees.

We have processed the 8C1 dataset with both the full Bayesian analysis method and the model-based clustering method described in Sections 3 and 4.

5.1 Full Bayesian analysis

The posterior distribution for the number k of components in the mixture is presented in Figure 1 a), from which we deduce that $k = 6$ or $k = 7$ is the most likely value. The post-processing algorithm was therefore carried out for both values of k and no significant differences were found concerning the main groups. We present here the results obtained with $k = 7$. Box plots of the posterior distributions for the weights, the standard deviations and the mean vector of the most populated cluster are presented in Figure 1 b), c) and d), respectively. In these box plots, the 10%, 15%, 25%, 50%, 75%, 85% and 90% percentiles are indicated. The obtained results and assignations coincide basically with the four main clusters detected in [4].

5.2 Model-based clustering algorithm

We have applied the adapted `mclust` algorithm to the 8C1 dataset, first carrying out the hierarchical agglomerative classification, and then computing the maximum likelihood estimators using the EM algorithm when the data are assumed to be partioned in k

groups, k ranging from 1 to 15 groups. For each of these possible number of groups, the BIC criterion is computed.

In Figure 2, the evolution of the BIC and the corresponding successive differences are plotted against the considered number of groups. The BIC value increases when the number of groups increases, tending to favor more clusters. From $k = 5$ the sucessive differences are relatively small, which would indicate that 4 to 7 clusters are present. More importantly, the assignation of the structures to the main clusters remain stable when k ranges from 4 to 7, and this assignation coincides basically with the results of the full Bayesian analysis and the results reported in [4].

6 Conclusions

We have implemented two approaches to conformational classification of m-membered rings. Both are based on the formulation of a multivariate mixture model for the observation of torsion angles. We can see several advantages of the full Bayesian approach to this applied problem: on the one hand, it easily allows to take into account, through an extension of the parameter space, the physical restrictions and the intricate relations these imply between the torsion angles. On the other hand, we have been able to include chemical knowledge as part of the prior specification. Moreover, the output includes a measure of the uncertainty linked to the inference procedure, which represents a useful information for chemists.

However the main disadvantage of the method consists in its difficult implementation and the fact that some experience is required to tune the parameters used in the MCMC chain in order to obtain good mixing.

On the contrary, the model-based clustering method is simple to implement and fast, and the results are satisfactory. We do not see though how we could, in this approach, take into account the intricate physical restrictions present in the data.

Acknowledgements. This work was supported in part by the European Community's Human Potential Programme under contract HPRN-CT-2000-00100, DYNSTOCH and by the Project MTM2005-08597 of the DGI, Ministerio de Ciencia y Tecnología, Spain.

References

[1] C. Fraley and A.E. Raftery. Model-based clustering, discriminant analysis and density estimation. *J. Amer. Statist. Assoc.*, 97(458):611–631, 2002.

[2] M. Zimmer. Molecular mechanics, data and conformational analysis of first-row transition metal complexes in the cambridge strutural database. *Coord. Chem. Rev.*, 212:133–163, 2001.

[3] P. J. Green. Reversible jump Markov chain Monte Carlo computation and Bayesian model determination. *Biometrika*, 82(4):711–732, 1995.

[4] F.H. Allen, J.A.K. Howard, and N.A. Pitchford. Symmetry-modified conformational mapping and classification of the medium rings from crystallographic data. iv. cyclooctane and related eight-membered rings. *Acta Cryst.*, B52:882–891, 1996.

[5] W. Mass. *Crystal Structure Determination*. Springer-Verlag, Berlin, second edition, 2004.

[6] S. Richardson and P. J. Green. Corrigendum: "On Bayesian analysis of mixtures with an unknown number of components" [J. Roy. Statist. Soc. Ser. B **59** (1997), no. 4, 731–792]. *J. R. Stat. Soc. Ser. B Stat. Methodol.*, 60(3):661, 1998.

[7] O. Cappé, C. P. Robert, and T. Rydén. Reversible jump, birth-and-death and more general continuous time Markov chain Monte Carlo samplers. *J. R. Stat. Soc. Ser. B Stat. Methodol.*, 65(3):679–700, 2003.

[8] J.D. Dunitz. Conformations of medium rings. In J.D. Dunitz and J.A. Ibers, editors, *Perspectives in Structural Chemistry, Vol II*, 1968.

[9] C. P. Robert and G. Casella. *Monte Carlo statistical methods*. Springer Texts in Statistics. Springer-Verlag, New York, second edition, 2004. xxx+645 pp.

[10] M. Stephens. Dealing with label switching in mixture models. *J. R. Stat. Soc. Ser. B Stat. Methodol.*, 62(4):795–809, 2000.

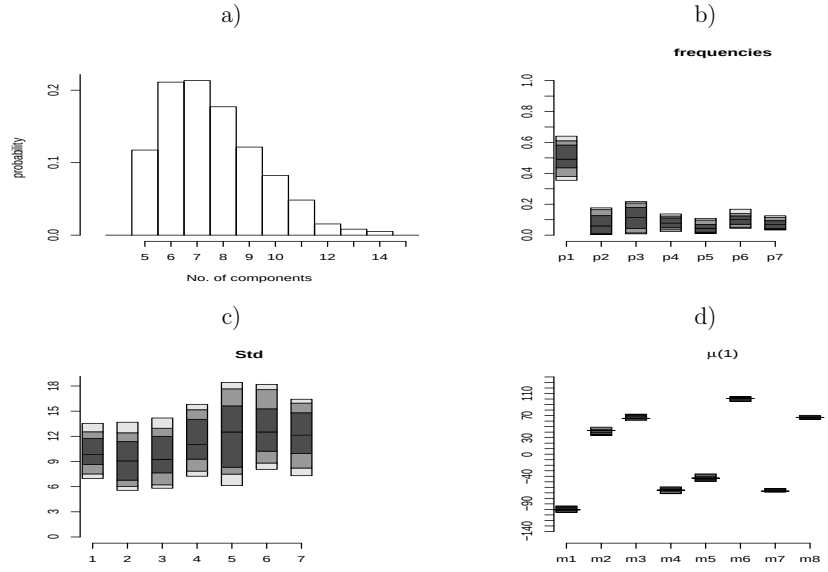

Figure 1: Cyclo-octane dataset of Section 5: a) posterior distribution for the number k of components; b), c) and d) Box plot-like diagrams of the posterior distributions of frequencies and standard deviations and the mean vector of the most populated cluster, when $k = 7$ components are chosen.

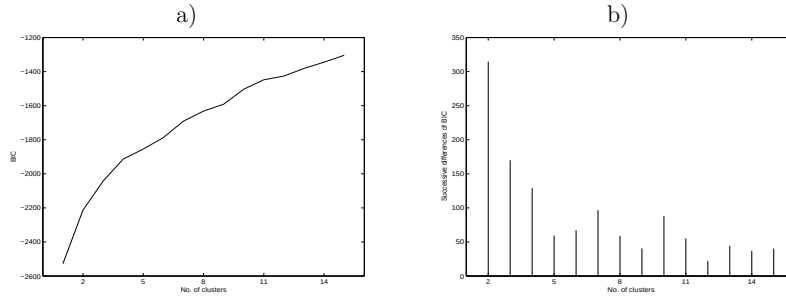

Figure 2: Cyclo-octane dataset of Section 5: BIC values vs. number of components a), and successive differences for the BIC values vs. number of components b).

Paper V

Estimating Functions with Prior Knowledge, (EFPK) for Diffusions

V

Working paper

Estimating Functions with Prior Knowledge, (EFPK) for Diffusions

Kim Nolsøe Mathieu Kessler Henrik Madsen

June 12, 2006

Abstract

In this paper a method is formulated in an estimating function setting for parameter estimation, which allows the use of prior information. The main idea is to use prior knowledge about the parameters, either specified as moment restrictions or as a distribution, and use it in the construction of an estimating function. The method may be useful on one hand when the full Bayesian analysis is difficult to carry out for computational reasons, which often is the case for diffusions. On the other hand, when few observations are available, the proposed method yields a simple way to incorporate prior knowledge.
Keywords: Small sample size, Estimating Functions, Diffusion Process, Cox Ingersoll & Ross (CIR) Process.

1 Introduction

Diffusion processes are widely used within engineering, physics, biology and finance since in many cases they are able to provide a good description of data using a limited number of parameters. Most importantly the continuous time formulation enables a direct use of prior physical knowledge in the model formulation and a direct interpretation of the estimated parameters. However, inference about the parameters from a discretely observed trajectory at equidistant times cannot in general be based on the likelihood since there is no analytical closed form available for it. Among the methods that were developed to overcome this difficulty, we can distinguish the ones which approximate the likelihood from the ones that intend to mimic the score function (the derivative of the loglikelihood with respect to the parameter).

In the first class, apart from the natural Gaussian approximation for the transition density of the observed Markov chain, attention has been paid to numerical approximations of the transition; examples are the iteration of Gaussian densities inspired by the Euler scheme, [Pedersen, 1995], and truncated series expansions of transformed Hermite functions, [Aït-Sahalia, 2002]. These methods proved to behave well on simulations but have the drawback of being time-consuming.

The estimating functions approach, that was initiated for discretely observed diffusions in [Bibby and Sørensen, 1995], can, to a certain extent, be seen as an attempt to mimic the unknown score function. Indeed, in a class, the optimal estimating function is the projection in some convenient sense of the score function. A nice feature of this methodology is that, even if you do not know how to approximate the derivative of the transition, any unbiased, or asymptotically unbiased, estimating function yields a reasonable estimator (consistent and $\sqrt{n}-$ asymptotically normal under mild conditions). For a review of these issues in diffusions models, see e.g [bib, 2004], while an introduction to the general theory for estimating functions can be found in [Heyde, 1997].

These methods provide good estimators when sufficient data are available, but are known to perform poorly when only few points in the trajectory are observed. When available, the incorporation of prior knowledge about the parameters is then desirable and it is well known that, in this case, the Bayesian methods usually outperform the frequentist approach. Of course, Bayesian inference for these models also requires the evaluation of the likelihood, and therefore the knowledge of the intractable transition density. To compute efficiently approximations to the posterior density, MCMC algorithms based on data augmentation schemes, were investigated in [Elerian et al., 2001], [Eraker, 2001] and [Roberts and Stramer, 2001]. However, as usual with these kind of schemes, the convergence is difficult to assess and implementation for multidimensional diffusions is not straightforward.

In this paper, we investigate an alternative approach to the full Bayesian method which consists in incorporating possible prior knowledge to estimating functions, forming the Estimating Functions with Prior Knowledge, *EFPK* from now on. These estimating functions turn out to be a simple way to produce an estimator that takes into account prior information about the parameter, they are easily implementable and perform better than the classical estimating functions when few data are observed, but prior information is available.

EFPK is introduced in Section 3.2. In Section 4 an optimality criterion is described. The behavior of the proposed estimator is investigated in Section 5 for a data set containing measurements of Nitrous Oxide concentrations in a measurement apparatus, previously addressed in [Pedersen, 2000]. Finally Section 6 contains concluding remarks.

2 Framework and notations

2.1 The model given the parameter

In this paper we consider one-dimensional diffusions characterized by

$$dX_t = a(X_t;\theta)dW_t + b(X_t;\theta)dt, X_0 = x_0, \tag{1}$$

where W_t is the one-dimensional standard Brownian motion. The parameter $\theta = (\theta_1, \ldots, \theta_p)$ is a p-dimensional vector from the parameter space $\Theta \subseteq \mathbb{R}^p$, $p \in \mathbb{N}$, the functions $a : \Omega \times \Theta \mapsto \mathbb{R}$ and $b : \Omega \times \Theta \mapsto \mathbb{R}$ are known up to θ. Let E denote the

state space of X, $E \subseteq \mathbb{R}$. $X_0 = x_0$ indicates that the process is known at t_0 and the true value of θ is denoted θ_0. The functions a and b are assumed to be smooth enough to ensure the uniqueness of the law of the solution to (1). We work on the canonical space endowed with the filtration generated by the projections, and denote by $\mathbb{P}_\theta$ the probability induced by the solution to (1) for $\theta \in \Theta$.
We assume that the trajectory is observed at discrete times: $t_1, \ldots, t_n$, with $t_1 < t_2 < \ldots < t_n$ and we denote the data by $(X_{t_1}, \ldots, X_{t_n}) = X_{1:n}$. Define $\Delta_i = t_i - t_{i-1}$, $i = 1, \ldots, n$

The sequence $\{X_{1:n}\}_{n\geq 1}$ is a Markov chain under $\mathbb{P}_\theta$, we assume that the distribution of X_{t_i} given $X_{t_{i-1}} = x$ under $\mathbb{P}_\theta$ admits a density with respect to the Lebesgue density, we denote this density by $p:\ y \mapsto p(\theta; x, y, \Delta_i), y \in E$.

We denote by $x_{1:n} \mapsto f(\theta; x_{1:n})$ the joint density of $(X_{1:n})$ for the value θ of the parameter.

The loglikelihood function $l : (\theta; X_{1:n}) \to l(\theta; X_{1:n})$ is then given by

$$l(\theta; X_{1:n}) = \sum_{i=1}^{n} \log p(\theta; X_{t_{i-1}}, X_{t_i}, \Delta_i), \tag{2}$$

and the score function $U : (\theta; X_{1:n}) \to U(\theta; X_{1:n})$, the derivative of the loglikelihood with respect to the parameter, is

$$U(\theta; X_{1:n}) = \sum_{i=1}^{n} \frac{\partial_\theta p(\theta; X_{t_{i-1}}, X_{t_i}, \Delta_i)}{p(\theta; X_{t_{i-1}}, X_{t_i}, \Delta_i)}. \tag{3}$$

We use the notation $\partial_\theta p(\theta; X_{t_{i-1}}, X_{t_i}, \Delta_i)$ for the column vector of the partial derivatives of the function p

$$\partial_\theta p(\theta; X_{t_{i-1}}, X_{t_i}, \Delta_i) = \left(\frac{\partial p(\theta; X_{t_{i-1}}, X_{t_i}, \Delta_i)}{\partial \theta_1}, \ldots, \frac{\partial p(\theta; X_{t_{i-1}}, X_{t_i}, \Delta_i)}{\partial \theta_p}\right)^T$$

where T denotes the transposed vector, it is implicitly assumed that the derivatives exist.

2.2 The prior information

We will assume that the prior information for each of the components will be given independently from each other. The prior distribution for $\theta \in \Theta$ will therefore be assumed to have the multiplicative form

$$\pi_1(\theta_1) \otimes \cdots \otimes \pi_p(\theta_p). \tag{4}$$

Moreover, for each of the components θ_i, $i = 1, \ldots, p$, we will consider two ways to incorporate the prior knowledge:

Either: Case A_i. A full prior distribution for θ_i is specified, in which case it is denoted by $\theta_i \mapsto \pi_i^*(\theta_i)$,

Or: Case B_i. Only some prior expectations are specified. That is, we do not want to provide a full distribution for θ_i, instead, we will only assume given k numbers $\mu_j^{(i)}, \quad j = 1, \ldots, k$ which represent the prior expectations of k user-specified functions $f_1^{(i)}(\theta_i), \ldots, f_k^{(i)}(\theta_i)$. Tipically, the prior specification could be done through prior moments; in this case the functions $f_1^{(i)}(\theta_i), \ldots, f_k^{(i)}(\theta_i)$ would be the appropiate polynomials, see example 1 below.

We will denote by Π_i, either the set of all probability distributions that fullfill the prior moments conditions in case B_i:

$$\Pi_i = \left\{ \pi : \ \pi \text{ prob. distributions such that } \forall 1 \leq j \leq k \ \int f_j^{(i)}(\theta_i)\pi(d\theta_i) = \mu_j^{(i)} \right\},$$

or the singleton $\Pi_i = \{\pi_i^*(\theta_i)\}$ in case A_i.

We denote the resulting set of probability distributions by Π:

$$\Pi = \{\pi(\theta) = \pi_1(\theta_1) \otimes \cdots \otimes \pi_p(\theta_p) : \pi_i(\theta_i) \in \Pi_i \quad , i = 1, \ldots, p\}.$$

The set Π is therefore to be interpreted as the set of all probability distributions that are compatible with our prior information specification.

EXAMPLE 1. *Consider a three-dimensional parameter $\theta = (\kappa, \varphi, \sigma^2)$, one choice of a prior specification could be*

$$\begin{aligned} B_1 &: \ E[\kappa] = \mu_1^{(1)}, \quad V[\kappa] = \mu_2^{(1)} \\ B_2 &: \ E[\varphi] = \mu_1^{(2)}, \quad V[\varphi] = \mu_2^{(2)} \\ A_3 &: \ \pi_3^* : \sigma^2 \sim \mathcal{IG}(\alpha, \beta) \end{aligned}$$

where $\forall x \quad f_1^{(1)}(x) = f_1^{(2)}(x) = x$, $f_2^{(1)}(x) = x^2 - (\mu_1^{(1)})^2$ *and* $f_2^{(2)}(x) = x^2 - (\mu_1^{(2)})^2$.

3 Estimating functions with prior knowledge

3.1 Estimating functions in the classical setting, a brief review

An estimating function G is a function of the parameter θ and the observation $X_{1:n}$ $G : (\theta; X_{1:n}) \to G(\theta; X_{1:n})$, that yields an estimator for θ by solving the p-dimensional equation

$$G(\theta; X_{1:n}) = 0.$$

Typically such an estimating function is required to be unbiased under $\mathbb{P}_\theta$ for all θ and in order to study the asymptotic behavior of the deduced estimator, a central limit theorem is assumed to hold for the sequence $\{G(\theta; X_{1:n})\}_n$. In the context of Markov chains, this is achieved by considering estimating functions of the form

$$G(\theta; X_{1:n}) = \sum_{i=1}^{n} g(\theta; X_{t_{i-1}}, X_{t_i}, \Delta_i),$$

for some well behaved function $g : y \mapsto g(\theta; x, y, \Delta)$, which satisfies

$$\int g(\theta; x, y, \Delta) p(\theta; x, y, \Delta) dy = 0, \quad \forall x, \forall \theta, \forall \Delta \tag{5}$$

further details can be found in e.g. [bib, 2004].

The construction of the estimating function G relies on the specification of some integrals of the transition density of the Markov chain: assume for example that we want to build estimating functions based on the specification of the first moment of the transition density, we will consider $g(\theta; x, y, \Delta) = \alpha_1 h_1(\theta; x, y, \Delta)$, with $h_1(\theta; x, y, \Delta) = (y - m_1(\theta; x, \Delta))$, where $m_1(\theta; x, \Delta) = \int u\, p(\theta; x, u, \Delta) du$ for all x and θ, and consider the class $\gamma_1(\theta; x, \Delta)$ of functions,

$$\gamma_1(\theta; x, \Delta) = \{g \in L_2(p(\theta; x, y, \Delta)dy), \ \exists\, \alpha_1 \in \mathbb{R}^p,\, g(\theta; x, y, \Delta) = \alpha_1 h_1(\theta; x, y, \Delta))\}\,.$$

Picking any function g in $\gamma_1(\theta; x, \Delta)$, we can construct an estimating function $G(\theta; X_{1:n}) = \sum_{i=1}^n g(\theta; X_{t_{i-1}}, X_{t_i}, \Delta_i)$ which, under $\mathbb{P}_\theta$ is unbiased and forms a martingale. We denote this class of estimating functions by

$$\begin{aligned} \mathcal{G}_1 \ &= \ \{G : (\theta; X_{1:n}) \mapsto G(\theta; X_{1:n}) \text{ s.t. } G(\theta; X_{1:n}) = \sum_{i=1}^n g(\theta; X_{t_{i-1}}, X_{t_i}, \Delta_i) \\ &\qquad \text{with } g \in \gamma_1(\theta; x, \Delta),\, \forall \theta, \forall \Delta, \forall x\}. \end{aligned}$$

Analogically we will consider estimating functions in

$$\begin{aligned} \gamma_2(\theta; x, \Delta) \ &= \ \Big\{g : y \mapsto g(\theta; x, y, \Delta) \in L_2(p(\theta; x, y, \Delta)dy), \exists\, \alpha_2 \in \mathbb{R}^{(p\times 2)}, && (6) \\ &\qquad g(\theta; x, y, \Delta) = \alpha_2 \begin{bmatrix} h_1(\theta; x, y, \Delta) \\ h_2(\theta; x, y, \Delta) \end{bmatrix} && (7) \\ &\qquad = \alpha_2 \begin{bmatrix} y - m_1(\theta; x, \Delta) \\ (y - m_1(\theta; x, \Delta))^2 - (m_2(\theta; x, \Delta) - m_1(\theta; x, \Delta)^2) \end{bmatrix} \Big\}. && (8) \end{aligned}$$

and refer to this class of estimating functions as $\mathcal{G}_2$.

More generally, we will consider, for all θ and x, linear finite dimensional subspaces $\gamma(\theta; x, \Delta)$ of $L_2^*(\mathbb{P}_\theta)$ - the subspace of functions $g(\theta; x, y, \Delta)$ in $L_2(\mathbb{P}_\theta)$ that satisfy (5) - and construct the class of estimating functions

$$\begin{aligned} \mathcal{G} \ &= \ \{G : (\theta; X_{1:n}) \mapsto G(\theta; X_{1:n}) \text{ s.t. } G(\theta; X_{1:n}) = \sum_{i=1}^n g(\theta; X_{t_{i-1}}, X_{t_i}, \Delta_i) \qquad (9) \\ &\qquad \text{with } g(\theta; x, y, \Delta) \in \gamma(\theta; x, \Delta)\, \forall \theta, \forall \Delta, \forall x\} \end{aligned}$$

The closer $G \in \mathcal{G}$ is to U in $L_2(\mathbb{P}_\theta)$, the closer will the estimator deduced from the "best" estimating function in $\mathcal{G}$ be to the maximum likelihood estimator, in the sense that the asymptotic variance will be closer to the optimal. The optimal estimating function in $\mathcal{G}$, is the orthogonal projection of U onto $\mathcal{G}$ in $L_2(\mathbb{P}_\theta)$, see [Heyde, 1997] or [bib, 2004] for more details.

3.2 Incorporating prior knowledge

The Maximum A Posteriori (MAP) estimator is found by maximizing the posterior score, or equivalently by solving

$$\frac{\partial_\theta \pi(\theta)}{\pi(\theta)} + \frac{\partial_\theta l(\theta; X_{1:n})}{l(\theta; X_{1:n})} = 0. \tag{10}$$

As pointed out in Section 2.2 we allow the flexibility for the specification of the prior knowledge for each of the parameters θ_i either through distributions **Case** A_i or alternatively by moment restrictions in **Case** B_i. Obviously when the prior information is specified through moment restrictions the prior distribution is not necessarily uniquely defined.

We define the class of prior functions

$$\mathcal{F} = \left\{ F : \theta \mapsto F(\theta) \text{ s.t. } F(\theta) = (F_1(\theta_1), \ldots, F_p(\theta_p))^T \text{ with } F_i \in \mathcal{F}_i \right.$$

where $\mathcal{F}_i$ for all i is, for some user-specified $k' \leq k$

$$\mathcal{F}_i = \left\{ F_i : \theta_i \mapsto F_i(\theta_i) = \left\{ \begin{array}{ll} \frac{\partial_{\theta_i} \pi_i^*(\theta_i)}{\pi_i^*(\theta_i)}, & \text{if we are in case } A_i \\ \sum_{j=1}^{k'} c_j^{(i)} (f_j^{(i)}(\theta_i) - \mu_j^{(i)}), & \text{for some real numbers } c_1^{(i)}, \ldots, c_{k'}^{(i)}, \\ & \text{if we are in case } B_i \end{array} \right. \right\}.$$

Remark: the number k' of terms that appear in the construction of F should be compatible with the specification of prior information in **case** B_i. We will see how, if the optimal estimating function is to be used, k' shall be strictly smaller than k.

Finally a class $\mathcal{H}$ is specified

$$\begin{aligned} \mathcal{H} = \{ H : (\theta; X_{1:n}) \mapsto H(\theta; X_{1:n}) \text{ s.t. } & H(\theta; X_{1:n}) = F(\theta) + G(\theta; X_{1:n}) \\ & \text{for some } F(\theta) \text{ in } \mathcal{F} \text{ and some } G(\theta; X_{1:n}) \text{ in } \mathcal{G} \}. \end{aligned} \tag{11}$$

We will refer to estimating functions in $\mathcal{H}$ as EFPK (Estimating Functions with Prior Knowledge).

Notice that an estimating function in $\mathcal{H}$ is not unbiased under $\mathbb{P}_\theta$ for a fixed sample size n, however asymptotically it is. The EFPK corrects the value of the estimates derived from $G(\theta; X_{1:n}) = 0$ by drawing it towards the most a posteriori likely value of θ. The correction has less and less influence asymptotically.

In Section 4.2, the optimal choice of $F \in \mathcal{F}$ and $G \in \mathcal{G}$ will be discussed.

Example 2. *(Example 1 continued) We are now ready to determine the expression of* $F \in \mathcal{F}$*, where the parametrization of the* $\mathcal{IG}(\alpha, \beta)$*,* $\pi^*(\sigma^2) = \frac{1}{\Gamma(\alpha)\beta^\alpha (\sigma^2)^{\alpha+1}} e^{-\frac{1}{\sigma^2 \beta}} \mathbb{I}_{(0,\infty)}(\sigma^2)$ *with* $\alpha > 0$ *and* $\beta > 0$ *was chosen*

$$F(\theta) = \begin{bmatrix} c_1^{(1)}(\kappa - \mu_1^{(1)}) \\ c_1^{(2)}(\varphi - \mu_1^{(2)}) \\ \frac{1}{\beta(\sigma^2)^2} - \frac{\alpha+1}{\sigma^2} \end{bmatrix}.$$

4 Optimality Criterion

This section describes the optimality criterion used for the proposed EFPK and derive an expression for the optimal EFPK. We begin by briefly sketching the basic idea behind optimal estimating functions in the classical sense.

4.1 Optimality Criterion, in the classical setting, a brief review

[Godambe and Heyde, 1987] defined the fixed sample optimal G^* in $\mathcal{G}$ of unbiased estimating functions as the one minimizing the dispersion distance to the U for all n and θ. They formulate three criteria which are equivalent if the class $\mathcal{G}$ is closed under finite summation. This is our case and we only mention one of them :
Criterion 1. $G^* \in \mathcal{G}$ is fixed sample optimal in $\mathcal{G}$ if

$$\begin{aligned} \|G^*(\theta; X_{1:n}) - U(\theta; X_{1:n})\|^2_{L_2(\mathbb{P}_\theta)} \quad &\leq \quad \|G(\theta; X_{1:n}) - U(\theta; X_{1:n})\|^2_{L_2(\mathbb{P}_\theta)}, \\ \forall G \in \mathcal{G},\, \forall\, \theta \in \Theta. & \end{aligned} \tag{12}$$

In the case of Markov processes, when the class of estimating functions is assumed to be constructed from linear subspaces $\gamma(\theta; x, \Delta)$ as is the case for the class $\mathcal{G}$ described in 3.1, see (9), the notion of projection can be formulated precisely: the optimal estimating function in $\mathcal{G}$ is

$$G^*(\theta; X_{1:n}) = \sum_{i=1}^{n} g^*(\theta; X_{t_{i-1}}, X_{t_i}, \Delta_i),$$

where $g^*(\theta; x, y, \Delta) = (g_1^*(\theta; x, y, \Delta), \ldots, g_p^*(\theta; x, y, \Delta))$ and, for all θ, x, $y \mapsto g_j^*(\theta; x, y, \Delta)$ is the orthogonal projection of $y \mapsto \partial_{\theta_j} \log(p(\theta; x, y, \Delta))$ onto $\gamma(\theta; x, \Delta)$ in $L_2(\mathbb{P}_\theta))$ see [Kessler, 1995].

Denote, for all x and θ, by $(y \mapsto h_1(\theta; x, y, \Delta), \ldots, y \mapsto h_N(\theta; x, y, \Delta))$ a basis of the linear subspace $\gamma(\theta; x, \Delta)$. For all $g(\theta; x, y, \Delta)$ in $\gamma(\theta; x, \Delta)$, there exists coefficients $\alpha_{ij}(\theta; x, \Delta)$, such that

$$g_i(\theta; x, y, \Delta) = \sum_{j=1}^{N} \alpha_{ij}(\theta; x, \Delta) h_j(\theta; x, y, \Delta).$$

For all x and θ, the orthogonality property,

$$\int h_j(\theta; x, y, \Delta)\left(\frac{\partial_{\theta_i} p(\theta; x, y, \Delta)}{p(\theta; x, y, \Delta)} - g_i^*(\theta; x, y, \Delta)\right) p(\theta; x, y, \Delta) dy = 0 \qquad i = 1, \ldots, p,\ j = 1, \ldots, N$$

is easily shown to be equivalent to the following equation for $\alpha_{ij}^*(\theta; \Delta, x)$

$$B(\theta; \Delta, x) = \begin{pmatrix} \alpha_{11}^*(\theta; \Delta, x) & \cdots & \alpha_{1N}^*(\theta; \Delta, x) \\ \vdots & & \vdots \\ \alpha_{p1}^*(\theta; \Delta, x) & \cdots & \alpha_{pN}^*(\theta; \Delta, x) \end{pmatrix} C(\theta; \Delta, x) \tag{13}$$

where $C(\theta;\Delta,x)=(c_{ij}(\theta;\Delta,x))_{1\le i,j\le N}$ with

$$c_{ij}(\theta;\Delta,x):=\int h_i(\theta;x,y,\Delta)h_j(\theta;x,y,\Delta)p(\theta;x,y,\Delta)dy$$

and $B(\theta;\Delta,x)=(b_{ij}(\theta;\Delta,x))_{1\le i\le p,1\le j\le N}$ with

$$b_{ij}(\theta;\Delta,x):=\int h_j(\theta;x,y,\Delta)\frac{\partial_{\theta_i}p(\theta;x,y,\Delta)}{p(\theta;x,y,\Delta)}p(\theta;x,y,\Delta)dy=-\int\partial_{\theta_i}h_j(\theta;x,y,\Delta)p(\theta;x,y,\Delta)dy.$$

EXAMPLE 3. *Consider the Cox-Ingersoll-Ross process given by the stochastic differential equation*

$$dC_t=\kappa(\varphi-C_t)dt+\sigma\sqrt{C_t}dW_t \tag{14}$$

where $\kappa>0,\varphi>0,\sigma^2>0$ *and* $\sigma^2\le 2\kappa\varphi$.

The optimal $G^*\in\mathcal{G}_2$ *is determined from* $B(\theta;\Delta,x)$ *and* $A(\theta;\Delta,x)$ *applying (13), after some straightforward calculations we obtain*

$$\begin{aligned}G^*(\theta;C_{1:n}) &= \sum_{i=1}^{n}a^*(\Delta,C_{i-1};\theta)[C_i-F(\Delta,C_{i-1};\theta)]\\ &\quad +b^*(\Delta,C_{i-1};\theta)[(C_i-F(\Delta,C_{i-1};\theta))^2-\phi(\Delta,C_{i-1};\theta)]\end{aligned} \tag{15}$$

with

$$a^*(\Delta,x;\theta) = -\frac{\partial_\theta\phi(\Delta,x;\theta)\eta(\Delta,x;\theta)-\partial_\theta F(\Delta,x;\theta)\psi(\Delta,x;\theta)}{\phi(\Delta,x;\theta)\psi(\Delta,x;\theta)-\eta(\Delta,x;\theta)^2} \tag{16}$$

$$b^*(\Delta,x;\theta) = -\frac{\partial_\theta F(\Delta,x;\theta)\eta(\Delta,x;\theta)-\partial_\theta\phi(\Delta,x;\theta)\phi(\Delta,x;\theta)}{\phi(\Delta,x;\theta)\psi(\Delta,x;\theta)-\eta(\Delta,x;\theta)^2} \tag{17}$$

Note: *The different signs of* $a^*(\Delta,C_{i-1};\theta)$ *and* $b^*(\Delta,C_{i-1};\theta)$ *compared to soerensen??, the sign obviously in* $\mathcal{G}$ *is not important however in this setup it is.*

where

$$\begin{aligned}F(\Delta,x;\theta) &= \int yp(\theta;x,y,\Delta)dy=xe^{-\kappa\Delta}+\varphi(1-e^{-\kappa\Delta})\\ \phi(\Delta,x;\theta) &= \int(y-F(\Delta,x;\theta))^2p(\theta;x,y,\Delta)dy=\frac{\sigma^2}{2\kappa}(1-e^{-\kappa\Delta})(\varphi(1-e^{-\kappa\Delta})+2xe^{-\kappa\Delta})\\ \eta(\Delta,x;\theta) &= \int(y-F(\Delta,x;\theta))^3p(\theta;x,y,\Delta)dy\\ &= \frac{(\sigma^2)^2}{2\kappa^2}\left(\varphi-3(\varphi-x)e^{-\kappa\Delta}+3(\varphi-2x)e^{-2\kappa\Delta}-(\varphi-3x)e^{-3\kappa\Delta}\right)\\ \psi(\Delta,x;\theta) &= \int((y-F(\Delta,x;\theta))^4-\phi(\Delta,x;\theta)^2)p(\theta;x,y,\Delta)dy\\ &= \frac{3(\sigma^2)^3}{4\kappa^3}\left((\varphi-4x)e^{-4\kappa\Delta}-4(\varphi-3x)e^{-3\kappa\Delta}+6(\varphi-2x)e^{-2\kappa\Delta}-4(\varphi-x)e^{-\kappa\Delta}+\varphi\right)\\ &\quad +2\phi(\Delta,x;\theta)^2.\end{aligned}$$

4.2 Optimal estimating functions with Prior Knowledge

The optimal $H^* \in \mathcal{H}$ is the one that minimizes for all candidate prior distribution π in Π, $\|.\|^2_{L_2(f(\theta;x_{1:n})\pi(\theta)dx_{1:n}d\theta)}$ to the posterior score (remember that $f(\theta;.)$ denotes the density of the data given θ.)

DEFINITION 4.1. *$H^* \in \mathcal{H}$ is optimal in $\mathcal{H}$ if*

$$\|H^*(\theta;X_{1:n})-U(\theta;X_{1:n})\|^2_{L_2(f(\theta;x_{1:n})\pi(\theta)dx_{1:n}d\theta)} \leq \|H(\theta;X_{1:n})-U(\theta;X_{1:n})\|^2_{L_2(f(\theta;x_{1:n})\pi(\theta)dx_{1:n}d\theta)} \tag{18}$$

$\forall H \in \mathcal{H}, \forall\theta \in \Theta, \forall\pi \in \Pi$.

PROPOSITION 4.1. *The optimal EFPK is*

$$H^*(\theta;X_{1:n}) = F^*(\theta) + G^*(\theta;X_{1:n}) \tag{19}$$

where $G^* \in \mathcal{G}$ minimizes

$$\|G(\theta;X_{1:n}) - \frac{\partial_\theta f(\theta;X_{1:n})}{f(\theta;X_{1:n})}\|^2_{L_2(f(\theta;x_{1:n})dx_{1:n})}, \quad \forall\theta \in \Theta,\ \forall G \in \mathcal{G} \tag{20}$$

and $F^* \in \mathcal{F}$ minimizes

$$\|F(\theta) - \frac{\partial_\theta \pi(\theta)}{\pi(\theta)}\|^2_{L_2(\pi(\theta)d\theta)}, \quad \forall\theta \in \Theta,\ \forall F(\theta) \in \mathcal{F}, \forall\pi \in \Pi. \tag{21}$$

Proof. Let H be an estimating function in $\mathcal{H}$

$$H(\theta;X_{1:n}) = F(\theta) + G(\theta;X_{1:n}).$$

First we will denote by P the posterior score

$$P(\theta;X_{1:n}) = \partial_\theta \log(f(\theta;x_{1:n})\pi(\theta)) = \partial_\theta \log(f(\theta;X_{1:n})\pi(\theta)) = \frac{\partial_\theta\pi(\theta)}{\pi(\theta)} + \frac{\partial_\theta f(\theta;X_{1:n})}{f(\theta;X_{1:n})}, \tag{22}$$

inserting the expression from (22) in

$$\|H(\theta;X_{1:n}) - P(\theta;X_{1:n})\|^2_{L_2(f(\theta;x_{1:n})\pi(\theta)dx_{1:n}d\theta)}$$

yields

$$\begin{aligned}
&\|F(\theta) - \frac{\partial_\theta\pi(\theta)}{\pi(\theta)}\|^2_{L_2(f(\theta;x_{1:n})\pi(\theta)dx_{1:n}d\theta)} \\
&+\|G(\theta;X_{1:n}) - \frac{\partial_\theta f(\theta;X_{1:n})}{f(\theta;X_{1:n})}\|^2_{L_2(f(\theta;x_{1:n})\pi(\theta)dx_{1:n}d\theta)} \\
&+2 < G(\theta;X_{1:n}) - \frac{\partial_\theta f(\theta;X_{1:n})}{f(\theta;X_{1:n})}, F(\theta) - \frac{\partial_\theta\pi(\theta)}{\pi(\theta)} >_{L_2(f(\theta;x_{1:n})dx_{1:n})\pi(\theta)d\theta)} \Rightarrow \\
\|H(\theta;X_{1:n}) \ - \ P(\theta;X_{1:n})\|^2_{L_2(f(\theta;x_{1:n})\pi(\theta)dx_{1:n}d\theta)} &= \|F(\theta) - \frac{\partial_\theta\pi(\theta)}{\pi(\theta)}\|^2_{L_2(\pi(\theta)d\theta)} \\
+ \ \|G(\theta;X_{1:n}) - \frac{\partial_\theta f(\theta;X_{1:n})}{f(\theta;X_{1:n})}&\|^2_{L_2(f(\theta;x_{1:n})\pi(\theta)dx_{1:n}d\theta)}
\end{aligned}$$

since

$$\int G(\theta; X_{1:n}) f(\theta; x_{1:n}) dx_{1:n} = \int \frac{\partial_\theta f(\theta; X_{1:n})}{f(\theta; X_{1:n})} f(\theta; x_{1:n}) dx_{1:n} = 0.$$

From (23) it is concluded that

$$H^*(\theta; X_{1:n}) = F^*(\theta) + G^{**}(\theta; X_{1:n}),$$

where $G^{**} \in \mathcal{G}$ minimizes (23) for all $\theta \in \Theta$ and all $G \in \mathcal{G}$

$$\|G(\theta; X_{1:n}) - \frac{\partial_\theta f(\theta; X_{1:n})}{f(\theta; X_{1:n})}\|^2_{L_2(f(\theta; x_{1:n})\pi(\theta) dx_{1:n} d\theta)} \tag{23}$$

and $F^* \in \mathcal{F}$ minimizes (21) for all $\theta \in \Theta$ and all $F \in \mathcal{F}, \forall \pi \in \Pi$. Next we need to prove that

$$G^{**}(\theta; X_{1:n}) = G^*(\theta; X_{1:n}).$$

This is however straightforward since, if $G^*(\theta; X_{1:n})$ solves (12) for all $\theta \in \Theta$ and all $H \in \mathcal{H}$, the inequality is still fulfilled integrating both sides w.r.t. $\pi(\theta) d\theta$ □

Note: To find the optimal $F^* \in \mathcal{F}$ in $L_2(\pi(\theta)d\theta), \forall \pi \in \Pi$ the orthogonal projection of $F \in \mathcal{F}$ to $\frac{\partial_\theta \pi(\theta)}{\pi(\theta)}$ in $L_2(\pi(\theta)d\theta)$ is carried out analogically to the calculations in Section 3.1. The elements $F_i^*(\theta_i)$ in A_i are trivial. In B_i for each $\pi_i \in \Pi_i$, the optimal $c_j^{*(i)}, j = 1, \ldots, k$ are found by solving

$$\int (f_l^{(i)}(\theta_i) - \mu_l^{(i)})(\frac{\partial_{\theta_i} \pi_i(\theta_i)}{\pi_i(\theta_i)} - \sum_{j=1}^{k'} c_{jm}^{*(i)} (f_j^{(i)}(\theta_i) - \mu_j^{(i)})) \pi_i(d\theta_i) = 0 \tag{24}$$

$$i = 1, \ldots, p,\ l = 1, \ldots, k',\ m = 1, \ldots, n'$$

or

$$B(\theta_i) = \begin{pmatrix} c_{1m}^{*(i)} & \cdots & c_{k'm}^{*(i)} \end{pmatrix} C(\theta_i)$$

where $C(\theta_i) = (c_{st}(\theta_i))_{1 \le s,t \le k'}$ with

$$c_{st}(\theta_i) := \int (f_s^{(i)}(\theta_i) - \mu_s^{(i)})(f_t^{(i)}(\theta_i) - \mu_t^{(i)}) \pi_i(d\theta_i)$$

and $B(\theta_i) = (b_1(\theta), \ldots, b_{k'}(\theta_i))$ with

$$b_s(\theta_i) := \int (f_s^{(i)}(\theta_i) - \mu_s^{(i)}) \frac{\partial_{\theta_i} \pi_i(\theta)}{\pi_i(\theta)} \pi_i(d\theta_i) = -\int \partial_{\theta_i} f_s^{(i)}(\theta_i) \pi_i(d\theta_i),\ s = 1, \ldots, k'.$$

Remark: When choosing k' and the functions $f_j^{(i)}$ in the construction of the estimating functions F, these should be compatible, in the case when the optimal EFPK is to be used, with the prior information specification in **Case** B_i. As an example, consider $B(\theta)$ as above, one needs to know the prior expectation of $\partial_{\theta_i} f_s^{(i)}$, which should therfore be one of the prior information specification.

EXAMPLE 4. *(Example 2 and 3 continued)*

Now we determine the expression of $H^*(\theta; C_{1:n})$ by finding the optimal $F^* \in \mathcal{F}$ and applying the $G^*(\theta; C_{1:n})$ from Example 3.

The optimal $F^* \in \mathcal{F}$ is determined by inserting in (24)

$$F^*(\theta) = \begin{bmatrix} -\frac{\kappa - \mu_1^{(1)}}{\mu_2^{(1)}} \\ -\frac{\varphi - \mu_1^{(2)}}{\mu_2^{(2)}} \\ \frac{1}{\beta(\sigma^2)^2} - \frac{\alpha+1}{\sigma^2} \end{bmatrix}.$$

Applying this $F^*(\theta)$ and the $G^*(\theta; C_{1:n})$ from Example 3 the $H^*(\theta; C_{1:n})$ can be determined, inserting in (23)

$$H^*(\theta; C_{1:n}) = G^*(\theta; C_{1:n}) + \begin{bmatrix} -\frac{\kappa - \mu_1^{(1)}}{\mu_2^{(1)}} \\ -\frac{\varphi - \mu_1^{(2)}}{\mu_2^{(2)}} \\ \frac{1}{\beta(\sigma^2)^2} - \frac{\alpha+1}{\sigma^2} \end{bmatrix}. \tag{25}$$

5 Estimating the Nitrous Oxide Emission Rate from the Soil Surface by Means of a Diffusion Model

Estimations have been carried out on data sets containing measurements at certain time points of Nitrous Oxide concentrations in a measurement apparatus, each trajectory presents measurements of the Nitrous Oxide concentrations for a certain geographical location. Different geographical locations were used to draw a more complete picture of the Nitrous Oxide emission due to the location dependency. In Figure 1 the measurements are graphically presented from 12 different locations, each trajectory containing approximately 12 measurements.

The emission rate of Nitrous Oxide is interesting since it plays an important role in the deterioration of the ozone layer. Long term consequences of increasing Nitrous Oxide concentration in the atmosphere encompass issues such as global worming the (greenhouse effect) and holes the the ozone layer see [Crutzen, 1970] or [Bouwman, 1996] for further details.

Previously estimation the of the emission rate was carried out not utilizing SDE [Hutchinson GL, 1981]. This approach however suffers from certain drawbacks from a parameter estimation point of view [Pedersen, 2000]. Only for a limited number of trajectories it was possible to estimate the parameters of interest. In [Pedersen, 2000] a CIR process was applied to model the Nitrous Oxide concentrations at time t to facilitate estimation of the emission rate. This approach does not suffer from the problem mentioned above. However we have chosen to carry out the estimation procedure using EFPK due to the limited number of observations in each trajectory and to incorporate the available prior knowledge.

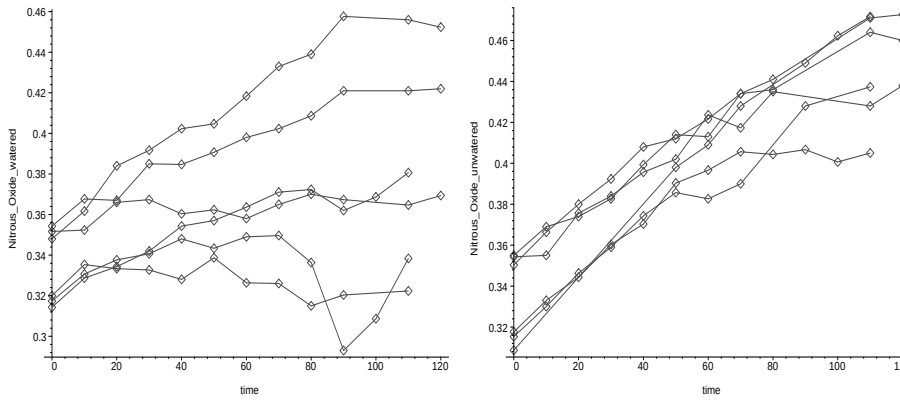

Figure 1: Data set watered (left). Data set unwatered (right). The data sets have been preprocessed as described in [Pedersen, 2000] by removing the same outliers. Concentrations are measured in ppmv (parts pr. million volume based), while time since placement of the soil cover is measured in minutes.

5.1 The Model

In [Pedersen, 2000] it was demonstrated that for each trajectory $C^j_{1:n}$ the CIR process from (14) models the data sufficiently well, for a certain value of the parameter $\theta^j = (\kappa^j, \varphi^j, \sigma^{2j})$ with j indicating the location and C^j_t describing the Nitrous Oxide concentration in the measurement apparatus at time t.

The initial emission rate r^j_0 is related to the parameters in the CIR model through

$$r^j_0 \;=\; \kappa^j(\varphi^j - C^j_0) = \frac{dE[C^j_t|C^j_0]}{dt}|_{t=0}, \tag{26}$$

hence a possible biased estimator of $\hat{r}^j_0$ is

$$\hat{r}^j_0 \;=\; \hat{\kappa}^j(\hat{\varphi}^j - C^j_0). \tag{27}$$

To reduce the bias the correction term proposed in [Pedersen, 2000] or $\hat{r}^j_0 = \hat{\kappa}^j(\hat{\varphi}^j - C_0) - Cov(\hat{\kappa}^j, \hat{\varphi}^j)$ could be used, however also as pointed out in [Pedersen, 2000] the compensator term might be rather poorly estimated giving rise to further complications, so the biased expression from (27) is used.

5.2 Estimation of the emission rate

It can be shown that the transition density for the CIR model is a non central chi-square distribution with non-integer parameters, which makes likelihood methods complicated. In [Pedersen, 2000] a second order polynomial martingale estimating functions, not being

$\mathcal{O}_F$ but having "sensible" weights, as in Example 3, was used to derive explicit. In in practice applying "sensible" weights in the construction of the estimating function little is gained compared to the $\mathcal{O}_F$ estimating function.

So to carry out the estimation the estimator from (25) was used.

5.3 Constructing the priors

The specification of the prior knowledge for our application is delicate since the priors need are for the parameter θ^i but the actual prior information is available for r_0

However in [Pedersen, 2000] it is commended that representative values for κ, φ and σ^2 are.

Type I $E[\kappa] = .02$, $E[\varphi] = .42$ and $E[\sigma^2] = 10^{-5}$.

Type II $E[\kappa] = .08$, $E[\varphi] = .34$ and $E[\sigma^2] = 10^{-4}$.

The variance is more questionable from [Nitrous Oxide Emission from Manure and Inorganic Fertilizers Applied to Spring Barley, S.O.Petersen] under normal circumstances $E[r_0] \simeq [0; .002]$ so the standard deviation should not be more informative than .0005.

Under the assumption of independency we easily see that $V[r_0] = E[\kappa]^2 V[\varphi] + V[\kappa]E[\varphi]^2 + V[\kappa]V[\varphi]$

Calculating φ and κ applying estimators from $\mathcal{G}_2$ for each of the data sets we get rough estimators for $V[\varphi]$ and $V[\kappa]$.

TYPE I $V[\varphi] \approx .007$, $V[\kappa] \approx .002$

TYPE II $V[\varphi] \approx .003$, $V[\kappa] \approx .002$

These rough estimators results in

TYPE I $V[r_0] \approx .00056$

TYPE II $V[r_0] \approx .00032$

which are less informative than .0005 in both cases.

Finally we choose values for α and β, not being to informative either with the median around 10^{-5} and 10^{-4} again obtained applying estimators from $\mathcal{G}_2$ for each of the data sets.

This is obtained by

TYPE I $\alpha = 1$ and $\beta = 50000$

TYPE II $\alpha = 1$ and $\beta = 5000$

This procedure is carried out first for the TYPE I data sets and next for TYPE II data sets.

5.4 Results

	k01	k02	k03	k04	k05	k06
$\hat{\varphi}\,(ppvm)$	.4207	.5161	.6162	.4528	.6248	.4919
$\hat{\kappa}\,(min^{-1})$	.0194	.0083	.00686	.015	.00477	.0124
$\hat{\sigma}^2\,(10^{-6})$	7.68	12.2	3.00	24.2	9.93	4.95
$\hat{r}\,(ppvm/min)(10^{-3})$	1.95	1.65	2.07	1.52	1.32	1.70
$\hat{\varphi}\,(ppvm)$	.4206	.4989	.584	.4545	.514	.480
(BEF)$\hat{\kappa}\,(min^{-1})$	.0193	.00929	.0079	.0141	.0096	.01447
(BEF)$\hat{\sigma}^2\,(10^{-6})$	6.97	10.05	3.50	18.5	9.55	5.5
(BEF)$\hat{r}\,(ppvm/min)(10^{-3})$	2.00	1.71	2.10	1.41	1.49	1.88

Table 1: Type I, Un-watered data sets: The index of estimator listed in left column specify estimation method, and the top indexes mark the certain data set, observations available in [Pedersen, 2000].

	k01	k02	k03	k04	k05	k06
$\hat{\varphi}\,(ppvm)$	.3267	.3357	.3837	.3651	.4754	.4352
$\hat{\kappa}\,(min^{-1})$	.1193	.07895	.02088	.0875	.01497	.0146
$\hat{\sigma}^2\,(10^{-5})$	3.58	13.37	.964	1.128	1.113	.873
$\hat{r}\,(ppvm/min)(10^{-3})$	.907	1.45	1.45	1.18	1.91	1.18
$\hat{\varphi}\,(ppvm)$	.3278	.3376	.3665	.3645	.4399	.408
(BEF)$\hat{\kappa}\,(min^{-1})$	.114	.0432	.0492	.1385	.0286	.0398
(BEF)$\hat{\sigma}^2(10^{-5})$	5.33	7.23	4.02	3.89	4.05	3.99
(BEF)$\hat{r}\,(ppvm/min)(10^{-3})$	.89	.88	2.50	1.77	2.63	2.13

Table 2: Type II, Watered data sets: The index of estimator listed in left column specify estimation method, and the top indexes mark the certain data set, observations available in [Pedersen, 2000].

6 Conclusion

The method Estimating Functions with Prior Knowledge is proposed as a method for parameter estimation which incorporates prior knowledge in the estimates. This is done by adding an additional term to the ordinary estimating equation. Adding this term in the estimating function results in equations from where explicit expressions of estimators in general are more difficult to derive. Due to the structure of estimating equations from $\mathcal{H}$ the method is applicable whenever ordinary estimating equations can be applied.

The EFPK approach is in particular useful for small sample sizes if some prior knowledge is available, since classical estimates in these situations might be very unreliable. The incorporated prior knowledge move estimates towards the prior and thereby "remove" extreme estimates and reduce the variation of the estimates. The basic idea behind EFPK is to create an estimating function which is maximal correlated with the

posterior score, contrary to the classical setup where the score function is imitated. The idea is formalized by minimizing the L_2 distance to the posterior score.

We have demonstrated how to implement EFPK for parameter estimation for discretely observed diffusions. As case studies the Cox, Ingersoll and Ross CIR process were chosen. For the Cox, Ingersoll and Ross CIR process the method illustrates its worth, since it clearly in many cases out performs ordinary EF.

7 Acknowledgement

Most of this research was done while Kim Nolsøe stayed at the Department of Statistics, University of Cartagena. This stay was supported by the European Commission through the Research Training Network DYNSTOCH under the Human Potential Programme. Further we would like to thank Bo Martin Bibby, Susanne Ditlevsen and Helle Sørensen for discussions and especially Søren O. Petersen for supplying the data and expert specification of the priors for the investigated experiment.

References

[bib, 2004] (2004). *Handbook of Financial Econometrics*, chapter Estimating Functions for Discretely Sampled Diffusion-Type Models. forthcoming.

[Aït-Sahalia, 2002] Aït-Sahalia, Y. (2002). Maximum likelihood estimation of discretely sampled diffusions: a closed-form approximation approach. *Econometrica*, 70(1):223–262.

[Bibby and Sørensen, 1995] Bibby, B. M. and Sørensen, M. (1995). Martingale estimation functions for discretely observed diffusion processes. *Bernoulli*, 1(1-2):17–39.

[Bouwman, 1996] Bouwman, A. F. (1996). Direct emission of nitrous oxide from agricultural soils. *Nutr. Cycl. Agroecosys.*, 46:53–70.

[Crutzen, 1970] Crutzen, P. (1970). The influence of nitrogen oxides on the atmospheric ozone content. *Quart. J. Roy. Meteor. Soc.*, 96:320–325.

[Elerian et al., 2001] Elerian, O., Chib, S., and Shephard, N. (2001). Likelihood inference for discretely observed nonlinear diffusions. *Econometrica*, 69(4):959–993.

[Eraker, 2001] Eraker, B. (2001). MCMC analysis of diffusion models with application to finance. *J. Bus. Econom. Statist.*, 19(2):177–191.

[Godambe and Heyde, 1987] Godambe, V. P. and Heyde, C. C. (1987). Quasi-likelihood and optimal estimation. *Internat. Statist. Rev.*, 55(3):231–244.

[Heyde, 1997] Heyde, C. C. (1997). *Quasi-likelihood and its application*. Springer Series in Statistics. Springer-Verlag, New York. A general approach to optimal parameter estimation.

[Hutchinson GL, 1981] Hutchinson GL, M. A. (1981). Improved soil cover method for field measurement of nitrous oxide fluxes. *Soil Science Society of America Journal*, 45.

[Kessler, 1995] Kessler, M. (1995). Martingale estimating functions for a markov chain. preprint. *Laboratoire de Probabilitès, Universitè Paris VI*.

[Pedersen, 2000] Pedersen, A. (2000). Estimating the nitrous oxide emission rate from the soil surface by means of a diffusion model. *Scandinavian Journal of Statistics*, 27:385–403.

[Pedersen, 1995] Pedersen, A. R. (1995). A new approach to maximum likelihood estimation for stochastic differential equations based on discrete observations. *Scand. J. Statist.*, 22(1):55–71.

[Roberts and Stramer, 2001] Roberts, G. O. and Stramer, O. (2001). On inference for partially observed nonlinear diffusion models using the Metropolis-Hastings algorithm. *Biometrika*, 88(3):603–621.

Paper VI

PREDICTION-BASED ESTIMATING FUNCTIONS FOR DIFFUSION PROCESSES WITH MEASUREMENT NOISE

Submitted to *Revstat*

PREDICTION-BASED ESTIMATING FUNCTIONS FOR DIFFUSION PROCESSES WITH MEASUREMENT NOISE

Authors: KIM NOLSØE
– Department of Mathematical Modelling,
Technical University of Denmark (kn@imm.dtu)

JAN NYGAARD NIELSEN
– Department of Mathematical Modelling,
Technical University of Denmark (jan.nygaard@netcompany.com)

HENRIK MADSEN
– Department of Mathematical Modelling,
Technical University of Denmark (hm@imm.dtu)

Abstract:

- The prediction-based estimating functions proposed by [Sørensen, 2000] are formulated explicitly for discretely observed stochastic differential equations, where the measurements are encumbered with additive white noise. Simple expressions are derived for the optimal estimating functions when the classes of prediction-based estimating functions are defined by a finite-dimensional space of predictors. Only unconditional moments are needed for this class of estimating functions. Particular attention is devoted to the Cox-Ingersoll-Ross model. Using Monte Carlo simulation the small-sample properties are examined, and the method is compared to a method based on particular nonlinear filtering.

Key-Words:

- *Martingale estimating functions, Monte Carlo simulation, nonlinear filtering, prediction-based estimating functions, stochastic differential equations.*

AMS Subject Classification:

- 49A05, 78B26.

1. Introduction

Until recently the only feasible solutions to the parameter estimation problem in discretely, partially observed stochastic differential equations (SDEs), where the measurements are contaminated with additive Gaussian white noise, has been to apply the particle filters [Doucet et al., 2001] or more approximatively to apply the Kalman-Bucy filter [Kalman and Bucy, 1961] for linear (in the narrow-sense) systems to compute the likelihood function. The filter is based on the evolution of the conditional moments of the underlying state variables, which is assumed to be described by SDEs. For nonlinear systems, ordinary differential equations describing the evolution of the conditional moments are obtained by Taylor expansions of functions of the drift and diffusion functions. For nonlinear systems, the extended Kalman filter (EKF) may be applied provided that the diffusion function does not depend on the state variables. Otherwise higher order filters must be applied [Jazwinski, 1970, Maybeck, 1982], see [Nielsen et al., 2000] for a recent application of second order filters. The EKF is particularly well-suited for handling a nonlinear measurement equation that describes the functions of the underlying state variables that are measured with additive noise.

The explicit treatment of measurement noise makes it possible to distinguish between process noise, i.e. the noise typically described by a Wiener process, that affects the future behavior of the states, and the measurement noise, which in technical and physical applications is merely due to uncertainty in the measurement device and in financial applications is due to rounding off prices, asynchronous trading, bid-ask spreads and other market imperfections. One-step ahead prediction errors are provided by these filters such that Quasi-Maximum Likelihood (QML) estimates may be obtained using a Prediction Error Decomposition [Schweppe, 1965] under the assumption that the prediction errors are, for instance, Gaussian distributed. However, the nonlinear filters are based on Taylor expansions in a way that makes explicit analysis of the validity of the approximations infeasible. The validity and the performance of the nonlinear filter may, to some extent, be tested using model validation tools.

The general theory of Estimating Functions (EFs) dates back to [Godambe, 1960], see also [McLeish and Small, 1988, Godambe and Kale, 1991, Heyde, 1997]. However, the development of EFs for discretely observed SDEs is of a more recent date. The Martingale Estimating Functions (MEFs) from the linear family for discretely observed SDEs developed by [Bibby and Sørensen, 1995] are inspired by the properties of the pseudo-score function, i.e. the score function obtained by discretizing the continuous-time likelihood function [Liptser and Shiryaev, 2001b] and [Liptser and Shiryaev, 2001a] provided that the diffusion function does not depend on the unknown parameters. Requiring the EF being a martingale implies that the asymptotic properties may be obtained without letting the time between measurements tend to zero. Unfortunately it also implies that the EFs involve conditional moments and that the optimal EFs involve derivatives of these moments with respect to the parameters, which, most often, must be com-

puted by simulation, see [Kloeden and Platen, 1995] for some approximate methods. If the diffusion function depends on the unknown parameter other classes of EFs should be used, e.g. the MEFs from the quadratic family attributable to [Bibby and Sørensen, 1995], that also requires computing the third and fourth order conditional moments. In [Kessler, 2000] a class of simple EFs that provides explicit expressions for the estimators of the parameters in univariate SDEs is proposed. These EFs can only be used to estimate parameters appearing in the stationary density, because it is based on unconditional moments. However, the martingale property is lost and asymptotically efficient estimators are not available. In [Kessler and Sørensen, 1999] another class of MEFs that are based on eigenfunctions of the generator associated with the SDE is proposed, see also [Bibby and Sørensen, 2001], which utilizes a combination of the latter two methods.

The PEFs proposed by [Sørensen, 2000] are applied on measurement error models for a simple choice of the functions spanning the space. For this class a simple expression for the optimal estimating functions (in the sense of fixed sample optimality) is available. We describe how to carry out the calculation for the CIR process and through a simulation study it is verified that the derived estimators slightly outperforms the implemented filtering method.

Other available methods are the Generalized Method-of-Moments [Hansen, 1982], Simulated Method-of-Moments [Duffie and Singleton, 1993], and Efficient Method-of-Moments [Gallant and Tauchen, 1996, Gallant and Long, 1997]. But none of these methods allow for measurement noise explicitly. This also holds for the nonparametric method proposed by [Jiang and Knight, 1997] and compared using Monte Carlo simulation by [Maekawa et al., 1998].

In Section 2 the modelling framework is put forth. A review of PEF will be presented in Section 3, where the particular problems involved in allowing for measurement noise will be discussed. A simple expression for the optimal estimating functions in the sense of [Heyde, 1997] is presented in Section 4. In Section 4.3, particular attention is devoted to the CIR model [Cox et al., 1985]; a class of SDEs that are used extensively in mathematical finance, where one of the states is not directly observed. In Section 5 the properties of the proposed method, simple and explicit estimating functions and a nonlinear filter used in combination with a QML method are studied using Monte Carlo simulation. Finally, Section 6 concludes.

2. The model

Consider a one-dimensional diffusion $X = (X_t)_{t\geq 0}$ defined on the state space $\mathcal{S} \subseteq \mathbb{R}$ satisfying the stochastic differential equations

$$dX_t = b(X_t;\boldsymbol{\theta})dt + \sigma(X_t;\boldsymbol{\theta})dW_t; \quad X_0 = x, \tag{2.1}$$

indexed by $\boldsymbol{\theta}$, where $\boldsymbol{\theta}$ belongs to $\boldsymbol{\Theta}$, an open subset of $\mathbb{R}^p$; $(W)_{t\geq 0}$ is the standard Wiener process; b and σ are known $\mathbb{R}$-valued functions defined on $\mathcal{S}\times\boldsymbol{\Theta}$, which are assumed to be smooth enough to ensure, for every $\boldsymbol{\theta}\in\boldsymbol{\Theta}$, the uniqueness in law of the solution to (2.1).

Let $s(x;\boldsymbol{\theta})$ denote the density of the scale measure

$$s(x;\boldsymbol{\theta}) = \exp\left(-\int_0^x \frac{2b(y;\boldsymbol{\theta})}{\sigma^2(y;\boldsymbol{\theta})}dy\right). \tag{2.2}$$

Condition 1. The following hold for all $\boldsymbol{\theta}\in\boldsymbol{\Theta}$

$$\int_0^\infty s(x;\boldsymbol{\theta})dx = \int_{-\infty}^0 s(x;\boldsymbol{\theta})dx = \infty \tag{2.3}$$

and

$$\int_{-\infty}^\infty [s(x;\boldsymbol{\theta})\sigma^2(x;\boldsymbol{\theta})]^{-1}dx = A(\boldsymbol{\theta}) < \infty. \tag{2.4}$$

Under these assumptions X is ergodic, and with respect to the Lebesgue measure its stationary density is $x\mapsto [A(\boldsymbol{\theta})s(x;\boldsymbol{\theta})\sigma^2(x;\boldsymbol{\theta})]^{-1}$.

The differential operator L defined by

$$L = b(x;\boldsymbol{\theta})\frac{\partial}{\partial x} + \frac{1}{2}\sigma^2(x;\boldsymbol{\theta})\frac{\partial^2}{\partial x^2} \tag{2.5}$$

for all twice differentiable functions is called the *generator* of the SDE (2.1). A twice continuously differentiable function $\varphi(x;\boldsymbol{\theta})$ is called an *eigenfunction* for L with eigenvalue $\lambda(\boldsymbol{\theta})$ if it satisfies

$$L\varphi(x;\boldsymbol{\theta}) = -\lambda(\boldsymbol{\theta})\varphi(x;\boldsymbol{\theta}) \tag{2.6}$$

for all x in the state space $\mathcal{S}$.

The observed process $(Y_{t_i})_{1\leq i\leq n}$ is assumed to be given by

$$Y_{t_i} = h(X_{t_i}) + \varepsilon_{t_i}, \tag{2.7}$$

where $\Delta_i = t_i - t_{i-1}$ is the sampling interval, n the number of measurements, h a specified function $h : x \to h(x)$ and $(\varepsilon_{t_i})_{1\leq i\leq n}$ is the Gaussian white noise process $N(0, \sigma_\varepsilon^2)$ that accounts for the measurement noise. The latter is independent of $(W_t)_{t\geq 0}$.

For computational reasons the following is assumed to hold, this is very often reasonable in practise.

Condition 2. h is a polynomial in x, i.e. $h(x) = A_m x^m + A_{m-1}x^{m-1} + \ldots + A_0$, $m \in \mathbb{N}$, $A_i \in \mathbb{R}, i = 1, \ldots, m$.

3. Prediction-based Estimating Functions

An estimating function $\mathbf{G}$ is a function of $\boldsymbol{\theta}$ and the observations $Y_{t_1}, \ldots, Y_{t_n}$, $\mathbf{G} : (Y_{t_1}, \ldots, Y_{t_n}; \boldsymbol{\theta}) \mapsto \mathbf{G}(Y_{t_1}, \ldots, Y_{t_n}; \boldsymbol{\theta})$ from where estimators $\hat{\boldsymbol{\theta}}$ are found by solving the p-dimensional equation

$$\mathbf{G}(Y_{t_1}, \ldots, Y_{t_n}; \boldsymbol{\theta}) = 0.$$

For Markov processes the $\mathbf{G}$ functions have a particular nice structure

$$\mathbf{G}(Y_{t_1}, \ldots, Y_{t_n}; \boldsymbol{\theta}) = \sum_{i=2}^{n} \mathbf{g}(Y_{t_i}, Y_{t_{i-1}}; \boldsymbol{\theta})$$

$\mathbf{g} : (Y_{t_i}, Y_{t_{i-1}}; \boldsymbol{\theta}) \mapsto \mathbf{g}(Y_{t_i}, Y_{t_{i-1}}; \boldsymbol{\theta})$. We refer readers to [Heyde, 1997] for an introduction to estimating function theory.

This review of Prediction-based Estimating Functions follows [Sørensen, 2000], however the aim at a less general framework sufficient for our setup, where Y is a stationary process. We refer readers to [Sørensen, 2000] for a more general setup, here details regarding convergence of the derived estimators can be found.

Now consider the construction of an estimating function for a non-Markovian process expressed as

$$\mathbf{G}(Y_{t_1}, \ldots, Y_{t_n}; \boldsymbol{\theta}) = \sum_{i=1}^{n-1} \bar{\mathbf{g}}_i(Y_{t_1}, \ldots, Y_{t_{i+1}}; \boldsymbol{\theta}). \tag{3.1}$$

The first restriction we choose for convenience is to let $\bar{\mathbf{g}}_i : (Y_{t_1}, \ldots, Y_{t_{i+1}}; \boldsymbol{\theta}) \mapsto \bar{\mathbf{g}}_i(Y_{t_1}, \ldots, Y_{t_{i+1}}; \boldsymbol{\theta})$ depends only on q lags of Y_{t_i}, $\bar{\mathbf{g}}_i : (Y_{t_{i-q}}, \ldots, Y_{t_i}; \boldsymbol{\theta}) \mapsto \bar{\mathbf{g}}_i(Y_{t_{i-q}}, \ldots, Y_{t_i}; \boldsymbol{\theta})$, $i = q+1, \ldots, n$ with $\bar{\mathbf{g}}_i(Y_{t_{i-q}}, \ldots, Y_{t_i}; \boldsymbol{\theta}) = \bar{\mathbf{g}}_j(Y_{t_{i-q}}, \ldots, Y_{t_i}; \boldsymbol{\theta}) = \mathbf{g}(Y_{t_{i-q}}, \ldots, Y_{t_i}; \boldsymbol{\theta})$, $i = q+1, \ldots, n$, $j = q+1, \ldots, n$, for this choice of $\bar{\mathbf{g}}_i$, (3.1) takes the form

$$\mathbf{G}(Y_{t_1}, \ldots, Y_{t_n}; \boldsymbol{\theta}) = \sum_{i=q+1}^{n} \mathbf{g}(Y_{t_{i-q}}, \ldots, Y_{t_i}; \boldsymbol{\theta}).$$

Next let us specify more structure on

$$\mathbf{g}(Y_{t_{i-q}}, \ldots, Y_{t_i}; \boldsymbol{\theta}) = \sum_{j=1}^{N} \mathbf{A}_j(Y_{t_{i-q}}, \ldots, Y_{t_{i-1}}; \boldsymbol{\theta})(f_j(Y_{t_i}) - \pi_j(Y_{t_{i-q}}, \ldots, Y_{t_{i-1}}; \boldsymbol{\theta})).$$

For $j = 1, \ldots, N$ let f_j and π_j, be one-dimensional functions $f_j : y \mapsto f_j(y)$ and $\pi_j : (y_{t_{i-q}}, \ldots, y_{t_{i-1}}; \boldsymbol{\theta}) \mapsto \pi_j(y_{t_{i-q}}, \ldots, y_{t_{i-1}}; \boldsymbol{\theta})$ and $\mathbf{A}_j$ be p-dimensional functions $\mathbf{A}_j : (y_{t_{i-q}}, \ldots, y_{t_{i-1}}; \boldsymbol{\theta}) \mapsto \mathbf{A}_j(y_{t_{i-q}}, \ldots, y_{t_{i-1}}; \boldsymbol{\theta})$ defined on the state space $\mathcal{S}$ in L_2. f_j are functions specified by the user. Next we turn to the specification of π_j and $\mathbf{A}_j$:
Consider the linear projection

$$\pi_j(Y_{t_{i-q}}, \ldots, Y_{t_{i-1}}; \boldsymbol{\theta}) = a_j(\boldsymbol{\theta}) + \mathbf{b}_j(\boldsymbol{\theta})^T \mathbf{Z}^j_{1:q} \tag{3.2}$$

with $\mathbf{Z}^j_{1:q} = (h^j_1(Y_{t_{i-q}}), \ldots, h^j_q(Y_{t_{i-1}}))$, $a_j : \boldsymbol{\theta} \to a_j(\boldsymbol{\theta})$, $\mathbf{b}_j : \boldsymbol{\theta} \to \mathbf{b}_j(\boldsymbol{\theta})$ and for each element $h_k(Y_{t_{i-q-1+l}}), k = 1, \ldots, q$ is a one-dimensional function $h_k : y \mapsto h_k(y)$, and finally a_j and $\mathbf{b}_j$ are determined by the linear projection

$$\begin{aligned} \mathbf{b}_j(\boldsymbol{\theta}) &= V[\mathbf{Z}^j_{1:q}]^{-1} Cov[f_j(Y_{t_i}), \mathbf{Z}^j_{1:q}]^T \\ a_j(\boldsymbol{\theta}) &= E[f_j(Y_{t_i})] - \mathbf{b}_j(\boldsymbol{\theta})^T E[\mathbf{Z}^j_{1:q}]. \end{aligned}$$

The next task is to specify the function $\mathbf{A}_j$: Since we know that the projection errors $(f_j(Y_{t_i}) - \pi_j(Y_{t_{i-q}}, \ldots, Y_{t_{i-1}}; \boldsymbol{\theta}))$ are orthogonal to all the elements $(1, \mathbf{Z}^j_{1:q}, j = 1, \ldots, N)$ a reasonable estimating function is

$$\mathbf{G}(Y_{t_1}, \ldots, Y_{t_n}; \boldsymbol{\theta}) = \sum_{i=q+1}^{n} \begin{pmatrix} 1(f_1(Y_{t_i}) - \pi_1(Y_{t_{i-q}}, \ldots, Y_{t_{i-1}}; \boldsymbol{\theta})) \\ \vdots \\ Z^1_q(f_1(Y_{t_i}) - \pi_1(Y_{t_{i-q}}, \ldots, Y_{t_{i-1}}; \boldsymbol{\theta})) \\ \vdots \\ \vdots \\ 1(f_N(Y_{t_i}) - \pi_N(Y_{t_{i-q}}, \ldots, Y_{t_{i-1}}; \boldsymbol{\theta})) \\ \vdots \\ Z^N_q(f_N(Y_{t_i}) - \pi_N(Y_{t_{i-q}}, \ldots, Y_{t_{i-1}}; \boldsymbol{\theta})) \end{pmatrix}. \tag{3.3}$$

Only parameters appearing in these moments for at least one j can be estimated using (3.3). For computational tractability this imposes some restrictions on the choice of the functions f_j and $h^j_{1:q}$ for all j. Often simple polynomials in Y_{t_i} are used. There is no available theory for the optimal choice of the functions f_j and $h^j_{1:q}$ due to the lack of a properly defined optimality criterion, but the choice must be guided by the (subset of the) parameters that should be estimated.

4. Optimal estimating functions

In this section explicit expressions for the optimal prediction-based estimating functions with measurement noise will be given. The presentation and notation in Section 4.1 follow [Sørensen, 2000] that also relies on optimality results from [Heyde, 1997]. Section 4.2 contains results regarding explicit expressions for unconditional moments of both $(X_t)_{t\geq 0}$ and $(Y_{t_i})_{1\leq i\leq n}$ and their interrelations.

4.1. Optimal estimating functions

In order to find the optimal $\mathbf{G}^*(Y_{t_1},\ldots,Y_{t_n};\boldsymbol{\theta})$ (3.3) is rewritten as

$$\mathbf{G}(Y_{t_1},\ldots,Y_{t_n};\boldsymbol{\theta}) = \mathbf{A}(\boldsymbol{\theta}) \sum_{i=q+1}^{n} \mathbf{H}^{(i)}(Y_{t_{i-q}},\ldots,Y_{t_i};\boldsymbol{\theta}), \tag{4.1}$$

where $\mathbf{A}(\boldsymbol{\theta})$ is some function we seek to determine optimally and $\mathbf{H}^{(i)}(Y_{t_{i-q}},\ldots,Y_{t_i};\boldsymbol{\theta})$ is specified through (3.3). As in [Sørensen, 2000] the $\mathcal{O}_F$-optimal criterion from [Heyde, 1997] is applied to find the optimal weighting function

$$\begin{aligned}\mathbf{A}^*(\boldsymbol{\theta}) \;=\; & -E[\sum_{i=q+1}^{n} \partial_{\boldsymbol{\theta}} \mathbf{H}^{(i)}(Y_{t_{i-q}},\ldots,Y_{t_i};\boldsymbol{\theta})^T] \\ & \left[E[(\sum_{i=q+1}^{n} \mathbf{H}^{(i)}(Y_{t_{i-q}},\ldots,Y_{t_i};\boldsymbol{\theta}))(\sum_{j=q+1}^{n} \mathbf{H}^{(j)}(Y_{t_{j-q}},\ldots,Y_{t_j};\boldsymbol{\theta}))^T]\right]^{-1}\end{aligned} \tag{4.2}$$

where

$$
\begin{aligned}
(4.3)\; & E[(\sum_{i=q+1}^{n} \mathbf{H}^{(i)}(Y_{t_{i-q}},\ldots,Y_{t_i};\boldsymbol{\theta}))(\sum_{j=q+1}^{n} \mathbf{H}^{(j)}(Y_{t_{j-q}},\ldots,Y_{t_j};\boldsymbol{\theta}))^T] \\
&= E[\mathbf{H}^{(q+1)}(Y_{t_1},\ldots,Y_{t_{q+1}};\boldsymbol{\theta})\mathbf{H}^{(q+1)}(Y_{t_1},\ldots,Y_{t_{q+1}};\boldsymbol{\theta})^T] \\
&\quad + \sum_{k=2}^{n-q} \frac{n-q+1-k}{n-q} \Big[E[\mathbf{H}^{(q+1)}(Y_{t_1},\ldots,Y_{t_{q+1}};\boldsymbol{\theta})\mathbf{H}^{(q+k)}(Y_{t_k},\ldots,Y_{t_{k+q}};\boldsymbol{\theta})^T] \\
&\qquad\qquad + E[\mathbf{H}^{(q+k)}(Y_{t_k},\ldots,Y_{t_{k+q}};\boldsymbol{\theta})\mathbf{H}^{(q)}(Y_{t_0},\ldots,Y_{t_q};\boldsymbol{\theta})^T]\Big]
\end{aligned}
$$

and

$$
\partial_{\boldsymbol{\theta}^T}\mathbf{H}^{(i)}(Y_{t_{i-q}},\ldots,Y_{t_i};\boldsymbol{\theta}) = \begin{pmatrix} \partial_{\theta_1}H_1^{(i)}(Y_{t_{i-q}},\ldots,Y_{t_i};\boldsymbol{\theta}) & \ldots & \partial_{\theta_p}H_1^{(i)}(Y_{t_{i-q}},\ldots,Y_{t_i};\boldsymbol{\theta}) \\ \vdots & & \vdots \\ \partial_{\theta_1}H_p^{(i)}(Y_{t_{i-q}},\ldots,Y_{t_i};\boldsymbol{\theta}) & \ldots & \partial_{\theta_p}H_p^{(i)}(Y_{t_{i-q}},\ldots,Y_{t_i};\boldsymbol{\theta}), \end{pmatrix}
$$

Remark 4.1. Conditions for invertibility of (4.3) is given in [Sørensen, 2000].

4.2. Computing unconditional moments

In most applications the functions f_j and $h_{1:q}^j$ will be polynomials in the measurements at different time instants. Thus in order to determine the unconditional mixed moments constituting $E[\mathbf{H}^{(i)}(Y_{t_{i-q}},\ldots,Y_{t_i};\boldsymbol{\theta})\mathbf{H}^{(i)}(Y_{t_{i-q}},\ldots,Y_{t_i};\boldsymbol{\theta})^T]$, expressions of the form

$$
E[Y_{t_1}^{j_1}Y_{t_2}^{j_2}\cdots Y_{t_m}^{j_m}] \tag{4.4}
$$

for $m \in \mathbb{N}$, j_1, …, $j_m \in \mathbf{N}_0^m$ and $t_1 < t_2 < \ldots < t_m$ being increasing sampling times must be determined. Using (2.7) together with Condition 2 this problem reduces to determining explicit expressions for moments on the form $E[X_{t_1}^{j_1}\cdots X_{t_m}^{j_m}]$ provided that the following condition holds.

Condition 3. Polynomials are eigenfunctions to the generator (2.5) of the diffusion process (2.1), i.e. the eigenfunctions

$$
\varphi_i(x;\boldsymbol{\theta}) = \sum_{j=0}^{i} \gamma_{ij}(\boldsymbol{\theta})x^j \tag{4.5}
$$

satisfy the equation

$$L\varphi_i(x;\boldsymbol{\theta}) = -\lambda_i\varphi_i(x;\boldsymbol{\theta}) \tag{4.6}$$

for $i = 1, \ldots, m$.

Remark 4.2. This is the case for several popular models in finance [Kessler and Sørensen, 1999]

Remark 4.3. The constants $\gamma_{ij}(\boldsymbol{\theta})$ are computed from (4.5). See Section 5.1 for an example.

Lemma 4.1. *Under Condition 3, it holds that*

$$\exp(-\lambda_i t)\sum_{j=0}^{i}\gamma_{ij}(\boldsymbol{\theta})x^j = \sum_{j=0}^{i}\gamma_{ij}(\boldsymbol{\theta})\sum_{k=0}^{j}\nu_{jk}(t;\boldsymbol{\theta})x^k; \quad i = 1, \ldots, m \tag{4.7}$$

from which the constants $\nu_{jk}(t;\boldsymbol{\theta})$ are determined.

Proof. Taking the conditional expectation on both sides of (4.5) yields

$$E[\varphi_i(X_t;\boldsymbol{\theta})|X_0 = x] = \sum_{j=0}^{i}\gamma_{ij}(\boldsymbol{\theta})E[X_t^j|X_0 = x]. \tag{4.8}$$

Under weak regularity conditions

$$E[\varphi_i(X_t;\boldsymbol{\theta})|X_0 = x] = \exp(-\lambda_i t)\varphi_i(x;\boldsymbol{\theta}) \tag{4.9}$$

see [Kessler and Sørensen, 1999]. Inserting (4.9) in (4.8) yields

$$\exp(-\lambda_i t)\varphi_i(x;\boldsymbol{\theta}) = \sum_{j=0}^{i}\gamma_{ij}(\boldsymbol{\theta})E[X_t^j|X_0 = x]. \tag{4.10}$$

Under Condition 3, Eq. (4.10) can be expressed as

$$\exp(-\lambda_i t)\varphi_i(x;\boldsymbol{\theta}) = \sum_{j=0}^{i}\gamma_{ij}(\boldsymbol{\theta})\sum_{k=0}^{j}\nu_{jk}(t;\boldsymbol{\theta})x^k \tag{4.11}$$

Inserting (4.5) in (4.11) completes the proof. □

Remark 4.4. It follows immediately from (4.10)–(4.11) that

$$E[X_t^j|X_0 = x] = \sum_{k=0}^{j} \nu_{jk}(t;\boldsymbol{\theta})x^k; \quad j \in \mathbb{N} \tag{4.12}$$

This leads to the main result given in the next Theorem.

Theorem 4.1. *Assume that the diffusion $(X_t)_{t\geq 0}$ solves (2.1). For $m \in \mathbb{N}$, $j_1, j_2, \ldots, j_m \in \mathbb{N}_0^m$ and the sampling times $t_1 < t_2 < \ldots < t_m$, it holds that*

$$\begin{aligned} E[X_{t_1}^{j_1} \cdots X_{t_m}^{j_m}] = & \sum_{i_m=0}^{j_m} \nu_{j_m,i_m}(t_m - t_{m-1};\boldsymbol{\theta}) \times \cdots \times \sum_{i_3=0}^{j_3+i_4} \nu_{(j_3+i_4),i_3}(t_3 - t_2;\boldsymbol{\theta}) \\ & \times \sum_{i_2=0}^{j_2+i_3} \nu_{(j_2+i_3),i_2}(t_2 - t_1;\boldsymbol{\theta}) E[X_{t_1}^{j_1+i_2}] \end{aligned} \tag{4.13}$$

Proof. The proof is made by induction. $E[X_{t_1}^{j_1}]$ obviously fulfills (4.13).

Assume that

$$\begin{aligned} E[X_{t_1}^{j_1} \cdots X_{t_m}^{j_m}] = & \sum_{i_m=0}^{j_m} \nu_{j_m,i_m}(t_m - t_{m-1};\boldsymbol{\theta}) \times \cdots \times \sum_{i_3=0}^{j_3+i_4} \nu_{(j_3+i_4),i_3}(t_3 - t_2;\boldsymbol{\theta}) \\ & \times \sum_{i_2=0}^{j_2+i_3} \nu_{(j_2+i_3),i_2}(t_2 - t_1;\boldsymbol{\theta}) E[X_{t_1}^{j_1+i_2}] \end{aligned}$$

Next let us prove that

$$\begin{aligned} E[X_{t_1}^{j_1} \cdots X_{t_m}^{j_m} X_{t_{m+1}}^{j_{m+1}}] = & \sum_{i_{m+1}=0}^{j_{m+1}} \nu_{j_{m+1},i_{m+1}}(t_{m+1} - t_m;\boldsymbol{\theta}) \times \cdots \times \\ & \sum_{i_3=0}^{j_3+i_4} \nu_{(j_3+i_4),i_3}(t_3 - t_2;\boldsymbol{\theta}) \\ & \times \sum_{i_2=0}^{j_2+i_3} \nu_{(j_2+i_3),i_2}(t_2 - t_1;\boldsymbol{\theta}) E[X_{t_1}^{j_1+i_2}] \end{aligned}$$

By conditioning on $X_{t_m}^{j_m}$, we get

$$\begin{aligned} E[X_{t_1}^{j_1}\cdots X_{t_{m+1}}^{j_{m+1}}] &= E[E[X_{t_1}^{j_1}\cdots X_{t_m}^{j_m}X_{t_{m+1}}^{j_{m+1}}|X_{t_m}^{j_m}]] \\ &= E[X_{t_1}^{j_1}\cdots X_{t_m}^{j_m}E[X_{t_{m+1}}^{j_{m+1}}|X_{t_m}^{j_m}]] \\ &= E[X_{t_1}^{j_1}\cdots X_{t_m}^{j_m}\sum_{i_{m+1}=0}^{j_{m+1}}\nu_{j_{m+1},i_{m+1}}(t_{m+1}-t_m;\boldsymbol{\theta})X_{t_m}^{i_{m+1}}] \\ &= \sum_{i_{m+1}=0}^{j_{m+1}}\nu_{j_{m+1},i_{m+1}}(t_{m+1}-t_m;\boldsymbol{\theta})E[X_{t_1}^{j_1}X_{t_2}^{j_2}\cdots X_{t_m}^{j_m+i_{m+1}}] \end{aligned}$$

According to the assumption by induction we obtain

$$\begin{aligned} E[X_{t_1}^{j_1}\cdots X_{t_{m+1}}^{j_{m+1}}] = &\sum_{i_{m+1}=0}^{j_{m+1}}\nu_{j_{m+1},i_{m+1}}(t_{m+1}-t_m;\boldsymbol{\theta})\sum_{i_m=0}^{j_m}\nu_{j_m,i_m}(t_m-t_{m-1};\boldsymbol{\theta}) \\ &\times\cdots\times\sum_{i_3=0}^{j_3+i_4}\nu_{(j_3+i_4),i_3}(t_3-t_2;\boldsymbol{\theta}) \\ &\times\sum_{i_2=0}^{j_2+i_3}\nu_{(j_2+i_3),i_2}(t_2-t_1;\boldsymbol{\theta})E[X_{t_1}^{j_1+i_2}], \end{aligned}$$

which completes the proof. □

Remark 4.5. The result in Theorem 4.1 is a generalization of a result in [Sørensen, 2000].

4.3. The CIR model

Consider the CIR model which is used extensively in mathematical finance as a model for e.g. spot interest rates

$$dX_t = \alpha(\beta - X_t)dt + \sigma\sqrt{X_t}dW_t; \quad X_0 = x, \tag{4.14}$$

where $\boldsymbol{\theta} = (\alpha, \beta, \sigma) \in (0,\infty)^3$ such that the process $(X_t)_{t\geq 0}$ is ergodic. It is well known that X_t is non-central chi-square distributed and that X (the stationary case) is gamma-distributed $\Gamma\left(\frac{2\alpha\beta}{\sigma^2}, \frac{\sigma^2}{2\alpha}\right)$. It follows that the stationary mean and

variance are given by $E[X] = \beta$ and $\mathrm{Var}[X] = \frac{\beta\sigma^2}{2\alpha}$, respectively. The higher order moments satisfy the recursive relation

$$E[X^m] = \left(\beta + \frac{(m-1)\sigma^2}{2\alpha}\right) E[X^{m-1}] \tag{4.15}$$

for $m \geq 2$. The spectrum (set of eigenvalues) is $\Lambda_{\boldsymbol{\theta}} = \{j\alpha \colon j \in \mathbb{N}_0\}$ with corresponding eigenfunctions $\phi_j(x;\boldsymbol{\theta}) = L_j^{(\eta)}(2\alpha x\sigma^{-2})$, where $L_j^{(\eta)}$ is the j'th order Laguerre polynomial with parameter $\eta = 2\alpha\beta\sigma^{-2} - 1$ [Karlin and Taylor, 1981].

The discrete trajectory $(Y_{t_i})_{1\leq i\leq n}$ with $t_i = i\Delta$ is assumed to be given by

$$Y_{t_i} = X_{t_i} + \varepsilon_{t_i}. \tag{4.16}$$

For notational simplicity, we assume that only one parameter is to be estimated, i.e. $p = 1$.

Let $N = 1, q = 5$ and $f_1 : y \mapsto f_1(y^2)$, i.e. (3.2) is

$$\pi(Y_{t_{i-5}}, \ldots, Y_{t_{i-1}}; \boldsymbol{\theta}) = a(\boldsymbol{\theta}) + \mathbf{b}(\boldsymbol{\theta})^T \mathbf{Z}^{(i-1)} = a + b_1 Y_{t_{i-1}}^2 + \ldots + b_5 Y_{t_{i-5}}^2$$

inserting in (3.3) yields

$$\mathbf{G}(Y_{t_1}, \ldots, Y_{t_n}; \boldsymbol{\theta}) = \sum_{i=5}^{n} \begin{bmatrix} Y_{t_i}^2 - \hat{a}_0 - \hat{a}_1 Y_{t_{i-1}}^2 - \ldots - \hat{a}_5 Y_{t_{i-5}}^2 \\ Y_{t_{i-1}}^2 (Y_{t_i}^2 - \hat{a}_0 - \hat{a}_1 Y_{t_{i-1}}^2 - \ldots - \hat{a}_5 Y_{t_{i-5}}^2) \\ \vdots \\ Y_{t_{i-5}}^2 (Y_{t_i}^2 - \hat{a}_0 - \hat{a}_1 Y_{t_{i-1}}^2 - \ldots - \hat{a}_5 Y_{t_{i-5}}^2) \end{bmatrix}.$$

In order to compute the optimal weights $\mathbf{A}^*(\boldsymbol{\theta})$ in (4.2), it is necessary to compute the matrix of partial derivatives $\partial_{\boldsymbol{\theta}^T} \mathbf{H}^{(i)}(Y_{t_{i-5}}, \ldots, Y_{t_i}; \boldsymbol{\theta})$ and the matrix in (4.3). The latter consists of (mixed) moments of Y_{t_i} that may be computed using that it is possible to derive a general expression that relates the simple unconditional moments of Y_{t_i} and X_{t_i}.

Lemma 4.2. *For the discretized trajectory $(Y_{t_i})_{1\leq i\leq n}$ given by (4.16), it holds that*

$$E[Y_{t_i}^{2m}] = \sum_{j=0}^{2m} \delta_j E[X_{t_i}^{2m-j}] \tag{4.17}$$

with

$$\delta_j = \begin{cases} \binom{2m}{j} \sigma_\varepsilon^j \prod_{k=1}^{j/2} (2k-1) & \text{for } j = 0, 2, 4, \ldots \\ 0 & \text{for } j = 1, 3, 5, \ldots \end{cases} \tag{4.18}$$

for $m \in \mathbb{N}$.

Proof. The binomial formula yields the result

$$E[Y_{t_i}^{2m}] = E[(X_{t_i} + \varepsilon_{t_i})^{2m}] = \sum_{j=1}^{2m} \binom{2m}{j} E[X_{t_i}^{2m-j} \varepsilon_{t_i}^{j}] \tag{4.19}$$

As $(\varepsilon_{t_i})_{1 \leq i \leq n}$ is Gaussian white noise, it holds that

$$E[X_{t_i}^{2i_1+1} \varepsilon_{t_i}^{2i_2+1}] = 0$$

for $i_1, i_2 \in \mathbb{N}_0^2$. As $E[\varepsilon_t^{2i+1}] = 0$ and $E[\varepsilon_t^{2j}] = \sigma_\varepsilon^{2j} \prod_{k=1}^{j}(2k-1)$ for $j \in \mathbb{N}_0$ the definition of the constants $\delta_j \in \mathbb{N}$ in (4.18), and hence (4.17), follows. □

From the lemma, it follows that e.g.

$$\begin{aligned}
E[Y_{t_i}^2] &= E[X_{t_i}^2] + \sigma_\varepsilon^2 \\
E[Y_{t_i}^4] &= E[X_{t_i}^4] + 6E[X_{t_i}^2]\sigma_\varepsilon^2 + 3\sigma_\varepsilon^4 \\
E[Y_{t_i}^6] &= E[X_{t_i}^6] + 15E[X_{t_i}^4]\sigma_\varepsilon^2 + 45E[X_{t_i}^2]\sigma_\varepsilon^4 + 15\sigma_\varepsilon^6 \\
E[Y_{t_i}^8] &= E[X_{t_i}^8] + 28E[X_{t_i}^6]\sigma_\varepsilon^2 + 210E[X_{t_i}^4]\sigma_\varepsilon^4 + 420E[X_{t_i}^2]\sigma_\varepsilon^6 + 105\sigma_\varepsilon^8
\end{aligned}$$

Furthermore, it holds that

$$\begin{aligned}
\mathrm{Var}[Y_{t_i}^2] &= E[X_{t_i}^4] + 4E[X_{t_i}^2]\sigma_\varepsilon^2 + 2\sigma_\varepsilon^4 - E[X_{t_i}^2]^2 \\
\mathrm{Cov}[Y_{t_{i_1}}^2, Y_{t_{i_2}}^2] &= E[(Y_{t_{i_1}}^2 - E[Y_{t_{i_1}}^2])(Y_{t_{i_2}}^2 - E[Y_{t_{i_2}}^2])] = \mathrm{Cov}[X_{t_{i_1}}^2, X_{t_{i_2}}^2];\ t_{i_1} \neq t_{i_2},
\end{aligned}$$

Using these relations higher order unconditional moments of $(Y_{t_i})_{1 \leq i \leq n}$ may be expressed in terms of the unconditional moments of $(X_{t_i})_{1 \leq i \leq n}$ given by (4.15). The same applies for mixed moments of $(Y_{t_i})_{1 \leq i \leq n}$, e.g.

$$\begin{aligned}
E[Y_{t_1}^2 Y_{t_2}^2 Y_{t_3}^2 Y_{t_4}^2] &= E[(X_{t_1} + \varepsilon_{t_1})^2 (X_{t_2} + \varepsilon_{t_2})^2 (X_{t_3} + \varepsilon_{t_3})^2 (X_{t_4} + \varepsilon_{t_4})^2] \\
&= E[X_{t_1}^2 X_{t_2}^2 X_{t_3}^2 X_{t_4}^2] + \sigma_\varepsilon^2 E[X_{t_1}^2 X_{t_2}^2 X_{t_3}^2] + \sigma_\varepsilon^2 E[X_{t_1}^2 X_{t_2}^2 X_{t_4}^2] \\
&\quad + \sigma_\varepsilon^2 E[X_{t_1}^2 X_{t_3}^2 X_{t_4}^2] + \sigma_\varepsilon^4 E[X_{t_2}^2 X_{t_3}^2] + \sigma_\varepsilon^4 E[X_{t_2}^2 X_{t_4}^2] \\
&\quad + \sigma_\varepsilon^4 E[X_{t_3}^2 X_{t_4}^2] + 4\sigma_\varepsilon^6 E[X_{t_1}^2] + \sigma_\varepsilon^8
\end{aligned}$$

Theorem 4.1 provides expressions for the mixed moments $E[X_{t_1}^2 X_{t_2}^2 X_{t_3}^2 X_{t_4}^2]$ in terms of $E[X_t^m]$, where the latter is given by (4.15).

Example 4.1. Let us now try to determine expressions of $\nu_{20}(t;\boldsymbol{\theta})$, $\nu_{21}(t;\boldsymbol{\theta})$ and $\nu_{22}(t;\boldsymbol{\theta})$ by applying (4.7). To ease the notation $\nu_{jk}(t;\boldsymbol{\theta})$ will be written as ν_{jk} and $\gamma_{jk}(\boldsymbol{\theta})$ as γ_{jk}. Inserting $i = 2$ in (4.7) yields

$$\exp(-\lambda_2 t) \cdot (\gamma_{20} + \gamma_{21} x + \gamma_{22} x^2) = \gamma_{20}\nu_{00} + \gamma_{21}(\nu_{10} + \nu_{11} x) + \gamma_{22}(\nu_{20} + \nu_{21} x + \nu_{22} x^2)$$

Collecting terms in x yields

$$\begin{aligned}\gamma_{20}\exp(-\lambda_2 t) &= \gamma_{20}\nu_{00} + \gamma_{21}\nu_{10} + \gamma_{22}\nu_{20}\\ \gamma_{21}\exp(-\lambda_2 t) &= \gamma_{21}\nu_{11} + \gamma_{22}\nu_{21}\\ \gamma_{22}\exp(-\lambda_2 t) &= \gamma_{22}\nu_{22}.\end{aligned}$$

These equations are then solved with respect to ν_{2j} for $j = 1, 2, 3$, which yields

$$\nu_{20} = \frac{\gamma_{20}}{\gamma_{22}}(\exp(-\lambda_2 t) - \nu_{00}) - \frac{\gamma_{21}}{\gamma_{22}}\nu_{10} \tag{4.20}$$

$$\nu_{21} = \frac{\gamma_{21}}{\gamma_{22}}(\exp(-\lambda_2 t) - \nu_{11}) \tag{4.21}$$

$$\nu_{22} = \exp(-\lambda_2 t) \tag{4.22}$$

Inserting the solutions for ν_{00}, ν_{10} and ν_{11}, which is obtained by solving

$$L\varphi_2(x;\boldsymbol{\theta}) = -\lambda_2\varphi_2(x;\boldsymbol{\theta}) \text{ and } L\varphi_1(x;\boldsymbol{\theta}) = -\lambda_1\varphi_1(x;\boldsymbol{\theta})$$

in (4.20)–(4.22) yields

$$\begin{aligned}\nu_{20} &= \frac{\gamma_{20}}{\gamma_{22}}(\exp(-\lambda_2 t) - 1) - \frac{\gamma_{21}}{\gamma_{22}}\frac{\gamma_{10}}{\gamma_{11}}(\exp(-\lambda_1 t) - 1)\\ \nu_{21} &= \frac{\gamma_{21}}{\gamma_{22}}(\exp(-\lambda_2 t) - \exp(-\lambda_1 t))\\ \nu_{22} &= \exp(-\lambda_2 t)\end{aligned}$$

Example 4.2. It follows that the second eigenfunction $\phi_2(x;\boldsymbol{\theta})$ is given by (up to a multiplicative constant)

$$\phi_2(x;\boldsymbol{\theta}) = \gamma_{20} + \gamma_{21}x + \gamma_{22}x^2 \tag{4.23}$$

where the constants γ_{2i} for $i = 0, 1, 2$ are determined as follows. For the CIR model, Eq. (4.6) takes the form

$$\alpha(\beta - x)(\gamma_{21} + 2\gamma_{22}x) + \gamma_{22}\sigma^2 x = -\lambda_2(\gamma_{20} + \gamma_{21}x + \gamma_{22}x^2)$$

Making the arbitrary choice $\gamma_{22} = 1$ and matching coefficients yields

$$\gamma_{21} = -\frac{2\alpha\beta + \sigma^2}{\alpha} \text{ and } \gamma_{20} = \frac{\beta(2\alpha\beta + \sigma^2)}{2\alpha}$$

such that

$$\phi_2(x;\boldsymbol{\theta}) = \frac{\beta(2\alpha\beta + \sigma^2)}{2\alpha} - \frac{2\alpha\beta + \sigma^2}{\alpha}x + x^2$$

It is clear that even for a small sample a huge amount of mixed moments need to be computed in order to determine the optimal PEF given by (4.1). These computations may be carried out using a symbolic mathematical package, say, Maple[a], or the moments may be computed by simulation. In both cases, it is

[a]The programs may be obtained from the authors on request.

convenient to introduce an algebra to handle all the special cases, where some of the indices in the mixed moment $E[X_{t_1}^2 X_{t_2}^2 X_{t_3}^2 X_{t_4}^2]$ coincide. Depending on the (autocorrelation and mixing) properties of the data, it may also be possible to simplify and reduce the number of mixed moments.

5. Monte Carlo studies

In this section the properties of the PEFs in our setup will be analyzed and compared to nonlinear filter used in combination with a QML method using Monte Carlo simulation. Discrete measurements of the CIR model are used, i.e. the model is given by (4.14) and (4.16).

5.1. A nonlinear filter

The general continuous-discrete time nonlinear filtering problem is described in [Jazwinski, 1970, Maybeck, 1982] with a recent application in finance given in [Nielsen et al., 2000]. Briefly the general idea is to infer information about the unobserved states X_{t_i} from the measurements Y_{t_i} for $i = 1, \ldots, n$ using two sets of equations: A propagation set describing the evolution of the states between the sampling times and an update set that updates the estimates of the states at the sampling times t_i. Let $\mathcal{Y}_{t_i}$ denote the information set provided by the measurements up to and including time t_i. The transition densities $p(X_{t_i}|X_{t_{i-1}};\boldsymbol{\theta})$ can, at least in principle, be found as the solution to the Chapman-Kolmogorov forward equation, and the conditional density $p(X_t|\mathcal{Y}_{t_{i-1}};\boldsymbol{\theta})$ may then be found from

$$p(X_t|\mathcal{Y}_{t_{i-1}};\boldsymbol{\theta}) = \int_{\mathcal{S}} p(X_t|X_{t_{i-1}};\boldsymbol{\theta}) p(X_{t_{i-1}}|\mathcal{Y}_{t_{i-1}};\boldsymbol{\theta}) dX_{t_{i-1}} \text{ for } t \in [t_{i-1}, t_i), \tag{5.1}$$

where $p(X_{t_i}|\mathcal{Y}_{t_{i-1}};\boldsymbol{\theta})$ is the conditional density for the previous measurement update that follows from Bayes' rule

$$p(X_{t_i}|\mathcal{Y}_{t_i};\boldsymbol{\theta}) = \frac{p(Y_{t_i}|X_{t_i}, \mathcal{Y}_{t_{i-1}};\boldsymbol{\theta}) p(X_{t_i}|X_{t_{i-1}};\boldsymbol{\theta})}{p(Y_{t_i}|\mathcal{Y}_{t_{i-1}};\boldsymbol{\theta})}. \tag{5.2}$$

Assuming that the measurement noise is Gaussian, the first numerator term may be simplified to $p(Y_{t_i}|X_{t_i}, \mathcal{Y}_{t_{i-1}};\boldsymbol{\theta}) = p(Y_{t_i}|X_{t_i};\boldsymbol{\theta})$, where the latter is Gaussian.

The denominator is given by

$$p(Y_{t_i}|\mathcal{Y}_{t_{i-1}};\boldsymbol{\theta}) = \int_{\mathcal{S}} p(Y_{t_i}|X_{t_i};\boldsymbol{\theta})p(X_{t_i}|\mathcal{Y}_{t_{i-1}};\boldsymbol{\theta})dX_{t_i} \tag{5.3}$$

Unfortunately, an explicit expression for the conditional density $p(X_t|\mathcal{Y}_{t_{i-1}};\boldsymbol{\theta})$ given in (5.1) cannot be obtained for the CIR model (4.14), which implies that an approximate solution to the continuous-discrete time filtering problem given by (5.1)–(5.3) must be found. Motivated by the linear Kalman filter [Kalman and Bucy, 1961] that is based on the first two conditional moments, i.e. the conditional mean and variance, the exact time propagation of the states are approximated by two Ordinary Differential Equations (ODEs) for the first two conditional moments of the conditional density, see e.g. [Maybeck, 1982]. However, for the CIR model (4.14), it turns out that these approximate ODEs coincide with the true ODEs[b]. Indeed these ODEs may be solved explicitly, i.e.

$$E[X_{t_i}|X_{t_{i-1}}] = \beta + (X_{t_{i-1}} - \beta)e^{-\alpha\Delta} \tag{5.4}$$

$$\mathrm{Var}[X_{t_i}|X_{t_{i-1}}] = \frac{\sigma^2}{\alpha}\left[\frac{\beta}{2} + (X_{t_{i-1}} - \beta)e^{-\alpha\Delta} - \left(X_{t_{i-1}} - \frac{\beta}{2}\right)e^{-2\alpha\Delta}\right] \tag{5.5}$$

with $\Delta_i = \Delta = t_i - t_{i-1}$. The approximate updating equations are given by

$$E[X_{t_i}|\mathcal{Y}_{t_i}] = E[X_{t_i}|\mathcal{Y}_{t_{i-1}}] + K_{t_i}(Y_{t_i} - E[X_{t_i}|\mathcal{Y}_{t_{i-1}}]) \tag{5.6}$$

$$\mathrm{Var}[X_{t_i}|\mathcal{Y}_{t_i}] = (1 - K_{t_i})\mathrm{Var}[X_{t_i}|\mathcal{Y}_{t_{i-1}}], \tag{5.7}$$

where the Kalman gain K_{t_i} is

$$K_{t_i} = \frac{\mathrm{Var}[X_{t_i}|\mathcal{Y}_{t_{i-1}}]}{\mathrm{Var}[X_{t_i}|\mathcal{Y}_{t_{i-1}}] + \sigma_\varepsilon^2} \tag{5.8}$$

The equations (5.4)–(5.8) constitute the modified truncated second order filter.

QML estimates of the parameter $\boldsymbol{\theta}$ are readily obtained by assuming that the one-step ahead prediction errors $Y_{t_i} - E[X_{t_i}|\mathcal{Y}_{t_{i-1}}]$ in (5.6) are Gaussian. Given that the first two conditional moments are correctly specified by the filter, it is conjectured from [Heyde, 1997] that the QML estimates attain the same nice properties as ML estimates.

[b]This statement holds for the socalled truncated second order filter that ignores all central moments of X_t of higher order than two.

Remark 5.1. It is noted that the assumption inherent to the applied filter is that the conditional mean and variance provide an adequate description of the transition density. This assumption only holds for narrow-sense linear SDEs with a Gaussian density.

5.2. Simulation studies

Two Monte Carlo simulation studies are reported in this section. In each study 20 stochastically independent time series each consisting of n=500 measurements have been simulated. The Milstein discretization scheme [Kloeden and Platen, 1995] is used to obtain a numerical solution to (4.14) and measurement noise is subsequently added to the simulated states. For computational convenience, one parameter is estimated at a time while the others are fixed at their true value. The nuisance parameter σ_ε^2 is also fixed. Due to the computational requirements of PEF only estimates of α and σ^2 are provided in both studies. The results obtained in Section 5.1 have been used extensively.

In the first study the parameter vector

$$\boldsymbol{\theta}^T = (\alpha, \beta, \sigma^2, \sigma_\varepsilon^2) = (0.08, 0.25, 0.0073, (0.015)^2)$$

is used. The sampling interval is $\Delta_i = \Delta = 0.1$. The results reported in Table 5.2 are obtained. The mean and standard deviation of the 20 samples of each parameter is listed. All the methods underestimate α, but almost the same level of efficiency is obtained. This, in particular, holds for the filtering/QML method. In our experience the filter method tends to underestimate the *speed-of-adjustment* parameter α when it is "small" compared to the sampling time Δ, see e.g. [Nielsen et al., 2000]. On the other hand, the filtering/QML method outperforms the EF-based methods regarding the estimate of σ^2.

In the second study the parameter vector

$$\boldsymbol{\theta}^T = (\alpha, \beta, \sigma^2, \sigma_\varepsilon^2) = (0.5, 0.25, 0.0225, 0.01)$$

is used. The sampling time is $\Delta_i = \Delta = 0.1$. The results reported in Table 2 are obtained. In this study the filtering/QML method and the PEF method provide almost identical results. The filtering estimates are slightly less biased, and the efficiency of the estimate of σ^2 is higher. Thus the value of α in this study is sufficiently large compared to the sampling time Δ to avoid the afore-mentioned problems with the filtering/QML method. Similar problems have not occurred with the PEF method.

	True	PEF	Filter
α	0.08	0.0743 (0.0145)	0.0546 (0.0144)
σ^2	0.0073	0.0124 (0.0091)	0.0074 (0.0013)

Table 1: Estimation results from the first simulation study. The estimates provided are obtained as the mean of 20 independent samples each consisting of 500 measurements from the CIR model (4.14). The standard deviations are given in parenthesis. The true values are $(\alpha, \beta, \sigma^2, \sigma_\varepsilon^2) = (0.08,\ 0.25,\ 0.0073,\ (0.015)^2)$.

	True	PEF	Filter
α	0.5	0.4911 (0.0553)	0.4959 (0.0584)
σ^2	0.0225	0.01873 (0.007322)	0.01973 (0.003349)

Table 2: Estimation results from the second simulation study. The estimates provided are obtained as the mean of 20 independent samples each consisting of 500 measurements from the CIR model (4.14). The standard deviations are given in parenthesis. The true values are $(\alpha, \beta, \sigma^2, \sigma_\varepsilon^2) = (0.5,\ 0.25,\ 0.0225,\ 0.01)$.

6. Conclusion

The simulation study has been limited by huge runtimes, generally we observed that the estimated parameters applying PEF and the filtering methods yield rather similar results, with a tendency that estimators obtained applying the filter seems to fluctuate more.

We explicitly formulate the prediction-based estimating functions proposed by [Sørensen, 2000] for measurement error models. The method is based on unconditional (mixed) moments and explicit results are presented in order to facilitate a computation of these moments. The CIR model is used to illustrate some of the moment calculations inherent to the method; an explicit expression for the relation between the measurements and the underlying states is derived. The method has been presented for univariate diffusion processes, but it may be generalized to multifactor models.

An obvious advantage of PEF is that optimal estimators may be derived

and their asymptotic properties are well-established. However, an obvious disadvantage is the huge number of unconditional and mixed moments that need be computed even for univariate SDEs. Furthermore some restrictions must be imposed on the SDE as well as the measurement function in order to be able to compute the unconditional moments. From a theoretical point of view it is possible to generalize the PEF method to cope with multivariate SDEs, but they may be very difficult to implement, unless suboptimal weights are used. Nonlinear filtering methods are not limited by these restrictions and are well-suited for multivariate SDEs, but the approximations that are inherent to the ODEs for the conditional moments are very difficult to assess such that the properties of the QML-estimates are difficult to establish. In our experience the bias imposed by these approximations are, however, negligible in most applications.

REFERENCES

[Bibby and Sørensen, 1995] Bibby, B. M. and Sørensen, M. (1995). Martingale estimation functions for discretely observed diffusion processes. *Bernoulli*, 1(1-2):17–39.

[Bibby and Sørensen, 2001] Bibby, B. M. and Sørensen, M. (2001). Simplified estimating functions for diffusion models with a high-dimensional parameter. *Scand. J. Statist.*, 28(1):99–112.

[Cox et al., 1985] Cox, J. C., Ingersoll, Jr., J. E., and Ross, S. A. (1985). A theory of the term structure of interest rates. *Econometrica*, 53(2):385–407.

[Doucet et al., 2001] Doucet, A., de Freitas, N., and Gordon, N., editors (2001). *Sequential Monte Carlo methods in practice*. Statistics for Engineering and Information Science. Springer-Verlag, New York.

[Duffie and Singleton, 1993] Duffie, D. and Singleton, K. J. (1993). Simulated moments estimation of Markov models of asset prices. *Econometrica*, 61(4):929–952.

[Gallant and Long, 1997] Gallant, A. R. and Long, J. R. (1997). Estimating stochastic differential equations efficiently by minimum chi-squared. *Biometrika*, 84(1):125–141.

[Gallant and Tauchen, 1996] Gallant, A. R. and Tauchen, G. (1996). Which moments to match? *Econometric Theory*, 12(4):657–681.

[Godambe, 1960] Godambe, V. P. (1960). An optimum property of regular maximum likelihood estimation. *Ann. Math. Statist.*, 31:1208–1211.

[Godambe and Kale, 1991] Godambe, V. P. and Kale, B. K. (1991). Estimating functions: an overview. In *Estimating functions*, volume 7 of *Oxford Statist. Sci. Ser.*, pages 3–20. Oxford Univ. Press, New York.

[Hansen, 1982] Hansen, L. P. (1982). Large sample properties of generalized method of moments estimators. *Econometrica*, 50(4):1029–1054.

[Heyde, 1997] Heyde, C. C. (1997). *Quasi-likelihood and its application*. Springer Series in Statistics. Springer-Verlag, New York. A general approach to optimal parameter estimation.

[Jazwinski, 1970] Jazwinski, A. H. (1970). *Stochastic Processes and Filtering Theory*. Academic Press.

[Jiang and Knight, 1997] Jiang, G. J. and Knight, J. L. (1997). A nonparametric approach to the estimation of diffusion processes, with an application to a short-term interest rate model. *Econometric Theory*, 13(5):615–645.

[Kalman and Bucy, 1961] Kalman, R. E. and Bucy, R. S. (1961). New results in linear filtering and prediction problems. *J. of Basic Engineering, Transactions ASMA, Series D*, 83:95–108.

[Karlin and Taylor, 1981] Karlin, S. and Taylor, H. M. (1981). *A second course in stochastic processes*. Academic Press Inc. [Harcourt Brace Jovanovich Publishers], New York.

[Kessler, 2000] Kessler, M. (2000). Simple and explicit estimating functions for a discretely observed diffusion process. *Scand. J. Statist.*, 27(1):65–82.

[Kessler and Sørensen, 1999] Kessler, M. and Sørensen, M. (1999). Estimating equations based on eigenfunctions for a discretely observed diffusion process. *Bernoulli*, 5(2):299–314.

[Kloeden and Platen, 1995] Kloeden, P. E. and Platen, E. (1995). Numerical methods for stochastic differential equations. In *Nonlinear dynamics and stochastic mechanics*, CRC Math. Model. Ser., pages 437–461. CRC, Boca Raton, FL.

[Liptser and Shiryaev, 2001a] Liptser, R. S. and Shiryaev, A. N. (2001a). *Statistics of random processes. I*, volume 5 of *Applications of Mathematics (New York)*. Springer-Verlag, Berlin, expanded edition. General theory, Translated from the 1974 Russian original by A. B. Aries, Stochastic Modelling and Applied Probability.

[Liptser and Shiryaev, 2001b] Liptser, R. S. and Shiryaev, A. N. (2001b). *Statistics of random processes. II*, volume 6 of *Applications of Mathematics (New York)*. Springer-Verlag, Berlin, expanded edition. Applications, Translated from the 1974 Russian original by A. B. Aries, Stochastic Modelling and Applied Probability.

[Maekawa et al., 1998] Maekawa, K., Knight, J. L., and Hisamatsu, H. (1998). Finite sample comparisons of the distributions of the OLS and GLS estimators in regression with an integrated regressor and correlated errors. *Econometric Rev.*, 17(4):387–413.

[Maybeck, 1982] Maybeck, P. S. (1982). *Stochastic Models, Estimation and Control*. Academic Press.

[McLeish and Small, 1988] McLeish, D. L. and Small, C. G. (1988). *The theory and applications of statistical inference functions*, volume 44 of *Lecture Notes in Statistics*. Springer-Verlag, New York.

[Nielsen et al., 2000] Nielsen, J. N., Vestergaard, M., and Madsen, H. (2000). Estimation in continuous-time stochastic volatility models using nonlinear filters. *Int. J. Theor. Appl. Finance*, 3(2):279–308.

[Schweppe, 1965] Schweppe, F. C. (1965). Evaluation of likelihood functions for Gaussian signals. *IEEE Trans. Information Theory*, IT-11:61–70.

[Sørensen, 2000] Sørensen, M. (2000). Prediction-based estimating functions. *Econom. J.*, 3(2):123–147.